Novel zebrafish models for autism spectrum disorder

Thesis submitted for the degree of

Doctor of Philosophy

at the University of Leicester

by

Elisa Dalla Vecchia (MSc)

Department of Neuroscience, Psychology and Behaviour

University of Leicester

2019

Nothing in life is to be feared,
it is only to be understood.
Now is the time to understand more,
so that we may fear less.

Maria Skłodowska-Curie

Abstract

Novel zebrafish models for autism spectrum disorder

Elisa Dalla Vecchia

Autism spectrum disorder (ASD) refers to a group of complex neurodevelopment disorders influenced by multiple genes and environmental factors. ASD is characterized by repetitive and stereotyped behaviour together with deficits in social communication and interaction. The lack of knowledge regarding the underlying genetics and neurobiology of this disorder has hindered the discovery of novel drugs. The aim of this project is to investigate the function of two ASD candidate genes, *reelin* (*reln*) and *ywhaz*, to gain insights into the neurological basis of ASD and improve drug treatments. To this end, we have used *reln* and *ywhaz* mutant lines to investigate the function of ASD-candidate genes in zebrafish.

The first results chapter focuses on *reln*, the archetypal ASD candidate gene. *reln*$^{-/-}$ exhibits an impaired behavioural phenotype which resembles specific symptoms of ASD and it provides significant insights into the relationship between Reln activity and the role of the serotoninergic system in ASD.

The second chapter describe the generation of a stable zebrafish *ywhaz*$^{-/-}$ mutant line using the Clustered Regularly Interspaced Short Palindromic Repeats/CRISPR associated protein-9 nuclease (CRISPR/Cas9) technique.

The third chapter focuses on the characterisation of *ywhaz*$^{-/-}$, highlighting the importance of functional *ywhaz* signalling in the adult brain, and shedding light on the role of both the serotoninergic and dopaminergic system in ASD. *ywhaz*$^{-/-}$ reveal an impaired behaviour which resembles some of the defects occurring in ASD and it can be rescued by fluoxetine and quinpirole treatment.

In summary, both the mutant lines analysed in this project can be considered suitable models to analyse some defects which occur in ASD, in particularly cerebellar defects. This study supports the idea that damage of certain cerebellar areas can result in the core symptoms of ASD.

Acknowledgments

I am really glad to have the opportunity to thank all the people who accompanied me during my time as PhD student. It has been an extraordinary experience, and I have been supported by so many people that I need to apologize in advance for the length of these acknowledgements.

First and foremost, I would like to thank my supervisor Will Norton for the opportunity to undertake this work. You represent everything I could have ever wanted in a supervisor and I cannot thank you enough for yours continued support, mentoring and enthusiasm during my PhD. You have been so supportive of me throughout my PhD, always taking time for me whenever I needed it, since the beginning of the PhD until the very end, and for that I am truly grateful. Your dedication to both your lab and science is admirable, and you know how hard it was for me to leave you and your lab. Without your support, advice and guidance, I probably would not be here. Thank you for believing in me and giving me this amazing chance in life.

I would like to thank all the present and past members of the Norton's lab. The biggest thank goes to Amir, a true friend of mine and invaluable mentor in the lab. I feel blessed ("Amir..bless me!") for having had the opportunity to get to know you as a friend and to take advantage of all your scientific knowledge. Together we "crispred" and it was such a big achievement. It has been a pleasure to work side by side with you, to share so many nice moments, dinners, butterflies, trips and chats. Let's "Feed Our Inner Smile" together and keep being friends no matter the distance. I could not thank my dear friend Irene enough, who firstly welcomed me in this group. Luckily, we were desk mates only for a short period, if not with all our chatting I would never have finished my PhD on time! I am extremely grateful to Hector, the pillar of the Norton's lab, for always being available for me, teaching me un uncountable numbers of techniques and for his encouragement, helpful comments and suggestions. I am grateful to Ceinwen for her kindness and all her technical assistance, especially during the last qPCR experiments. No one knows the departments better than her and she has always been there when I

needed help. I am thankful to Florian, for all the suggestions and scientific discussions. I would also like to thank Pelumi, for adding an extra smile to our group. It was always nice to have her around in the lab, and I will never forget the “non-spiciness” of her Jollof rice. Finally, I would like to thank Cassiano, one of the kindest person I have got to know. He brought such a Brazilian happiness to the lab, and I still smile when I think about him and his yerba mate tea.

I am very grateful to the MiND network. Sharing this journey with this amazing PhD student team made all the working meeting enjoyable moments in which we did not only share knowledge that helped us to grow up as scientists, but we also shared pure moment of fun travelling and discovering the world (..of course always being lost in a new city and late for the meetings!).

Another massive acknowledgment goes to all the friends who became my second family in Leicester, you have all made my time in Leicester a unique experience, to say the least! To Laura and Giorgio, who welcomed me in Leicester at the beginning of my Erasmus and supported me until the very end of this PhD adventure. I will never thank them enough for their friendship. Our family could not be completed without Irene and Peppe, who were part of this amazing “gruppo trifamiliare” too. I have probably had dinner more time at your place than mine own, and this is worthy ten thousand thanks. We spent endless time together, which usually started with an aperitivo and ended in the most various ways from visiting allotment, to talk to the weirdest people in town, to have a Maryland Chicken (second) dinner on the streets, to celebrate the Leicester city football club victory singing and dancing outside the stadium (and being interviewed by the Italian television!). A “grazie Alessandro” goes to the best flat mate I could ever asked for. Regardless the disagreement between smart lights, the usefulness of google home and technology in general, we were perfectly in synchrony when it was the time to cook (pizza, risotto, pasticcio, paella and minestrine), to choose the series for the movie nights or to fight against bees and broken windows. It was nice to know that I had in Stanley Court a friend on whom I could always count. Nevertheless, thanks to you I met Betty. Despite the “Greek pastitsio” still makes me shiver, I am glad that I can call her friend and that I have an ally always by my side.

How not to mention my best friend Anna, despite the distance you have been very close to me during all these years spent abroad. We have been friends for more than 20 years and you still manage to surprise me. From coming at surprise to collect me at the airport (well, of course you were late also in this occasion), to take me to Gardaland as a surprise for my birthday. I could have not asked for a better best friend in life: “Siamo come al sole a mezzogiorno, baby”.

I have had so much support from my family, both emotionally and practically. You were even happier than me every time that I got a tiny positive result, and knowing that you have always been proud of me and what I was doing gave me the strength to be where I am now. I will never thank you enough for all the times that you took me to the airport (most of the times getting a fine on your way!), or you organised a welcome dinner when I was visiting home. You were never really far away from me: Mum, you tried so hard to be even closer to me, that you started to go to English classes, but it did not work out very well, didn’t? Dad, you reached the next level when you fixed my bicycle through a video call, I am still amazed. I also became an auntie by phone, when Elena and Berti called me at 5.00 am announcing that Mattia was happily born, but I just though they typed the wrong number. My family has been my solid pillar during these years, I couldn’t have done this without you.

Thank to my grandparents, aunts, uncles and cousins too, for always welcoming me back home and supporting me while I was in Leicester.

I want to make a special mention too, of Marco. During all these years you brought out the best in me, always encouraging me to follow my dreams and ambitions. Is wonderful how much we grew up in these years, becoming the people that we are now, loving and supporting each other. Live apart from each other during these years it has been the most difficult challenge of this PhD. But finally, the long distances are over and I am so looking forward to move to Innsbruck and start to live our life together. Thanks for being the love of my life.

Table of contents

List of tables

List of figures

List of abbreviations

5-HIAA	5-hydroxyindoleacetic acid
5-HT	serotonin
aa	amino acid
Ach	acetylcholine
AD	Alzheimer's disease
ADHD	attention deficit and hyperactivity disorder
Akt	protein Kinase B
aldoca	aldolase Ca
ApoER2	apolipoprotein E receptor 2
ASD	autism spectrum disorder
AUTS1	first autism susceptibility locus
BP	bipolar disorder
CACNA1C	calcium channel, voltage-dependent, l type, alpha 1c subunit
CamKII	calmodulin-dependent protein kinase II
Cas	CRISPR associated proteins
CC	crista cerebellaris
CCe	corpus cerebelli
cDNA	complementary DNA
CeP	cerebellar plate
CFs	climbing fibers
CJD	Creutzfeldt–Jakob disease
CNS	central nervous system
CNVs	copy number variations
COMT	catechol o-methyl transferase
CR	Cajal-Retzius
CREB	cAMP response element-binding protein
CRISPR	Clustered Regularly Interspaced Short Palindromic Repeats
crRNA	CRISPR RNA
CT	cycle time
CTR	carboxy-terminal region
DA	dopamine
DAB	3,3'-Diaminobenzidine
Dab1	adaptor protein Disabled-1
Dat	dopamine transporter
DlP	dorsal lateral pallium
Dm	medial part of the dorsal telencephalon
DmP	dorsal medial pallium
DOPAC	3,4-dihydroxyphenylacetic acid
dpf	days post fertilisation

$DR_{1;5}$	D1-like receptor
$DR_{2;3;4}$	D2-like receptor
drd	dopamine receptor
DT	dorsal thalamus
elf1a	elongation factor 1a
ELISA	enzyme-linked immunosorbent assay
FDA	Food and Drug Administration
FMR1	fragile x mental retardation 1
FSCV	fast-scan cyclic voltammetry
Fw	forward
GABA	γ-aminobutyric acid
Gad	glutamate decarboxylase enzyme
GCL	granule cell layer
GEF	GTP exchange factor
GOI	gene of interest
GSK3β	glycogen synthase kinases 3β
Ha	habenula
hpf	hours post fertilization
HPLC	high precision liquid chromatography
HRM	heterozygous *reeler* mice
HVA	homovanillic acid
Hy	hypothalamus
IEGs	immediate-early gene
IHC	immunohistochemistry
IID	inter-individual distance
IMGSAC	International Molecular Genetic Study of Autism Consortium
indels	insertions/deletions
IO	inferior olive nuclei
ISH	*in situ* hybridization
L-DOPA	L-3,4-dihydroxyphenylalanine
LCa	lobus caudalis cerebelli
LCH	cerebellar hypoplasia
LDLR	low-density lipoprotein receptor
LTP	long-term potentiation
mao	monoamine oxidase
MDS	Miller-Dieker syndrome
MECP2	methyl cpg binding protein 2
MFs	mossy fibers
ML	molecular layer
MLS	multipoint maximum LOD score
MO	medulla oblongata

NA	noradrenaline
NCBI	National Center for Biotechnology Information
NDD	nearest neighbour distance
NFTs	neurofibrillary tangles
NIH	National Institute of Health
nin	interpeduncular nucleus
NLGN	neuroligin
NMD	nonsense-mediated mRNA decay
NMDA	N-methyl-D-aspartate receptors
NPD	neuropsychiatric disorders
NRXN	neurexin
ORF	open reading frame
Oxt	oxytocin
P	proline
PAM	proto-spacer adjacent motif
PBS	phosphate-buffered saline
PBT	phosphate-buffered saline + Tween-20
PCL	Purkinje cell layer
PET	positron emission tomography
PFA	paraformaldehyde
PKA	protein kinase A
pmat	plasma membrane monoamine transporter
Po	preoptic region
PPI	prepulse inhibition
pS	phosphoserine
PSD-95	postsynaptic density protein 95
pT	phosphothreonine
PTB	phosphotyrosine binding
PTC	premature termination codon
PTU	1-phenyl 2-thiourea
R	arginine
Rap1	repression and activation protein GTPase
REF	reference gene
Reln	Reelin
RF	reticular formation
rpl13	ribosomal protein L13a
RR	reelin repeats
RT	room-temperature
RT-PCR	reverse transcription polymerase chain reaction
Rv	reverse
S	signal peptide

sac	stratum album centrale
sert	serotonin transporter
SFKs	Src-family kinases
sfm	stratum fibrosum marginale
sgRNA	guide RNA
SH2	Src-homology domains
SHANK	sh3 and multiple ankyrin repeat domains
SL	F-spondin-like domain
slc18	solute carrier family 18
slc6a3	solute carrier family 6, member 3
SNPs	single nucleotide polymorphisms
SNVs	single-nucleotide variants
so	stratum opticum
sp	stratum periventriculare
SSC	saline-sodium citrate buffer
SSRI	selective serotonin reuptake inhibitor
SZ	schizophrenia
T7EI	T7 Endonuclease I
T	thalamus
TeO	optic tectum
Th	tyrosine hydroxylase
TL	torus longitudinalis
Tph	tryptophan hydroxylase
tracrRNA	trans-activating RNA
tRNA	total RNA
TSC	TSC complex subunit
Val	lateral part of the valvula cerebelli
Vam	medial part of the valvula cerebelli
VLDLR	very low-density lipoprotein receptor
VMSP	visually-mediated social preference test
VT	ventral thalamus
Vv	ventral nucleus of the ventral telencephalon
WES	whole exome sequencing
ZIRC	Zebrafish International Resource Center

Chapter 1 Autism spectrum disorder

1.1 Neurodevelopmental disorders (NPD)

Neurodevelopmental and neuropsychiatric disorders (NPD) are complex diseases that are influenced by multiple genes and environmental factors. The spectrum of NPD symptoms is wide and ranges from specific limitations in the control of executive function or learning to global impairments in intelligence and social skills (Cristino et al., 2014). NPD include different disorders such as intellectual disability, autism spectrum disorder (ASD), fragile-X syndrome, attention deficit and hyperactivity disorder (ADHD) and schizophrenia. NPD place a significant strain on society, with mental health problems costing developed countries between 3 and 4% of the gross national product (Salvage, 2011). Nevertheless, in spite of this burden, little is known about the underlying neurobiology of NPDs, and candidate genes are difficult to detect since affected individuals harbour different risk alleles in heterogeneous genetic backgrounds. However, thanks to modern genetic screening techniques, progress has been made in unravelling the genetics of NPD and hundreds of candidate genes have now been identified, including single nucleotide polymorphisms (SNPs) and copy number variations (CNVs) in affected individuals. Hypotheses regarding the molecular pathways that underlie NPD can then be made by coupling whole-genome sequencing with protein interaction information through computational approaches (Cristino et al., 2014; Mitchell, 2011).

1.2 Autism spectrum disorder

The term “autism” derives from the Greek word *autos*, which means “oneself”. In 1911, the psychiatrist Eugène Bleuler, first used this term to describe symptoms of self-absorption that impaired communication in schizophrenic patients (Bleuler, 1930). Later in 1943, Leo Kanner defined autism as “enclosure in oneself”, an independent clinical syndrome which is already present at birth (Kanner et al., 1943). Since then extraordinary progress has been made in understanding the pathophysiology

underlying this complex disorder. Nowadays autism is classified as a spectrum: autism spectrum disorder (ASD) (DSM-5, Edition 2013), which encompass autism together with the less severe Asperger's disorder, childhood disintegrative disorder and pervasive developmental disorder not otherwise specified. This group of neurodevelopmental syndromes is characterized by deficits in communication and social interactions as well as restricted interests and repetitive behaviours with an onset prior to 3 years of age (DSM-5, Edition 2013). In fact, the main clinical features of ASD are atypical social interactions, impaired language production and comprehension, insistence on uniformity, unusual learning, hypo- or hyper-reactivity to sensory stimuli, stereotypies (repetitive movement or utterances) and impaired motor adjustment. ASD has multiple comorbidities, including attention deficit and hyperactivity disorder, intellectual developmental disorder, language disorder, obsessive compulsive behaviours, tics, eating disorders and sleep disorders (Leyfer et al., 2006). Moreover, autistic patients often experience depression and anxiety disorders (Gotham et al., 2015). Estimation of the prevalence of ASD has evolved constantly through the years starting from 1 birth out of 2500 in the early 70's (Fombonne, 2003) and now reaching 1 in 68 eight-year-old American children (Christensen et al., 2016). Autistic patients require comprehensive care across the lifespan, and although several medications are used to treat the symptoms of ASD, currently only risperidone and aripiprazole are approved by the U.S. Food and Drug Administration (FDA) for use in autism, specifically for the treatment of severe irritability (Politte et al., 2014). There are new medications under development that show promise for ASD, and in particular oxytocin is one of the most promising targets to ameliorate social interactions (Penagarikano, 2015).

1.2.1 Aetiology of autism spectrum disorder

Since the beginning, ASD was thought to be innate in new-borns with the possibility of being genetically transmitted (Frith et al., 1991; Kanner et al., 1943). Approximately 25% of autism cases are caused by known mutations in known genes, whereas about 75% of cases are still classified as idiopathic (Huguet et al., 2013). Although much effort has concentrated on identifying genes linked to ASD, there is also an increasing amount of research into possible environmental causes. According to data from different

countries, the relative contribution of environmental and genetic factors may be region-specific and could also change over time. Several susceptibility genes and loci have been identified through linkage and association studies and it is possible that the striking clinical heterogeneity of ASD may reflect the high degree of underlying aetiological heterogeneity (Persico and Napolioni, 2013).

1.2.1.1 Genetics of autism spectrum disorder

In a first pioneering genetic study of ASD, the occurrence of autism in same-sex monozygotic pairs of twins was diagnosed as 4 pairs out of the 11 monozygotic twins studied, whereas it was not present in the 10 other dizygotic twins (Folstein and Rutter, 1977). Nowadays, concordance for autism in monozygotic pairs of twins is estimated to be 88% (Rosenberg et al., 2009), recognising an important role for genetic factors in this disease. Since ASD occurs approximately four times more frequently in males than females (Hampson and Blatt, 2015; Werling and Geschwind, 2013), the possible involvement of the X chromosome in ASD was investigated revealing that mutations on the sex chromosome are associated with ASD. For example, mutations in the X-linked genes, *NEUROLIGIN 3* (*NLGN3*) and *NEUROLIGIN 4X* (*NLGN4X*), have been link to ASD (Delavest et al., 2012; Jamain et al., 2003; Thomson et al., 2004). More than 200 genes are linked to ASD, and most of them are involved in pathways that might alter synaptic homeostasis. In fact, both mutations and CNVs are frequently reported in glutamatergic and GABAergic pathway genes that are involved in synaptogenesis, long term potentiation and neuronal functions (Delorme et al., 2013; Szatmari et al., 2007). Examples include mutations in the *SH3* and *MULTIPLE ANKYRIN REPEAT DOMAINS 2* and 3 genes (*SHANK2*, *SHANK3*) and in the gene coding for Neurexin (*NRXN*). *SHANK* genes code for proteins located in the post-synaptic density of glutamatergic synapses that are essential for neuronal functioning. Mutations in these genes seem to be most frequently observed in autistic patients (Durand et al., 2007; Leblond et al., 2012). NRXN is a presynaptic membrane protein which interacts with NLGN in glutamatergic and GABAergic synapses (Kim et al., 2008). Specific chromosomal regions have also been associated with ASD, in fact the International Molecular Genetic Study of Autism Consortium (IMGSAC) identified six different regions within the chromosomes 4, 7, 10,

16, 19 and 22 which are likely to be involved in the aetiology of ASD (Consortium, 2001). Among these regions the long arm of chromosome 7 (7q) gave the most significant multipoint maximum LOD score (MLS) and other studies found associations between mutations in 7q and autism (Ashley-Koch et al., 1999; Barrett et al., 1999; Philippe et al., 1999). This region is now referred to as the first autism susceptibility locus (AUTS1).

1.2.1.2 Epigenetic and environmental factors in autism spectrum disorder

Genetic factors alone are not responsible of the symptoms of ASD; epigenetic factors may contribute to the aetiology of this disease (Flashner et al., 2013; Hallmayer et al., 2011), and environmental factors may also increase its risk (Carter and Blizard, 2016; Vijayakumar and Judy, 2016). The contribution of genetic and environmental factors varies between each autistic patient and environmental factors have different effects according to the developmental stage of the individual at the time of exposure (Tordjman et al., 2014). The prenatal factors associated with increased ASD risk are advanced parental age at birth, gestational bleeding and diabetes, multiple birth (Gardener et al., 2009) and *in utero* exposure to thalidomide and valproate which are teratogenic medications (Bromley et al., 2008). During the perinatal period, preterm birth is positively correlated with the development of ASD, while severe deficits in very early social interactions, such as profound early social deprivation can also increase the risk of ASD (Rutter et al., 1999). Epigenetic effects, which are functional modifications to the genome that modulate gene expression without changing the nucleotide sequence, can affect the interactions between genetic and environmental factors (Tordjman et al., 2014). These modifications can modulate synaptic plasticity and neuronal excitability, and they can be transmitted across generations (Fagiolini et al., 2009). Therefore, ASD progression might be the result of intricate interactions between a number of genetic mutations, environmental factors and epigenetic modifications in specific critical developmental time windows.

1.2.1.3 Neurochemical involvement in autism spectrum disorder

Irregularities in several neurotransmitter systems have been implicated in the pathology of ASD. Several studies indicate involvement of serotonin (5-HT), dopamine (DA), *γ*-aminobutyric acid (GABA), glutamate, noradrenaline (NA), acetylcholine (ACh) and oxytocin (Oxt) dysfunction in the development of ASD (Lam et al., 2006). The main function of neurotransmitters in the central nervous system (CNS) is to regulate synaptic signalling, brain maturation and cortical organization including neuronal migration and positioning (Manent and Represa, 2007).

Serotonin:

Serotonin (5-HT), is involved in brain development, cell division and differentiation, neurite growth, and synaptogenesis (Chugani, 2002). The regulation of 5-HT in the CNS has also been implicated in the control of behaviour including social interactions, anxiety, reward behaviour, aggression, mood, impulsivity, sleep and psychosis (Cook and Leventhal, 1996; Kiser et al., 2012; Kriegebaum et al., 2010). Therefore, the role of 5-HT in neuropsychiatric disorders has been a major topic of research. Autistic patients demonstrate impairments in many of the functions modulated by 5-HT. The association between abnormal 5-HT activity and autism was first identified in 1961 when a pioneering study reported increased levels of whole blood 5-HT in approximately 30% of autistic patients (Schain and Freedman, 1961). Since then, more studies have replicated this finding, showing that one third of autistic individuals suffer from hyperserotonemia (Anderson et al., 1987; Hanley, 1977; Leboyer et al., 1999; Leventhal et al., 1990; Ritvo, 1970; Takahashi et al., 1976). Additional evidence that impaired 5-HT signalling contributes to ASD is the fact that depletion of the precursor of 5-HT, tryptophan, can aggravate repetitive behaviours in autism (McDougle et al., 1996). Positron emission tomography (PET) studies indicate impaired 5-HT synthesis rates in ASD children (Chugani et al., 1999). Moreover, selective serotonin transporter inhibitors (SSRI) sometimes reduce anxiety, rituals and obsessive-compulsive behaviours in autistic individuals (McDougle et al., 1996; Williams et al., 2011) even though side effects may occur and SSRIs are not effective in all cases (Williams et al., 2011). In contrast to this, there is recent evidence that hyposerotonemia at neurodevelopmental stages may cause autism, since it has been reported that plasma 5-HT levels in the

mothers of patients with autism were significantly lower than in mothers of normal children. Moreover, plasma 5-HT values were significantly lower in autistic children than their fathers (Connors et al., 2006). It therefore seems likely that low maternal plasma 5-HT might contribute to impaired brain development in autism.

Dopamine:

Dopamine (DA) plays several important roles in reward, motivation and motor actions. Among the distinct DAergic neurons subpopulations present in the brain, the ventral tegmental area and substantia nigra are involved in the regulation of functions which are usually impaired in ASD (Haber, 2014). The ventral tegmental area projects to the prefrontal cortex and the ventral striatum to the nucleus accumbens to form the mesocorticolimbic circuit that is associated with higher-order brain functions such as reward and motivation (Chevallier et al., 2012). A key hallmark of ASD is reduced social interaction which could arise from mesocorticolimbic circuit dysfunction. In fact, it has been shown that ASD is characterized by hypoactivation of the reward system (Dichter et al., 2010), and deficits occur for both social and non-social rewards (Dichter et al., 2011; Scott-Van Zeeland et al., 2010). Other studies have shown that autistic patients have alterations in the mesocorticolimbic DAergic pathway, with reduced release of DA in the prefrontal cortex and reduced neural activity in the nucleus accumbens (Ernst et al., 1997; Scott-Van Zeeland et al., 2010). Therefore, deficits in the DAergic system at the level of the mesocorticolimbic pathway could represent one of the events which lead to the social deficits observed in ASD. The substantia nigra DAergic neurons might also be involved in the ASD. These neurons project to the dorsal striatum, forming the nigrostriatal circuit, which regulates motor output for specific goal-directed-behaviour and stereotypies (Chevallier et al., 2012; Haber, 2014; Lewis and Kim, 2009). The stereotyped behaviours detected in ASD patients could arise from defects in the DAergic system at the level of the nigrostriatal pathway. This theory is confirmed by a number of different studies, such as induced dysfunction of the nigrostriatal pathway in mice which leads to stereotyped behaviours (Lewis et al., 2007), and the administration of dopamine D_1 receptor antagonists which ameliorate spontaneous stereotypies in mice (Presti et al., 2003). Moreover, mice carrying a 16p11.2 deletion, a mutation found in autistic patients, exhibit nigrostriatal lesions and stereotyped patterns of behaviour

(Horev et al., 2011). In autistic patients polymorphisms in the *dopamine D_3 receptor* gene are associated with an increased striatal volume and stereotyped behaviour (Staal et al., 2015) while polymorphisms in the *dopamine D_4 receptor* and the *dopamine transporter* genes are linked to repetitive behaviour (Gadow et al., 2010). Therefore, deficits in the DAergic system at the level of the mesocorticolimbic and nigrostriatal circuits could cause autistic-like behaviour by altering the reward system and the regulation of motor actions.

GABA and glutamate:

γ-aminobutyric acid (GABA) is the main inhibitory neurotransmitter in the mammalian CNS. It reduces neuronal excitability throughout the nervous system, whereas glutamate is the most abundant excitatory neurotransmitter (Watanabe et al., 2002). GABA and glutamate signalling play a role in normal cell migration during brain development. A correct balance between glutamatergic and GABAergic systems is essential for the positioning of principal, pyramidal and interneurons in the cerebral cortex (Manent and Represa, 2007) and its disruption might lead to severe alterations to CNS function and homeostasis (Levitt, 2005). Hussman first proposed that ASD may arise from an imbalance between excitatory glutamate and inhibitory GABA signalling (Hussman, 2001). In fact, GABAergic interneurons are active across cortical domains and could be involved in the pathophysiology of cortical dysfunction in autism (Casanova et al., 2003). GABA dysfunction could result in hyperstimulation of neurons leading to seizures (Tuchman and Rapin, 2002) and impairments in reacting to external stimuli (Casanova et al., 2006). Furthermore, defects in either $GABA_A$ or $GABA_B$ receptors might heighten postsynaptic neuronal excitability and impair glutamate release. Genetic studies, animal models and *in vivo* and *in vitro* studies of humans support the idea that the GABAergic system is involved in the pathogenesis of ASD (Cellot and Cherubini, 2014; Coghlan et al., 2012). In fact, genetic studies have revealed abnormalities in the 15q11-13 region which contains several $GABA_A$ receptor subunit genes associated with autism (Buxbaum et al., 2002; Wolpert et al., 2000). In addition, animal models lacking different GABA receptor subunits exhibit autistic-like behaviours (Cheh et al., 2006; Delorey et al., 2008; Tabuchi et al., 2007). *In vivo* studies have reported increased GABA plasma levels in ASD patients (Dhossche et al., 2005; El-Ansary and Al-Ayadhi, 2014;

Russo, 2013), and reduced GABA levels in the frontal lobe (Harada et al., 2011), sensorimotor (Puts et al., 2017) and auditory regions (Gaetz et al., 2014) as well as the anterior cingulate cortex (Brix et al., 2015) of ASD patients. Post-mortem studies have shown that some autistic patients have a reduction in GABAergic Purkinje cells in the cerebellum (Bauman and Kemper, 2005) and fewer neurons in the lateral amygdala and fusiform gyrus (Amaral et al., 2008; van Kooten et al., 2008), whereas in the hippocampus the density of GABAergic interneurons is increased (Lawrence et al., 2010). $GABA_A$ (Blatt et al., 2001; Fatemi et al., 2014; Guptill et al., 2006) and $GABA_B$ receptor levels are also decreased in the hippocampus and superior frontal cortex of autistic patients (Fatemi et al., 2010; Fatemi et al., 2008). Animal models of ASD also display GABAergic alterations, as observed in mice carrying a mutation in the *Neuroligin 3* gene (Földy et al., 2013; Pizzarelli and Cherubini, 2013). Moreover, mouse embryos exposed to the convulsant valproic acid *in utero* exhibit autistic-like behaviours postnatally together with a decreased level of both pre- and post-synaptic GABAergic signalling (Banerjee et al., 2012). The suggestion that autism could arise from an increased glutamate/GABA ratio is also support by pharmacological studies which show that administration of GABA agonists and glutamate receptor antagonists has promising preliminary results in both an ASD animal model and a small-scale phase II human trial of autistic patients (Berry-Kravis, 2014; Oberman, 2012).

Overall there is plenty of evidence for altered neurotransmitter signalling in ASD. Alterations during critical periods of brain development could lead to permanent changes in neural circuits which in turn can affect behaviour. Impairment of brain development can be caused by mutations in genes directly linked to the transmitter signalling (including syntheses and degradation enzymes, receptors and transporters) as well as environmental perturbations. The involvement of many different neurotransmitters in the aetiology of ASD seems likely to contribute to the high level of heterogeneity seen in this disease.

1.2.2 Neurophysiological features of autism spectrum disorder

The first two years of life, when the brain develops and triples in size, are essential for the creation of mature cerebral circuitry (Courchesne et al., 2000). Since ASD symptoms typically occur between 2 and 4 years of age, when the initial phase of neural development is complete, it was hypothesised that ASD may arise from developmental deficits in the cerebral circuitry (Courchesne, 2004). Therefore, structural and morphological brain abnormalities associated with ASD have been studied. Analysis of head circumference measurements in ASD have shown that brain growth is impaired in autistic patients (Amaral et al., 2008; Courchesne, 2003). The onset of the core symptoms of ASD is preceded by two phases of brain growth abnormalities: a reduced head size at birth, followed by a sudden increase growth between 1–2 months and 6–14 months of age (Courchesne, 2004; Courchesne et al., 2004). This excessive growth is followed by an abnormally slow or arrested growth rate during the end of the second year of life, when most of the main autistic symptoms start to appear (Dawson, 2008; Redcay and Courchesne, 2005). The early overgrowth finally leads to an abnormally large brain, with a 10% increment in volume compared to controls (Courchesne, 2004). In particular the frontal lobe, cerebellum, amygdala, and limbic volumes are larger than the controls and are subject to structural alterations as well (Courchesne, 2004; Courchesne and Pierce, 2005; Courchesne et al., 2004; Schumann, 2004). In fact, abnormalities in the laminar cytoarchitecture of the cerebral cortex have been reported (Kemper and Bauman, 1998), together with loss and atrophy of Purkinje cells in the cerebellum (Ritvo et al., 1986) and a decreased number of neurons in the amygdala of post-mortem autistic brains (Schumann and Amaral, 2005; Schumann and Amaral, 2006). Altogether, these defects are the most prominent neuropathological abnormalities in ASD (Bailey, 1998; Kemper and Bauman, 1998) and these brain regions are intimately involved in the development of the higher-order cognitive, emotional, language, and social functions known to be altered in autism. The cerebral overgrowth occurs during a particular vulnerable stage of development when the circuits that regulate these functions are being formed (Dobbing, 1982). Thus, it is quite likely that neuronal underdevelopment and abnormal circuitry formation might lead to the development of autistic behaviours. Taken together, this evidence supports the

hypothesis that autism is underpinned by cortical organisational defects which arise during early brain development and cause impairments of information processing at different levels of the nervous system, from dendritic and synaptic organisation to pathway connectivity and brain structure (Geschwind and Levitt, 2007; Minshew and Williams, 2007).

1.2.3 Autism spectrum disorder endophenotypes

The diagnoses of neuropsychiatric disorders used to be based on subjective assessments of symptoms (Bearden and Freimer, 2006). Recent research has proposed that more measurable parameters, such as endophenotypes, are needed as objective criteria for diagnoses. An ideal endophenotype should be heritable, controlled by a single gene, associated with the risk of the disorder in the population and be expressed even when the disease is not active (Gottesman and Gould, 2003; Rommelse, 2008). The use of endophenotypes in neuropsychiatric research provides biological descriptions, including neurophysiological, neuroanatomical and cognitive information that can be reliably measured in different animal models. There are currently no medical tests or biological markers that can be used to diagnose ASD (Lai et al., 2013). This makes it crucial to identify endophenotypes to help with diagnosis. The study of ASD endophenotypes is complicated by the fact that their expression could change developmentally over time (Viding and Blakemore, 2007; Volkmar and McPartland, 2014). Some of the promising autistic endophenotypes that have been identified so far include language, social skills, anxiety, seizure, head size and measures of behaviour and cognition, which allow for reliable testing of autistic dysfunction (DiLalla et al., 2017; Rubenstein et al., 2015).

1.3 Model organisms used in NPD research

Model organisms can be defined as non-human species which are used to model and study biological phenomena, including human disorders, in order to acquire new knowledge which can be applied to more complex organisms such as humans (Leonelli

and Ankeny, 2013). To ensure that the data collected from an animal model can be translated to humans it must: i) have similar biological dysfunction, such as the same gene mutation or anatomical abnormality as the human disorder (construct validity); ii) have sufficiently homologous symptoms with those of the human disorder (face validity); iii) and respond to the clinical treatments that prevent or reverse symptoms in the human disorder (predictive validity) (Gould and Gottesman, 2006; Willner, 1991). The inventory of model organisms compiled by the U.S. National Institute of Health (NIH) comprises thirteen different species, including the yeast *Saccharomyces cerevisiae*, the nematode worm *Caenorhabditis elegans*, the plant *Arabidopsis thaliana*, the fruit fly *Drosophila melanogaster*, the zebrafish *Danio rerio* and the mouse *Mus musculus* (NIH, 2010). In particular, animal models allow the role of susceptibility genes and environmental factors for diseases such as ASD to be characterised. In this project we have chosen zebrafish as a model organism to investigate the function of two ASD candidate genes.

1.3.1 Animal models of autism spectrum disorder

Animal models are often used to study the pathophysiology of neuropsychiatric disorders and to screen for novel treatments (Willner, 1991). Even though a single model cannot mimic all aspects of a complex disorder such as autism some underlying symptoms can be studied. Several animal models targeting different aspects of the disorder are currently available. Among these are models which harbour mutations in the major candidate loci for autism, 15q11–13 and 7q (Consortium, 2001; Cook et al., 1998; D'Arcangelo et al., 2017; Folsom and Fatemi, 2013; Piochon et al., 2014) and in important candidate genes including *NLGN3* and *NLGN4X* (El-Kordi et al., 2013; Hamilton et al., 2014; Thomas et al., 2017), *SHANK2* and *SHANK3* (Jiang and Ehlers, 2013) and *NRXN* (Born et al., 2015). Other model organisms have mutations in genes linked to syndromes that are comorbid with ASD, such as mutations in the *FRAGILE X MENTAL RETARDATION* 1 gene (*FMR1*) which lead to Fragile X syndrome (Gauducheau et al., 2017; Kaiser-McCaw et al., 1980); *METHYL CPG BINDING PROTEIN 2* gene (*MECP2)* which is involved in Rett's syndrome (Liu et al., 2016; Meloni et al., 2000); mutations in the *TSC COMPLEX SUBUNIT* genes (*TSC1* and *TSC2*) related to tuberous sclerosis (Green

et al., 1994; Tsai et al., 2012); and a mutation in the *CALCIUM CHANNEL, VOLTAGE-DEPENDENT, L TYPE, ALPHA 1C SUBUNIT* gene (*CACNA1C*) which is linked to Timothy syndrome (Gillis et al., 2011; Kabir et al., 2017). Further models are represented by animals which have an altered 5-HTergic system, either caused by the administration of chemical substances or mutagenesis of genes involved in the 5-HTergic pathway (Muller et al., 2016). Moreover, it is known that prenatal air pollution and valproate exposure could lead to epigenetic modifications which might affect brain structure and function leading to the emergence of autistic behaviours (Mabunga et al., 2015; Nicolini and Fahnestock, 2017). Therefore, many animal models of ASD are induce by valproate administration during prenatal life (Markram, 2007; Markram and Markram, 2010).

1.3.2 Zebrafish

Zebrafish have been the vertebrate model of choice in developmental biology for a long time. More recently they have also become a popular model organism for biomedical research thanks to several features (Kalueff et al., 2014; Tropepe and Sive, 2003). Among these features are some practical qualities such as their small size, short generation time and external fertilisation that together with the fact that embryos are transparent allows for *in vivo* monitoring of neural circuits during development. The zebrafish genome is fully sequenced, and more than 70% of human genes have at least one zebrafish orthologue (Howe et al., 2013). Genetic manipulation techniques have been established, and it is easy to manipulate zebrafish pharmacologically (Stewart et al., 2014). By 6 days larval fish demonstrate a range of innate behaviours including swimming continuously and searching for food. Zebrafish also exhibit elaborate social and cognitive responses which are similar to those observed in other vertebrates.

1.3.2.1 Zebrafish models of autism spectrum disorder

To understand the genetic and developmental basis of ASD, the development of reliable animal models is needed. Although it is impossible to develop an animal model that represents all the aspects of a complex brain disorder, zebrafish are a promising tool to

study candidate genes, analyse the role of specific neural pathways and screen for novel drugs (Dalla Vecchia et al., 2018; Stewart et al., 2014) through the characterisation of the behavioural phenotype of mutant lines (Mathur and Guo, 2010; Morris, 2009). The features that make zebrafish a good model for ASD are described below.

Their behavioural phenotype can resemble human behaviour:

One feature of zebrafish related to the study of ASD is the fact that zebrafish have a wide range of behavioural phenotypes that might resemble aspects of the human disorder (Kalueff et al., 2013; Kalueff et al., 2014; Stewart et al., 2014). In fact, zebrafish are highly social animals, and most of the time they shoal, staying close to conspecifics and permitting social behaviour to be quantified (Stewart et al., 2014). They are also able to perform complex behaviours such as learning and memory (Blaser and Vira, 2014). Social behaviour can be evaluated with the shoaling and social preference test whereas spatial working memory and memory performance can be accurately measured through the habituation to novelty test and using different mazes (Stewart et al., 2014). Most of these behavioural assays have been established for both larval and adult fish permitting behaviour to be studied throughout development (Ahmad et al., 2012; Kalueff et al., 2013).

It is possible to quantify altered physiological functions:

In addition to behavioural analyses, it is also possible to examine changes to neurochemistry caused by genes link to ASD. The basal levels of neurotransmitters in the brain can be measured by high precision liquid chromatography (HPLC) and the enzyme-linked immunosorbent assay (ELISA). Moreover, fast-scan cyclic voltammetry (FSCV) is an electrochemical procedure that permits the detection of neurotransmitter reuptake and release, and its use in zebrafish was recently established in our laboratory (Jones et al., 2015).

It is possible to perform pharmacological studies in zebrafish:

Zebrafish are also a valuable model system for pharmacological studies. Drug development and testing studies are easily performed at all the developmental stages. In fact, wild type zebrafish are often used for high throughput drug screening, providing

the opportunity to study the behavioural effects of compounds at early stages, mimicking the action of external factors that can act during development (Rihel et al., 2010). It is possible to test novel ASD treatment drugs by administering them to zebrafish ASD models because zebrafish are highly sensitive to all major classes of neuroactive drugs including cognitive enhancers, antipsychotics, anxiolytics, and hallucinogens (Kalueff et al., 2014; Neelkantan et al., 2013). Moreover, the zebrafish's responses to these drugs often resemble the behavioural reaction observed in rodents treated with the same compounds allowing information to be translated across species.

Their neuroanatomy is similar to mammals:

The zebrafish CNS contains all the major structures, neurotransmitters, pathways and receptors found in mammals (Mueller, 2012; Panula et al., 2010; Rink and Wullimann, 2001; Wullimann et al., 1996). One of the most striking difference is the telencephalon, which in mammals consist of a six-layered laminar structure which develops through evagination (Mueller et al., 2011; Nieuwenhuys, 1994). Due to developmental differences, the zebrafish telencephalon has a non-laminar structure which develops through eversion (Folgueira et al., 2012). This means that the forebrain has a different structure in zebrafish compared to humans. However, it does contain regions that are functionally equivalent to their mammalian counterpart. In particular, the dorsal medial pallium (DmP) has been characterised as being structurally and functionally homologous to the mammalian amygdala (Ganz et al., 2014), the dorsal lateral pallium (DlP) to the hippocampus (Salas et al., 1996), and the subpallium to the striatum (Rink and Wullimann, 2001). Furthermore, the neurotransmitter pathways which are relevant to ASD, such as DA, 5-HT, GABA and glutamate, are conserved in the zebrafish brain and have been well characterised (Panula et al., 2006).

Serotoninergic system in zebrafish

The majority of the behavioural functions of 5-HT seem to be preserved in zebrafish and drugs which act in this system have conserved effects. 5-HT is synthesized in a two-step reaction using the rate-limiting enzyme Tryptophan hydroxylase (Tph). Upon synthesis, 5-HT is transported into vesicles by the *solute carrier family 18* (*slc18*) (Ren et al., 2013; Wen et al., 2008) and then to the extracellular environment by two transport systems,

one mediated by the *serotonin transporter* (*sert*), and the other that is dependent on sodium and the *plasma membrane monoamine transporter* (*pmat*) (Duan and Wang, 2010; Norton et al., 2008). After uptake, 5-HT is metabolized to 5-hydroxyindoleacetic acid (5-HIAA) and the rate-limiting enzyme for this reaction is Monoamine oxidase (Cotzias and Dole, 1951). Due to the genome duplication events in teleost fish, many genes are duplicated in zebrafish, including 5-HT pathway components. For instance, humans have only two isoforms of *TRYPTOPHAN HYDROXYLASE*, whereas zebrafish have three isoforms of which *tryptophan hydroxylase 1* (*tph1*) is duplicated, while *tryptophan hydroxylase 2* and *3* (*tph2 and tph3*) exist in a single form (Bellipanni et al., 2002; Teraoka et al., 2004). At least sixteen 5-HT receptor subtypes have been described in mammals whereas only three have been characterized in zebrafish so far (Gaspar et al., 2003; Kriegebaum et al., 2010; Norton et al., 2008). Zebrafish appear to have only one isoform of *monoamine oxidase* (*mao*) instead of the two isoforms present in humans (Setini et al., 2005). Neuroanatomically, 5-HTergic nuclei in the zebrafish adult brain are found in the pretectal complex, the hypothalamic periventricular nuclei, the rostral and caudal raphe populations and in the area postrema (Gaspar and Lillesaar, 2012; Maximino and Herculano, 2010; Maximino et al., 2013; Panula et al., 2010). Each 5-HTergic cluster projects to specific areas of the CNS from the telencephalon and olfactory bulb to the hypothalamus, spinal cord and cerebellum (Herculano and Maximino, 2014).

Dopaminergic system in zebrafish

The zebrafish DAergic system has been extensively studied, revealing potential similarities with the human DAergic system and adding validity to the zebrafish as model for translational research (McLean and Fetcho, 2004; Panula et al., 2010; Rink and Guo, 2004; Rink and Wullimann, 2002b). The production of DA is regulated by Tyrosine hydroxylase (Th) which converts the amino acid L-tyrosine to L-3,4-dihydroxyphenylalanine (L-DOPA), the precursor of DA (Kaufman, 1995). Zebrafish possess two *th* genes, *th1* and *th2*. *th1* is more similar to the mammalian *Th* than *th2* (83.5% and 71.6% amino acid similarity with the rodent homologue *Th* at the protein level), and *th1* and *th2* share 72.9% similarity at the amino acid level (Candy and Collet, 2005). By 3 – 4 days post fertilisation (dpf) all the DAergic tracts have fully developed

(McLean and Fetcho, 2004; Rink and Wullimann, 2001) and DAergic clusters are located throughout the telencephalon and diencephalon. However, in contrast to mammals, they are not found in the mesencephalon and midbrain (substantia nigra and ventral tegmental area) (McLean and Fetcho, 2004; Panula et al., 2010; Rink and Wullimann, 2002a). Once synthesised, DA is packaged into synaptic vesicles by *slc18* and released into the synaptic cleft. In both mammals and zebrafish there are two isoforms of *slc18*, the members *a1* and *a2* (Wang et al., 2016). Once in the synapse DA binds to and activates dopamine receptors. Mammals have five dopamine receptor subtypes which are divided into two groups: the D1-like receptor (DR_1 and DR_5) which activate adenylyl cyclase and upregulates cAMP signalling, and the D2-like receptor (DR_2, DR_3 and DR_4) which inhibit adenylyl cyclase activity. In zebrafish, eight dopamine receptor subtypes have been found: *drd1*, *drd2a*, *drd2b*, *drd2c*, *drd3*, *drd4a*, *drd4b* and *drd4C*. *drd1* is considered the homologue of the mammalian D1-like receptor type, whereas all the rest belong to the mammalian D2-like receptor type (Panula et al., 2010). DA's activity is terminated by its reuptake through the *Dopamine transporter* (*Dat*); one single isoform of this gene is present in zebrafish and named *solute carrier family 6*, *member 3* (*slc6a3*) (Chen and Reith, 2000; Eriksen et al., 2010). After reuptake DA can be either recycled into synaptic vesicles by SLC18A2 or degraded by monoamine oxidase (MAO) and catechol o-methyl transferase (COMT) (Männistö and Kaakkola, 1999). The metabolism of DA in zebrafish is not thought to be dependent on the homologue of MAO, but rather on COMT, which is coded for by two genes in zebrafish (Panula et al., 2010).

GABAergic and glutamatergic system in zebrafish

In mammals, GABA, the principal inhibitory neurotransmitter of the CNS, has a prominent role in the cerebellum (Farrant and Nusser, 2005; Roberts and Kuriyama, 1968). GABA is synthesized from glutamate by two isoforms of the glutamate decarboxylase enzyme (*Gad65* and *Gad67*) (Kaufman et al., 1991; Roberts and Kuriyama, 1968). Three isoforms of *gad* enzymes have been identified in zebrafish (Delgado and Schmachtenberg, 2008; Kim et al., 2004). *gad1a* and *gad1b* are homologous to mammalian *Gad67* and *gad2* resembles GAD65. *gad2* was identified in the adult fish cerebellum (Delgado and Schmachtenberg, 2008) and *gad1b* in the

forebrain during embryonic development (MacDonald et al., 2013). Moreover, the zebrafish genome contains 22 genes encoding for $GABA_A$ receptor subunits (α1– α6b, β1– β4, γ1– γ3, δ, π, ζ, ρ1– ρ3a) and 7 subunit-like genes (α2-like, α3-like, two β2-like, π-like, ρ1-like, ρ3-like). The α1 subunit is localised within the cerebellum (Delgado and Schmachtenberg, 2008) and α1, α3, ρ1, ρ1-like, ρ2a, ρ2b in the retina (Connaughton et al., 2008). Three homologous isoforms of the $GABA_B$ receptors have also been found in the zebrafish cerebellum (Delgado and Schmachtenberg, 2008). *gabbr1a* and *gabbr1b* are homologous to the human gene coding for subunit B1 of the $GABA_B$ receptors and *gabbr2* is homologous to the B2 subunit. In conclusion, the homologues of GABA, Gad65, and the receptor subunits $GABA_{A\alpha1}$ and $GABA_{B1}$ are widely expressed in the zebrafish cerebellum with a distribution pattern which resembles the mammalian ones. In fact, GABAergic neurons are found throughout the corpus cerebelli, vestibulolateral lobe and valvula cerebelli, with a higher intensity in the molecular layer. Therefore, the expression patterns of GABAergic system genes seem to be conserved between zebrafish and mammals (Cocco et al., 2017; Delgado and Schmachtenberg, 2008).

All together, these features make zebrafish a powerful model to study the genetic, molecular, and neural basis of ASD and have led to the recent increase in using zebrafish as model organism for ASD.

1.4 Aims of this thesis

The overall objective of the studies presented in this thesis was to investigate the function of two ASD candidate genes: *reelin* (*reln*) and *ywhaz* (Lammert and Howell, 2016; Toma et al., 2014), to gain insights into the neurological basis of this disease. The experiments are organised and presented in three separate chapters, as described below:

Chapter 3

The third chapter focuses on *reelin*. Investigating one of the archetypal ASD candidate genes is an ideal opportunity to demonstrate which features might be altered in a zebrafish model of ASD. A $reln^{-/-}$ mutant line was already available in our laboratory, as part of a collaboration with Dr Filippo Del Bene at the Curie Institute, Paris. To

investigate the function of this gene, we first characterised Reln localisation within the brain and checked for the presence of potential neuroanatomical abnormalities. We then performed behavioural experiments using a platform present in our laboratory, focusing on social behaviour and cognitive deficits linked to ASD. We also investigated the possible changes to brain function which might underpin the compromised social behavioural phenotype using HPLC. Finally, we tested therapeutic agents in order to see if their administration could rescue the impaired phenotype.

Chapter 4

The fourth chapter describes the generation of a stable zebrafish *ywhaz*$^{-/-}$ mutant line using the Clustered Regularly Interspaced Short Palindromic Repeats/CRISPR associated protein-9 nuclease (CRISPR/Cas9) technique. We described step by step establishment of this line, starting with designing the synthetic guide RNA (sgRNA) to its production together with the Cas9 mRNA, and microinjection in one-cell stage embryos. This is followed by the description of the methods used to screen for positive mutants and the selection of the founder. The chapter ends with the validation of the mutant line by gene expression analysis using the reverse transcription polymerase chain reaction (RT-PCR).

Chapter 5

The fifth chapter focuses on the characterisation of *ywhaz*$^{-/-}$. As a first step towards understanding its behavioural function we first characterised *ywhaz* expression at both developmental stages and in the adult brain using *in situ* hybridization and immunochemistry. In a similar way to *reln*$^{-/-}$ we then characterised the behavioural phenotype and neurochemistry of *ywhaz*$^{-/-}$ mutants. Furthermore, using RT-PCR we analysed the expression level of genes involved in the neurotransmitter pathways which are impaired in *ywhaz*$^{-/-}$. Finally, we used this information to select and test three different drugs to verify whether they can rescue the abnormal behaviour observed in *ywhaz*$^{-/-}$.

Chapter 2 Material and Methods

2.1 Zebrafish strains, care and maintenance

Adult zebrafish (*Danio rerio*) were maintained in the Preclinical Research Facility (PRF) at the University of Leicester using standard fish-keeping protocols and in accordance with institute guidelines for animal welfare. The zebrafish were maintained in three-litre tanks, each containing 15 zebrafish. The water temperature was approximately 28°C and the light cycle was 14 h lights on (6:00–20:00), 10 h lights off. Zebrafish were fed two times a day. Embryos were obtained through natural mating and kept in an incubator at 28°C up to 5 days post fertilization (dpf), before being transferred into the system. In this thesis we refer to embryos when fish are between 0 hpf and 5 dpf, larvae when they are between 5 and 30 days old, juveniles for fish between 1 and 3 months old and adult for fish which are older than 3 months. A detailed description of the zebrafish strains used in this study can be found in Table 1.

Table 1. Description of zebrafish mutant and transgenic lines used in this study.

Wild-type, mutant and transgenic zebrafish line	Gene	Description	References
Wild-type (WT)		Wild-type AB strain zebrafish from the Zebrafish International Resource Center (ZIRC).	ZIRC
reln$^{-/-}$	*reln*	TALEN-mediated loss-of-function allele of *reelin.* The mutation introduces a STOP codon after 1689 of 3468 aa. ENSEMBL reference sequence: ENSDART00000157663.1	(Di Donato et al., 2018)
dab1a$^{-/-}$	*dab1a*	CRISPR/Cas9-mediated loss-of-function allele of *dab1a.* The mutation causes a complete change of sequence after amino acid 36 out of 537. ENSEMBL reference sequence: ENSDART00000145841.2	(Di Donato et al., 2018)
vldlr$^{-/-}$	*vldlr*	CRISPR/Cas9-mediated loss-of-function allele of *vldlr.* The mutation introduces a STOP codon after amino acid 406 out of 846. ENSEMBL reference sequence: ENSDART00000139047.1	(Di Donato et al., 2018)
ywhaz$^{-/-}$	*ywhaz*	CRISPR/Cas9-mediated loss-of-function allele of *ywhaz*. The mutation introduces a STOP codon after amino acid 126 out of 244. ENSEMBL reference sequence: ENSDARG00000032575.7	*ywhaz*$^{-/-}$ was generated as part of this PhD thesis
Tg(*olig2*:*egfp*)^{vu12}		The transgenic reporter enables labelling of Eurydendroid cells with EGFP.	(Shin et al., 2003)
Tg(*aldoca*:*gap43-Venus*)^{rk22}		A promoter fragment of the *aldoca* gene that drives expression of membrane-tagged Venus in Purkinje cells.	(Tanabe et al., 2010)

2.2 *In situ* hybridization (ISH) and Immunohistochemistry (IHC)

2.2.1 Preparation of *ywhaz* mRNA probe

2.2.1.1 Cloning and plasmid construction

Total RNA (tRNA) was extracted from whole frozen adult zebrafish brains using the TRIzol reagent and according to the manufacturer's instructions. Complementary DNA (cDNA) was synthesized from 1 μg tRNA using the RevertAid First Strand cDNA Synthesis Kit (Thermo Scientific). The *ywhaz* mRNA sequence was taken from the National Center for Biotechnology Information (NCBI) web site (NCBI Reference Sequence: NM_212757.2). Primers to amplify the open reading frame (ORF) of the gene were designed as follow: forward (Fw) primer 5'- AACCTGCTCTCTGTGGCCTA -3' and reverse (Rv) primer 5'- GCTCAGAAATGGCATCATCA -3'. The 481 bp amplicon was generated by PCR reaction, performed in a final volume of 20 μl with 1 μl of cDNA, 10 μl of ReadyMix™ Taq PCR Reaction Mix with MgCl2 (Sigma-Aldrich), 1 μl of forward primer (10 μM), 1 μl of reverse primer (10 μM) and water up to 20 μl. The thermo-cycling profile used consisted of 35 cycles with an annealing temperature of 57°C. The *ywhaz* fragment was cloned into a plasmid using the StrataClone PCR cloning Kit (Agilent) according to the manufacturer's instructions. The plasmids were collected and purified Using GeneJET Plasmid Maxiprep Kit (Thermo Scientific) and the product was sequenced by GATC Biotech to check the orientation of the insert in the plasmid and the identity of the sequence.

2.2.1.2 Plasmid linearization and *in vitro* transcription

The StrataClone PCR Cloning Vector pSCA-Amp/Kan containing the *ywhaz* insert was linearized with *NotI* restriction enzyme (5 μl of plasmid DNA, 5 μl of 10X restriction enzyme buffer, 2 μl of *NotI* restriction enzyme in a final volume of 50 μl). *ywhaz* DIG-antisense RNA probe was then generated by *in vitro* transcription (1 μg of linearized template DNA, 4 μl of 5X transcription buffer, 2 μl of 10X DIG-NTP-Mix, 1 μl of RNase inhibitor, 1 μl of T3 RNA polymerase and H_2O to make 20 μl). The product was DNase

treated and cleaned using sodium acetate/ethanol precipitation. The final *ywhaz* probe was stored at -20°C.

2.2.2 Preparation of the samples for ISH and IHC

Embryos were treated with 1-phenyl 2-thiourea (PTU) at 24 hours post fertilization (hpf) to prevent pigmentation. Embryos, larvae and dissected brains from adult fish were fixed overnight at 4°C in 4% paraformaldehyde (PFA) in phosphate-buffered saline (PBS). Specimens were then dehydrated with a gradient of methanol/PBS (25%, 50%, 75% and 100% methanol) before being stored for at least one hour and up to several months at -20°C.

2.2.3 First day of *in situ* hybridization

Samples were rehydrated with a gradient of methanol/PBS (75%, 50%, 25% and 0% methanol) and then digested with proteinase K (10 μg/ml in PBS) at room temperature (30 minutes for a whole adult brain and 9 dpf embryos, 25 minutes for 6 dpf embryos, 15 minutes for 3 dpf embryos and 10 minutes for 2 dpf embryos). Samples were then fixed in 4% PFA for 20 minutes and rinsed in phosphate-buffered saline + 0.1% Tween-20 (PBT). Samples were prehybridized at 68°C for at least 2 hours in 300 μl of HYB^+ buffer (65% formamide, 5X saline-sodium citrate (SSC) buffer, 50 μg/ml heparin, 0.5 mg/ml torula RNA, 0.1% Tween-20, 9.2 mM citric acid, pH 6.0). HYB^+ was then replaced with fresh HYB^+ containing the DIG-labelled probe (at a concentration of 5 ng/μl) and incubated overnight at 68°C.

2.2.4 Second day of *in situ* hybridization

The HYB^+/probe mix was removed and stored at -20°C for future use. Samples were washed with a gradient of HYB^+/2X SSC (75%, 50%, 25% and 0% HYB) for 10 minutes each, and then twice with 0.05X SSC for 30 minutes each. For ISH on sections, adult brains were fixed for 20 min with 4% PFA and embedded in 3% agarose dissolved in

water. Samples were sectioned at 100 μm using a vibratome and sections were collected in PBS. Specimens were blocked for 1 hour at room-temperature (RT) in blocking solution (2% normal goat serum, 2 mg/ml bovine serum albumin in PBT) and then incubated overnight with anti-DIG-AP antibody (1:4000 dilution in blocking solution).

2.2.5 Third day of *in situ* hybridization

Samples were washed several times in PBT and then three times for 10 minutes each in Xpho solution (100 mM Tris-HCl pH 9.5, 50 mM $MgCl_2$, 100 mM NaCl and 0.1% Tween-20). Xpho solution was replaced with NBT/BCIP solution (225 μg/ml of NBT and 175 μg/ml of BCIP in Xpho) and the specimens were incubated in the dark to develop the stain. Samples were monitored with a dissecting microscope every 30 minutes. The reaction was stopped by several washes in PBS and were fixed in 4% PFA for 20 minutes. Embryos were stored in 80% glycerol and 20% PBT at 4°C, whereas sections were mounted on slides and covered with Mowiol solution. The NBT/BCIP signal was imaged using a GX microscope, a CMEX 5.0 camera and Image focus 4 software.

2.2.6 Immunohistochemistry

The primary and secondary antibodies used for the IHC and their concentrations are reported in Table 2. Adult brains were rehydrated with a gradient of methanol/PBS (75%, 50%, 25% and 0% methanol) and then digested with proteinase K (10 μg/ml in PBS) at room temperature for 30 minutes followed by post-fixation in 4% PFA for 20 minutes. Samples were then rinsed in PBT. Specimens were embedded in 3% agarose dissolved in water and sectioned at 100 μm using a vibratome. Sections from *Tg*(*olig2*:*egfp*)^{vu12} were blocked for 1 hour at RT with blocking solution and then incubated overnight in primary antibody. The day after, samples were washed several times in PBT, blocked with blocking solution for an hour at RT and incubated in secondary antibody diluted in blocking solution for 1 hour at RT. For *reln*$^{-/-}$, *ywhaz*$^{-/-}$ and *Tg*(*aldoca*:*gap43-Venus*)^{rk22} the Vectastain universal *Elite* ABC Kit (Vector, #PK-6200) was used. Therefore, the sections were blocked for 1 hour at RT with the blocking serum.

The blocking serum consists of 1:10 normal horse serum in blocking diluent, which is 1% bovine serum albumin (BSA) in PBT. The specimens were then exposed overnight to primary antibody, followed by 1 hour incubation in secondary antibody, and 3 hours' incubation with Vectastain *Elite* ABC Reagent solution. After several washes in PBT, peroxidase activity was detected using 3,3'-Diaminobenzidine (DAB, Sigma, #D4293) according to the manufacturer's instruction. For double *in situ* hybridization/antibody labelling, the ISH was performed first (with NBT/BCIP staining) followed by the IHC (with DAB staining).

Table 2. Antibodies used in the IHC.

Primary antibody	Secondary antibody	Genotype
Anti-Reelin (Millipore, #MAB5366) Dilution 1:500	Biotinylated Universal Antibody anti mouse and rabbit IgG (H+L) (Vectastain universal *Elite* ABC Kit, Vector)	*reln*$^{-/-}$
Anti-GFP (Amsbio, #TP401) Dilution 1:500	Peroxidase Anti-Rabbit IgG (H+L) (Vector, #PI-1000) Dilution 1:1000	*Tg*(*olig2*:*egfp*)^{vu12}
Anti-Parvalbumin antibody (Millipore, #MAB1572) Dilution 1:1000	Biotinylated Universal Antibody anti mouse and rabbit IgG (H+L) (Vectastain universal *Elite* ABC Kit, Vector)	*ywhaz*$^{-/-}$
Anti-GFP (Amsbio, #TP401) Dilution 1:500	Biotinylated Universal Antibody anti mouse and rabbit IgG (H+L) (Vectastain universal *Elite* ABC Kit, Vector)	*Tg*(*aldoca*:*gap43-Venus*)^{rk22}

2.2.7 Nissl Staining

For Nissl staining brains were prepared as described in paragraph 2.2.2. They were then rehydrated in a gradient of methanol/PBS (75%, 50%, 25% and 0% methanol) and were cut into 100 μm sections with a vibratome (see paragraph 2.2.4). The sections were stained for 3 minutes with cresyl violet solution (0.1% cresyl violet acetate and 0.25%

acetic acid in H_2O). The staining was stopped by washing with PFA and the slides were mounted on slides and covered with Mowiol solution. The Nissl staining was photographed using a GX microscope, a CMEX 5.0 camera and Image focus 4 software. Comparable areas were defined in every section for both WT and *reln*$^{-/-}$, and the cells within the selected areas were counted using the "Manual Cell Counting and Marking" function of ImageJ software based upon computational approaches (Cristino et al., 2014; Mitchell, 2011).

2.3 Behavioural methods

Unless specified, behavioural analyses were performed on 3- to 5-month-old adult zebrafish of both sexes. After being genotyped, all fish were maintained in groups of 15, by genotype, until the day of testing. Behavioural experiments were recorded using FlyCapture2 2.5.2.3 software and a digital camera from Point Grey Research. The same room was always used for experiments, with constant illumination and temperature. All behavioural experiments were completed between 10:00 and 17:00. Fish were transported to the testing room in holding tanks on the same day as analysis. The fish were left for 30 minutes to habituate to the testing room. The age, sex, and size were carefully matched between fish of different genotypes.

2.3.1 Visually-mediated social preference test (VMSP)

The experiment was performed in a transparent rectangular tank composed of five chambers. One central chamber (19 × 13 cm) was surrounded by four identical chambers (9.5 × 6.5 cm). The transparent walls dividing the chambers contained perforated holes, so that the fish were separated physically but were able to see and smell each other. A group of three unfamiliar "stranger" zebrafish was placed in the top left chamber. The test fish was placed in the central chamber and its behaviour was recorded for five minutes from above. In a second step, another group of three unfamiliar zebrafish were placed in the right bottom chamber and the test zebrafish was recorded for five more minutes. In order to measure the interactions with conspecifics, the videos were then

analysed with Noldus Ethovision XT software quantifying time spent in different zones of the tank or the time spent freezing. The same procedure was used to test juvenile fish using a similar tank which had a 1:3 reduction in size.

2.3.2 Shoaling test

The shoaling experiment was performed following the protocol from Parker et al., 2013. Group of five fish (familiar individuals with a mix of males and females) were placed in a large open tank (20.5 × 29 × 19 cm). The fish were left to acclimatise for 5 minutes and then filmed from above for 10 minutes. Using software from ViewPoint Life Sciences it was possible to measure the nearest neighbour distance (NDD: the distance between each individual and its closest neighbour) and the inter-individual distance (IID: the mean distance from each individual to all other fish). Replaying the films it was possible to calculate the cluster score: virtually dividing the tank into eight equal sections and counting the maximum number of fish in one section divided by the total number of sections occupied by the fish every 30 seconds (Parker et al., 2013). The same procedure was used to test juvenile fish using a similar tank which had a 1:3 reduction in size.

2.3.3 Anxiety-like behaviour and exploratory activity

2.3.3.1 Novel tank test (NTT)

The NTT was performed in a standard 1.5 L trapezoid tank (Egan et al., 2009) where the fish were placed and recorded for 5 minutes. Noldus Ethovision XT software was used to measure the amount of time spent in the bottom (geotaxis) and top third of the tank, time spent freezing, the total distance swum, velocity and the absolute angular velocity.

2.3.3.2 Open field test

The open field test was performed in a large open tank (20.5 × 29 × 19 cm) where the fish were recorded from above for 5 minutes. To quantify the duration of thigmotaxis (time spent swimming at a distance of 2 cm or less from the walls), the time spent in the

periphery and in the center, the time spent freezing, the distance swum and the velocity the films were analysed using Noldus Ethovision XT software.

2.3.4 Aggression test

Aggression was measured using the mirror-induced stimulation protocol (Norton et al., 2011). The setup consists of a glass aquarium (15 × 10 × 30 cm) with both the long sides and one short side covered with a white opaque material. A mirror was placed outside of the clear fourth side of the tank offset at an angle of 22.5° (Gerlai et al., 2000). To habituate the fish to the setup, they were placed in holding tanks with walls covered in white paper on the night before the experiment. Single fish were recorded for 5 minutes. The time spent in agonistic interaction was manually quantified using LabWatcher software from ViewPoint Life Sciences. To avoid observer bias, manual quantification was performed by an independent researcher unaware of the genotype being analysed.

2.4 High precision liquid chromatography (HPLC) analysis of monoamines and metabolites

2.4.1 Preparation of the samples

Fish were decapitated and their brains were dissected and divided into four areas: telencephalon (Tel), diencephalon (DI), optic tectum (TeO) and hindbrain (Hb), under a dissecting microscope. Samples were weighed, homogenised in 100 μl ice-cold 0.1 N perchloric acid using a pellet pestle (Sigma, #Z359971) and centrifuged at 12,000 rcf for 15 min at 4°C. The supernatant was collected and stored at -80°C until use.

2.4.2 HPLC settings

HPLC analysis for dopamine (DA), serotonin (5-HT), 3,4-dihydroxyphenylacetic acid (DOPAC), homovanillic acid (HVA) and 5-hydroxyindoleacetic acid (5-HIAA) was carried out using electrochemical detection as described by (Young, 2004). Samples (15 μl) were injected using a Spark Triathlon refrigerated autosampler and separation was achieved

on a Luna C18(2), 5 μm, 100 Å, 100 x 1 mm (Phenomenex Ltd) reverse phase column. The mobile phase (75 mM sodium dihydrogen phosphate, 1 mM EDTA, 0.6 mM octane sulphonic acid (OSA) in deionised water containing 5% methanol, pH 3.7) was delivered by a Rheos 4000 pump (Presearch, UK). Electrochemical detection was performed using a glass carbon working electrode set at 700 mV relative to an Ag/AgCl reference electrode, using an Antec Intro detectorincorporating a low volume (VT-03) flow cell (Antec, Netherlands).

2.4.3 Analysis of the data

Samples were quantified by comparison with standard solutions of known concentrations of monoamines and metabolites using Chrom Perfect data analysis software (Justice Laboratories, NJ). Each sample was run in duplicate and the mean content of monoamine and neurotransmitter for sample was calculated and normalised to the weight of tissue. The results are expressed as picomoles per milligram of brain tissue.

2.5 Drug treatments

Treatment duration and concentrations were chosen according to published studies and pilot experiments in our lab. Table 3 summarizes the pharmacological treatments performed in this project.

Table 3. Pharmacological treatments performed in this study.

Drug	Concentration	Diluted in	Method of administration	Duration of the treatment	Supplied by
Buspirone	10 mg/L	H_2O	Immersion	1 hour	Tocris #0962
Oxytocin	10 ng/kg	Saline 0.9%	Injection	30 minutes	Sigma #O3251
Risperidone	170 μg/L	DMSO	Immersion	15 minutes	Tocris #2865
Fluoxetine	5 mg/L	DMSO	Immersion	2 hours	Tocris #0927
Quinpirole	0.25 mg/L	H_2O	Immersion	1 hour	Tocris #1061

2.6 Gene expression analysis

2.6.1 RNA extraction

Total RNA was extracted from the whole brain using the GenElute™ Mammalian Total RNA Miniprep Kit (Sigma-Aldrich) following the manufacturer's instructions. The samples were DNase treated with TURBO™ DNase (ThermoFisher Scientific) to remove any genomic DNA contamination. The concentration and quality of RNA was determined using a NanoDrop 2000 spectrophotometer (LabTech International). 2 μl of tRNA was run on a 1.5% (w/v) agarose gel to check for degradation.

2.6.2 First strand cDNA synthesis

First strand cDNA was synthesised from 0.25 μg of tRNA using the RevertAid First Strand cDNA Synthesis Kit (ThermoFisher Scientific) following the manufacturer's instructions. Both oligo dT and random primers were used in a 20 μl reaction. The reaction was then diluted 1:2 dilution in H_20 prior to use in the PCR reaction.

2.6.3 Reverse-transcription quantitative PCR (RT-qPCR)

RT-qPCR was performed on 8 brains per genotype with three replicates for each brain using a CFX Connect™ Real-Time System machine (BioRad Laboratories) and the SensiFAST™ SYBR No-ROX Mix (Bioline). The RT-qPCR mixture consisted of 10 μL SYBR, 250 nM of Fw and Rv primers (Table 4) and 1 μl diluted cDNA in a total volume of 20 μL. The RT-qPCR cycling conditions were: 95°C for 3 min followed by 40 cycles of 95°C for 30 s, 60°C for 30 s, and 72°C for 30 s.

Table 4. Primers used for RT-qPCR analysis (purchased from Sigma).

Target Gene	GenBank accession no.	Fw primer (5'-3')	Rv primer (5'-3')	bp	References
tyrosine hydroxylase (th)	AF075384	AATCCACCATCTTGAAACC	TGCTAACATCCGACAGG	101	(Filby et al., 2010)
tyrosine hydroxylase 2 (th2)	NM_001001829	AGCAAAACGGAGCAGTAAAGG	CTCATTAGAAAGGGCATACAACAG	80	(Filby et al., 2010)
tryptophan hydroxylase 1a (tph1a)	AF548566	CAGTTCAGTCAGGAGATTGG	GACAGTGCGTGCTTCAG	176	(Filby et al., 2010)
tryptophan hydroxylase 1b (tph1b)	NM_001001843	TTATATTATTATCTGCCTTGTCTG	AGTGCTCTGTGGTATTTGG	106	(Filby et al., 2010)
tryptophan hydroxylase 2 (tph2)	NM_214795	CAAGAGACAACAGCAACTATG	AAGCCCAACAGGTGATTTAG	84	(Filby et al., 2010)
dopamine receptor 1 (*drd1*)	NM_001135976	AAGCCCGTTTCGCTATGAG	GCACAGGGATGAAGGAGATAAG	101	(Bertotto et al., 2018)
dopamine receptor 2a (*drd2a*)	NM_183068	TGCGAATCCTGCCTTTGT	TTCCGGAGTACCACGTAGAT	102	(Bertotto et al., 2018)
dopamine receptor 2b (*drd2b*)	NM_197936	GGTTCTACGCAAGCGGCGGA	GGCAGGTACACCCCCGTTGG	154	(Puttonen et al., 2018)
dopamine receptor 4 (*drd4*)	NM_001012620	GGCCTTGATCACCGCCACCT	GGTTCCTGTTCGGCACCTGGTT	86	(Puttonen et al., 2018)
ywhaz	NM_212757	GAGTACCGTGAGAAGATCGAAGC	CGGATCAGAAACTTGTCCAGCAG	80	Dr Norton's lab
ywhae	NM_212605	AAGAAAGCTACAAGGACTCGACG	TCTTGCAGCGCCTCTTTATTCTG	115	Dr Norton's lab
solute carrier family 6 (neurotransmitter transporter), member 3 (*slc6a3*)	NM_131755	AGACATCTGGGAAGGTGGTG	ACCTGAGCATCATACAGGCG	151	(Barreto-Valer et al., 2012)

2.6.4 RT-qPCR efficiency

A melting curve step (50–95°C) was performed to verify that only single products had been amplified. No-template and no-reverse transcriptase controls were also performed for each primer pair and cDNA, respectively. To assess RT-qPCR efficiency, a 2-fold dilution series of cDNA template were processed. Their threshold cycle (Ct) values were plotted on a logarithmic scale along with corresponding concentrations to generate a linear regression curve through the data points. The value of the slope of the trend line represented the efficiency of the RT-qPCR.

2.6.5 Data analysis

Results were normalised to the expression level of one of these two housekeeping genes: the ribosomal protein L13a (*rpl13*) and the elongation factor 1a (*elf1a*). The relative expression of the genes and the fold change were calculated using the 2^{-ddCT} comparative method (Livak and Schmittgen, 2001; Schmittgen and Livak, 2008). The dCT value for each sample was calculated by subtracting the cycle time (CT) value of the gene of interest (GOI), the CT value of the reference (REF) gene: [dCT (sample) = $CT_{(sample\ GOI)} - CT_{(sample\ REF)}$]. This was also determined for the control sample (calibrator): [dCT (calibrator) = $CT_{(calibrator\ GOI)} - CT_{(calibrator\ REF)}$]. The ddCT value for each sample was then determined by subtracting the dCT value of the calibrator from the dCT value of the sample: [ddCT = dCT (sample) – dCT (calibrator)]. The fold change of the normalized level of GOI expression was calculated by using the formula: 2^{-ddCT}.

Chapter 3 REELIN

3.1 Introduction

3.1.1 The structure of REELIN

The reeling gait of spontaneous Edinburgh *reeler* mutant mice was first described by Falconer in 1951. The mutant brains also exhibited hypoplasia of the cerebellum, which causes a peculiar neurological phenotype characterised by ataxia and dysregulation of motor coordination (Falconer, 1951). Finally, more than forty years later, the gene responsible for the *reeler* phenotype was identified and named *Reelin* (*Reln*) (Bar et al., 1995; D'Arcangelo et al., 1995; Hirotsune et al., 1995; Ogawa et al., 1995). RELN is a large 3460 amino acid (aa) secreted glycoprotein that can be divided into three regions. At the N-terminal region, there is a signal peptide (S) and a 200 aa F-spondin-like domain (SL) which is followed by a region of about 400 aa which does not have sequence similarity to any previously characterized proteins. This region is followed by an eightfold series of tandem repeats, named reelin repeats (R). Each reelin repeat domain is further divided in two subrepeat domains (A and B) linked by an EGF-like domain. *RELN* ends with a carboxy-terminal region (CTR; Figure 1) (Arcangelo et al., 1995; DeSilva et al., 1997; Ichihara et al., 2001; Lee and D'Arcangelo, 2016). Functionally, the subrepeat domain 6A binds to the canonical Reelin receptors apolipoprotein E receptor 2 (ApoER2) and the very low-density lipoprotein receptor (VLDLR), whereas the CTR is necessary for efficient phosphorylation of the intracellular adaptor protein Disabled-1 (Dab1) *in vitro* (Yasui et al., 2010). After secretion, RELN protein is cleaved by metalloproteases to generate three fragments: an N-terminal (Nt), a central (C) and a C-terminal (Ct) fragment. Even though the C fragment alone is able to activate intracellular signalling, the full-length protein is more potent. This means that RELN processing downregulates the activity of the full-length protein (Jossin, 2004; Lee and D'Arcangelo, 2016; Yasui et al., 2007).

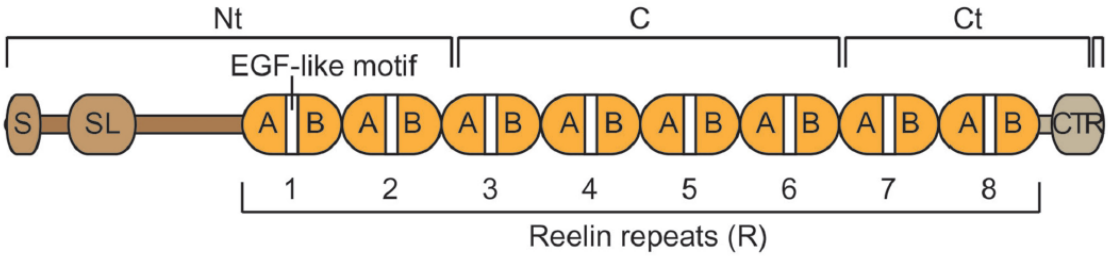

Figure 1. REELIN structure and its cleavage fragments. At the N-terminal RELN consists of a signal peptide (S), an F-spondin-like domain (SL). This region is followed by eight consecutive reelin repeats (R) each divided into two subdomains (A and B) which are connected by an epidermal growth factor (EGF) like motif. RELN ends with a positively charged carboxy-terminal region (CTR). After secretion, full-length RELN is subjected to cleavage which produces three fragments: the N-terminal (Nt), the central (C) and the C-terminal (Ct) fragment. Adapted from Lee, 2016.

3.1.2 REELIN function

RELN is mainly expressed in the brain where it plays critical roles in both the positioning of neurons during neurodevelopment and in the regulation of postnatal synaptic function. Little is known about the roles of RELN in the periphery. In mammals, Reln is mostly secreted by Cajal-Retzius (CR) cells in the marginal zone of the cerebral cortex which coordinates the arrangement of postmitotic cortical neurons in a 6-layer structure (O'Dell et al., 2012). The mammalian neocortex has a laminar structure that develops in an inside-out manner in which late-born neurons are placed more superficially than earlier-born neurons, following a birth-date-dependent pattern (Bock and May, 2016; Sekine et al., 2012). The migration of new born neurons from germinal zones to specific layers of the cerebral cortex is a critical step during neuronal development. In mammals, the Cajal-Retzius cells form the most superficial layer of the cerebral cortex (layer 1), whereas cells of the cortical plate generate layers 2 to 6, producing the inside-out arrangement. Specifically, neurons born in the ventricular zone migrate to their final sites in one of the six layers of the cortex. This process is mediated by Reln, which is secreted by Cajal-Retzius cells in layer 1 (light blue cells in Figure 2) and promotes the migration of postmitotic cells along the radial glial cells to form the cortical plate and subplate (orange and yellow cells respectively in Figure 2). As more cells arrive, the cortical plate creates an organized set of layers (2 to 6) where the later cells migrate along the radial system (Figure 2) (Hatten, 2002; Meyer, 2007).

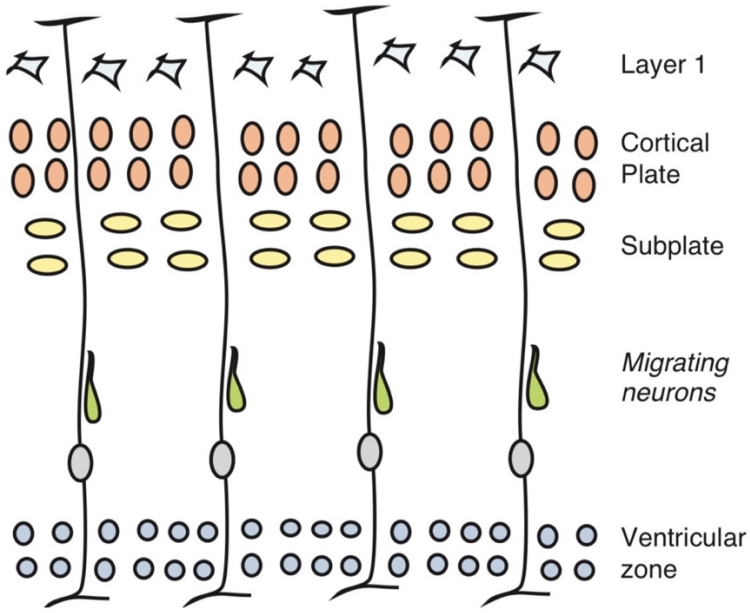

Figure 2. Formation of the layered cerebral cortex. The ventricular zone generates neurons destined to migrate along the radial glial system to specific layers in the cortex. The very first generated cells migrate to the most superficial layer (layer 1, Cajal-Retzius cells, light blue), which afterwards secrete RELN. Thereafter, new-born cells migrate and form the cortical plate (orange) and subplate (yellow) via the RELN pathway. In a second step, as more cells arrive, cortical plate neurons continue the migration generating a set of layers (2 to 6) according to an inside-outside gradient. Figure adapted from Mary E. Hatten, 2002.

In the *reeler* mouse the new born cells fail to migrate and form the cortical plate and its layered structure, causing an inversion of the cortical layering (Figure 3) (Goffinet, 1983; Miyata et al., 1997).

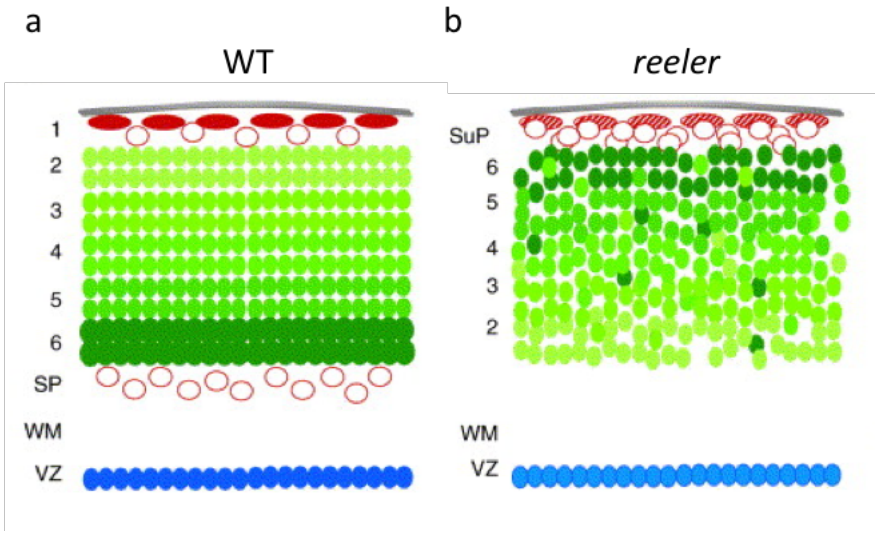

Figure 3. Structure of mammalian neocortex in WT and *reeler*. a) WT neocortex comprises six cellular layers. Layer 1 is the most superficial layer and it is constituted of Cajal-Retzius cells which secrete RELN (red). Layers 2 to 6 form the cortical plate (green) which sits above the subplate (SP). A band of white matter (WM) is present right below the SP and beneath it is the ventricular zone which generates neurons (blue). **b)** Analysis of *reeler* mouse cortex shows that Cajal-Retzius cells do not express RELN. Therefore, the cortical plate (green) develops underneath the subplate (named now as superplate [SuP]), causing an inversion of the cortical layering in the cortical plate. Figure adapted from Olson and Walsh, 2002.

RELN regulates radial neuronal migration not only in the cerebral cortex but also in other laminated brain structures such as the cerebellum and hippocampus (D'Arcangelo, 2014). In fact, the *reeler* mouse not only has disorganized cortical layering, but also displays cerebellar hypoplasia, a condition characterized by cerebellar underdevelopment with a decreased number of cells, which likely is caused by the failure of Purkinje neurons to form a cellular layer (Goffinet, 1983; Miyata et al., 1997). Parallel abnormalities have been identified in human patients, where homozygous null mutations in *RELN* lead to lissencephaly (smooth brain) with cerebellar hypoplasia (LCH) (Hong et al., 2000). After birth CRs degenerate, and in the adult brain Reln is preferentially expressed in glutamatergic granule cells of the cerebellum, whereas in the cortex and hippocampus it is almost exclusively expressed in γ-aminobutyric acid (GABA)ergic neurons (Pesold et al., 1998). In addition to its prenatal roles, RELN modulates the formation and function of synaptic circuits promoting the maturation of dendrites, synaptogenesis, synaptic transmission, plasticity and neurotransmitter release (D'Arcangelo, 2005; Förster et al., 2010; Herz and Chen, 2006; Levenson et al., 2008; Levy et al., 2014). The cellular and molecular mechanisms underlying RELN's role during and after brain development are mediated by a molecular signalling pathway. The signalling mechanism is activated by the binding of Reln to its cell surface receptors

apolipoprotein E receptor-2 (Apoer2) and very low density-lipoprotein receptor (Vldlr). Src/Fyn kinases and the adaptor protein Dab1 are part of this core signalling machinery as well. RELN signalling in turn modulates the activity of adaptor proteins and downstream protein kinase cascades, regulating several aspects of brain development and synaptic function (Bock and May, 2016; Lee and D'Arcangelo, 2016).

3.1.2.1 REELIN signalling transduction

3.1.2.1.1 REELIN receptors: VLDLR and ApoER2

The two high-affinity RELN receptors are members of the low-density lipoprotein receptor (LDLR) family which is involved in lipoprotein trafficking. LDLR is a family of transmembrane glycoproteins that share common structural motifs: an extracellular domain necessary to bind the ligands, a single transmembrane domain and a cytoplasmic tail that transduces signals and harbours an NPxY motif allowing internalization of the binding protein (Figure 4) (Go and Mani, 2012). Among all the family members, it has been shown that VLDLR and ApoER2 have an important role in embryonic development (Howell and Herz, 2001). In fact, double *Apoer2/Vldlr* knock-out mice display a *reeler*-like neuroanatomical phenotype (Trommsdorff et al., 1999). ApoER2 and VLDLR play distinct roles in neuronal migration due to their different expression pattern. ApoER2 is mostly expressed in hippocampal and cortical neurons, and single *Apoer2* knock-out mice show defects in forebrain structures. VLDLR is mainly expressed in the Purkinje cells of the cerebellum, correlating with defects in this structure in single VLDLR knock-out mice (Trommsdorff et al., 1999).

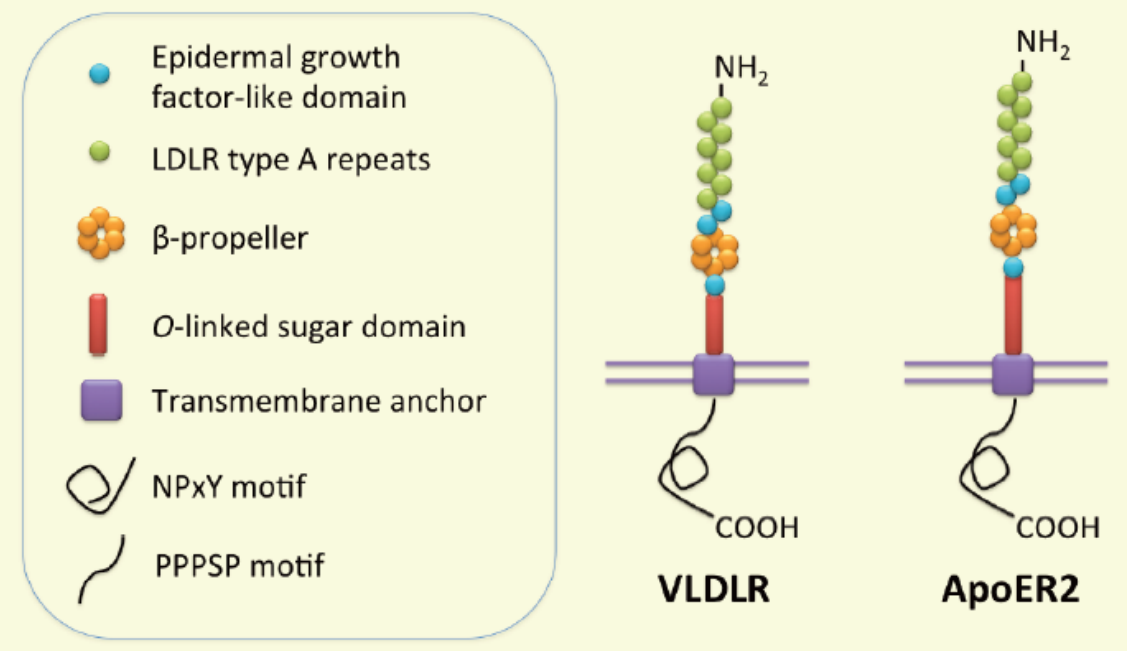

Figure 4. Schematic structure of VLDLR and ApoER2. As members of the LDLR family, both proteins share common structural motifs: LDLR type A repeats which are essential for ligand binding, an epidermal growth factor (EGF)-like domain, transmembrane anchor, and a cytoplasmic domain that includes the NPxY motif, which mediates clustering of the receptors. Adapted from Go and Mani, 2012.

3.1.2.1.2 The canonical REELIN signalling cascade and the involvement of Dab1

Upon binding, VLDLR and ApoER2 internalize RELN, a process that requires the NPxY motif. As a result, Dab1 binds to the cytoplasmic tail of these receptors near the internalization domain (Howell et al., 1999) leading to the activation of downstream signalling molecules crucial for migration. The mammalian homolog of *Drosophila* dab1 was the first essential transducer of the Reln signalling pathway to be identified, when Sheldon and colleagues demonstrated that *scrambler* and *yotari*, two mouse mutants for Dab1, show a similar phenotype as the *reeler* mutant (Sheldon et al., 1997). Dab1 is an intracellular adaptor protein that, when phosphorylated on tyrosine residues, can interact with the Src-homology (SH2) domains of Src-family kinases (SFKs) (Howell, 1997). This adaptor protein also contains a phosphotyrosine binding (PTB) domain which allows Dab1 to bind receptor internalization domains and phosphoinosites (Homayouni et al., 1999; Howell et al., 1999; Stolt et al., 2003). Dab1 localisation is almost complementary with RELN's, being present at high levels in the Purkinje cells of the cerebellum and in the neurons of the embryonic cerebral cortex and hippocampus

(Meyer et al., 2003; Rice et al., 1998). When the receptors bind RELN, they initiate a phosphorylation cascade starting with Dab1 being phosphorylated on tyrosine residues by Fyn and Src kinases, and thus activating downstream signalling events crucial for i) neuronal migration and lamination, ii) dendrite and spine development and iii) synaptic function (Figure 5) (Arnaud et al., 2003; Bock and Herz, 2003; Howell et al., 1997; Howell et al., 1999; Rice et al., 1998). Dab1 tyrosine phosphorylation also leads to ubiquitination by the E3 ubiquitin ligase component Cullin 5, and therefore to its degradation by the proteasome system, ensuring that the signal is transitory (Feng et al., 2007). In the following paragraphs the main downstream mechanisms associated with the canonical Reln signalling cascade via ApoER2/Vldlr and Dab1 will be described.

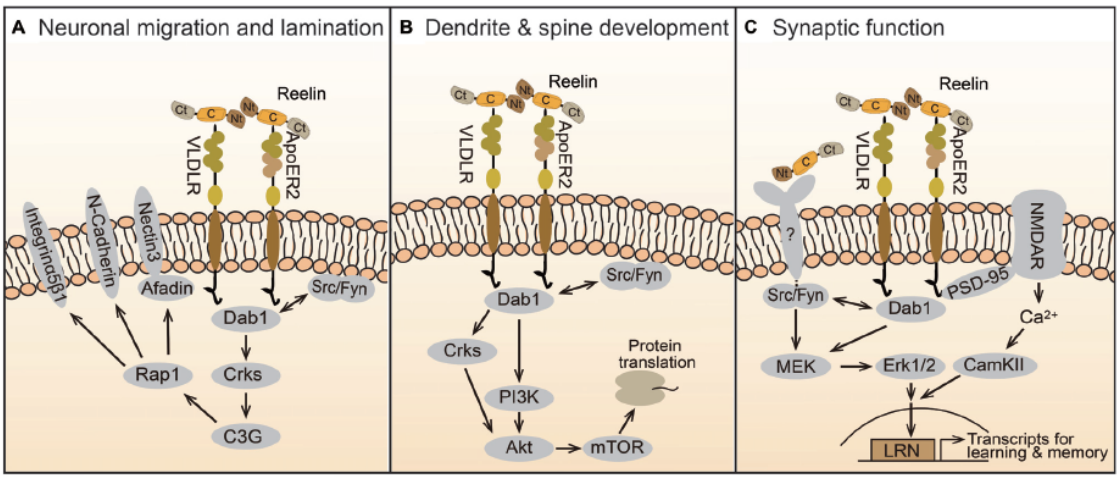

Figure 5. Reelin core signalling transduction. Upon binding to its receptors ApoER2 and VLDLR, the Reln central domain is internalized and its signal is transduced by the activation of Src/Fyn kinases that phosphorylate the adaptor protein Dab1. Downstream of this canonical pathway, different signalling pathways regulate distinct biologic activities prenatally and postnatally. **(a)** At developmental stages, RELN is involved in neuronal migration and cortical layer formation through the Crk/C3G/Rap1 pathway. **(b)** Early postnatally, RELN regulates protein translation, dendrite outgrowth and spine development through the Crk adaptor proteins and the PI3K-Akt-mTOR pathway. **(c)** Postnatally RELN affects synaptic function and plasticity through the expression of immediate-early genes involved in learning and memory. This activity is mediated by ApoER2, through the NMDAR/PSD-95/CamKII pathway and by an unknown receptor which activates the MEK-Erk1/2 pathway by Src/Fyn kinases. Adapted from Lee and D'Arcangelo, 2016.

3.1.2.1.3 REELIN signalling transduction in the control of neuronal migration

Dab1 is necessary for glia-independent somal translocation in radially migrating neurons, but not for glia-guided locomotion (Franco et al., 2011). The molecular

mechanism of translocation starts with phosphorylated Dab1 which recruits Crk adaptor proteins, causing the activation of the GTP exchange factor (GEF) C3G and leading to the activation of repression and activation protein (Rap1) GTPase (Brunne et al., 2013; Jossin and Cooper, 2011). Dab1 ultimately regulates cortical lamination via the Crk/C3G/Rap1 pathway since when activated Rap1 acts on adhesion molecules including N-Cadherin, nectins and integrin$\alpha 5\beta 1$ enabling terminal neuronal translocation and inside-out layer formation (Gil-Sanz et al., 2013) (Figure 5a).

3.1.2.1.4 REELIN signalling transduction in the control of dendrite and spine development

The canonical RELN pathway (ApoER2/VLDLR, Dab1, SFKs and Crks) also controls dendrite and spine development. The precise mechanisms underlying these actions are still unclear, but it is known that Phosphoinositide 3-kinase (PI3K) and Protein Kinase B (Akt) are involved in this process downstream of Dab1 (Figure 5b). In fact, upon Reln binding, Dab1 activates P13K through direct binding at its regulatory subunit p85α, regulating phosphorylation of Akt and inhibiting glycogen synthase kinases 3β (GSK3β) (Bock and Herz, 2003). Downstream of Akt, mTOR and proteins such as p70S6K and ribosomal protein S6 are activated and mediate the effects of RELN upon dendritic growth (Jossin and Goffinet, 2007).

3.1.2.1.5 REELIN signalling transduction in the modulation of synaptic function

In the adult brain RELN modulates synaptic function and plasticity through both canonical and non-canonical signalling pathways. The non-canonical signalling pathway does not require ApoER2 and VLDLR. Rather, it involves the full-length form of Reln which is able to activate the MEK-Erk1/2 signalling pathway through an unknown receptor leading to synaptic immediate-early gene (IEGs) expression, and thus affecting synaptic function (Lee et al., 2014). Through the canonical signalling pathway, RELN intensifies long-term potentiation (LTP) in the hippocampus, a cellular mechanism underlying memory and learning. This effect depends upon the presence of VLDLR and

a specific splice variant of ApoER2 (Beffert et al., 2005; Weeber et al., 2002). ApoER2 is located at the postsynaptic densities of excitatory synapses and an alternatively spliced variant of exon 19 interacts with N-methyl-D-aspartate (NMDA) receptors through the postsynaptic density protein 95 (PSD-95). This complex mediates RELN–induced calcium (Ca^{2+}) entry (Beffert et al., 2005; Chen, 2005)(Figure 5c). The increase of intracellular Ca^{2+} concentrations in the postsynaptic neuron activates Ca^{2+}/calmodulin-dependent protein kinase II (CamKII), generating a series of downstream signals that enhance the expression of genes involved in dendrite development and neurite outgrowth, and that can also induce long-term changes in synaptic strength (Chen, 2005). For example, the transcription factor cAMP response element-binding protein (CREB) is part of this cascade. Therefore, RELN function is crucial for controlling Ca^{2+} influx during synaptic signal transmission, regulating synaptic strength and ensuring correct learning and memory (Chen, 2005). Recently, it has been shown that Dab1 is also required for the Reln-induced enhancement of hippocampal LTP and is a critical regulator for hippocampal-dependent behavioural tasks such as associative and spatial learning (Trotter et al., 2013). Together, these signalling pathways regulate postnatal synaptic plasticity and activity by inducing the immediate-early genes which are involved in learning and memory.

In conclusion, RELN is a multifunctional extracellular glycoprotein that is essential for correct neuronal positioning during brain development and for synaptic plasticity in the adult brain. Its core signalling machinery includes ApoER2/VLDLR receptors, Src/Fyn kinases and Dab1. Specific downstream mechanisms control distinct functions such as neuronal migration and lamination through the CrK/Rap1 pathway, and dendrite and spine development via the P13K/Akt/mTOR pathway. Activity at NMDA receptors and the MEK/Erk1/2 pathway enhance the expression of genes important for synaptic plasticity and learning.

3.1.3 REELIN and neuropsychiatric disorders

At embryonic stages, RELN is involved in neuronal migration and cortical formation, vital processes required for higher brain function in mammals. In adulthood RELN is a key

regulator of synaptic plasticity which is strongly related to cognitive function. Therefore, abnormal RELN expression has been thought to impair cortical development and synaptic function, leading to cognitive deficits which are one of the main hallmarks of neuropsychiatric disorders (NPD). This theory is further supported by genetic studies, which have demonstrated that the RELN locus is associated with several neuropsychiatric disorders without gross malformations in brain structure such as autism spectrum disorder (ASD) (Wang et al., 2014c), schizophrenia (SZ) (Li et al., 2015; Ovadia and Shifman, 2011), Alzheimer's disease (AD) (Bufill et al., 2013) and bipolar disorder (BP) (Ovadia and Shifman, 2011). The idea that a decreased level of RELN leads to impaired brain function linked to NPD in humans is also supported by animal studies. For example, both homozygous and heterozygous *reeler* mice (HRM) exhibit behavioural and cognitive defects (Costa, 2002; Qiu et al., 2006; Tueting et al., 1999). The specific *Reln* haploinsufficiency in HRM shows defects in sensory motor gating with impaired prepulse inhibition (PPI), a phenotype which is usually associated with SZ (Barr et al., 2008; Kutiyanawalla et al., 2011; Teixeira et al., 2011; Tueting et al., 1999). HRM also exhibit dendritic spine density and defects in the prefrontal cortex LTP (Iafrati et al., 2013), and they show learning deficits related to the hippocampus including an impairment in hippocampal plasticity (Qiu et al., 2006). Interestingly, a reduced amount of RELN protein has been found in the brain and blood of human patients affected by neuropsychiatric disorders (NPD) (Eastwood and Harrison, 2006; Fatemi et al., 2005; Guidotti et al., 2000). Furthermore, genes that are part of the signalling pathway downstream of RELN were shown to be involved in NPD. For instance, abnormalities in ApoER2-NMDA receptor signalling can lead to SZ and AD (Chen et al., 2010; Zhou and Sheng, 2013), VLDLR and ApoER2 single knock-out mice display defects in LTP (Weeber et al., 2002); and Dab1-conditional knockout mice exhibit deficits in working memory and spatial reference, hyperactivity and a decreased level of anxiety (Imai et al., 2016). Impaired mTOR signalling causes cognitive and behavioural deficits in different animal models of schizophrenia (Gururajan and van den Buuse, 2013). In conclusion, even though not all of the molecular abnormalities in the RELN pathway are fully understood yet, different studies show that RELN signalling is involved in the aetiology of NPD and can be targeted for therapeutic intervention. In fact, administration of RELN protein into the brain of a mouse model of Angelman syndrome ameliorates the cognitive

behavioural deficits and synaptic plasticity (Hethorn et al., 2015). Furthermore, GSK3 is a well-known target for antipsychotics and mood stabilizers (De Sarno et al., 2002; Emamian et al., 2004) and rapamycin inhibition of mTORC1 is able to rescue cognitive defects in different animal models of NPD (Meffre et al., 2012).

3.1.3.1 REELIN signalling is impaired in autism spectrum disorder

A better comprehension of how candidate genes contribute to ASD at the molecular level is essential to understand the aetiology of this disorder. Due to RELN's role in neurodevelopment and its location at chromosome 7q22, which was previously described as the peak region of linkage and first autism susceptibility locus (AUTS1; IMGSAC, 1998), this gene quickly emerged as a candidate for ASD and whole exome studies of autistic individuals were carried out (De Rubeis et al., 2014). In the past years over 15 linkage and epidemiologic studies have been performed to examine RELN gene polymorphisms as a risk factor for ASD. Both positive and negative findings have emerged making the results controversial and inconclusive (Bonora et al., 2003; Dutta et al., 2006; Dutta et al., 2008; He et al., 2011; Krebs et al., 2002; Li et al., 2008; Li et al., 2004; Persico et al., 2001; Serajee et al., 2006; Zhang et al., 2002). Finally, in 2014, Wang et al., conducted a meta-analysis incorporating all the available results from case-control and transmission disequilibrium test studies to evaluate the associations between RELN genetic variants and the risk of ASD. Among the three RELN variants that have drawn the most attention in previous studies, only the single nucleotide polymorphism rs362691 segregates with ASD (Wang et al., 2014c). In addition to this, many more unique inherited and *de novo* Reln variants have been identified by exome sequencing of ASD patients (Bonora et al., 2003; De Rubeis et al., 2014; Koshimizu et al., 2013; Neale et al., 2012; Yuen et al., 2015; Zhang et al., 2015b). However, even if the contribution of heterozygous RELN mutations in ASD is supported by genetic studies, their role in the aetiology and neural basis of the disorder still remains elusive (Lammert and Howell, 2016). Further evidence for a role of Reln in the aetiology of ASD is the reduction of Reln levels in the cerebellum and blood of ASD patients (Fatemi, 2001; Fatemi, 2002; Fatemi et al., 2005). Fatemi and colleagues not only showed that different cleaved Reln proteins were all significantly reduced in the frontal and cerebellar brain

areas of autistic patients, but also that mRNA levels of *Reln* and *Dab1* were significantly reduced as well. Conversely, *vldlr* mRNA levels were increased in exactly the same areas (Fatemi et al., 2005). ASD is a disorder that originates during development and continues into postnatal life; and Reln is important during neurodevelopment and later on in synaptic function (Folsom and Fatemi, 2013). Additionally, the same brain areas express RELN and are altered in ASD. In fact, RELN is expressed in the developing cerebral cortex and postnatally in the cerebellum, and both structures have anatomical defects in autistic individuals (Butts et al., 2014; Stoner et al., 2014; Tsai et al., 2012; Wang et al., 2014b). Indeed, Purkinje cells are significantly decreased in ASD patients (Skefos et al., 2014). Intriguingly, the RELN signalling pathway directly interacts with two principal ASD protein networks: i) the protein translation control networks mediated by mTOR, which is the second largest candidate gene network for Fragile X syndrome and tuberous sclerosis (Davis et al., 2015; Laggerbauer, 2001); and the ii) NMDAR cascade, which is essential for controlling synaptic plasticity and memory formation. Increasing evidence links the dysfunction of NMDA receptors with ASD (Lee et al., 2015), and general synapse functions have been investigated in ASD research since different mutations found in ASD individuals map to their key regulatory genes (De Rubeis et al., 2014).

As already discussed in the Chapter 1, autism is a complex disorder resulting from the combination of genetic and environmental factors. Environmental factors could affect gene expression and Reln is especially susceptible to sex-linked changes. For example, male heterozygous *reeler* mice (HRM) have a decreased number of Purkinje cells compared to female and WT HRM (Hadj-Sahraoui et al., 1996), and more recently it has been shown that oestradiol administration to male HRM can correct this deficit in the short-term, and that testosterone and oestrogen have different effects in male and female HRM (Biamonte et al., 2009).

3.1.3.2 REELIN-based models of autism spectrum disorder

It is still debated whether animal models in which *reln* expression is reduced or absent are suitable models for ASD. Mice with a complete deletion of RELN exhibit cerebellar

alterations which lead to death shortly after weaning. It is therefore not possible to utilize RELN KO mice to model ASD at adult stages (Michetti et al., 2014). While still alive, young homozygous *reeler* mice show massive neuroanatomical defects including decreased brain volume, a non-foliated cerebellum with a reduced number of Purkinje cells, impaired lamination of the hippocampus and disorganization of the amygdala (Boyle et al., 2011). Intriguingly, post-mortem studies of autistic patients reveal shared defects with the *reeler* mice models, such as altered cortical lamination, and a reduced number of Purkinje neurons (Bauman and Kemper, 2005). Due to these morphological changes, this model undergoes serious physical impairments defined as the *reeler* phenotype. Therefore, they are not suitable for basic behavioural research, but they have been used to study neuronal migration and the aetiology of human lissencephaly (Hong et al., 2000). Instead, the so called heterozygous *reeler* mice (HRM), have been proposed as a model of ASD and schizophrenia by researchers who have reported that RELN haploinsufficiency causes loss of Purkinje neurons of the cerebellum (Biamonte et al., 2009; Maloku et al., 2010) and decreases of the number of dendritic spines in cortical and hippocampal neurons (Pappas et al., 2002). Moreover, it has been reported that HRM have an increased level of anxiety, abnormal prepulse inhibition (PPI), impaired executive function, motor impulsivity, decreased contextual fear conditioning and impairments in associative learning (Krueger et al., 2006; Qiu et al., 2006; Tremolizzo et al., 2002; Tueting et al., 1999). However, other groups have reported that HRM show normal activity, anxiety, coordination, spatial learning, social behaviour, PPI and they behave normally in the light–dark transition test (Podhorna and Didriksen, 2004; Qiu et al., 2006). Due to these inconsistent results from different groups, it is still debatable whether HRM can be used as a genetic model for ASD. Locomotion, anxiety, learning and cognitive functions have been studied intensively by several groups, but surprisingly, only few studies have investigated the effects of RELN haploinsufficiency on social interactions and communication, which are the main hallmarks of ASD. Regarding this Michetti et al. recently demonstrated that HRM do not show deficits in social and vocal repertoires during courtship (Michetti et al., 2014) while Podhorna et al. showed that HRM spend more time engaging in social investigation (Podhorna and Didriksen, 2004). To overcome this controversy, alternative models to HRM were generated. Kohno et al. created a knock-in mouse in which the positively-charged CTR

of RELN is deleted attenuating the signalling pathway downstream of RELN. These mice showed impaired social behaviours, hyperactivity, a reduced anxiety phenotype and their working memory was impaired when compared to WT (Kohno et al., 2015; Sakai et al., 2016). Usually, studies that are based on an ASD-model only consider one genetic component, excluding all the environmental factors that could affect the onset of this complex multifactorial disorder. This limiting aspect of animal model research has to be considered when interpreting data and translating them to human patients. Therefore, other alternative models have been created on the basis of the "double-hit" theory, which state that some behavioural abnormalities become evident only after a "second hit" (Picci and Scherf, 2015). To test this hypothesis, HRM mice have been subjected to different stressful stimuli such as saline injections (causing higher locomotor activity (Michetti et al., 2014)) or to repeat maternal separation which does not seem to affect the behaviour of HRM (Laviola et al., 2009).

Despite the controversial behavioural results from the HRM models, the evidence that implicates RELN deficiency as a vulnerability factor for ASD is still strong. These include its key role in neuronal migration and synaptic plasticity, the genetic studies which link the RELN locus with ASD and the reduced amount of RELN protein found in brain and blood samples from autistic patients. For these reasons, we have investigated the effect of RELN depletion in zebrafish. Since homozygous *reln*$^{-/-}$ zebrafish fish are viable and they reach adult stages, they have been studied in this project together with a heterozygous *reln*$^{+/-}$ line to determine anatomical and behavioural alterations, changes in brain monoamine levels and finally to test drugs. Even though heterozygous mutations in RELN are associated with ASD in human patients, and classically the HRM is used to model ASD in mouse, in this project only the results from the analysis of *reln*$^{-/-}$ zebrafish will be presented since *reln*$^{+/-}$ did not show any abnormalities (data not shown).

3.2 Results

3.2.1 Localisation of Reelin by IHC

All vertebrates show *Reln* expression in the adult brain including the zebrafish (Alcántara et al., 1998; Costagli et al., 2002; Ikeda and Terashima, 1997). We first mapped the localisation of Reln in the adult zebrafish brain building upon results from previous studies.

Forebrain:

Reln is detected in the medial part of the dorsal telencephalon (Dm) and in the ventral nucleus of the ventral telencephalon (Vv, Figure 6a). Reelin is not expressed in *reln*$^{-/-}$ mutants (Figure 6b).

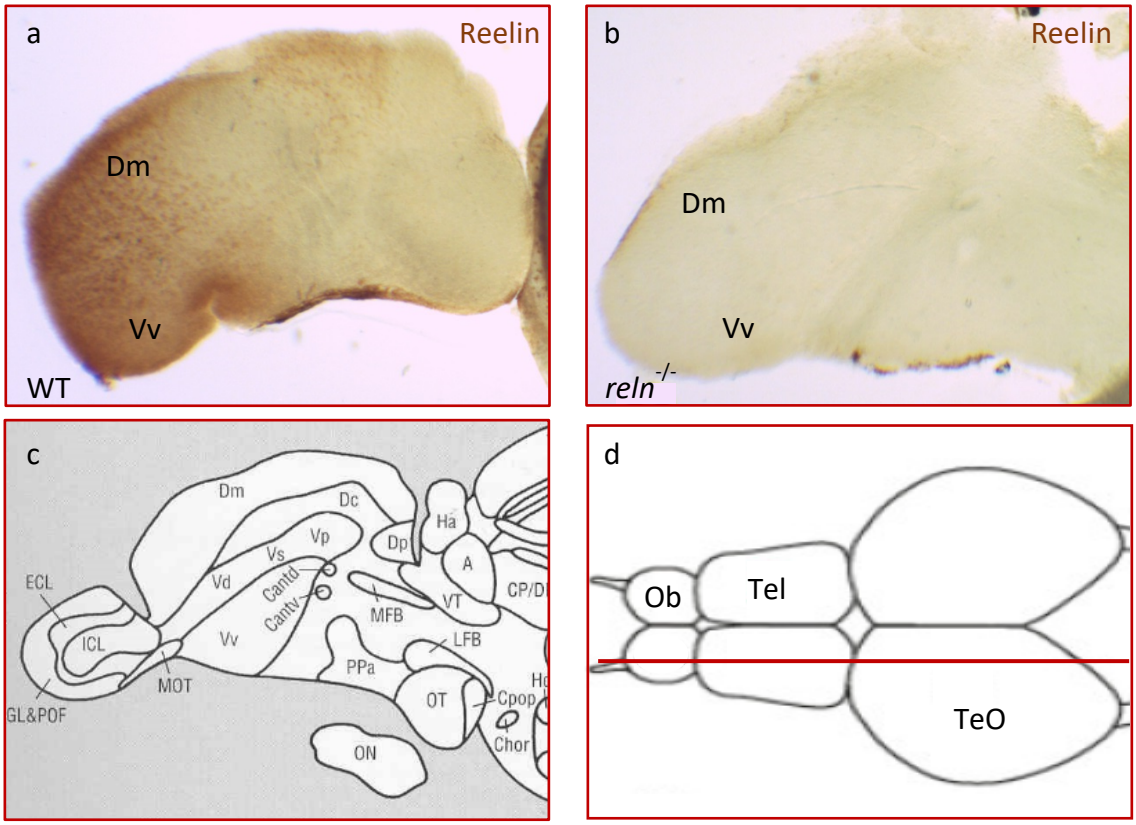

Figure 6. Reelin localisation in the forebrain. (a) In WT Reln is localised to the medial part of the dorsal telencephalon (Dm) and the ventral nucleus of the ventral telencephalon (Vm). **(b)** Reln is not expressed in *reln*$^{-/-}$. **(c)** Schematic sagittal view of the zebrafish forebrain, modified from Wullimann et al., 1992. **(d)** Schematic view of an adult zebrafish brain, adapted from Wullimann et al., 1992. The red line illustrates the location of sections shown in the previous panels. Abbreviations: Dm, dorsal telencephalon; Vv, ventral telencephalon.

Midbrain and Diencephalon

In the diencephalon, moderate levels of Reln are found in the ventral thalamic nuclei (Figure 7a) and in the ventral hypothalamic nuclei (Figure 7b). In the midbrain Reln is localised to the torus longitudinalis (Figure 7c) and also in a layer-specific manner in the optic tectum, specifically in the stratum fibrosum marginale (sfm) and in the stratum opticum (so, Figure 7g). A few labelled cells are observed in the interpeduncular nucleus (nin, Figure 7i). Reln is not expressed in *reln*$^{-/-}$ mutants (Figure 7d-f,h,j).

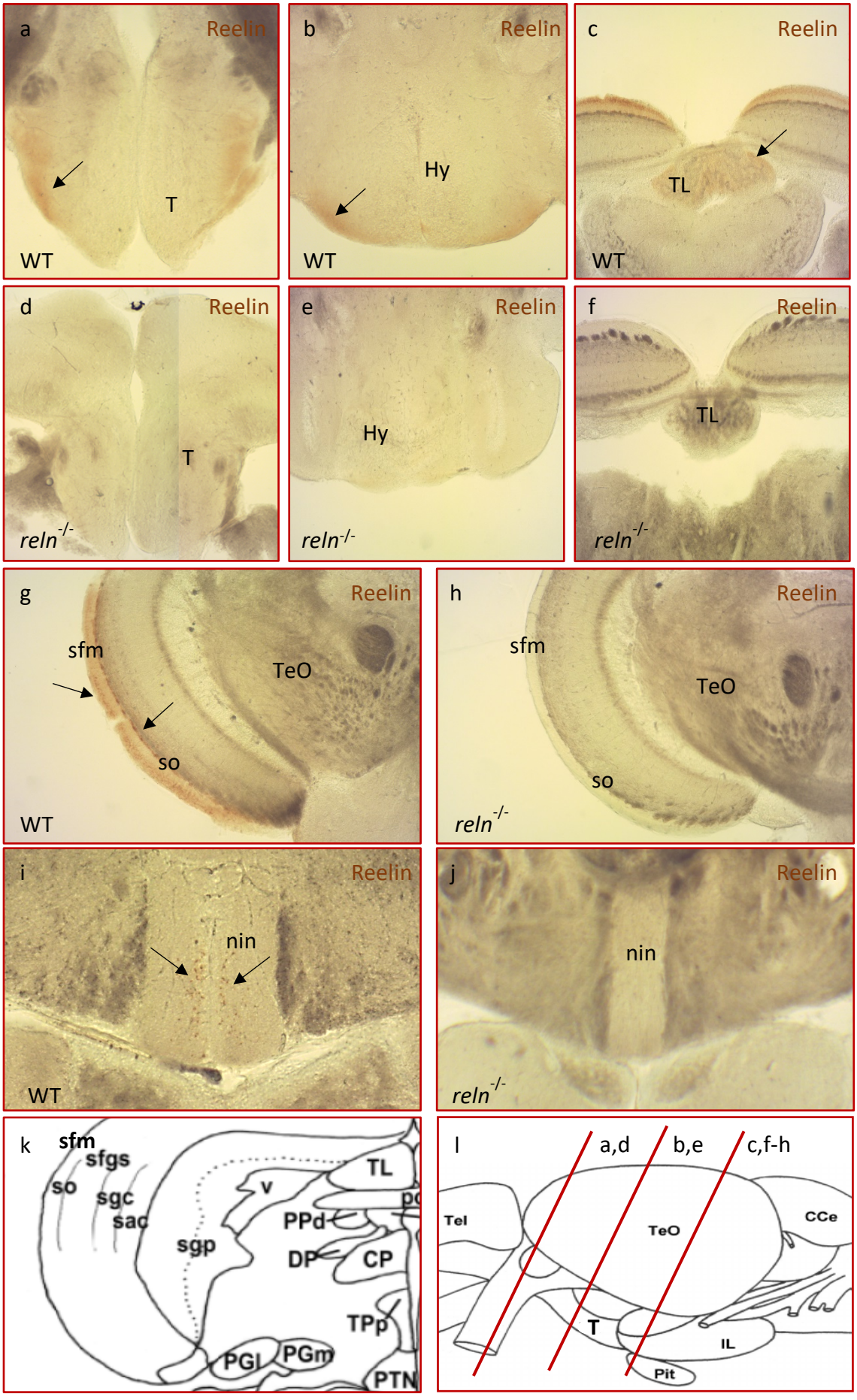
a
Reelin
T
WT
b
Reelin
Hy
WT
c
Reelin
TL
WT
d
Reelin
T
reln-/-
e
Reelin
Hy
reln-/-
f
Reelin
TL
reln-/-
g
Reelin
sfm
TeO
so
WT
h
Reelin
sfm
TeO
so
reln-/-
i
Reelin
nin
WT
j
Reelin
nin
reln-/-
k
sfm
sfgs
so
sgc
sac
sgp
v
TL
PPd
DP
CP
TPp
PGl
PGm
PTN
l
a,d
b,e
c,f-h
Tel
TeO
CCe
T
IL
Pit

Figure 7. Reelin localisation in the midbrain and diencephalon. In the WT diencephalon, Reln localises to **(a)** the ventral thalamic nuclei and **(b)** the ventral hypothalamic nuclei. In the midbrain Reln is highly localised in **(c)** the torus longitudinalis, **(g)** the stratum fibrosum marginale (sfm) and stratum opticum (so) of the optic tectum. **(i)** A few labelled cells are observed in the interpeduncular nucleus (nin) **(d-f,h,j)** Reln is not expressed in *reln*$^{-/-}$. **(k)** Schematic coronal view of the zebrafish optic tectum, modified from Costagli et al., 2002. **(l)** Schematic view of a zebrafish adult brain, modified from Wullimann et al., 1992. The red lines illustrate the location depicted in the previous panels. Abbreviations: Hy, Hypothalamus; nin, interpeduncular nucleus; sfgs, stratum griseum et album superficiale; so, stratum opticum; TeO, optic tectum; T, thalamus; TL, torus longitudinalis.

Hindbrain

In the hindbrain, Reln is highly localised to three areas of the cerebellum: the corpus cerebelli (CCe), the lobus caudalis cerebelli (LCa) and the crista cerebellaris (CC) (Figure 8a). Specifically, in the CCe Reln is only found in the granular cell layer, and no Reln was detected in the Purkinje and molecular cell layer. As already mentioned, the torus longitudinalis shows high levels of Reln (Figure 8a). Reln-positive cells are also present in the intermediate and inferior part of the reticular formation (RF) in the medulla oblongata (Figure 8b). Reln is not detected in *reln*$^{-/-}$ mutants (Figure 8c,d).

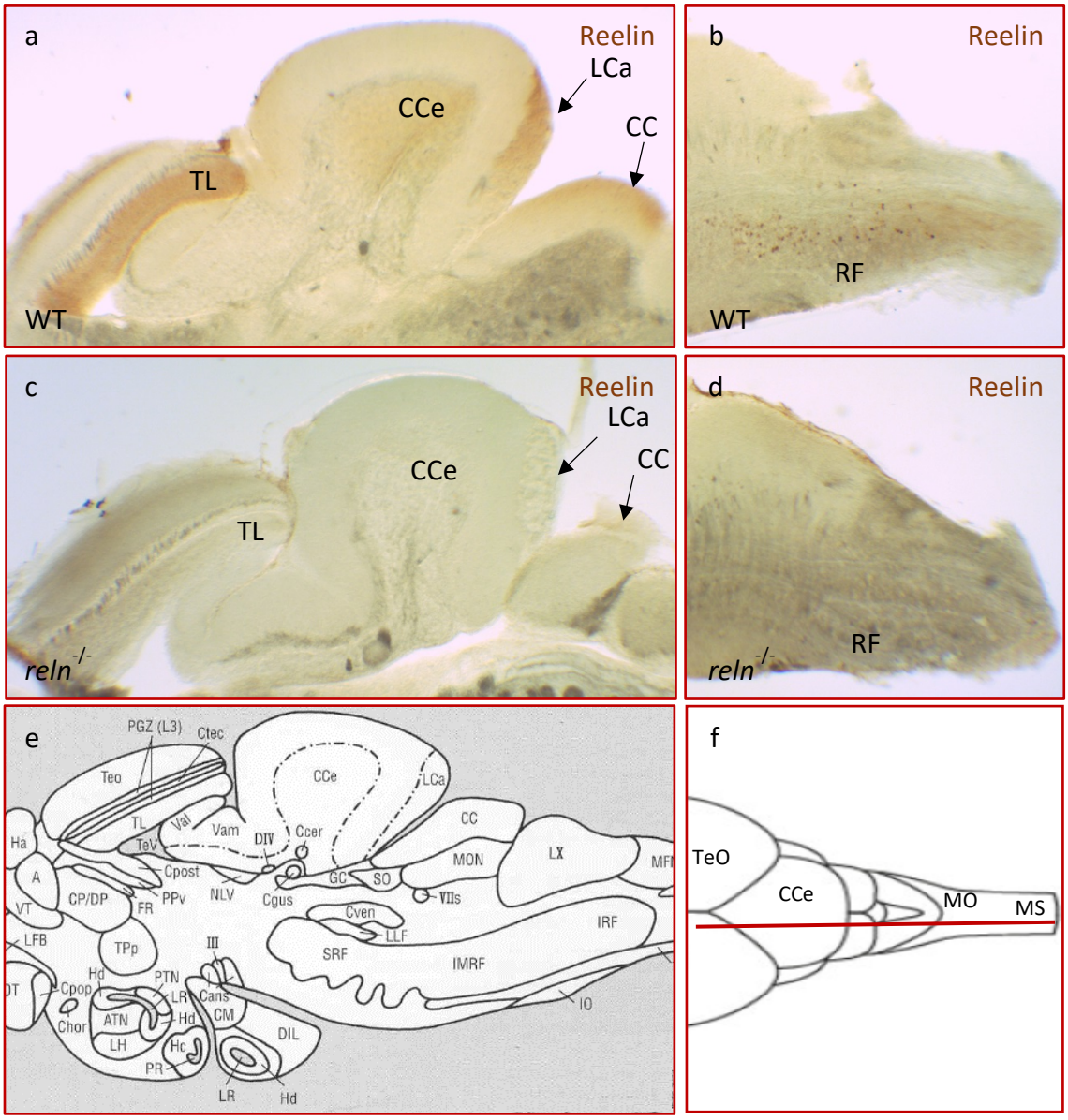

Figure 8. Reelin localisation in the hindbrain. In the WT hindbrain, Reln localises to **(a)** the corpus cerebelli (CCe), the lobus caudalis cerebelli (LCa) and the crista cerebellaris (CC), and to **(b)** the intermediate and inferior part of the reticular formation (RF). **(c,d)** Reln is not expressed in *reln*$^{-/-}$. **(e)** Schematic sagittal view of the zebrafish hindbrain adapted from Wullimann et al., 1992. **(f)** Schematic view of a zebrafish adult brain, modified from Wullimann et al., 1992. The red lines illustrate the location depicted in the previous panels. Abbreviations: CC, crista cerebellaris; CCe, corpus cerebelli; LCa, lobus caudalis cerebelli; RF, reticular formation; TL, torus longitudinalis.

3.2.2 Analysis of cytoarchitecture by Nissl Staining

One of the first defects observed in *reeler* mice was a severe hypoplasia of the cerebellum, which lacked foliation. In addition, histological studies of the *reeler* brain reported impaired cytoarchitecture with neuronal ectopia (abnormal positioning of

neurons) in other laminated brain structures such as the cerebral cortices and the hippocampus. Interestingly, patients with psychiatric disorders, including autism, show malpositioning of neurons (D'Arcangelo and Curran, 1998; Katsuyama and Terashima, 2009). Hence to better understand Reln's function we examined the cytoarchitecture of WT and *reln*$^{-/-}$ fish with the Nissl staining technique that uses cresyl violet as dye. Cresyl violet binds the acidic components of the neuronal cytoplasm, including the RNA-rich ribosomes, cell nuclei and nucleoli, making it possible to count the number of cells that are present in a defined area (Alvarado et al.) When observed in a sagittal plane the zebrafish telencephalon is very rich in neuronal somata (Figure 9a). Defined areas in the Dm and Vv, the two principals zones that show high levels of Reln in the IHC experiment, were selected and the numbers of cells presented in these areas were counted (Figure 9a,b). In this experiment only one brain per genotype was analysed therefore it was not possible to statistically analyse these results. However, we observed similar cell counts between these two areas in WT (71 cells in Dm, 102 cells in Vv) and *reln*$^{-/-}$ (79 cells in Dm, 105 cells in Vv), suggesting that the mutant may not have cytoarchitectural defects in Dm and Vv (Figure 10). Moving caudally, the cytoarchitecture of the optic tectum was analysed. A previous study described three main structural layers in the zebrafish optic tectum: the stratum opticum (so) together with the stratum marginale, the stratum fibrosum et griseum superficiale (sfgs), and the stratum album centrale (sac) together with the stratum periventriculare (sp) (Kim et al., 2004). The same laminar structure was observed in this analysis (Figure 9c,d). The cell counts for each of these layers showed similar values for the so and the sac layers between WT (63 cells in so, 56 cells in sac) and *reln*$^{-/-}$ (54 cells in so, 40 cells in sac), whereas *reln*$^{-/-}$ seem to have a decreased number of cells in the sfgs (100 cells in WT, 50 cells in *reln*$^{-/-}$, Figure 10). The cytoarchitecture of the cerebellum was also characterized using the Nissl stain. Three distinctive cell layers of the cerebellar cortex were identified: i) the external molecular layer (ML), which contains only few labelled cells since it mainly constitutes parallel fibres and small stellate cells, ii) the Purkinje cell layer (PCL) which contains bigger cells and iii) the deepest granule cell layer (GCL) which has an high concentration of small cells (Figure 9e,f). Cell counts were performed in a defined area across the PCL for both WT and *reln*$^{-/-}$, showing no substantial differences in the number of neurons between the genotypes (56 cells in WT, 53 cells in *reln*$^{-/-}$,

Figure 10). Finally, the reticular formation (RF) was analysed (Figure 9g,h). Little is known about the large population of excitatory interneurons that constitute the RF in zebrafish (Gray, 2013). The mammalian RF is better characterized and is divided into three main columns: raphe nuclei, gigantocellular reticular nuclei, and parvocellular reticular nuclei. Indeed, the results from the Nissl staining show the presence of large cell bodies which are likely to be the so-called giant neuronal cells, that are surrounded by many smaller cells (Figure 9). Two equal areas were defined in both WT and *reln*$^{-/-}$ sections and the number of stained cells were counted for each section resulting in similar numbers (179 cells in WT, 194 cells in *reln*$^{-/-}$, Figure 10).

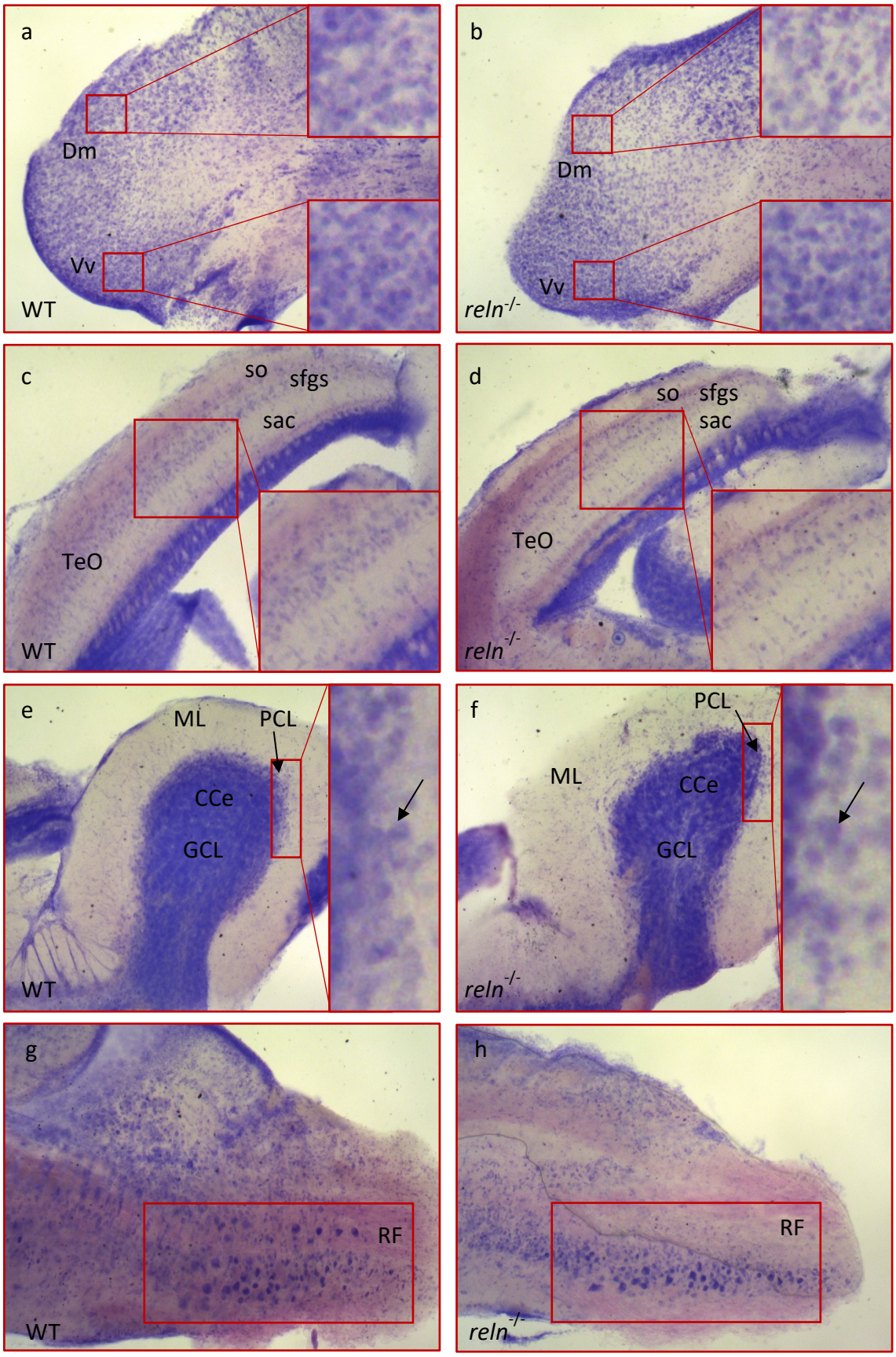
a
Dm
Vv
WT
b
Dm
Vv
reln-/-
c
so
sfgs
sac
TeO
WT
d
so
sfgs
sac
TeO
reln-/-
e
ML
PCL
CCe
GCL
WT
f
PCL
ML
CCe
GCL
reln-/-
g
RF
WT
h
RF
reln-/-

Figure 9. Nissl staining of zebrafish brain. Photographs of 100 µm thick sagittal sections labelled with cresyl violet. For each section, areas within the red squares were analysed (see results in Figure 10). **(a)** Rostral telencephalon of WT, with higher magnification of the two defined areas where the cells were counted for Dm and Vv respectively. **(b)** The same areas were selected for section of the *reln*$^{-/-}$ brain. **(c)** Optic tectum of WT, Nissl stain shows three main structural layers: the stratum opticum (so), the stratum fibrosum et griseum superficiale (sfgs), and the stratum album centrale (sac). The red squares show the area selected for cell counts with its related higher magnification view. **(d)** The same analysis was performed in a *reln*$^{-/-}$ section. **(e)** Cytoarchitecture of the WT cerebellum, with higher magnification of the area selected for cell counts across the PCL. The arrows point to Purkinje neuron cell bodies. **(f)** The same area was selected for a section of the *reln*$^{-/-}$ brain. **(g)** Medulla oblongata of WT. In red is shown the area of the reticular formation selected for cell counts, and **(h)** the corresponding area in *reln*$^{-/-}$.

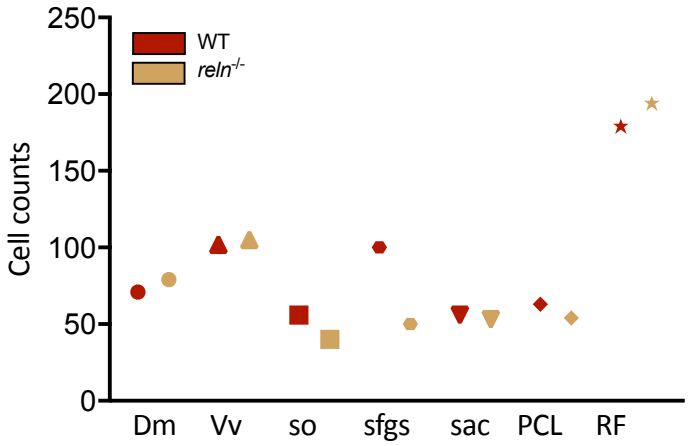

Figure 10. Summary plot showing cell counts. Dm, medial part of the dorsal telencephalon; Vv, ventral nucleus of the ventral telencephalon; so, stratum opticum; sfgs, stratum fibrosum et griseum superficiale; sac, stratum album centrale; PCL, Purkinje cell layer; RF, reticular formation.

3.2.3 Behavioural analysis of *reln*$^{-/-}$

The core symptoms of ASD are deficits in social communication and language, and repetitive and restrictive behaviours which cause significant distress for affected individuals. We assessed several behaviours including anxiety, boldness, aggression and social behaviour to demonstrate which behaviours might be altered in a zebrafish model of ASD.

3.2.3.1 Analysis of social behaviour

3.2.3.1.1 Visually-mediated social preference for novelty test (VMSP)

WT and *reln*$^{-/-}$ behaviour was analysed in the VMSP test as described in Chapter 2. The time spent in the different zones of the tank is used as an index to quantify social preference and the preference for novelty. During the social preference step of the experiment, both genotypes reacted in the same way, spending the majority of the time

swimming close to the first group of strangers (1st strangers; $p < 0.0001$ for both WT and *reln*$^{-/-}$, Figure 11a). During the preference for social novelty step, a difference in the behaviour of *reln*$^{-/-}$ was observed. They spent significantly less time in the area close to the second group of strangers compared to WT. Thus, mutants do not switch preference to the second group of unfamiliar fish (2nd strangers; $p < 0.0001$), whereas WT spend an equal amount of time near both groups of unfamiliar fish (2nd strangers; $p = 0.94$, Figure 11b). A representative tract of each genotype swimming in the tank is shown in Figure 11c-f.

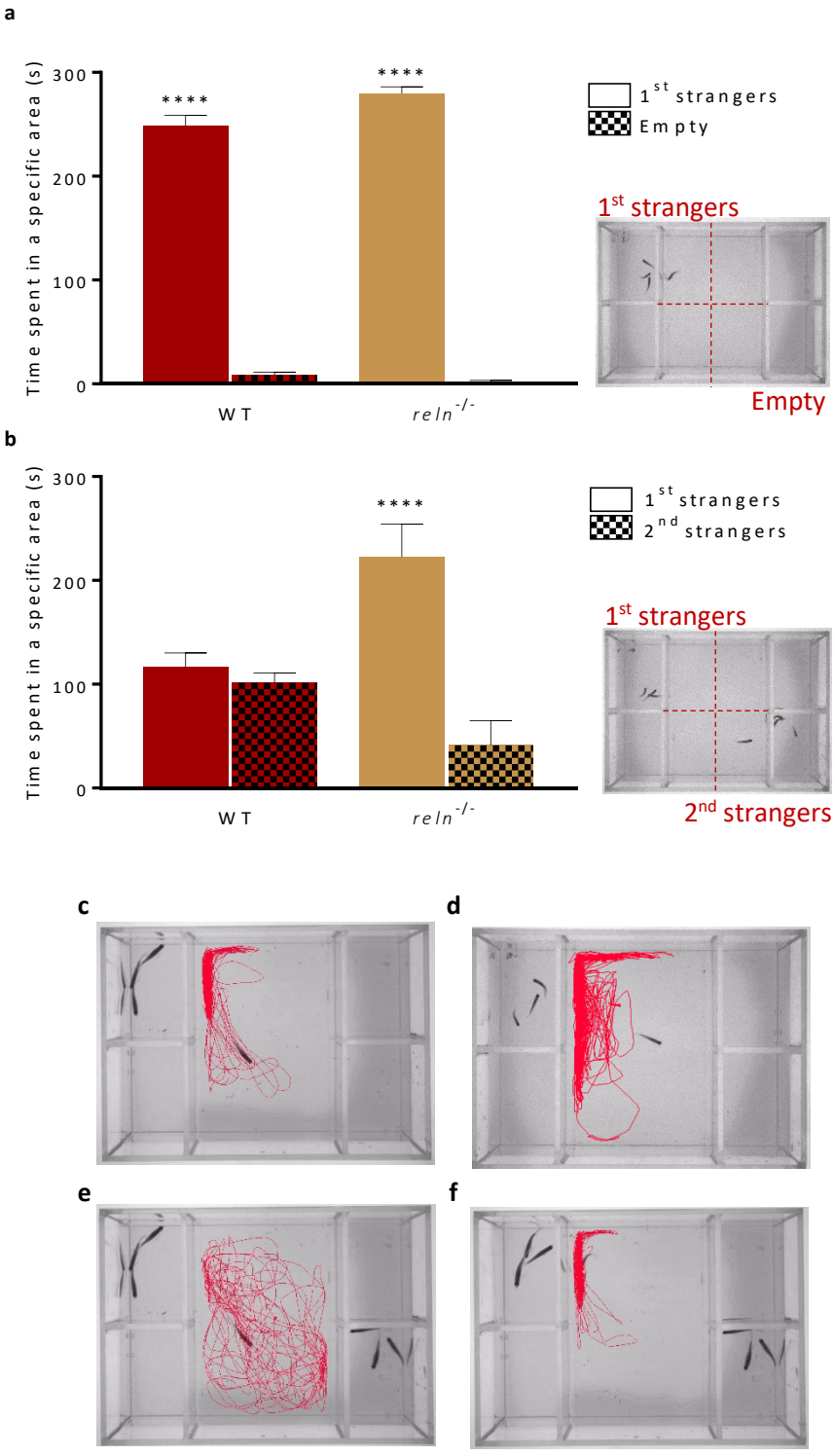

Figure 11. Visually-mediated social preference test. (a) Social preference. Both WT and *reln*$^{-/-}$ show a significant preference to spend time near a group of unfamiliar fish (1st strangers; $p < 0.0001$ for both WT and *reln*$^{-/-}$). **(b)** Preference for social novelty. WT spend an equal amount of time near both groups of unfamiliar fish (2nd strangers; $p = 0.94$). *reln*$^{-/-}$ do not switch preference to the second group of unfamiliar fish (2nd strangers; $p < 0.0001$). Two-way ANOVA with Tukey's post hoc comparisons. n = 12 wild-type and n = 10 *reln*$^{-/-}$. **** $p < 0.0001$. Mean ± SEM. **(c-f)** Swimming trajectory of focal fish in the behavioural arena. Representative traces for **(c)** WT and **(d)** *reln*$^{-/-}$ during the social preference test. **(e)** WT and **(f)** *reln*$^{-/-}$ show a difference in preference for the second group of unfamiliar fish.

3.2.3.1.2 Shoaling test

We next examined social behaviour in a group by measuring the proximity to other conspecifics. Analysis of groups of five fish revealed that *reln*$^{-/-}$ does not differ significantly in shoal cohesion compared to WT. This is showed by both the nearest neighbour distance (NDD, p = 0.22, Figure 12a) and the inter-individual distance (IID, p= 0.09, Figure 12b). Moreover, this phenotype is also confirmed by cluster analysis which can be used as an index for social cohesion (Parker et al., 2013) (p = 0.24, Figure 12g). The cluster score is measured every 30 seconds (t), dividing the maximum number of fish in one section (Max) by the total number of sections occupied by the fish (Total): Cluster score$_t$ = Max$_t$/Total$_t$ (Figure 12h). The polarization (p = 0.85, Figure 12e) and the velocity (p = 0.41, Figure 12f) of the shoal were similar between *reln*$^{-/-}$ and WT.

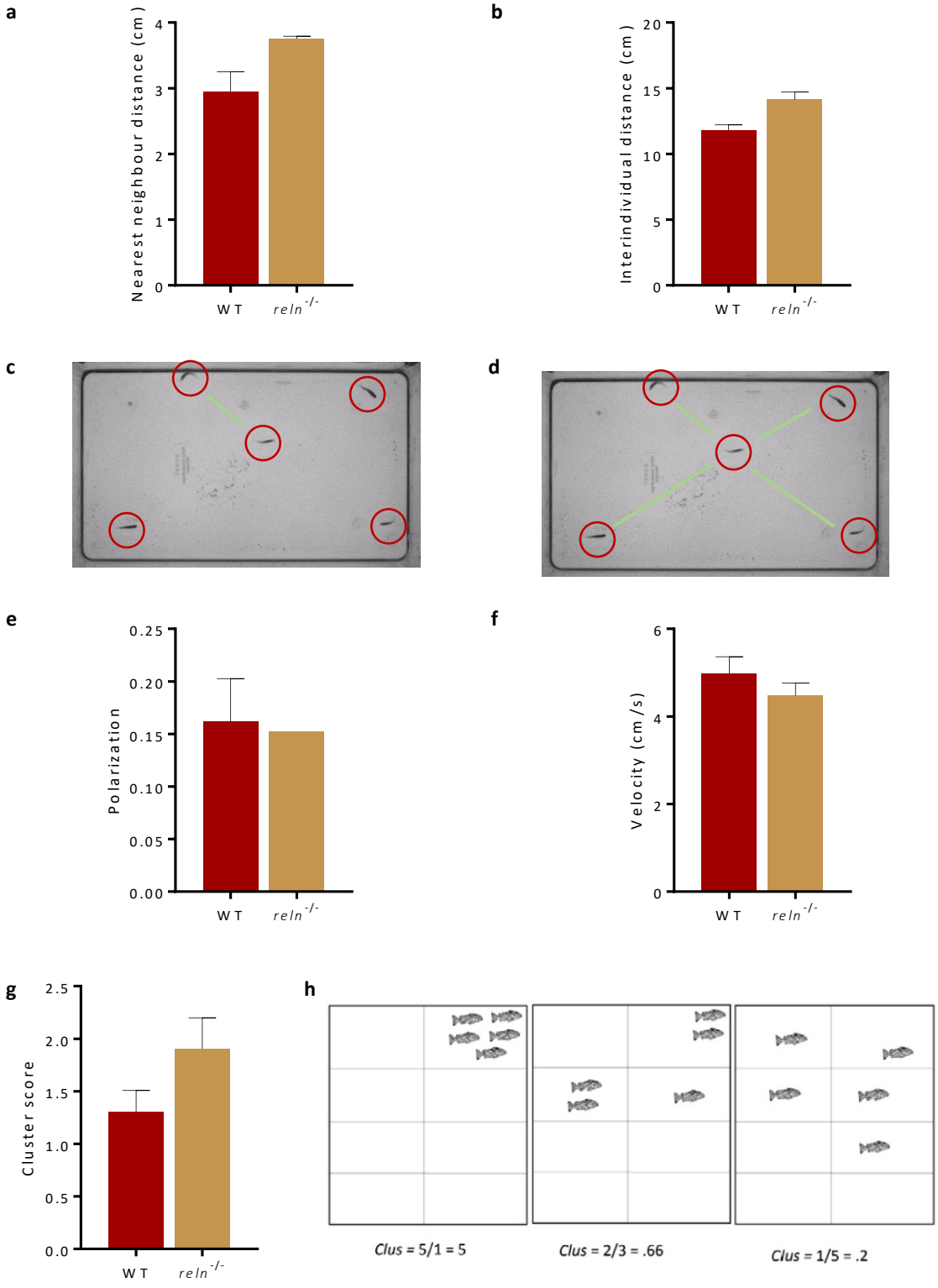

Figure 12. Shoaling behaviour. *reln*$^{-/-}$ display normal shoaling. **(a)** Nearest neighbour distance (p = 0.22), **(b)** inter-individual distance (p = 0.09), **(e)** polarization (p = 0.85), **(f)** velocity (p = 0.41) and **(g)** cluster score (p = 0.24). n = 2 groups of 5 wild-type, n = 2 groups of 5 *reln*$^{-/-}$. Unpaired t-test with Welch's correction. Mean ± SEM. Schematic representation of **(c)** nearest neighbour distance (the distance between each individual and its closest neighbour) and **(d)** inter-individual distance (the mean distance from each individual to all the other fish). **(h)** Example of cluster analysis adapted from Parker et al., 2013.

3.2.3.2 Analysis of anxiety-like behaviour and exploratory activity

3.2.3.2.1 Novel tank test (NTT)

We examined anxiety-like behaviour using the NTT. When zebrafish are placed in an unfamiliar tank they tend to dive to the tank floor avoiding the exposed upper regions until they acclimatise. The time spent near the bottom of the tank can be used as indication of anxiety-like behaviour (Bencan and Levin, 2008). Both genotypes spent about 95% of the time of the experiment at the bottom, showing a general baseline of anxiety-like behaviour. No significant difference was found between WT and *reln*$^{-/-}$ in the time spent at the bottom (p = 0.21, Figure 13a) and at the top (p = 0.69, Figure 13b) of a novel tank. Further parameters were analysed within the same test and the two genotypes do not show any significant differences in the time spent freezing (p = 0.94, Figure 13c), in locomotion (p = 0.36, Figure 13d), velocity (p = 0.29, Figure 13e) or angular velocity (p = 0.94, Figure 13f) in the novel tank.

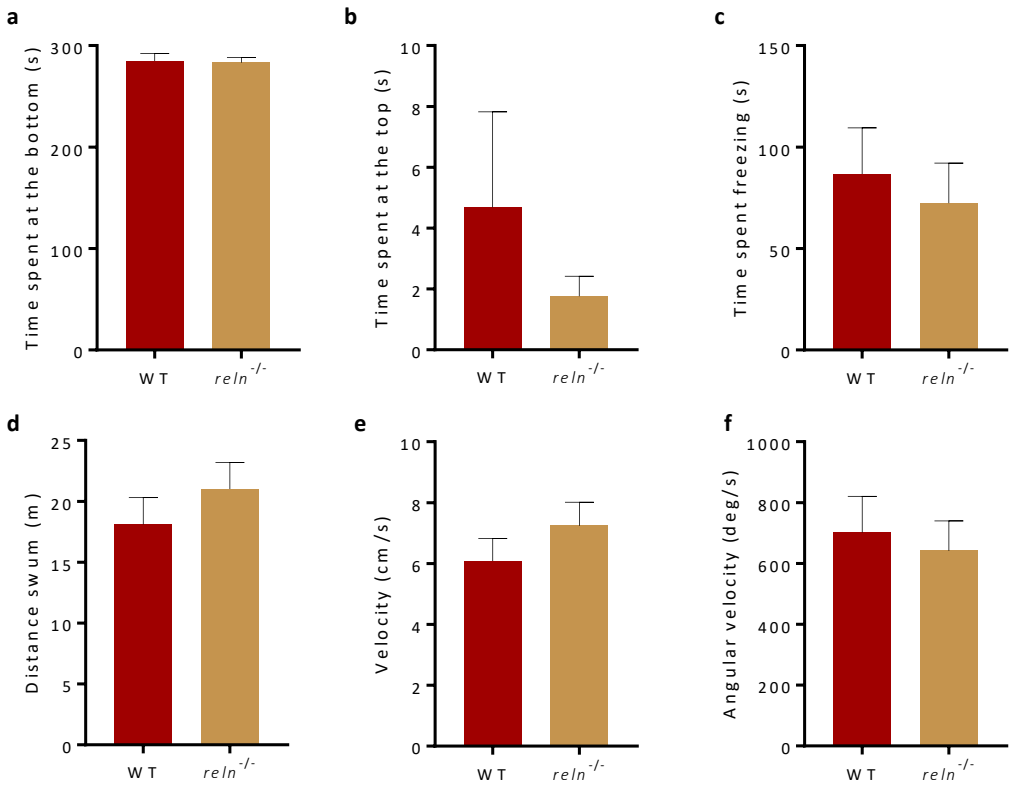

Figure 13. Novel tank test. *reln*$^{-/-}$ exhibit normal anxiety-like behaviour. Time spent **(a)** at the bottom (p = 0.21), **(b)** at the top (p = 0.69), and **(c)** freezing (p = 0.94) in a novel tank. n = 13 wild-type, n = 12 *reln*$^{-/-}$. Mann-Whitney U test. **(d)** Locomotion (p = 0.36), **(e)** velocity (p = 0.29) in a novel tank. n = 13 wild-type, n = 12 *reln*$^{-/-}$. Unpaired t-test with Welch's correction. **(f)** angular velocity (p = 0.94) in a novel tank. n = 13 wild-type, n = 12 *reln*$^{-/-}$. Mann-Whitney U test. Mean ± SEM.

3.2.3.2.2 Open field test

The lack of anxiety-like phenotype was also confirmed in the open field test by measuring the time spent in the center, periphery and side of a large tank. Again, both genotypes spent about 70% of the time in thigmotaxis (a preference for the side of the tank), showing a general baseline level of anxiety. No significant differences were found in the time spent in thigmotaxis (p = 0.91, Figure 14a), in the periphery (p = 0.24, Figure 14b) and in the center (p = 0.73, Figure 14c) of the open field tank between WT and *reln*$^{-/-}$. The time spent freezing (p = 0.98, Figure 14d), locomotion (p = 0.41, Figure 14e) and velocity (p = 0.40, Figure 14f) were also not affected in the open field.

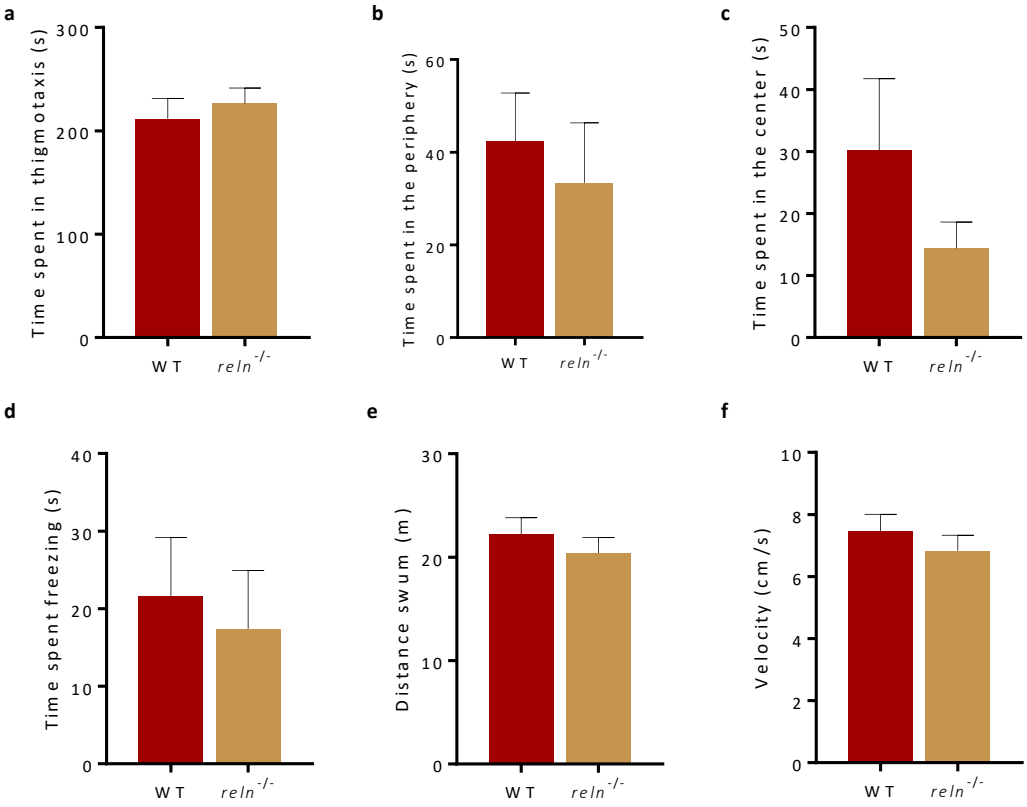

Figure 14. Open field test. *reln*$^{-/-}$ behave similarly to WT in the open field test. **(a)** Time at the side of the tank (p = 0.91), **(b)** in the periphery (p = 0.24) and **(c)** in the center of the tank (p = 0.73). n = 12 WT, n = 12 *reln*$^{-/-}$. Mann-Whitney U test. **(d)** Time spent freezing (p = 0.98), **(e)** locomotion (p = 0.41) and **(f)** velocity (p = 0.40) are not affected in the open field test. n = 12 WT, n = 12 *reln*$^{-/-}$. Unpaired t-test with Welch's correction. Mean ± SEM.

3.2.3.3 Mirror-induced aggression

We next investigated the behaviour of *reln* mutants in the mirror-induced aggression test. The mutants did not show a different level of aggression compared to WT (Figure 15).

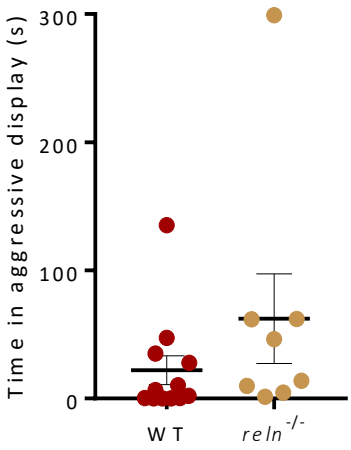

Figure 15. Mirror-induced aggression test. No difference in aggression levels between WT and *reln*$^{-/-}$ were observed (p = 0.10). n = 12 wild-type, n = 8 *reln*$^{-/-}$. Mann-Whitney unpaired t-test. Mean ± SEM.

3.2.4 Analysis of monoamines and their metabolites levels by high-performance liquid chromatography (HPLC)

To investigate whether mutation of *reln* influences levels of monoamines and their metabolites, we performed HPLC analyses to assess the basal level of 3,4-dihydroxyphenylacetic acid (DOPAC), dopamine (DA), 5-hydroxyindoleacetic acid (5HIAA), homovanillic acid (HVA) and serotonin (5-HT) in the brain. There was a significant genotype effect on 5-HT levels in the hindbrain, with *reln*$^{-/-}$ having increased level of this neurotransmitter (p = 0.0021, Figure 16d). No further alterations were found neither in others area of the brain (Figure 16a-c) nor in the turnover of neurotransmitters (Figure 16e-g).

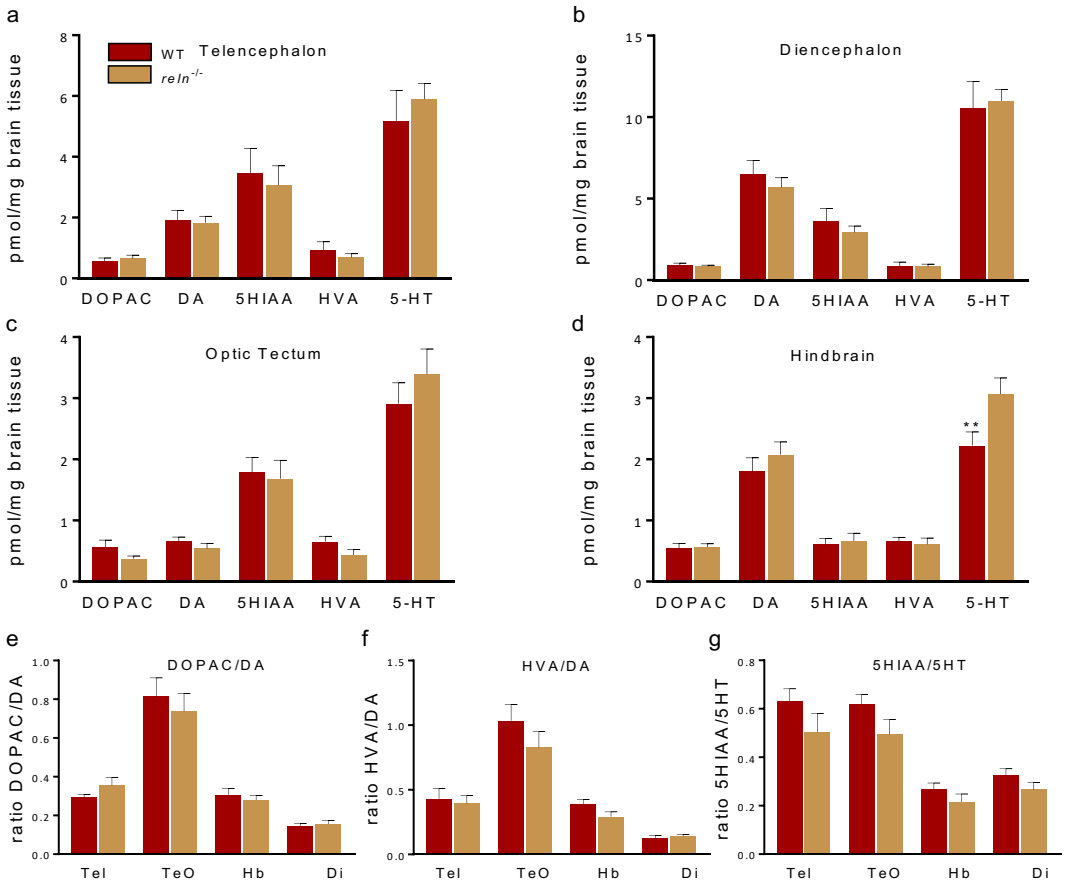

Figure 16. High precision liquid chromatography. 5-HT levels are increased in the hindbrain of *reln*$^{-/-}$ compared to WT ($p = 0.0021$). **(a)** Telencephalon, **(b)** diencephalon, **(c)** optic tectum and **(d)** hindbrain. No differences in the breakdown of **(e)** DOPAC/DA, **(f)** HVA/DA, **(g)** 5-HIAA/-5HT. T-tests with Holm-Sidak correction for multiple comparisons. Abbreviations: DA, dopamine; Di, diencephalon; DOPAC, 3,4-dihydroxyphenylacetic acid; Hb, hindbrain; HVA, homovanillic acid; Tel, telencephalon; TeO, optic tectum; 5-HIAA, 5-hydroxyindoleacetic acid; 5-HT, 5-hydroxytryptamine. n = 8 WT, n = 8 reln$^{-/-}$. ** $p < 0.01$. Mean ± SEM.

3.2.5 Pharmacological treatment of *reln*$^{-/-}$

The main defect in neurotransmitter signalling that we observed in *reln*$^{-/-}$ was an increase in the level of 5-HT in the hindbrain. Therefore, we applied buspirone, a 5-HT$_{1A}$ receptor agonist (Ohlsen and Pilowsky, 2005) to investigate the connection between 5-HT and the behavioural phenotype observed of *reln*$^{-/-}$. Buspirone, acting as a partial agonist for the 5-HT$_{1A}$ receptors, inhibits firing of 5-HT neurons and the synthesis and use of 5-HT thus decreasing 5-HT activity (Loane and Politis, 2012). Treatment with 10 mg/L buspirone increased the preference for social novelty in WT (1st strangers; $p = 0.0039$, Figure 17a), but did not rescue the impaired preference for social novelty of

reln$^{-/-}$ (2nd strangers; p = 0.0120, Figure 17b), although drug application increased the time spent close the new group of unfamiliar fish (Cohen's d effect size = 0.46, Figure 17b).

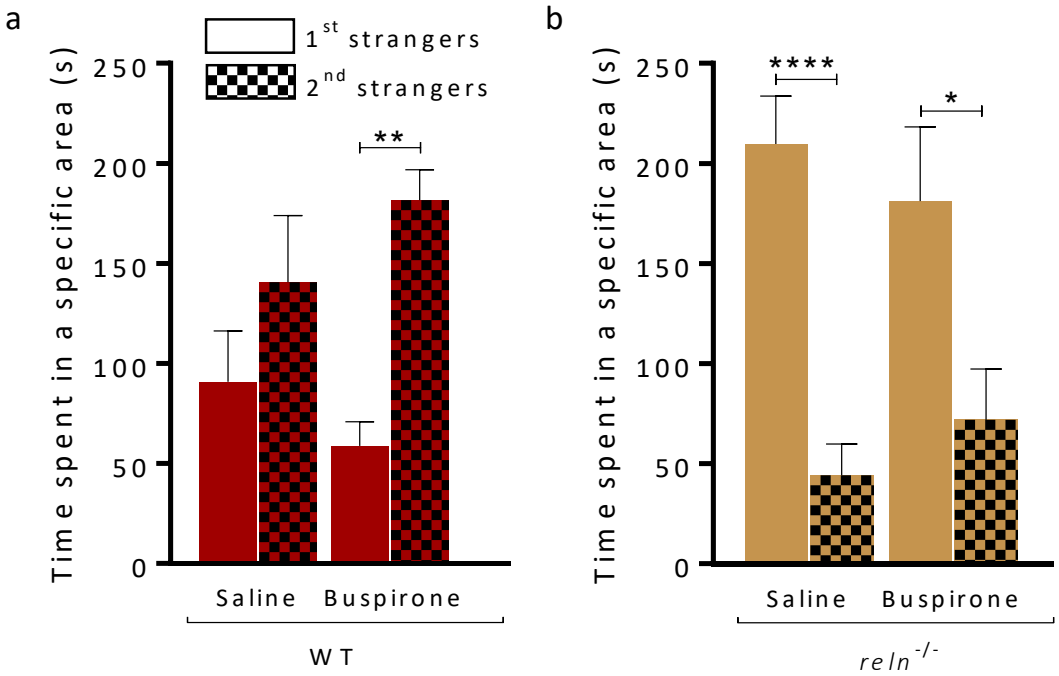

Figure 17. Buspirone increases the preference for social novelty in WT but does not rescue it in *reln*$^{-/-}$. **(a)** WT treated with saline spent equal time near the two groups of unfamiliar fish (p = 0.51), whereas WT treated with buspirone switched preference and spent more time near the new group of unfamiliar fish (p = 0.0039). **(b)** Buspirone treatment did not rescue the impaired preference for social novelty of *reln*$^{-/-}$ zebrafish (p = 0.0120; saline control, p < 0.0001), although drug application increased the time that *reln*$^{-/-}$ spent close the new group of unfamiliar fish (Cohen's d effect size = 0.46). Three-way ANOVA with Sidak's multiple comparisons. n = 8 WT and n = 8 *reln*$^{-/-}$. * p < 0.05, ** p < 0.01, ** p < 0.0001. Mean ± SEM.

The impaired social behavioural phenotype suggests that *reln*$^{-/-}$ might be a good model for some aspects of ASD. Therefore, the mutants were treated with two drugs that are used to treat ASD in human patients, oxytocin and risperidone. Oxytocin has been recently shown to improve social function and reduce repetitive behaviour in individuals with ASD (Andari et al., 2010; Guastella et al., 2010; Hollander et al., 2003). Risperidone has a long history in ASD treatment with a recognized moderate efficacy and safety for treating the disorder (Canitano, 2008). Neither treatment with 0.01 ng/kg oxytocin or 170 µg/L risperidone are able to rescue the impaired preference for social novelty observed in *reln*$^{-/-}$ (2nd strangers; p = 0.048 and p = 0.0023, Figure 18b).

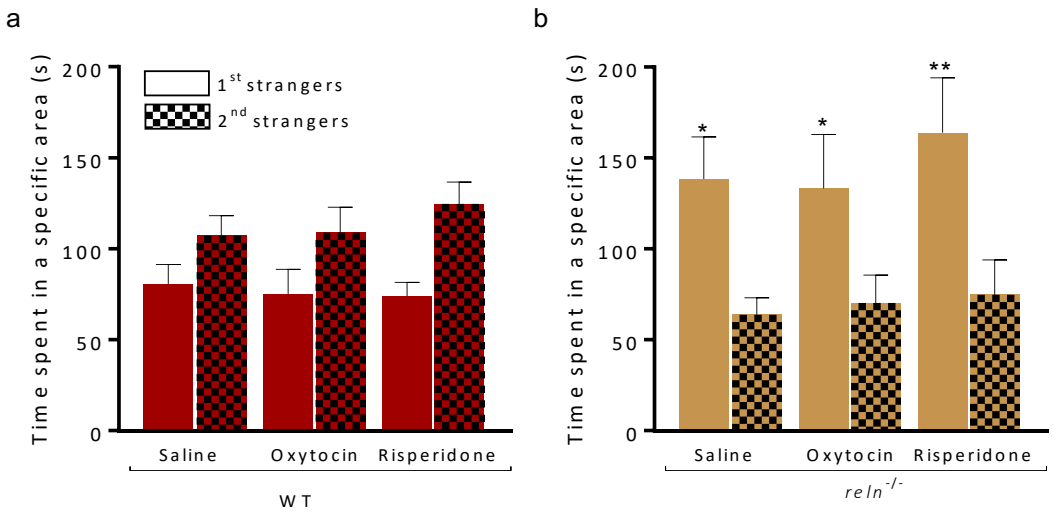

Figure 18. Oxytocin and risperidone do not rescue preference for social novelty. **(a)** WT treated with saline (p = 0.57), oxytocin (p = 0.53) and risperidone (p = 0.14) spend equal time near the two groups of unfamiliar fish. **(b)** Neither oxytocin (p = 0.048) nor risperidone (p = 0.0023) treatment rescues the impaired preference for social novelty of *reln*$^{-/-}$ zebrafish (saline control, p = 0.014). Three-way ANOVA with Sidak's multiple comparisons. n = 9 WT and n = 9 *reln*$^{-/-}$. * p < 0.05, ** p < 0.01. Mean ± SEM.

3.2.6 Behavioural analysis of *dab1a*$^{-/-}$ and *vldlr*$^{-/-}$

Components of the RELN signalling pathway such as Dab1 and VLDLR are also associated with ASD. We therefore analysed the behaviour of both *dab1a*$^{-/-}$ and *vldlr*$^{-/-}$ mutant zebrafish. *dab1a*$^{-/-}$ exhibited similar behaviour to WT in the open field test. Specifically, mutants and WT spent the same amount of time at side (p = 0.75, Figure 19a) and in center of the tank (p = 0.87, Figure 19b), and the distance swum was also comparable between genotypes (p = 0.61, Figure 19c). In the mirror-induced aggression test *dab1a*$^{-/-}$ displayed heightened aggression levels compared to WT (p = 0.0445, Figure 19d). Even though anxiety-like behaviour was not altered in the novel tank test (p = 0.06, Figure 19e), *dab1a*$^{-/-}$ were more active (p = 0.0133, Figure 19f). In the visually-mediated social preference test, both genotypes preferred to spend time near a group of unfamiliar fish (1st strangers; p = 0.0005 for WT and p < 0.0001 for *dab1a*$^{-/-}$, Figure 19g) and they spent equal time near both groups when a second unfamiliar group was added (2nd strangers; p = 0.61 for WT and p = 0.44 for *dab1a*$^{-/-}$, Figure 19h).

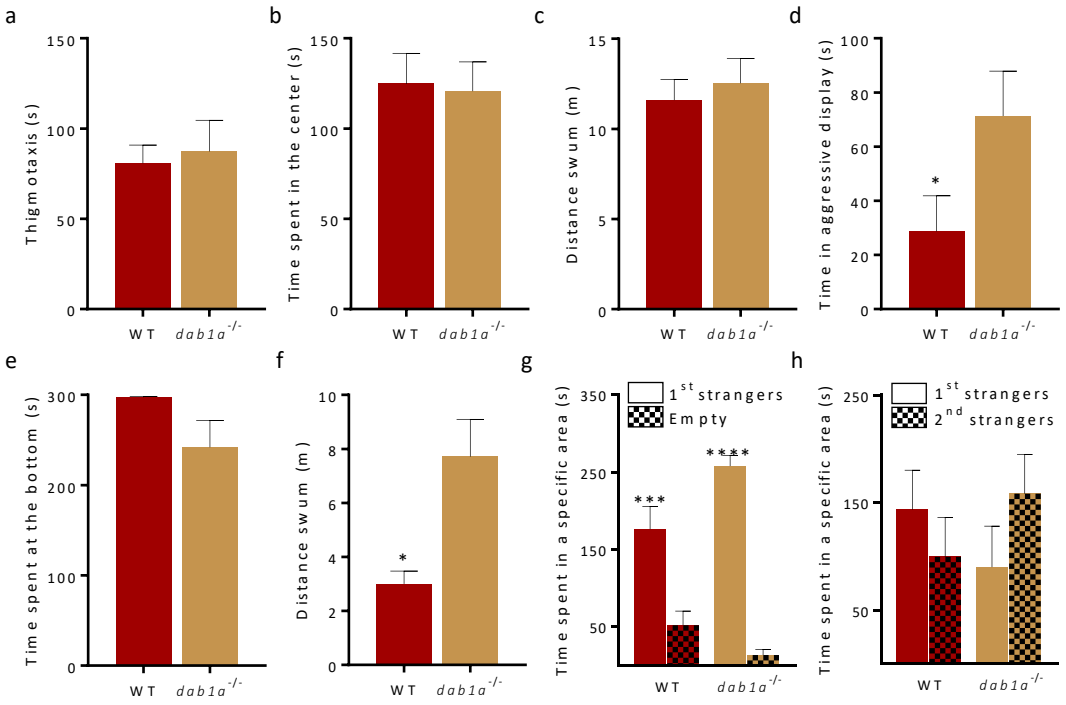

Figure 19. Behaviour of *dab1a*$^{-/-}$ zebrafish. (a-c) *dab1a*$^{-/-}$ exhibit normal behaviour in the open field test. **(a)** Time at side of the tank (p = 0.75) and **(b)** time in center of the tank (p = 0.87). **(c)** Locomotion (p = 0.61). n = 10 WT and n = 7 *dab1a*$^{-/-}$. Unpaired t-tests with Welch's correction. **(d)** *dab1a*$^{-/-}$ display heightened aggression levels compared to WT (p = 0.0445). **(e)** *dab1a*$^{-/-}$ exhibit normal anxiety-like behaviour. Time at the bottom of novel tank (p = 0.06). **(f)** *dab1a*$^{-/-}$ fish are more active in the novel tank test (p = 0.0133). n = 10 WT and n = 7 *dab1a*$^{-/-}$. Mann Whitney U test (*) p < 0.05. **(g,h)** Visually-mediated social preference test. **(g)** Both genotypes prefer to spend time near a group of unfamiliar fish (1st strangers; p = 0.0005 and p < 0.0001 respectively). **(h)** WT and *dab1a*$^{-/-}$ spend equal time near both groups when a second unfamiliar group is added (2nd strangers; p = 0.61 for WT and p = 0.44 for *dab1a*$^{-/-}$). Two-way ANOVA with Tukey and Sidak's post hoc comparisons. n = 10 WT and n = 7 *dab1a*$^{-/-}$. *** p < 0.001, **** p < 0.0001. Mean ± SEM.

vldlr$^{-/-}$ mutants spent significantly more time in center of the novel tank (p = 0.03, Figure 20b), while the time spent at the side (p = 0.15, Figure 20a) and locomotion were not affected (p = 0.71, Figure 20c). No difference in aggression levels between WT and *vldlr*$^{-/-}$ were found (p = 0.09, Figure 20d) nor did they exhibit anxiety-like behaviour, since the time spent at the bottom of novel tank (p = 0.32, Figure 20e) and the locomotion were comparable between the two genotypes (p = 0.86, Figure 20f). Regarding the visually-mediated social preference test, both WT and *vldlr*$^{-/-}$ preferred to spend time near a group of unfamiliar fish (1st strangers; p < 0.0001 for both genotypes, Figure 20g). They also spent equal time near both groups when a second unfamiliar group was added (2nd strangers; p = 0.58 for WT and p = 0.73 for *vldlr*$^{-/-}$, Figure 20h).

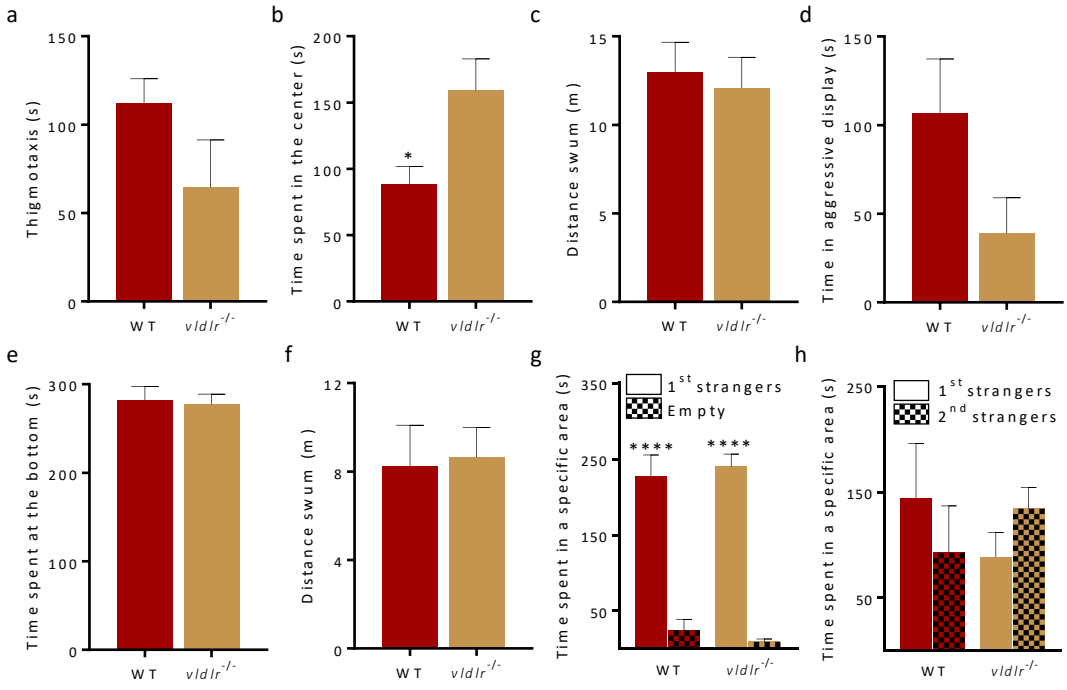

Figure 20. Behaviour of *vldlr*$^{-/-}$ zebrafish. (a-c) *vldlr*$^{-/-}$ behaviour in the open field test. **(a)** *vldlr*$^{-/-}$ spent the same time at side of the tank (p = 0.15) compared to WT but **(b)** more time in center of the tank (p = 0.03). **(c)** Locomotion (p = 0.71). n = 10 WT and n = 7 *vldlr*$^{-/-}$. Unpaired t-tests with Welch's correction. **(d)** No difference in aggression levels between WT and *vldlr*$^{-/-}$ (p = 0.09). **(e)** *vldlr*$^{-/-}$ exhibit normal anxiety-like behaviour. Time at the bottom of novel tank (p = 0.32), **(f)** locomotion in a novel tank (p = 0.86). n = 10 WT and n = 7 *vldlr*$^{-/-}$. Mann Whitney U test. (*) p < 0.05. **(g,h)**. Visually-mediated social preference test. **(g)** Both genotypes prefer to spend time near a group of unfamiliar fish (1st strangers; p < 0.0001 for both genotypes). **(h)** WT and *vldlr*$^{-/-}$ spend equal time near both groups when a second unfamiliar group is added (2nd strangers; p = 0.58 for WT and p = 0.73 for *vldlr*$^{-/-}$). Two-way ANOVA with Tukey and Sidak's post hoc comparisons. n = 7 wild-type and n = 7 *vldlr*$^{-/-}$. **** p < 0.0001.

3.3 Discussion

3.3.1 Reelin is localised to laminated areas of the brain that are important for cognition, emotion and learning

The zebrafish brain is an interesting system to study Reln function because of its distinctive anatomical features compared to other organisms. The zebrafish telencephalon has a non-laminar structure. It develops through eversion when the dorsal region of the telencephalic neural tube (pallium) folds over the ventral region (subpallium), generating an everted non-laminar telencephalon (Folgueira et al., 2012). Conversely, the mammalian cortex has one of the most complex architectures in the vertebrate CNS, characterized by a six-layered laminar structure and expanded surface areas (Nieuwenhuys, 1994) that develops through evagination (Mueller et al., 2011).

Nevertheless, the zebrafish brain possesses several laminar structures such as the optic tectum, the cerebellum, the torus semicircularis and the retina. These anatomical differences have to be considered during the analysis of Reln localisation and function in zebrafish. In the zebrafish telencephalon, Reln function is unlikely to be associated with lamination *per se*, although it might still be linked to a general role in axon guidance. High levels of Reln are found in the medial part of the dorsal telencephalon (Dm) and in the ventral nucleus of the ventral telencephalon (Vv). Interestingly, the Dm has been proposed to be homologous to the pallial amygdala in tetrapods (Ganz et al., 2014). Pallial structures are known to control motor, sensory and cognitive functions, like learning, memory and emotion. In agreement with the suggestion from Costagli et al., it is likely that Reln has a key role in the integration of sensory afferent information coming from tectum and diencephalon directly to the dorsal telencephalon (Costagli et al., 2002). The link between Reln and the processing of sensory information could be mediated by the NMDAR/PSD-95/CamKII pathway, which influences calcium levels controlling synaptic plasticity (Lee and D'Arcangelo, 2016). The presence of Reln in this area, which is important for cognition, might be relevant for the role of Reln in the aetiology of ASD. Moving caudally Reln is localised in a layer-specific manner in two layers of the optic tectum: the stratum fibrosum marginale (sfm) which is underneath the pia mater and glia limitans membranes, and the stratum opticum (so) directly below it. The optic tectum is the principal retinorecipient brain region in zebrafish and it is homologous to the superior colliculus in mammals (Gebhardt et al., 2013). The sfm is a plexiform-type layer filled with a dense assortment of axons, axon terminals and dendrites, whereas the so is formed of bundles of optic nerve terminals (Corbo et al., 2012). In fact, the so layer is targeted by retinal ganglion cells axons (Gebhardt et al., 2013). Reln localisation in the laminated optic tectum might suggest that Reln could be involved in the positioning of cell groups in zebrafish. Even higher levels of Reln are found in the torus longitudinalis which is a paired, longitudinal eminence of granular cells attached to the medial margins of the optic tectum. It is specific to ray-finned fish (Evans and Claiborne, 2005). Interestingly, the granule cells present in the torus longitudinalis project unmyelinated axons through the sfm of the adjacent optic tectum, to synapse with the spiny dendrites of tectal pyramidal cells. Therefore, the torus longitudinalis seems to be involved in learning complex visual scenes (Northmore, 2017)

and learning impairments are another hallmark of ASD. More caudally, in the region of the isthmic tegmentum, Reln is found in a few cells at the level of the interpeduncular nucleus, which is a structure that receives projections from the dorsal habenula nuclei (Amo et al., 2010). The dorsal habenula has been shown to be involved in stress, depression, memory function and nicotine withdrawal (Viswanath et al., 2014). In the hindbrain Reln is present in cerebellum structures and in the medulla oblongata. Specifically, in the CCe, Reln is found in the granule cell layer of the corpus cerebelli and no expression of Reln has been found in the Purkinje and molecular cell layer of the CCe. Reln is also present in the LCa of the cerebellum which consists only of granule cells, and in the CC which is a cerebellum-like structure proposed to function as part of the cerebellum. The granule cells of the CCe send their axons to Purkinje cells in the molecular layer of the cerebellum, whereas the granule cells of the LCa also send their axons to the dendrites of crest cells in the CC of the dorsal hindbrain (Takeuchi et al., 2015). Therefore, the areas where Reln localises are also all functionally linked to each other. Recent work has focused on the implication of the cerebellum in cognition and emotion, suggesting that impairments in cerebellar function may lead to disorders such as ASD (Reeber et al., 2013). The possible involvement of the cerebellum with ASD will be discussed in more detail in the general discussion (paragraph 6.2). Scattered Reln-positive cells are also present in the intermediate and inferior part of the reticular formation (RF) throughout the medulla oblongata. The RF is an intricate network of excitatory and inhibitory neurons and diffuse nuclei, which extends from the spinal cord throughout the medulla oblongata to the mesencephalon. The reticular formation integrates sensory inputs with its network of neurons being involved in the control of breathing, vasomotor tone, pain, somatomotor functions, and other homeostatic processes (Gray, 2013).

Taken together, all this information leads to two main conclusions: i) Reln is present in laminated structures of the optic tectum and cerebellum. Therefore, its role in neuronal migration could be conserved in zebrafish. This hypothesis has been recently confirmed by a study that shows that synaptic lamination in the larval zebrafish optic tectum is regulated by an attractive Reln concentration gradient (Di Donato et al., 2018). ii) High levels of Reln are found in central nervous system structures that are important for

cognition, emotion, learning and sensory information processing. The impairment of these features is the main hallmark of ASD, and defects in synaptic plasticity are one of the fundamental causative factors underlying ASD pathology (Gilbert and Man, 2017). Thus, the presence of Reln in these regions strengthens the idea of Reln being involved in the aetiology of ASD.

3.3.2 *reln*$^{-/-}$ mutant zebrafish do not show striking neuroanatomical defects

reeler mice have severe hypoplasia of the cerebellum and impaired cytoarchitecture of other laminated brain structures. We therefore, decided to characterize the cytoarchitecture of the *reln*$^{-/-}$ CNS. Given the low number of samples analysed per genotype it was not possible to perform statistical analysis, therefore this is just a descriptive analysis of what was observed. The only difference found between WT and *reln*$^{-/-}$ was a decreased number of neurons in the sfgs layer of the optic tectum. The optic tectum is a multi-layered structure with a dense neuropil, and it has been shown that many of the large type I interneurons of the sfgs express high levels of *reln* mRNA (Costagli et al., 2002). Therefore, if confirmed, neuronal ectopia defects in the tectal sfgs layer of *reln*$^{-/-}$, could be explained not only by the expression of *reln* in the tectal sfgs layer and Reln protein localisation in the sfm and so layer of the optic tectum, but also by Reln's role in the regulation of synaptic lamination (Costagli et al., 2002; Di Donato et al., 2018).

3.3.3 Visually-mediated preference for social novelty is impaired in *reln*$^{-/-}$

In order to investigate whether Reln dysfunction might be a vulnerability factor in ASD we characterised the behaviour of *reln*$^{-/-}$. Mutants do not show any abnormal aggression or anxiety-like behaviour. We assessed the social phenotype using two different tests: the VMSP and shoaling, which measure different aspects of social behaviour. Typically, zebrafish have strong shoaling tendencies and they tend to approach a group of conspecifics. *reln*$^{-/-}$ and WT have comparable value of NND and IID, meaning that they have a conserved tendency to shoal. Other shoaling parameters such as polarization and velocity were not impaired in *reln*$^{-/-}$. The cluster score analysis

confirmed this finding since the level of group cohesion for *reln*$^{-/-}$ was not significantly different from WT. The VMSP test is based on the fact that zebrafish are visually drawn to conspecifics. It is possible to utilize this innate inclination to test preference for social interaction and novelty. In agreement with their normal shoaling behaviour, during the social preference step of the experiment *reln*$^{-/-}$ behaved in the same way as the WT, spending most of the time swimming close to the first group of strangers. Very interestingly during the preference for social novelty step of the experiment, *reln*$^{-/-}$ behave differently from the WT, since they do not switch preference to the second group of unfamiliar fish. The social behavioural defects of *reln*$^{-/-}$ are very specific and occur only with the presence of a novel social stimulus (second group of strangers) when a first one is already present (first group of strangers) and not during normal shoaling. There are two points that have to be considered when interpreting this behaviour. Although social interaction plays a fundamental role in this experiment, the ability to attend to two simultaneous stimuli might also be measured. One interpretation of this behaviour might be based on the fact that simply *reln*$^{-/-}$ fish have a preference for the first stimulus and they are not attracted by the novelty. Another hypothesis could be that mutants are so focussed on the first stimulus that they do not switch attention to the second one. Indeed, one of the diagnostic criteria for ASD reported by the Diagnostic and Statistical Manual of Mental Disorders (DSM-5, Edition 2013) includes information about restricted interests and repetitive patterns of behaviour, stating that autistic patients might have highly restricted, fixated interests that are abnormal in intensity or focus.

3.3.4 HPLC analysis of monoamines and metabolites reveals increased level of serotonin in the hindbrain of *reln*$^{-/-}$

To correlate the behavioural phenotype of *reln*$^{-/-}$ to changes in basal levels of monoamine neurotransmitters in the CNS, we carried out HPLC and identified increased levels of 5-HT in the mutant hindbrain. The effect of RELN haploinsufficiency on the serotoninergic system, has been already studied in HRM (Varela et al., 2015). Due to the localisation of RELN to dendritic spines, which are the primary location where synaptic connections are established, Varela et al hypothesized that RELN

haploinsufficiency may affect the expression of serotonin 5-HT_{2A} receptors. They questioned whether abnormalities in RELN could contribute to impaired serotoninergic neurotransmission. Indeed, they show that the expression of 5-HT_{2A} receptors is increased in the striatum and are decreased in the cerebral cortex (Varela et al., 2015). We have demonstrated that *reln*$^{-/-}$ have an increased level of 5-HT in the hindbrain. This alteration might be explained by the fact that most of the serotonergic nuclei in the zebrafish are found in the hindbrain specifically in the raphe populations and in the area postrema (Herculano and Maximino, 2014). Moreover, other serotoninergic pathways components are expressed in the hindbrain or even in the same cell populations that express Reln, and therefore they could be affected by the lack of Reln. For example, *tph2* and *vmat* are also expressed in the raphe nuclei and in the RF (Ren et al., 2013; Teraoka et al., 2004; Wen et al., 2008) while *serta* is only expressed in the raphe nuclei (Norton et al., 2008). As previously shown in section 3.2.1, Reln is highly expressed in scattered cells in the RF throughout its extension in the medulla oblongata.

5-HT not only regulates important aspects of human behaviour related to NPD, such as social behaviour, but also regulates brain development, cell division and differentiation, neurite growth, and synaptogenesis (Chugani, 2002). The association between abnormal 5-HT activity and autism has been investigated through the years, showing that both hyperserotonemia and hyposerotonemia occurs in ASD patients (Connors et al., 2006; Schain and Freedman, 1961; Yang et al., 2014). It is therefore tempting to hypothesise that the increased level of 5-HT in the hindbrain caused by the lack of Reln could lead to the impaired social behaviour that we observed.

3.3.5 Buspirone, oxytocin and risperidone do not alter preference for social novelty in *reln*$^{-/-}$

Three different compounds were tested to try and rescue the impaired preference for social novelty of *reln*$^{-/-}$. The first drug tested was buspirone, which is an agonist of 5-HT_{1A} receptors and decreases serotonin levels. Buspirone decrease firing of dorsal raphe serotonin neurons, synthesis and release of serotonin (Baldessarini, 1996). Numerous studies have already shown that buspirone can have anxiolytic and pro-social effects in zebrafish (Barba-Escobedo and Gould, 2012; Bencan et al., 2009; File and Seth, 2003;

Gould, 2011; Gould et al., 2012; Maaswinkel et al., 2013; Maaswinkel et al., 2012). According to these results, buspirone treatment increases the preference for social novelty in both WT and *reln*$^{-/-}$, but not enough to completely rescue this impairment in mutants. The second compound tested in this study was oxytocin. Oxytocin signalling has been suggested to be impaired in ASD patients and clinical evidence demonstrates that acute oxytocin administration can improve social function and reduced repetitive behaviour in autistic individuals (Andari et al., 2010; Guastella et al., 2010; Higashida et al., 2012; Hollander et al., 2007; Hollander et al., 2003; Striepens et al., 2011). Oxytocin administration can ameliorate social deficits and repetitive behaviour in mouse models with a different effect according to the dose and genotype. In fact, two different mice strains exhibited increased sociability upon sub-chronic intraperitoneal oxytocin administration, and one of the two strains had decreased motor stereotypy after a single acute exposure to oxytocin (Teng et al., 2013). In this project acute oxytocin administration did not rescue the impaired preference for social novelty observed in *reln*$^{-/-}$, with the mutants still spending most of the time close to the first group of unfamiliar fish. The final compound that we tested was risperidone, an atypical antipsychotic medication. Risperidone is one of the most widely used drugs in the treatment of ASD. Together with aripiprazole, they are the only two medications which are approved by the Food and Drug Administration (FDA) to treat symptoms of ASD (DeFilippis and Wagner, 2016; Kumar et al., 2008; Kumar et al., 2009; Prieto, 2014; Prieto et al., 2014; Prieto et al., 2011; Silva et al., 2012) even though evidence of its efficacy are still controversial. Several studies support ameliorations in the overall severity of ASD (Luby et al. 2006; Nagaraj et al. 2006) or in specific primary symptoms including language, communication, socialization, stereotyped and repetitive behaviours (Nagaraj et al., 2006; Pandina et al., 2006; Shea, 2004). However, the biggest randomized placebo-controlled test of risperidone did not show improvements in core ASD symptoms (McDougle et al., 2005), and other studies report the amelioration effect only for irritability (McPheeters et al., 2011). In this project the impaired preference for social novelty observed in *reln*$^{-/-}$ was not rescued by risperidone application.

None of the drugs tested in this study were able to rescue the impaired social phenotype of *reln*$^{-/-}$. But among them, buspirone, seems to be the most promising drug,

since it has a Cohen's d medium size effect in increasing the preference for social novelty in *reln*$^{-/-}$. Usually drug treatments for ASD patients are effective only when administrated chronically for months (DeFilippis and Wagner, 2016). Oxytocin administration to mouse models with face validity to core ASD symptoms, was only able to ameliorate social deficits and repetitive behaviour upon chronic administration that lasted for weeks (Teng et al., 2013). Given the medium size effect of buspirone with single acute administration, our preclinical findings indicate that buspirone might have beneficial effects in treating social defects in *reln*$^{-/-}$, but its effect has to be further tested using a chronic administration regimen.

3.3.6 Behaviour of *dab1a*$^{-/-}$ and *vldlr*$^{-/-}$ mutant zebrafish

Genetic and epigenetic defects in members of the Reln-signalling pathway are linked to ASD risk. *scrambler* and *yotari* are two mouse strains carrying mutations in the mouse homologues of the *Drosophila* gene *disabled 1* (*mDab1*). Similar to *reeler* they both exhibit a reduction in cerebellar size, abnormal cerebral cortical lamination together with neural cell ectopia (Kojima et al., 2000; Sheldon et al., 1997; Yoneshima et al., 1997). *scrambler* mutants are less anxious in the elevated plus-maze but exhibit higher latencies in the emergence test. They show impaired vocalization responses, freezing behaviour, and severe motor coordination impairments on the stationary beam and rotorod tests, even though they are more active in the open field test (Jacquelin et al., 2013; Jacquelin et al., 2012). They also have an abnormal grooming activity (Strazielle et al., 2012). Furthermore, *Dab1* downregulation in mouse causes deficits in memory, pre-pulse inhibition and maternal care (Teixeira et al., 2014). Mice with a selective deletion of *Dab1* in excitatory neurons of the adult forebrain exhibit deficits in learning and memory confirming the hypothesis that *Dab1* is essential for normal hippocampal synaptic plasticity (Trotter et al., 2013). Mice with *Dab1* insufficiency also show impaired neonatal vocalization patterns (Fraley et al., 2016). Moreover, *Dab1* polymorphisms have been shown to be associated with ASD risk in the Chinese Han population (Li et al., 2013). Due to the association of *Dab1* with ASD, we examined the behaviour of *dab1a*$^{-/-}$. *dab1a*$^{-/-}$ exhibit heightened aggression levels compared to WT during the mirror induce aggression test and hyperactivity in the novel tank test. But

the behaviour that could mimic the sociability core symptoms of ASD, analysed with the visually-mediated social preference for novelty test, was unaffected.

The evidence that associate VLDLR insufficiency as a risk for ASD is less strong than the evidence for Dab1. *Vldlr* knock-out mice appear neurologically normal with a normal life span (Frykman et al., 1995), and only mice lacking both *Vldlr* and *ApoER2* exhibit a neurological phenotype. In fact, double *Vldlr*$^{-/-}$/*ApoER2*$^{-/-}$ mice have inverted cortical neuronal layers and a phenotype which is indistinguishable from *reeler* and *scrambler* (Curran and D'Arcangelo, 1998; Gallagher et al., 1998; González et al., 1997; Howell et al., 1997; Sheldon et al., 1997; Sweet et al., 1996; Ware et al., 1997). It has recently been shown that mice with VLDLR insufficiency have abnormal neonatal vocalization patterns (Fraley et al., 2016). Opposite to this it has been reported that post-mortem *VLDLR* mRNA levels are increased in the brain of autistic patients (Fatemi et al., 2005), therefore rats overexpressing VLDLR were generated and tested (Iwata et al., 2012). The overexpression of VLDLR in rats does not cause neuroanatomical abnormalities, but it does lead to have increased locomotor activity with minor deficits in the radial maze task, indicating that VLDLR levels might be involved in regulating locomotor activity and memory function. Given this evidence it is intriguing to test whether a *vldlr*$^{-/-}$ zebrafish model have an impaired behavioural phenotype. In this project we have demonstrated that *vldlr*$^{-/-}$ mutants behave normally overall, with only a minor difference compared to WT in the open field test, where the mutant spent slightly more time in center of the tank that could be related to an increased level of boldness.

Neither *dab1a*$^{-/-}$ or *vldlr*$^{-/-}$, show striking impairments in any of the core features of ASD. Even though *scrambler* and *yotari* mouse strains exhibit severe neurological and behavioural damages, *dab1a*$^{-/-}$ have heightened aggression levels and they are hyperactive in the novel tank test, but the social behaviour was unaffected. This might be due to the fact that zebrafish have two isoforms of the *dab1* gene (*dab1a* and *dab1b*), and the ablation of only one of the two isoforms might not be enough to alter the function of the entire *reln* signalling pathway due to compensation by the remaining isoform. It is debateable whether *VLDLR* ablation or overexpression causes any impairment related to the aetiology of ASD. We have shown that *vldlr*$^{-/-}$ mutants behave normally overall, confirming the evidence from *Vldlr* knock-out mice. VLDLR deficits on

their own might not to be enough to cause any behavioural phenotype resembling ASD symptoms. This might be because RELN and the aetiology of ASD are not connected by the RELN canonical signalling pathway, which relies on VLDLR. Conversely, because of compensatory effects, deficits in VLDLR alone may not enough to cause the disorder.

Chapter 4 Generation of a *ywhaz* mutant line

Associations have been found between the 14-3-3ζ isoform (YWHAZ) of the 14-3-3 protein and autism spectrum disorder (ASD) (Toma et al., 2014). In order to shed light on the potential role of YWHAZ dysfunction in ASD we used the Clustered Regularly Interspaced Short Palindromic Repeats/CRISPR associated protein-9 nuclease (CRISPR/Cas9) technique to establish a stable zebrafish *ywhaz* mutant line. To do so, we modified protocols from Auer and Del Bene, Gagnon and colleagues, and Hwang and colleagues (Auer and Del Bene, 2014; Gagnon et al., 2014; Hwang et al., 2013).

4.1 CRISPR/Cas9 mutagenesis

Clustered Regularly Interspaced Short Palindromic Repeats (CRISPR), together with CRISPR associated (Cas) proteins, provide bacteria and archaea an acquired resistance to invading viruses and plasmids (Wiedenheft et al., 2012). The type II CRISPR-Cas system is composed of a CRISPR RNA (crRNA), a trans-activating RNA (tracrRNA) and the Cas9 endonuclease which directs sequence-specific silencing of foreign nucleic acids (Gasiunas et al., 2012). A synthetic guide RNA (sgRNA), consisting of a single chimeric version of tracrRNA and crRNA, can direct Cas9 endonuclease-mediated cleavage of target DNA *in vitro* (Jinek et al., 2012). Customizable sgRNAs can be used to induce small insertions/deletions (indels) in embryos through incorrect repair of double-strand breaks, producing loss-of-function alleles for genes of interest due to frameshift mutations (Brocal et al., 2016; Hwang et al., 2013). In conclusion, Cas9 endonucleases together with CRISPR sequences constitute the basis of a technology which can be used for genome editing (Zhang et al., 2014).

4.1.1 Design of the target sequence and sgRNA

We used the CHOPCHOP web tool (Labun et al., 2016; Montague et al., 2014) to design the sgRNA targeting *ywhaz* used in this project. CHOPCHOP identifies sequences in the

gene of interest that can be used as a target site when they meet the following criteria: 5'-GG-$(N)_{18}$-NGG-3', whereby NGG is a small motif known as the proto-spacer adjacent motif (PAM). In bacteria and archaea, the PAM is recognised by the Cas9 protein and is only present in the foreign sequence (invading viruses and plasmids), allowing Cas9 to distinguish between self and non-self (Marraffini and Sontheimer, 2010). We therefore selected a target sequence containing the PAM motif within the genomic sequence of *ywhaz*. Conversely, the sgRNA was designed without it, with the purpose of leading the Cas9 protein to cleave the target DNA. The target sequence that we designed is GGGTGACTATTACCGCTACCTGG, where TGG is the PAM motif, and it is complementary to a sequence in the third exon of *ywhaz* gene. The sgRNA corresponds to GGGTGACTATTACCGCTACC (Figure 21).

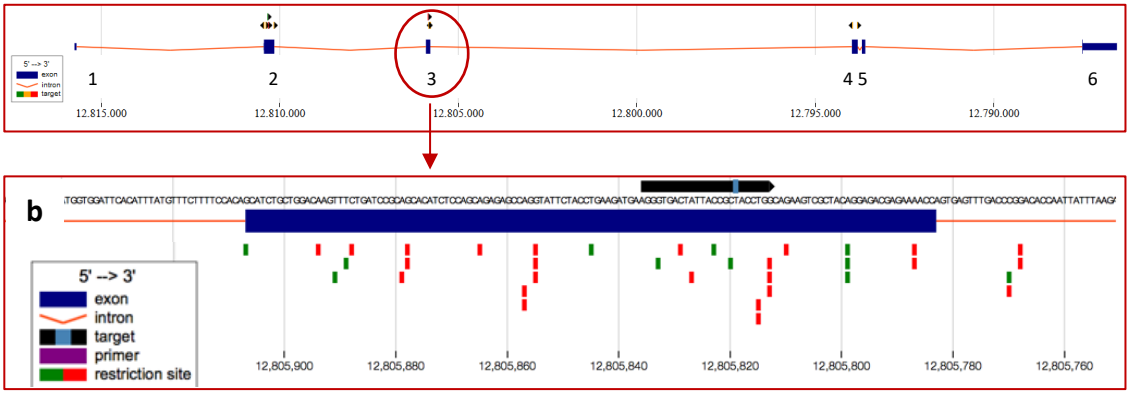

Figure 21. Design of target sequence and sgRNA for *ywhaz* using the CHOPCHOP web tool. (a) All the possible target sequences in *ywhaz* (arrowhead) found by CHOPCHOP are shown above every exon (blue bars). Introns are represented as red lines in between exons. **(b)** The target sequence selected (black bar) within the third exon (blue bar) is represented here in greater details. Figures are taken and adapted from http://chopchop.cbu.uib.no.

4.1.2 Checking for single nucleotide polymorphisms in and around the target sequence using the T7 Endonuclease I assay

Single nucleotide polymorphisms (SNPs) in and around the target sequence can affect enormously the efficiency of CRISPR/Cas9 itself and the subsequent ease with which mutations can be identified. Thus, the first step after designing the target sequence is to check for SNPs or other variants in and around the target site in the WT breeding stock. Five pairs of fish which to be used to generate the embryos for the sgRNA/Cas9 microinjection were first selected. After extracting genomic DNA from 10 adult WT fish (5 of each sex), we amplified the area around the CRISPR target site by PCR with primers

designed to anneal approximately 150-200 base pairs (bp) upstream and downstream of the expected cut site: forward (Fw) primer 5'- TGACCTGGTTTCTGAGCTGA -3' and reverse (Rv) primer 5'- TGCTGAACATCAAAGACCATCT -3'. The master mix consisted of 1 µl genomic DNA, 5 µl ReadyMix™ Taq PCR Reaction Mix with $MgCl_2$ (Sigma-Aldrich), 0.5 µl forward primer (10 µM) and 0.5 µl reverse primer (10 µM) in a final volume of 10 µl. The thermo-cycling conditions were: 95°C for 5 min followed by 35 cycles of 95°C for 30 s, 57°C for 30 s, and 72°C for 60 s. At this point we used the T7 Endonuclease I (T7EI) assay to check if any mutation was present in and around the target site. This assay is useful at two stages of the CRISPR procedure: at the very beginning to confirm the absence of mutations in the WT breeding stock, and after sgRNA/Cas9 microinjection to detect the occurrence of mutations. T7EI recognises and cleaves heteroduplexes and non-perfectly matched DNA in one of the first three phosphodiester bonds that is 5' to the mismatch. This means that when a WT sequence is hybridized with a sequence containing a mutation (SNP or indel), the T7EI cleaves immediately upstream of the specific mismatch, whereas if two WT sequences are hybridized perfectly together the T7EI does not cleave the amplicon. 5 µl of PCR product derived from each male was mixed with 5 µl of genomic DNA from each female and the samples were diluted to a final volume of 20 µl. We denatured the samples and then reannealed them with the addition of 2 µl of NEBuffer 2 (New England Biolabs) using a thermocycler and the following protocol (95°C, 5 min; 95-85°C at −2°C/s; 85-25°C at −0.1°C/s; hold at 4°C). Hybridized PCR products were then treated with 2 U T7EI at 37°C for 1 hour in a reaction volume of 20 µl. The action of the T7EI can be visualized by gel electrophoresis, where the presence of two bands, of 225 and 136 bp, represents a mutation in the target sequence whereas a wild type sequence will be displayed as a single band of 361 bp. To select WT fish for the breeding stock in this project, we performed the T7EI assay, and chose fish which have as result of the treatment a single band of 361 bp (Figure 22).

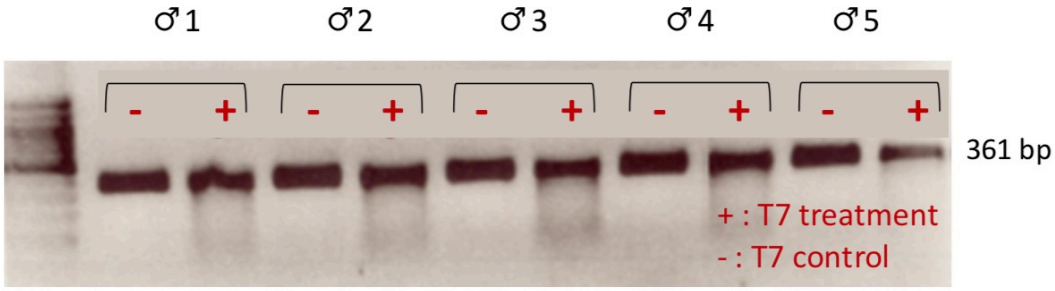

Figure 22. Gel showing an example of the results of the T7EI assay. The genomic DNA of female number 1 (♀1) was mixed individually with the genomic DNA of each male (♂ 1 to 5), and the samples obtained were subject to T7EI assay. + denotes the samples that were treated with the T7 endonuclease enzyme and – denotes the negative control that was not treated with the enzyme.

4.1.3 Production of sgRNA

We used the pDR274 vector, a gift from Keith Joung (Addgene plasmid #42250) (Hwang et al., 2013) to generate the template for sgRNA transcription. This vector harbours a T7 promoter upstream of a partial guide RNA sequence (Figure 23). In order to construct a plasmid containing the designed sgRNA, the vector was digested with *BsaI* restriction enzyme (New England Biolabs), dephosphorylated using Antarctic phosphatase following the manufacturer's instructions (New England Biolabs) and purified from a gel.

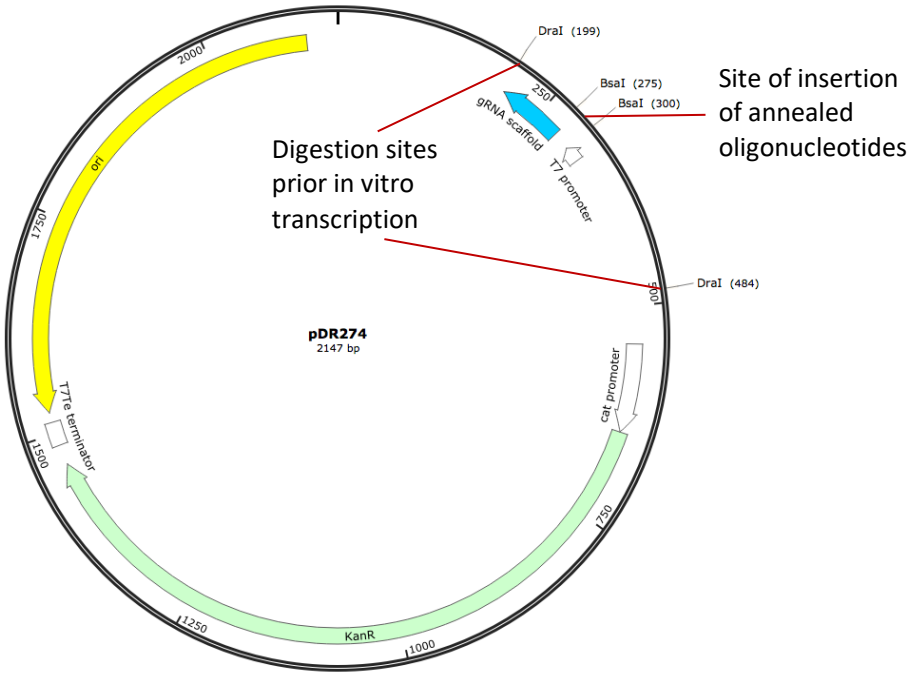

Figure 23. Structure of pDR274 vector. The empty backbone of the pDR274 gRNA expression vector is used to produce a sgRNA of a specific sequence. A pair of annealed oligonucleotides with the designed sequence are cloned into the vector backbone at the level of the *BsaI* restriction enzyme site. After digestion with the *DraI* restriction enzyme the T7 promoter is used for the *in vitro* transcription, resulting in the final sgRNA which is composed of the sgRNA specific sequence and its scaffold. Picture adapted from Addgene plasmid website, #42250.

A pair of annealed oligonucleotides were then cloned into the vector backbone. For directional cloning into the *BsaI*-digested vector, the annealed oligonucleotides have to have the specific overhangs shown in bold in Table 5. Before the cloning step, the oligonucleotides were phosphorylated using T4 Polynucleotide Kinase following the manufacturer's instructions (New England Biolabs) and annealed by incubation at 95°C for 5 minutes follow by slowly decreasing the temperature.

Table 5. Oligonucleotides designed to generate sgRNA. The oligonucleotides were purchased from Thermo Fisher Scientific.

Target site (5'-3') (PAM is in bold)	
GGGTGACTATTACCGCTACC**TGG**	
Oligonucleotide 1 (5'-3')	**Oligonucleotide 2 (5'-3')**
TAGGGTGACTATTACCGCTACC	**AAAC**GGTAGCGGTAATAGTCAC

The sgRNA was transcribed using a mMESSAGE mMACHINE® Kit following the manufacturer's instructions (Life Technologies) using the *DraI*-digested gRNA

expression vector as a template. The sgRNA was DNase treated and precipitated with ammonium acetate/ethanol following standard procedures. The RNA concentration was quantified using a NanoDrop spectrophotometer, diluted to 100 ng/µl and stored at -80°C.

4.1.4 Production of Cas9 mRNA

Cas9 mRNA was transcribed from the pMLM3613 vector using a mMESSAGE mMACHINE® T7 Ultra Kit following the manufacturer's instructions (Life Technologies). The pMLM3613 was a gift from Keith Joung (Addgene plasmid #42251)(Hwang et al., 2013). This vector has a unique *PmeI* restriction site positioned 3' at the end of the Cas9 coding sequence. The *Cas9* mRNA was DNase treated and precipitated with ammonium acetate/ethanol following standard procedures. The RNA concentration was quantified using a NanoDrop spectrophotometer, diluted to 500 ng/µl and stored at -80°C.

4.1.5 Microinjection of sgRNA/Cas9 in one-cell stage embryos

Embryos were collected by natural mating of pairs of wild-type zebrafish. 200-250 one-cell stage embryos were co-injected with approximately 1 nl total volume of Cas9-encoding mRNA (250 ng/µl) and sgRNA (25 ng/µl) each.

4.1.6 Checking the efficiency of the CRISPR/Cas9 method and identifying founders

The day after the microinjection, ten injected embryos which had developed normally were tested to check the efficiency of the CRISPR/Cas9 method using the T7EI assay. Once positive results had been obtained using the T7E1 assay, specific target site mutations were identified with the MiSeq System. For the T7EI assay, genomic DNA was extracted from a single embryo while for MiSeq analysis samples consisted of a pool of five embryos.

4.1.6.1 Embryonic genomic DNA extraction for T7EI assay and MiSeq analysis

For genomic DNA extraction a single embryo was placed into a microcentrifuge tube containing 20 µl of base solution (25 mM NaOH and 0.2 mM EDTA) and heated to 95°C for 30 minutes. The tube was then cooled to 4°C and 20 µl of neutralization buffer (40 mM Tris-HCl pH 5.0) were added. The sample was centrifuged and the supernatant was used directly as template for PCR. For pools of 5 embryos, 40 µl of base solution were used to cover the embryos and 40 µl of neutralization buffer were subsequently added.

4.1.6.2 Checking the efficiency of the CRISPR/Cas9 with T7EI assay

We checked the occurrence of mutations and the efficiency of the method by using the T7EI assay. Genomic DNA was extracted from ten 24 hpf injected embryos and every individual sample was mixed with WT genomic DNA. Three out of ten embryos analysed carried indels in the target sequence, which were visualized as two extra bands at 225 and 136 bp by gel electrophoresis (Figure 24). Given the positive outcome of the procedure, the rest of the injected embryos were raised to adulthood to form the F0 generation.

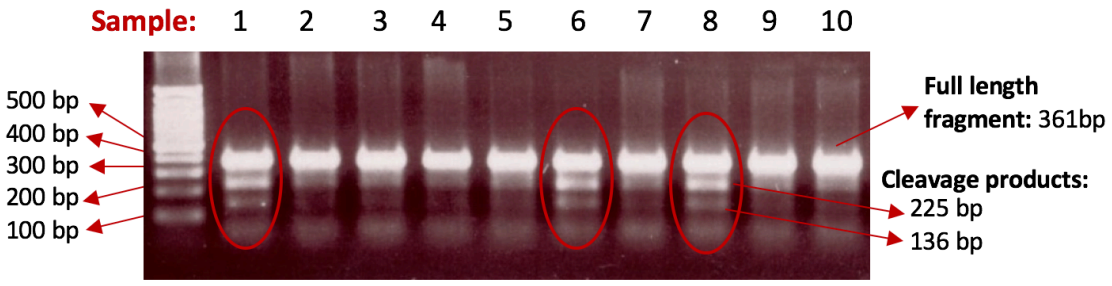

Figure 24. CRISPR/Cas9-mediated indels in *ywhaz*. The genomic DNA of 10 injected embryos (1 to 10) was mixed individually with WT genomic DNA, and the samples obtained were subject to T7EI. The results from the T7EI assay indicate that CRISPR/Cas9 induced cleavage in three out of ten embryos (samples 1, 6 and 8), which have two extra bands at 225 and 136 bp.

4.1.6.3 Screening by amplicon sequencing

In order to identify a founder carrying a mutation of interest that can be transmitted through the germline, we outcrossed a single F0 fish with a WT fish and collected groups

of five embryos produced by each breeding pair. After the extraction of genomic DNA from these pools of embryos, the samples were analysed by MiSeq Illumina sequencing. This technique allows CRISPR-induced indels to be identified and is important for recovering alleles transmitted to the germline. Specific primers containing a partial Illumina adaptor sequence were designed to amplify a region of about 230 bp surrounding the CRISPR target site (Table 6). These primers permit the creation of sequencing-ready libraries by PCR. PCR amplifications were performed in a final volume of 50 µl with 10 µl 5X Q5 Reaction Buffer, 1 µl 10 mM dNTPs, 2.5 µl 10 µM Forward Primer, 2.5 µl 10 µM Reverse Primer, 1 µl Template DNA (genomic DNA from the pools of 5 embryos), 0.5 µl Q5 High-Fidelity DNA Polymerase and 10 µl 5X Q5 High GC Enhancer. The following thermo-cycling profile used was: 95°C for 3 min followed by 35 cycles of 95°C for 30 s, 60°C for 30 s, and 72°C for 30 s.

Table 6. MiSeq Illumina primers. Primers designed for MiSeq Illumina analysis. The sequence underline is the partial Illumina adaptor sequence whereas the rest of the sequence is the part that specifically recognizes the *ywhaz* CRISPR target site. The oligonucleotides were purchased from Thermo Fisher Scientific.

Forward Primer	5'-TCGTCGGCAGCGTCAGATGTGTATAAGAGACAGCATCTGCTGGACAAGTTTCTGA-3'
Reverse Primer	5'-GTCTCGTGGGCTCGGAGATGTGTATAAGAGACAGATAATTGGTGTCCGGGTCAAAC-3'

The quality and size of the amplicons produced by PCR were checked by running 5 µl of each PCR product on an agarose gel. In case of good quality and right size the rest of the samples were purified using a PCR & DNA Cleanup Kit (5 µg) (Monarch®). The DNA concentrations were quantified using a Qubit spectrophotometer and the amplicons were diluted to 15-25 ng/µl prior to analysis. Samples were sequenced using a MiSeq Illumina platform in collaboration with Dr Jason Rihel, University College London, UK. The read out of this analysis are FastQ data files, which were analysed using Geneious software. The MiSeq Illumina sequencing produces files containing the amplicon sequences in both forward and reverse direction. Therefore, the reads have to be paired and aligned to the gene-specific reference sequence. A successful CRISPR experiment will show insertions and deletions in paired sequencing reads around the CRISPR target site. We identified a F0 fish that carries deletions of 6 and 7 bp that are transmitted through the germline to the F1 (Figure 25). The 7 bp deletion (Δ7) at the level of the 380 nt in the third exon of *ywhaz* (380_387delCCTGGCA) causes a frameshift that leads to a

premature stop codon in the third exon. We therefore decided to select this F0 fish which carries the Δ7 mutation as a founder to generate the stable *ywhaz* mutant line.

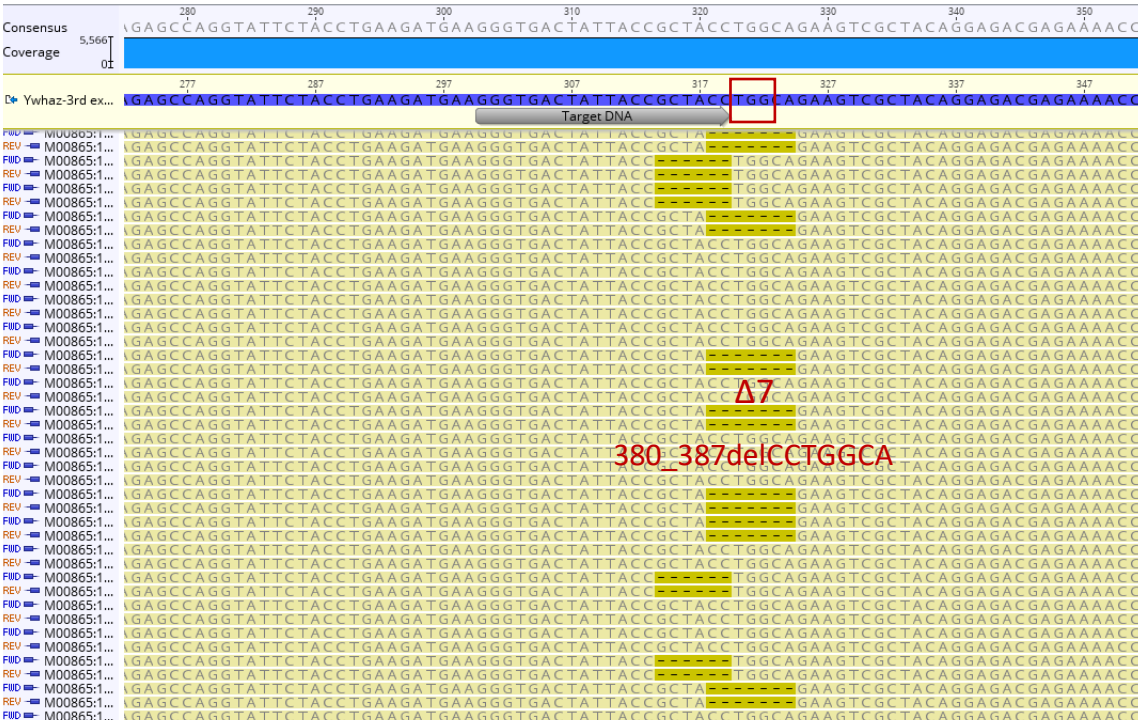

Figure 25. CRISPR/Cas9-mediated deletions of 6 and 7 bp in *ywhaz*. Read out of the MiSeq Illumina analysis indicating the deletions of 6 and 7 bp in *ywhaz* caused by the microinjection of Cas9 mRNA and sgRNA. The grey arrow represents the *ywhaz* target sequence, and the red rectangle the PAM sequence. In yellow, the MiSeq reads are paired and aligned to the gene-specific reference sequence which is shown in purple. Deletions are represented by the dashed line.

4.1.7 Generation of a stable mutant line

The F1 embryos born from the cross between the selected F0 founder carrying the Δ7 mutation and WT were raised to adulthood so that they could be genotyped without sacrificing them. Only the F1 fish carrying the Δ7 mutation, which should be present in heterozygosis, were kept. These fish were then in-crossed to obtain a final F2 stable mutant line homozygous for Δ7. We tested forty F1 fish with the T7EI assay, and found nine carrying indels in the CRISPR target site (data not shown). We further analysed these nine fish with Sanger sequencing and found that five of them (three females and two males) were positive for the presence of the Δ7 mutation (Figure 26).

Figure 26. CRISPR-mediated Δ7 mutation in *ywhaz*. **(a)** The CRISPR target sequence within the third exon of *ywhaz* is aligned with the correspondent sequence carrying the Δ7 mutation. The CRISPR target site, PAM motif and the mutation are indicated. **(b)** Example of a result from the Sanger sequencing showing the frameshift introduced by the Δ7 mutation.

4.1.8 Checking for the presence of off-target cleavage sites

Although the action of Cas9 and its targeting specificity should be tightly controlled by the specific 20 nucleotides of the sgRNA and the presence of the PAM motif next to the target sequence in the genome, potential off-target cleavage activity could still happen at genomic sequences with similarity to the one targeted. It is reported that off-target activity can occur even with only three to five base pair mismatches within the PAM-distal part of the sgRNA sequence (Fu et al., 2013; Zhang et al., 2015a). Therefore, we needed to check that the five F1 fish carrying the Δ7 mutation did not have any off-target cleavage before crossing them to generate the stable mutant line. The CHOPCHOP web tool determines potential off-target sites for all given sgRNAs, and the ones suggested for our sgRNA are summarised in Table 7.

Table 7. Off-target sequences determined by CHOPCHOP.

Number of mismatches	Off-target sequences	Alignment between CRISPR target sequence and off-target sequences	Position	Gene name
2	GGGAGATTATTACCGCTACCTGG	1 GGGTGACTATTACCGCTACCTGG 23 1 GGGAGATTATTACCGCTACCTGG 23	Exonic	*ywhag2*
4	GGGGGCCTATTACGGCTCCCGGG	1 GGGTGACTATTACCGCTACCTGG 23 1 GGGGGCCTATTACGGCTCCCGGG 23	Intronic	*tspan9b*

We used PCR to amplify the areas around these two off-target sites. The primers used were: forward primer 5'- CCTCTTGTCAGTGGCGTACA -3' and reverse primer 5'- TTCTCGGAGGACTCAACCAC -3', for the off-target site present in *ywhag2*, whereas for the one in *tspan9b* the forward primer was 5'- GCAGAGGAATTACGGATGGA -3' and reverse primer was 5'- CGCGTTTATCCTGAGCTTTC -3'. Both PCR reactions were performed in a final volume of 50 µl with 10 µl 5X Q5 Reaction Buffer, 1 µl 10 mM dNTPs, 2.5 µl 10 µM Forward Primer, 2.5 µl 10 µM Reverse Primer, 1 µl genomic DNA (from the F1 fish carrying the Δ7 mutation), 0.5 µl Q5 High-Fidelity DNA Polymerase and 10 µl 5X Q5 High GC Enhancer. The following thermo-cycling profile used was: 95°C for 3 min followed by 35 cycles of 95°C for 30 s, 60°C for 30 s, and 72°C for 30 s. PCR products were purified using a PCR & DNA Cleanup Kit (5 µg) (Monarch®), and analysed by Sanger sequencing. No extra mutations were found in the off-target areas (data not shown).

4.1.9 Genotyping

To discriminate between WT, *ywhaz*$^{+/-}$ and *ywhaz*$^{-/-}$ fish, we designed a genotyping strategy with specific primers that recognise the presence or the absence of the Δ7 allele (Table 8).

Table 8. *ywhaz* genotyping primers. Primers designed to discriminate between WT, *ywhaz*$^{+/-}$ and *ywhaz*$^{-/-}$ fish.

Primers which recognise Δ7 allele	
Ywhaz Forward (5'-3')	TGACCTGGTTTCTGAGCTGA
Mutant Reverse (5'-3')	TGTAGCGACTTCTAGCGGT
Primers which recognise WT allele	
Ywhaz Forward (5'-3')	TGACCTGGTTTCTGAGCTGA
WT Reverse (5'-3')	TAGCGACTTCTGCCAGGTAG
Primers use for internal control	
Control Forward (5'-3')	TGTACAAGTGCAGAAACCCAC
Control Reverse (5'-3')	TATCCGAATCAAGGCCAGGA

The mutant and WT reverse primers only recognise the mutated and WT sequence respectively. Therefore, the mutant reverse primer will amplify only the mutant allele,

when it is present, giving a band of 235 bp, whereas the WT reverse primer will produce a band of 235 bp only in the presence of WT allele. As result, *ywhaz*$^{-/-}$ fish will have a 235 bp amplified band only when the PCR is performed with the reverse mutant primer, whereas WT fish will show the amplicon only when analysed with the reverse WT primer. *ywhaz*$^{+/-}$ will have this fragment amplified in both situations. We also designed a pair of control primers which amplify a region 615 bp upstream in the *ywhaz* gene. The presence of this amplicon in both PCR reactions guarantees the efficiency of the PCR reaction (Figure 27).

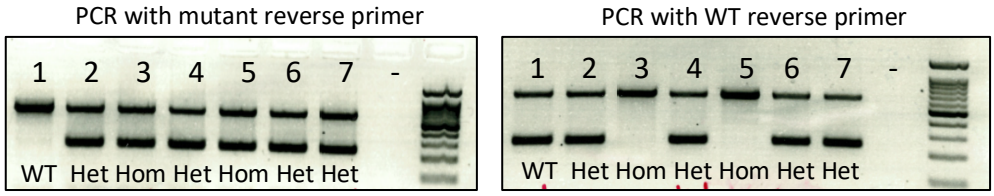

Figure 27. Genotyping PCR for the Δ7 allele. The results of these two PCR reactions allow us to discriminate between WT, *ywhaz*$^{+/-}$ and *ywhaz*$^{-/-}$ fish for Δ7 allele. The amplicon at 615 bp is an internal control that guarantees the efficiency of the PCR reaction and has to be present in every sample. Sample 1 is a WT fish, because there is not the 235 bp amplicon when the sample is analysed with the mutant reverse primer. On the contrary, samples 3 and 5 are homozygous for the Δ7 mutations because, the WT reverse primer does not amplify the 235 bp amplicon. Samples 2, 4, 6 and 7 are heterozygous for the mutations having the 235 bp amplicon amplified with both primers.

4.1.10 Gene expression analysis

The deletion of 7 bp at the level of the 380 nt in the third exon (380_387delCCTGGCA) of *ywhaz* causes a frameshift that led to a premature termination codon (PTC) within the third exon (Figure 28).

Figure 28. Schematic representation of the *ywhaz* locus. The gene consists of five coding exons. The Δ7 mutation 380_387delCCTGGCA introduces a premature stop codon into exon 3.

When indels result in a frameshift and generate a PTC, the corresponding truncated mRNA is predicted to be recognised by the nonsense-mediated mRNA decay (NMD) pathway. The NMD system is able to degrade transcripts harbouring PTCs in a translation-dependent manner resulting in a knock-out (Karousis et al., 2016). However,

NMD does not recognise all the PTC-containing transcripts with the same efficacy, since its activity depends on the position (Eberle et al., 2008; Neu-Yilik et al., 2011) and sequence composition of the PTC (Loughran et al., 2014). Consequently, transcripts harbouring a PTC might still lead to the transcription of C-terminally truncated proteins which could have residual or dominant negative functions. Thus, it is important to check whether the Δ7 mutation in *ywhaz* gives rise to a truncated protein or if the PTC is recognised and degraded by the NMD process. In the first case the mutated protein should consist of 126 amino acids (aa), where the full size Ywhaz protein is 244 aa meaning that 49% of the protein should be lost in the mutant. Ywhaz mediates most of its action thanks to conserved KRRY residues that recognise phosphorylated serine and threonine targets. Since in the mutated truncated protein this KRRY domain is impaired, it would be tempting to hypothesis that the mutated protein would not have a residual function. It is possible to check if the truncated transcript is degraded by the NMD process by analysing the level of *ywhaz* mRNA expression by RT-qPCR. We therefore processed WT and *ywhaz*$^{-/-}$ brains by RT-qPCR as previously described (see paragraph 2.6), observing a significantly decreased level of *ywhaz* expression in *ywhaz*$^{-/-}$ compared to WT ($p < 0.0001$, Figure 29). This suggests that NMD degradation of the truncated *ywhaz* transcript has occurred in mutants.

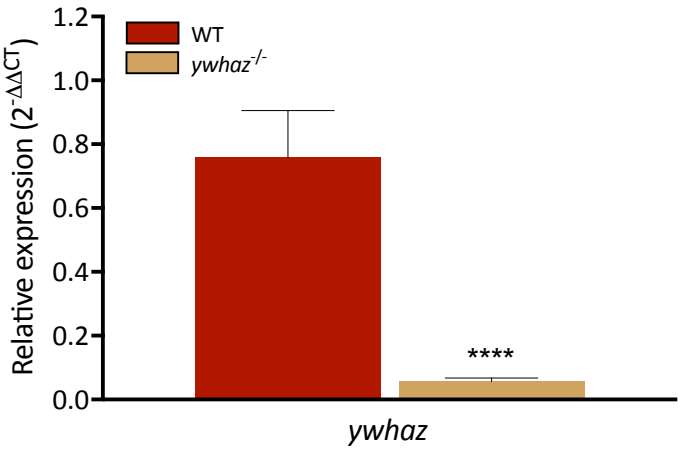

Figure 29. Effects of Δ7 allele on *ywhaz* gene expression. Relative expression profile of *ywhaz* normalised to the reference gene *elongation factor 1a* (*elf1a*). *ywhaz*$^{-/-}$ have a significantly decreased level of *ywhaz* expression ($p < 0.0001$) compared to WT. Mann-Whitney unpaired t-test. n = 10 WT, n = 10 *ywhaz*$^{-/-}$. **** $p < 0.0001$. Mean ± SEM.

In conclusion the *ywhaz*$^{-/-}$ CRISPR/Cas9 mutant line that we generated carries a 7 bp deletion. This causes a frameshift leading to degradation of the truncated *ywhaz* mRNA

possibly via NMD. Therefore, our novel *ywhaz*$^{-/-}$ mutant line can be used to examine Ywhaz function in zebrafish.

Chapter 5 Tyrosine 3-monooxygenase / tryptophan 5-monooxygenase

5.1 Introduction

5.1.1 Tyrosine 3-monooxygenase/tryptophan 5-monooxygenase

The tyrosine 3-monooxygenase/tryptophan 5-monooxygenase activation proteins (also called 14-3-3 proteins or YWHA proteins) were initially described in 1967 as acidic proteins that are abundant in the brain (Perez, 1967). Their name is derived from their elution and migration position on a DEAE-cellulose chromatography gel (Ichimura et al., 1988). 14-3-3 proteins are encoded by seven *YWHA*-genes and the seven isoforms in mammals are named with Greek letters; beta (β), gamma (γ), epsilon (ε), eta (η), zeta (ζ), sigma (σ) and tau (τ). This family of ubiquitously conserved regulatory molecules is expressed in all eukaryotic cells. However, the highest concentration of 14-3-3 proteins is found in the brain, comprising approximately 1% of its total soluble protein (Aitken, 2006; Berg et al., 2003). 14-3-3 proteins are highly conserved. They share 46% of sequence identity between isoforms suggesting functional redundancy (Obsil and Obsilova, 2011). However, most 14-3-3 proteins have high specificity for their binding targets and isoforms have distinct activity, with only some minor overlapping functions. In fact, each isoform has specific binding partners that cannot be bound by other 14-3-3 proteins (Aitken, 2006; Comparot et al., 2003b; Lau et al., 2006; Muslin and Lau, 2005).

5.1.2 The structure of 14-3-3 proteins

14-3-3 proteins are a family of highly homologous 30 kDa acidic proteins that exist as both hetero- and homodimers. An exception to this rule is the 14-3-3σ isoform which preferentially forms homodimers (Benzinger et al., 2005; Bridges and Moorhead, 2005; Gardino et al., 2006; Obsilova et al., 2008; Wilker et al., 2005). One of the first 14-3-3 structures to be determined was the ζ isoform. The mammalian ζ isotype has a cup-shaped dimeric structure. Each monomer is composed of nine α-helices organized in an

antiparallel manner to form an L-shaped structure (Liu et al., 1995; Xiao et al., 1995). The inner part of each monomer consists of two α-helices (α3 and α5) with several charged and polar amino acids and two other alpha helices (α7 and α9) composed of only hydrophobic amino acids, which together form a highly conserved concave amphipathic groove (Figure 30). This amphipathic groove is the site of interaction between 14-3-3 proteins and their phosphorylated and non-phosphorylated ligands (Petosa et al., 1998; Wang et al., 1998). The residues covering the concave surface of the groove are mainly conserved among different isoforms of the 14-3-3 family, whereas the outer surface is variable (Liu et al., 1995; Petosa et al., 1998; Wang et al., 1998; Yaffe et al., 1997). Therefore, the specificity of interaction between 14-3-3 isoforms and specific target proteins may involve the outer surface of the protein, whereas the interaction of ligands which bind well to all isoforms might be mediated by the conserved amphipathic groove (Aitken, 2011; Benzinger et al., 2005; Gardino et al., 2006; Yang et al., 2006). Both the N-terminal and C-terminal of all 14-3-3 isoforms are highly variable. The N-terminal has an essential role in dimer formation, with its sequence determining the number of heterodimer combinations that can occur. This further determines the specificity of targets that can bind each dimer (Aitken, 2011; Chaudhri et al., 2003; Fischer et al., 2008; Kligys et al., 2009; Liang et al., 2008). The carboxyl tail is thought to either regulate the function of 14-3-3 proteins or to stabilize the unliganded structure by interacting with the two internal grooves of the 14-3-3 dimer (Liu et al., 1995).

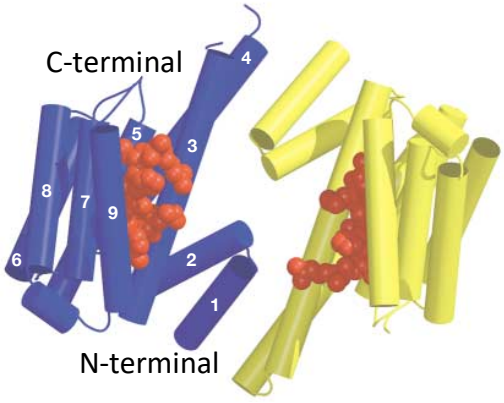

Figure 30. Schematic structure of the 14-3-3ζ dimer. Each monomer contains nine α-helices. The red parts represent phosphopeptides that bind to the amphipathic groove. Image adapted from Berg et al, 2003 and Liddington, The Burnham Institute, La Jolla, California, USA.

5.1.2.1 The 14-3-3 binding motif

The 14-3-3 proteins were the first molecules identified to specifically bind phosphoserine/phosphothreonine (pS/pT) containing motifs (Muslin et al., 1996; Yaffe et al., 1997). In fact, the most common binding site for 14-3-3 proteins is a phosphorylated serine residue (pS) flanked by an arginine (R) and proline (P) residue (Aitken, 2006; Obsil and Obsilova, 2011). The three principal binding motifs of 14-3-3 proteins have been identified: mode I: RSXpSXP, mode II: RX(Y/F)XpSXP, and mode III: pS/pT X_{1-2}-CO_2H (Aitken, 2006; Rittinger et al., 1999; Yaffe et al., 1997). The residues that are important for the binding of these motifs are conserved within all 14-3-3 isoforms, and are localised within the third and fifth helices (α3 and α5) in each monomer (Aitken, 2006). These residues are not solely responsible for binding, since other parts of the protein, such as the C-terminal domain, can modulate 14-3-3 binding as well (van Hemert et al., 2001). Therefore, in addition to the specificity caused by the phosphopeptide-binding motifs, target–protein interactions also depend upon the contacts with the surface of the protein outside of the binding groove (Berg et al., 2003; Truong et al., 2002). Furthermore, in some cases 14-3-3 proteins can also bind non-standard phosphorylated serine/threonine sites and non-phosphorylated targets (Campbell et al., 1997; Fu et al., 1993; Masters et al., 1999; Muslin et al., 1996).

5.1.3 14-3-3 function

The first function of 14-3-3 proteins to be described was activation of Tyrosine and Tryptophan hydroxylase (Th and Tph, respectively) (Aitken, 2006; Ichimura et al., 1987). Nowadays, over 200 binding partners are known to interact with 14-3-3 proteins, suggesting a general regulatory role for these proteins (Aitken, 2011). Once 14-3-3 proteins have bound their targets, they mediate different functions through one of the following mechanisms: i) Covering phosphorylated sites on targeted proteins, blocking the action of phosphatases and causing several alterations to protein activity and localization (Figure 31a) (Toyo-oka et al., 2003; Tzivion and Avruch, 2001). ii) Masking protein-protein interaction sites or protein-DNA interaction sites, thereby physically blocking structural features of target proteins (Figure 31b) (Obsil and Obsilova, 2011).

iii) Occluding the nuclear localisation sequence and altering the subcellular localisation of their binding partners (Figure 31c) (Brunet et al., 2002; Davezac et al., 2000; Obsil et al., 2003). iv) Reshaping the conformation of target proteins by acting as a rigid structure (Figure 31d) (Ganguly et al., 2001; Obsil et al., 2001; Obsil and Obsilova, 2011). v) Acting as a scaffold to facilitate protein-protein interactions, assisting in the creation of protein complexes (Figure 31e) (Ferl et al., 2002; Fu et al., 2000; Ottmann et al., 2007; Vincenz and Dixit, 1996). vi) Regulating the ubiquitination and degradation of targets by masking or exposing the ubiquitination sites of their targets (Figure 31f) (Cornell et al., 2016; Dar et al., 2014; Foote and Zhou, 2012; Mizuno et al., 2007; Toyo-oka et al., 2014).

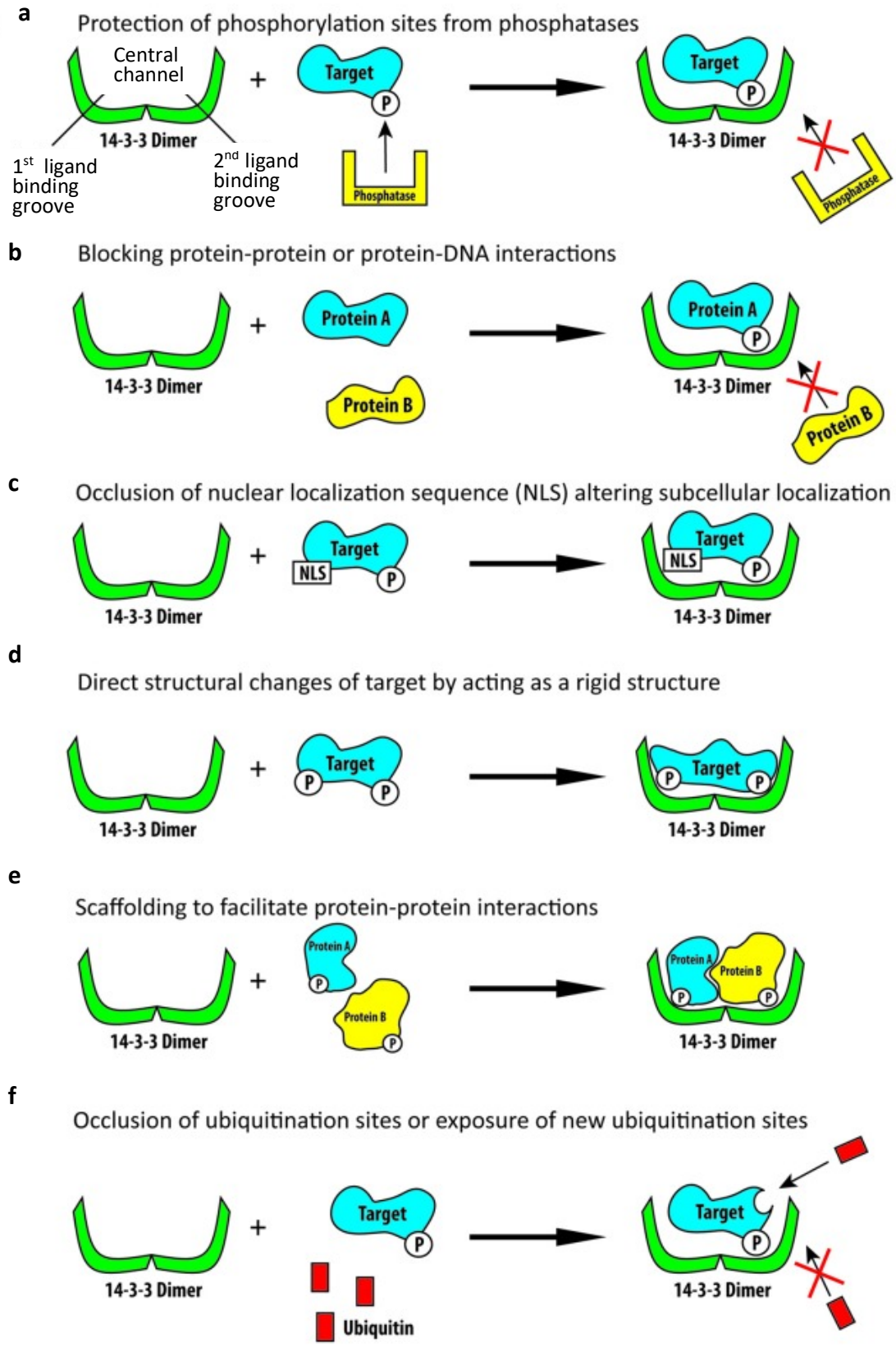

Figure 31. Schematic representation of the functions of 14-3-3 proteins. 14-3-3 proteins can bind phosphorylated targets and **(a)** protect them by phosphatase activity or **(b)** block protein-protein and protein-DNA interaction sites. **(c)** 14-3-3 proteins binding their targets can block localization signals, altering the target's subcellular localization. Acting as rigid structures, 14-3-3 proteins **(d)** can direct structural changes on their targets and **(e)** facilitate the interaction between multiple targets. **(f)** 14-3-3 proteins can either block or expose ubiquitination sites of the targets, regulating their subsequent degradation. Figure adapted from Cornell and Toyo-oka, 2017.

Upon interaction with their effector proteins, 14-3-3 proteins influence a wide range of diverse biological processes including cell growth control, apoptosis, cell signalling, intracellular trafficking/targeting, transcription and cytoskeletal structure, the control of metabolism, transcriptional regulation of gene expression, DNA damage response and neural development (Comparot et al., 2003a; Freeman and Morrison, 2011; Fu et al., 2000; Gardino and Yaffe, 2011; Hermeking and Benzinger, 2006; van Hemert et al., 2001). Although 14-3-3 proteins have such a wide range of molecular functions, they do not seem to have any intrinsic enzymatic properties. Rather, their activity is the result of regulating their protein targets. 14-3-3 proteins can also be subjected to post-translational modifications such as polyglycylation, phosphorylation, fatty acetylation, and alterations caused by oxidative stress (Hamaguchi et al., 2003; Lalle et al., 2010; Martin et al., 1993; Musiani et al., 2011). These post-translational modifications can have different effects on 14-3-3 proteins, including functional regulation, interaction with targets, cellular localization and specificity of dimerization (Aitken, 2011).

5.1.4 14-3-3 proteins and neuropsychiatric disorders

Due to their diverse cellular and molecular roles, 14-3-3 proteins have been associated with many human disorders from cardiomyopathy and cancer to neuropsychiatric disorders (NPD) (Cornell and Toyo-oka, 2016; Foote and Zhou, 2012; Kosaka et al., 2012; Morrison, 2009), including Parkinson's disease (PD), Alzheimer's disease (AD), Creutzfeldt-Jakob disease, schizophrenia and bipolar disorder (Berg et al., 2003; Foote and Zhou, 2012). The involvement of 14-3-3 proteins in so many neurological disorders might be explained by the fact that high levels of 14-3-3 proteins are found in the brain (Berg et al., 2003). They also play an important role in the development of the nervous system, in particular in three key stages of cortical development: neurogenesis and differentiation, neuronal migration and synaptogenesis (Cornell and Toyo-Oka, 2017). In fact, several findings have linked 14-3-3 proteins to neuronal migration defects. Mutations in *Drosophila 14-3-3* genes lead to disruption of neuronal differentiation and synaptic plasticity (Skoulakis and Davis, 1998). Regarding human neurodegenerative disorders, patients affected by Miller-Dieker syndrome (MDS), a more severe form of the neuronal migration disorder lissencephaly, have an extensive deletion of 17p13.3,

the chromosomal segment that includes the gene encoding 14-3-3ε (Nagamani et al., 2009; Toyo-oka et al., 2003). The cortex of embryos with Down's syndrome, have significantly decreased levels of 14-3-3γ, indicating a possible impairment of neuronal differentiation, synaptic plasticity and signalling pathways (Peyrl et al., 2002). Another neurodegenerative disorder associated with abnormal levels of 14-3-3 proteins is Creutzfeldt–Jakob disease (CJD), a condition characterized by dementia and other neurological features. In fact, patients affected by CJD have elevated levels of 14-3-3β, γ, ε, and η isoforms in their cerebrospinal fluid (Wiltfang et al., 2002). Similarly, high levels of 14-3-3γ and ε are found in several brain regions of patients with AD (Fountoulakis et al., 1999). The pathological hallmarks of AD are amyloid plaques and neurofibrillary tangles (NFTs) (Dai and Murakami, 2002) and positive 14-3-3 staining was detected in NFT but not in the amyloid plaques of AD patients (Layfield et al., 1996). Furthermore, based on their localization, binding partners, and neuroprotective function, 14-3-3 proteins have also been associated with PD. PD is characterized by presence of Lewy bodies (Cookson and Bandmann, 2010) and a reduction of dopamine levels in the brain. It has been shown that 14-3-3ε, γ, σ, and ζ colocalise with Lewy bodies (Berg et al., 2003; Kawamoto et al., 2002; Ubl et al., 2002) and 14-3-3ζ is as an endogenous binding partner and activator of TH, the rate-limiting enzyme in dopamine synthesis (Wang et al., 2009). Moreover α-synuclein, one of the main components of Lewy bodies, binds to 14-3-3 proteins and shares over 40% homology with 14-3-3 as well as binding the same partners including TH (Ostrerova et al., 1999). Thus, the interaction between α-synuclein, 14-3-3 and TH might be important in the regulation of dopamine biosynthesis in PD. Moreover, the 14-3-3η isoform binds to and negatively regulates *PARKIN*, an E3 ubiquitin ligase. When mutated, the interaction between *PARKIN* and 14-3-3η is disrupted (Kitada et al., 1998; Sato et al., 2005) and this could be functionally significant for autosomal recessive juvenile Parkinsonism. With regards to neuropsychiatric disorders, genetic analyses have suggested a link between schizophrenia and 22q12-13, the chromosomal region comprising *14-3-3η* gene (Muratake et al., 1996). Moreover, single nucleotide polymorphisms (SNP) in the *14-3-3η* and *ζ* genes have been linked to schizophrenia in a number of human studies (Bell et al., 2000; Jia et al., 2004; Toyooka et al., 1999; Wong et al., 2003). Other 14-3-3 isoforms, such as *14-3-3ε* and *ζ* were identified as potential susceptibility genes for

schizophrenia by post-mortem mRNA analyses (Ikeda et al., 2008; Jia et al., 2004; Wong et al., 2005). A decreased level of *14-3-3η* mRNA was found in the cerebellum of schizophrenics (Vawter et al., 2001), whereas the expression levels of *14-3-3β*, *η*, *ε*, *σ*, *ϑ*, and *ζ* mRNA were significant reduced in their prefrontal cortices (Middleton et al., 2005). Moreover, some schizophrenic brain samples have a reduced level of 14-3-3ζ (English et al., 2011).

5.1.4.1 14-3-3 models of neurological disorders

Given the associations between 14-3-3 family members and several psychiatric disorders, 14-3-3 isoform-specific knockout (KO) mice have been generated to investigate the function of these proteins in the brain. Ablation of 14-3-3ζ in Sv/129 background mice causes neurodevelopmental defects similar to those observed in neuropsychiatric disorders such as schizophrenia, autism spectrum disorder (ASD) and bipolar disorder (Cheah et al., 2012). *14-3-3ζ* KO mice (also called *Ywhaz*$^{-/-}$) exhibit hyperactivity and behavioural and cognitive defects such as a reduced ability to learn, impaired memory and altered sensorimotor gating (Cheah et al., 2012). These defects are accompanied by aberrant development of the hippocampus caused by impaired neuronal migration (Cheah et al., 2012). The hyperactivity of *Ywhaz*$^{-/-}$ mice can be rescued by the antipsychotic drug clozapine, an antagonist of dopamine (DA) and serotonin (5-HT) receptors which is used as a medication for schizophrenia (Ramshaw et al., 2013). *Ywhaz*$^{-/-}$ mice also have increased total tissue DA levels and reduced levels of DA transporter (DAT) (Ramshaw et al., 2013). Since epistatic interactions play an important role in disease pathogenesis, the effects of YWHAZ ablation were also tested in the BALB/c background to define the impact of genetic interactions on the *Ywhaz*$^{-/-}$ phenotype (Xu et al., 2015). Compared to the Sv/129 background, *Ywhaz*$^{-/-}$ BALB/c mice exhibit similar defects including aberrant mossy fibre connectivity and impaired spatial memory. However, they also have additional defects such as enlarged lateral ventricles, reduced synaptic density and mis-patterning of pyramidal neurons in all subfields of the hippocampus. In contrast, the *Ywhaz*$^{-/-}$ BALB/c mice did not display locomotor hyperactivity, a finding that is underscored by normal levels of DAT and DAergic signalling. Taken together, these results demonstrate that dysfunction of *Ywhaz* in mice

causes several pathological hallmarks associated with neuropsychiatric disorders in humans, although the genetic background plays a significant role in the pathophysiology, and severity of disease presentation (Xu et al., 2015). Homozygous 14-3-3ε KO mice (*Ywhae*$^{-/-}$) display abnormal brain development with neuronal migration defects in the cortex and the hippocampus and most of them die at birth (Toyo-oka et al., 2003), whereas heterozygous *Ywhae*$^{+/-}$ mice show a milder migration defect and appear healthy and fertile. *Ywhae*$^{+/-}$ mice exhibit weak defects in working memory in the eight-arm radial maze and moderately enhanced anxiety-like behaviour in the elevated plus-maze (Toyo-oka et al., 2003). Therefore, *Ywhae* is a possible susceptibility gene that functions protectively in schizophrenia (Ikeda et al., 2008), and *Ywhae*$^{+/-}$ may be a model for some aspects of this disease. 14-3-3γ deficient mutant mice (*Ywhag*$^{-/-}$) have also been characterised. They display a normal morphology of the cortex and cerebellum, with normal behaviour and life span (Steinacker et al., 2005). Therefore, the specificity of action of 14-3-3 proteins is reflected in mice with mutations in different *14-3-3* genes since they show distinct anatomical and behavioural features. Epistatic interactions also play an important role in disease pathogenesis as observed in *Ywhaz*$^{-/-}$ mice with different backgrounds.

5.1.4.2 14-3-3 ζ and autism spectrum disorder

Associations have been found between the 14-3-3ζ isoform and ASD. The ζ isoform (YWHAZ) codes for a postsynaptic protein that physically interacts with numerous ASD gene products (Toma et al., 2014). Toma and colleagues performed a study to uncover novel ASD candidate genes using whole exome sequencing (WES). WES permits the identification of rare single-nucleotide variants (SNVs) that may contribute to the complex genetic architecture of autism. They sequenced the exomes of 10 autism multiplex families and identified about 220 rare variants that were predicted to be pathogenic. These variants were transmitted from each parent to at least two affected siblings. All the variants were heterozygous, and no variant was found in more than one family. They identified a considerable number of genes already associated with autism or other NPDs suggesting a common genetic background for psychiatric conditions. Interestingly, they found a major role for truncating mutations in autism, and among

the genes that they discovered with unknown function and no previous link to autism was *YWHAZ* (Toma et al., 2014). To better understand the potential role of YWHAZ dysfunction in ASD we need to further investigate the mechanism by which this protein controls brain development and function. Therefore, we established a stable zebrafish *ywhaz* mutant line using the CRISPR/Cas9 technique. Using this line, we have investigated the expression and function of the zebrafish *ywhaz* homologue. We have determined behavioural alterations, changes in brain monoamine levels and the expression of genes implicated in dopaminergic and serotoninergic signalling in *ywhaz*$^{-/-}$. We also tested drugs to try and rescue the impaired behavioural phenotype. Even though heterozygous mutations in *YWHAZ* are associated with ASD in human patients, in this project only the results from the analysis of *ywhaz*$^{-/-}$ zebrafish will be presented since *ywhaz*$^{+/-}$ did not show strong abnormalities (data not shown).

5.2 Results

5.2.1 Expression of *ywhaz* by *in situ* hybridization

In humans and other vertebrates, 14-3-3 proteins are mostly present in adult brain structures with a small quantity found in other tissues. We first mapped the expression pattern of *ywhaz* in embryos, juveniles and the adult zebrafish brain by *in situ* hybridisation (ISH).

Embryonic expression

In 3 days post fertilization (dpf) WT embryos, *ywhaz* expression is widespread covering almost all brain areas. There is strong signal in the cerebellum of whole mounted embryo (Figure 32a). Sections of the stained tissue confirmed that *ywhaz* is expressed in the torus longitudinalis (TL), optic tectum (TeO), habenula (Ha), thalamus (ventral VT and dorsal DT), the preoptic region (Po) (Figure 32b), cerebellar plate (CeP) and the medulla oblongata (MO) (Figure 32c). *ywhaz* is not expressed in *ywhaz*$^{-/-}$ embryos confirming the loss of gene function in this mutant line (Figure 32d-f).

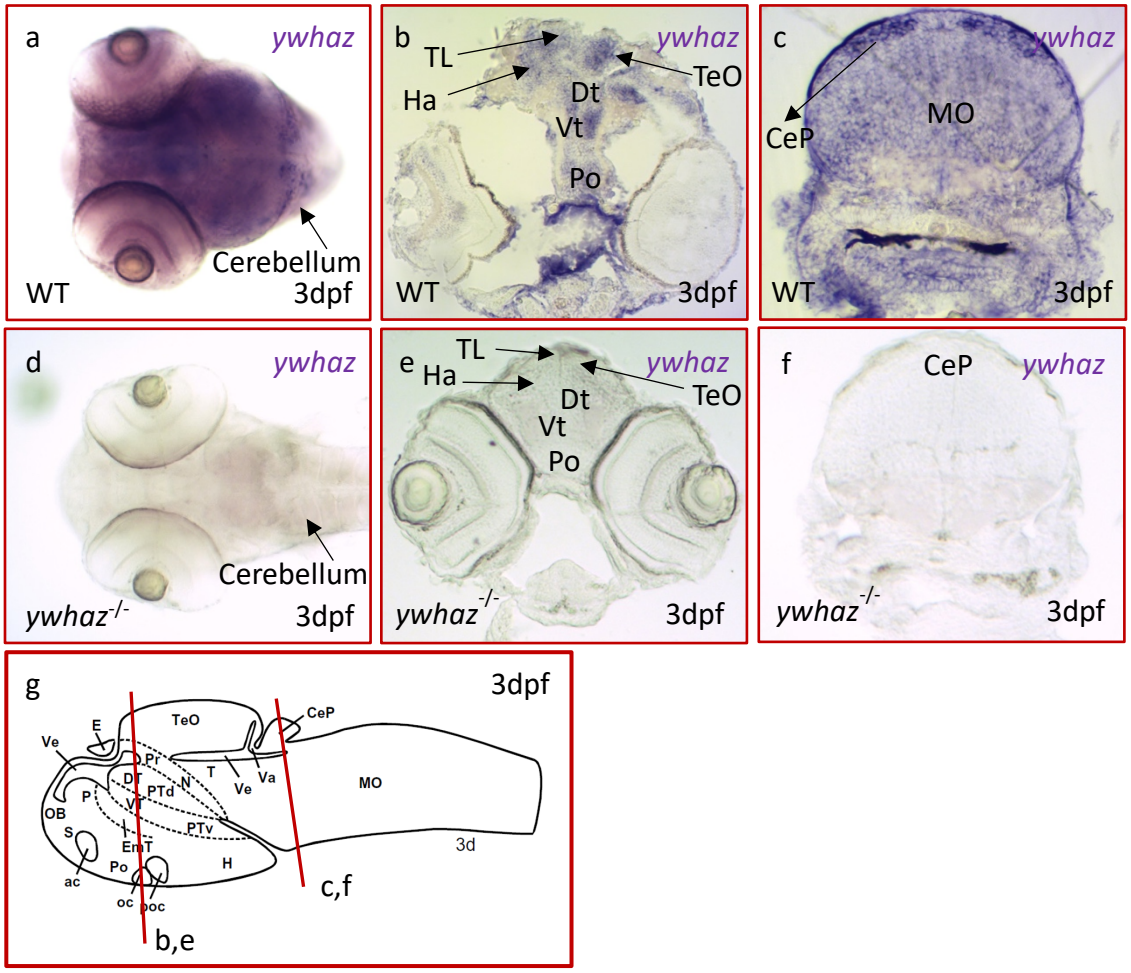

Figure 32. *ywhaz* expression in 3 dpf embryos by ISH. (a-c) In WT, *ywhaz* expression is widespread covering almost all brain areas. **(a)** Strong signal is detected in the cerebellum of whole mounted embryos. **(b)** There is visible signal in the torus longitudinalis (TL), optic tectum (TeO), habenula (Ha), thalamus (ventral VT and dorsal DT), the preoptic region (Po), **(c)** the cerebellar plate (CeP) and in the medulla oblongata (MO), in 20 µm sections of embryonic tissue. **(d-f)** *ywhaz* is not expressed in *ywhaz*$^{-/-}$ embryos. **(g)** Schematic sagittal view of a 3 dpf zebrafish embryo adapted from "Atlas of Early Zebrafish Brain Development", 2016 Elsevier B.V. The red lines illustrate the locations of sections depicted in the previous panels.

Juvenile expression

In juveniles (6 and 9 dpf) *ywhaz* expression is similar to that observed in embryos (3 dpf). There is still an extensive *ywhaz* signal covering almost all brain areas including the torus longitudinalis (TL), optic tectum (TeO), habenula (Ha), thalamus (ventral VT and dorsal DT), the preoptic region (Po) (Figure 33a,c), cerebellar plate (CeP) and medulla oblongata (MO) (Figure 33b,d).

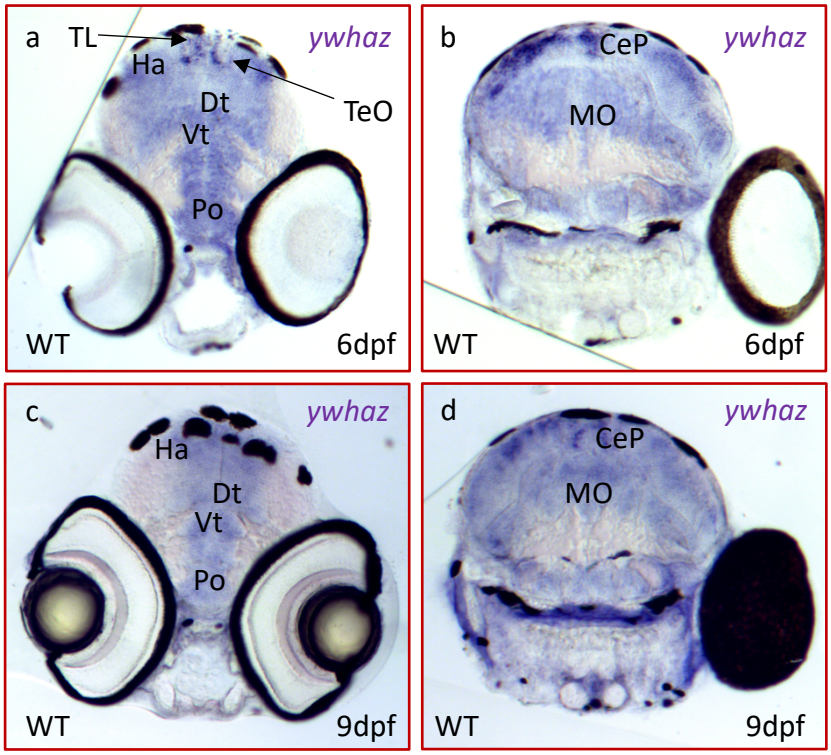

Figure 33. *ywhaz* expression in 6 and 9 dpf juveniles by ISH. *ywhaz* expression is widely spread covering **(a,c)** the torus longitudinalis (TL), optic tectum (TeO), habenula (Ha), thalamus (ventral VT and dorsal DT), the preoptic region (Po), **(b,d)** the cerebellar plate (CeP) and the medulla oblongata (MO), in 50 µm sections of juvenile zebrafish.

Adult expression

In adult zebrafish the expression of *ywhaz* is restricted to the cerebellum. In cross sections, starting from the rostral part there is visible signal in the lateral and medial part of the valvula cerebelli (Val and Vam) (Figure 34a-c). Moving more caudally the staining is observable also in the corpus cerebelli (CCe) (Figure 34d,e), but not in the lobus caudalis cerebelli (LCa) or in the crista cerebellaris (CC) (Figure 34e,f). The sagittal section is more informative, showing that *ywhaz* is distributed above the granule cell layer (GCL) of the Va and CCe (Figure 34j), most likely within the Purkinje cell layer (PCL), and it is not expressed in the LCa or CC (Figure 34j). *ywhaz* is not expressed in the PCL of *ywhaz*$^{-/-}$ confirming the loss of gene function in the mutant line (Figure 34k).

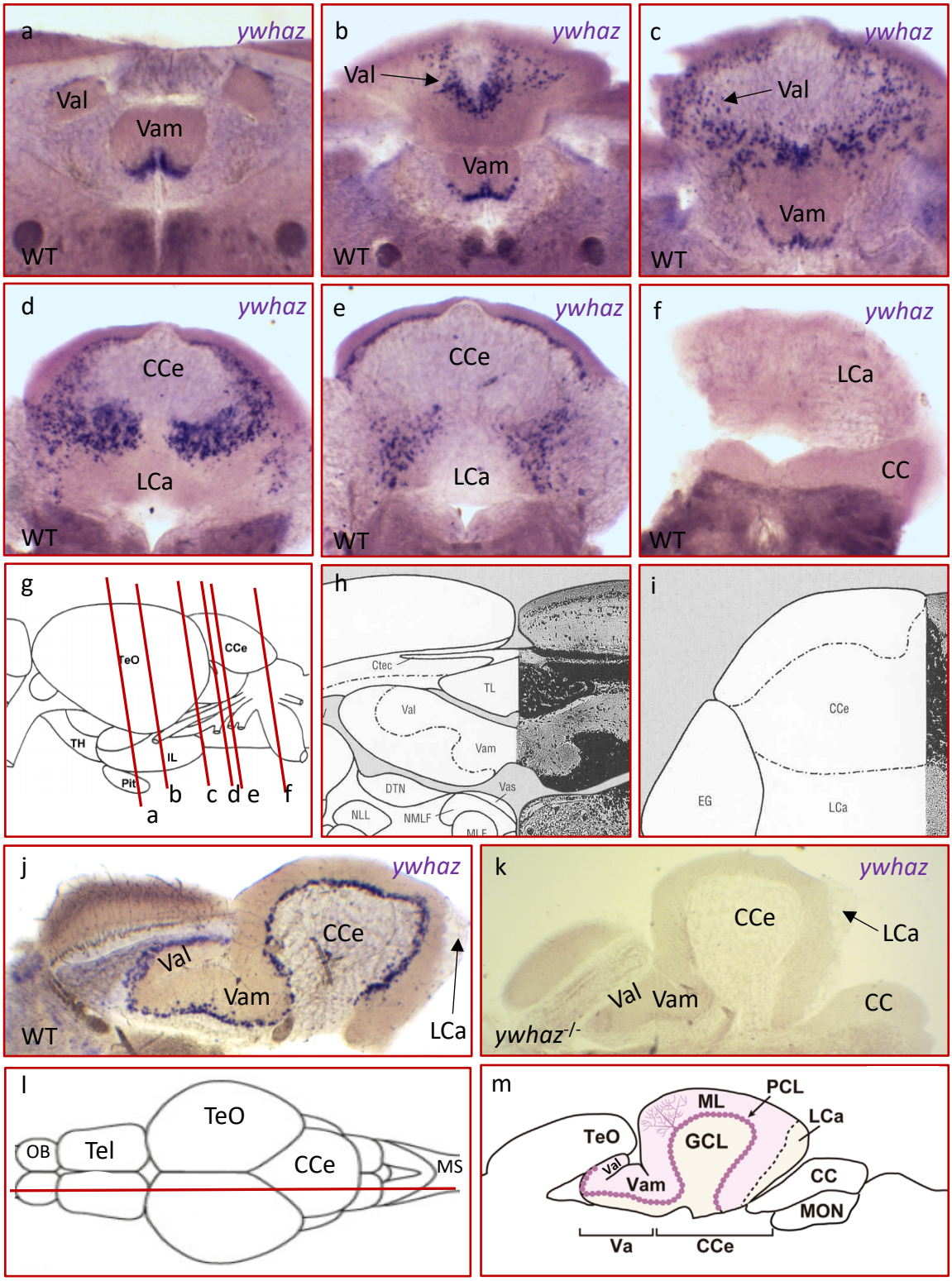
a
ywhaz
Val
Vam
WT
b
ywhaz
Val
Vam
WT
c
ywhaz
Val
Vam
WT
d
ywhaz
CCe
LCa
WT
e
ywhaz
CCe
LCa
WT
f
ywhaz
LCa
CC
WT
g
TeO
CCe
TH
IL
Pit
a
b
c
d
e
f
h
Ctec
TL
Val
Vam
DTN
Vas
NLL
NMLF
MLF
i
CCe
EG
LCa
j
ywhaz
Val
CCe
Vam
LCa
WT
k
ywhaz
CCe
LCa
Val
Vam
CC
ywhaz-/-
l
TeO
OB
Tel
CCe
MS
m
PCL
ML
LCa
TeO
GCL
Val
Vam
CC
MON
Va
CCe

Figure 34. *ywhaz* expression in adult zebrafish brains by ISH. (a-c) In WT cross sections, *ywhaz* is expressed in the lateral and medial part of the valvula cerebelli (Val and Vam), **(d,e)** in the corpus cerebelli (CCe), **(e,f)** but not in the lobus caudalis cerebelli (LCa) or in the crista cerebellaris (CC). **(j)** In a sagittal section, *ywhaz* is distributed above the granule cell layer (GCL) of the Va and CCe, most likely within the Purkinje cell layer, **(j)** but it is not expressed in the LCa or CC. **(k)** *ywhaz* is not expressed in *ywhaz*$^{-/-}$. **(g,l)** Schematic view of a zebrafish adult brain, modified from Wullimann et al., 1992. The red lines illustrate the locations of sections depicted in the previous panels. **(h,i)** Schematic coronal view of the zebrafish cerebellum, modified from Wullimann et al., 1992. **(m)** Schematic sagittal view of the zebrafish cerebellum, modified from Takeuchi et al., 2015.

The identity of cell type expressing *ywhaz* within the Purkinje cell layer was confirmed using a *Tg*(*aldoca:gap43-Venus*) line. In this line the promoter of the *aldolase Ca* (*aldoca*) gene, which encodes Zebrin II (Ahn et al., 1994), is used as a driver. Thus the line expresses a fluorescent protein that marks Purkinje cells. Using this line, we combined *ywhaz* ISH with an anti-GFP antibody stain. The result shows that *ywhaz* staining (purple) overlaps with Purkinje cells staining (brown), meaning that *ywhaz* is expressed within Purkinje cells (Figure 35).

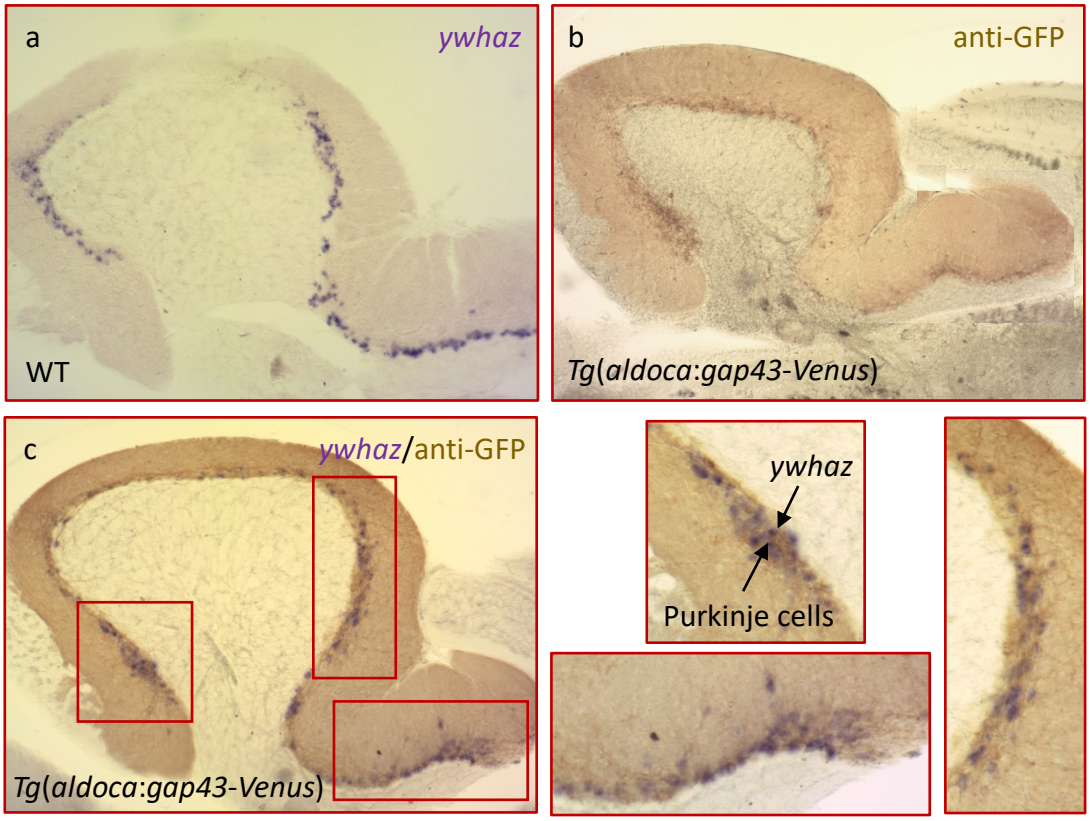

Figure 35. Co-staining of the Tg(aldoca:gap43-Venus) cerebellum with anti-GFP antibody and ywhaz riboprobe. (a) *ywhaz* riboprobe staining performed by ISH on a sagittal section of WT cerebellum. **(b)** Staining of the *Tg*(*aldoca*:*gap43-Venus*) cerebellum with anti-GFP antibody by IHC. **(c)** Co-staining of the *Tg*(*aldoca*:*gap43-Venus*) cerebellum with *ywhaz* riboprobe that has purple staining, and anti-GFP antibody that has brown staining in sagittal section. The overlap between the two staining (black arrows) indicates that *ywhaz* is localised within Purkinje cells.

In order to exclude expression of *ywhaz* in Eurydendroid cells, excitatory neurons that are present in the cerebellum and are situated more ventrally than Purkinje cells (Biechl et al., 2016), we performed an ISH with the *ywhaz* probe followed by IHC with an anti-GFP antibody in the *Tg*(*olig2*:*egfp*)^{vu12} transgenic line (Figure 36). In the zebrafish cerebellum, *olig2*$^{+}$ neurons localize to the vicinity of the PCL and have long axons similar to those of Eurydendroid cells. Therefore EGFP^{+} cells in the *Tg*(*olig2*:*egfp*)^{vu12} fish label Eurydendroid cells (McFarland et al., 2008). The result of the ISH followed by IHC (Figure 36) clearly shows that *ywhaz* staining (purple) does not overlap with Eurydendroid cell staining (brown) meaning that *ywhaz* is not expressed within Eurydendroid cells.

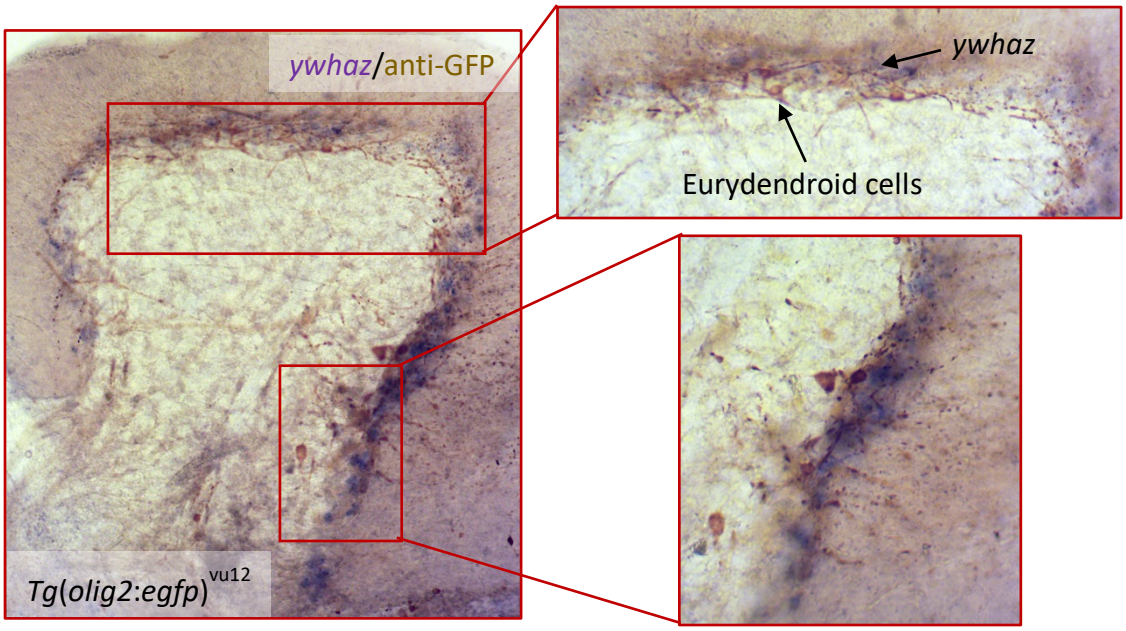

Figure 36. Co-staining of the *Tg*(*olig2*:*egfp*)^{vu12} cerebellum with a *ywhaz* riboprobe (purple staining), and anti-GFP antibody (brown staining) in a sagittal section. The fact that there is no overlap between the two stains means that *ywhaz* is not localized to Eurydendroid cells.

5.2.2 Behavioural analysis of *ywhaz*$^{-/-}$

The main hallmarks of ASD are impairments in social communication and language, associated with repetitive and restrictive behaviours which cause significant distress for autistic individuals. We assessed several behaviours including anxiety, boldness, aggression and social behaviour to analyse if the behaviour of *ywhaz*$^{-/-}$ mutants is altered.

5.2.2.1 Analysis of social behaviour

5.2.2.1.1 Visually-mediated social preference for novelty test (VMSP)

WT and *ywhaz*$^{-/-}$ behaviour was analysed in the VMSP test. During the social preference step of the experiment, both genotypes reacted in the same way, spending the majority of the time swimming close to the first group of strangers (1st strangers; $p < 0.0001$ for both WT and *ywhaz*$^{-/-}$; Figure 37a). During the preference for social novelty step, WT switched preference to the second group of unfamiliar fish (2nd strangers; $p = 0.0475$,

Figure 37b). However, *ywhaz*$^{-/-}$ do not have a preference between the two groups, spending equal time close to both of them (2nd strangers; p = 0.98, Figure 37b).

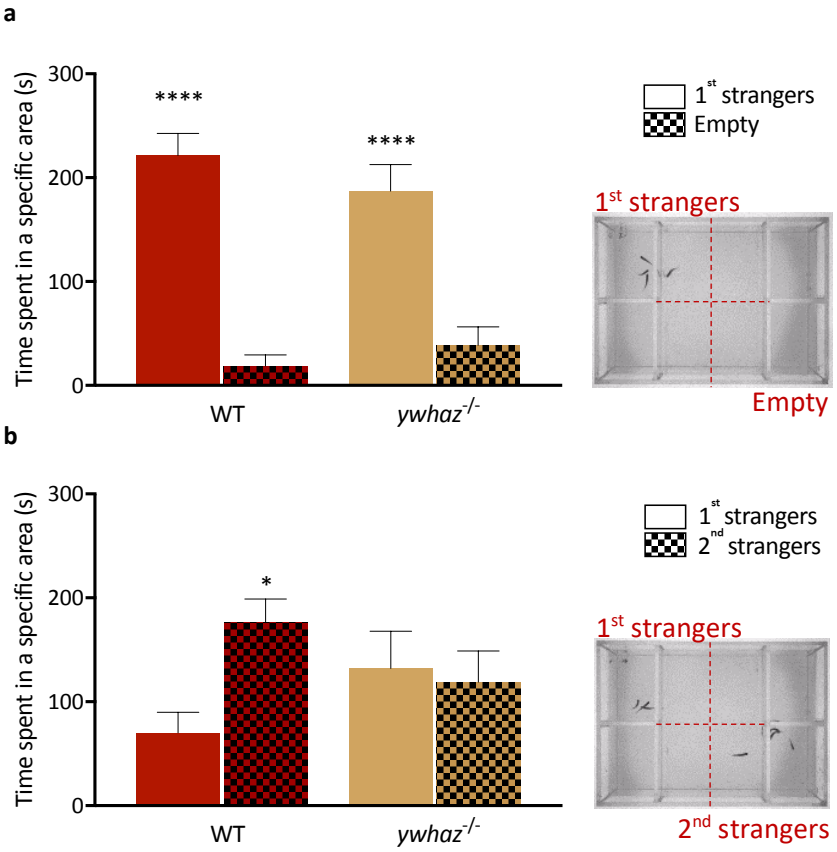

Figure 37. Visually-mediated social preference test. (a) Social preference. Both WT and *ywhaz*$^{-/-}$ show a significant preference to spend time near a group of unfamiliar fish (1st strangers; p < 0.0001 for both WT and *ywhaz*$^{-/-}$). **(b)** Preference for social novelty. WT switch preference and spend more time close to the second group of unfamiliar fish (2nd strangers; p = 0.0475). *ywhaz*$^{-/-}$ spend an equal amount of time near both groups of unfamiliar fish (2nd strangers; p = 0.98). Two-way ANOVA with Tukey's post hoc comparisons. n = 12. **** p < 0.0001, * p < 0.1. Mean ± SEM.

However, upon closer observation we noted that immediately after the addition of the second group of unfamiliar fish *ywhaz*$^{-/-}$ mutants tended to freeze. After this immobility, they started moving again, swimming close to either the first or the second group of unfamiliar fish in a way that appeared to be random (Figure 38a). We therefore analysed how much time the fish froze during the first two minutes following the addition of the second group of unfamiliar fish. *ywhaz*$^{-/-}$ mutants spent a significant amount of time freezing compared to the wild types (p = 0.0035; Figure 38b). This peculiar freezing behaviour is novel for *ywhaz*$^{-/-}$ and has not been observed in *reln*$^{-/-}$ or any other mutant line in our laboratory.

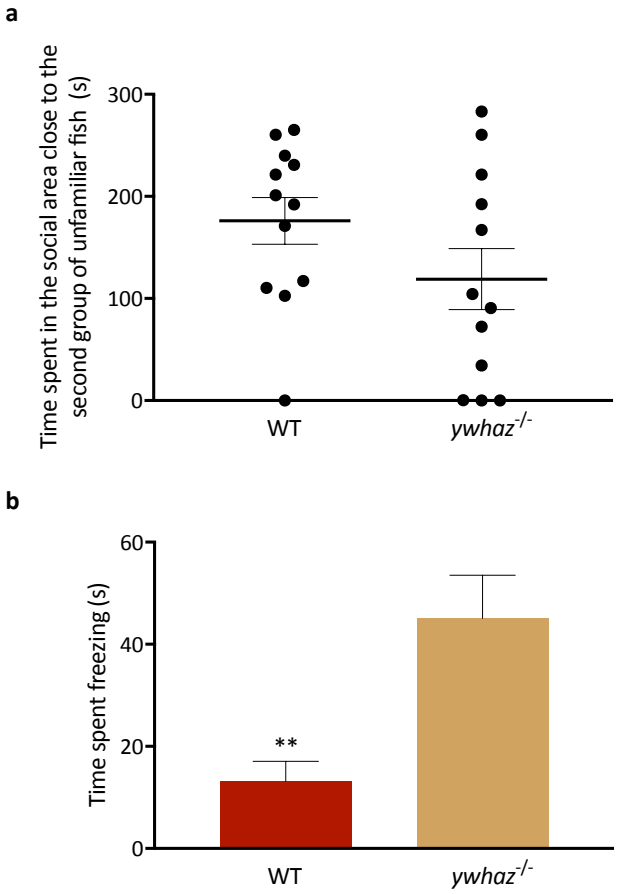

Figure 38. Second step of the visually-mediated social preference test. (a) Time spent in the social area close to the second group of unfamiliar fish. WT fish mostly behave in the same way with a small internal variability, whereas the mutants have a more heterogenous behaviour spending from 0 to almost 300 seconds in the area close to the second group of unfamiliar fish. **(b)** Time spent freezing during the first two minutes after the addition of the second group of strangers in the behavioural tank ($p = 0.035$). Unpaired t-test with Welch's correction. $n = 12$. ** $p < 0.01$. Mean ± SEM.

In order to verify whether the freezing behaviour that we observed was specifically caused by the introduction of fish, or if it can be induced also by other inanimate and odourless stimuli, we repeated the test adding marbles instead of the second group of unfamiliar fish. Again, we observed that immediately after the addition of marbles, *ywhaz*$^{-/-}$ mutants freeze compared to WT ($p = 0.0251$, Figure 39). This is followed by random movement whereby the fish swim close to either stimulus.

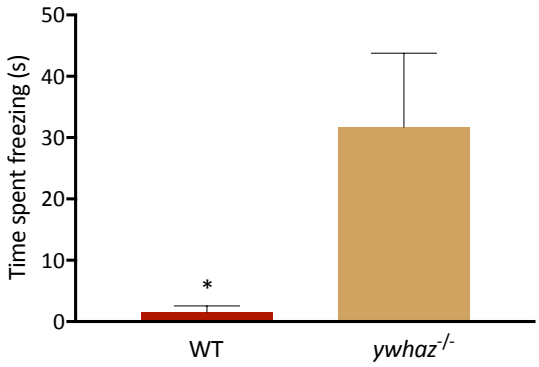

Figure 39. Addition of marbles instead of the second group of unfamiliar fish during the second step of the visually-mediated social preference test. Time spent freezing during the first two minutes after the addition of marbles in the behavioural tank ($p = 0.0251$). Mann-Whitney U test. $n = 10$. * $p < 0.1$. Mean ± SEM.

In order to analyse whether this defect is present only at adult ages or if it also appears earlier in life, we repeated the VMSP using juvenile (1-month-old) fish. During the social preference step of the experiment, both genotypes spent most of the time swimming close to the first group of strangers behaving in a similar way to adults (1st strangers; $p < 0.001$ for both WT and *ywhaz*$^{-/-}$, Figure 40a). During the preference for social novelty step, WT and *ywhaz*$^{-/-}$ spent equal time close to both groups of unfamiliar fish (2nd strangers; $p = 0.077$ and $p = 0.63$ respectively, Figure 40b) and did not show any freezing reaction ($p > 0.99$, Figure 40c).

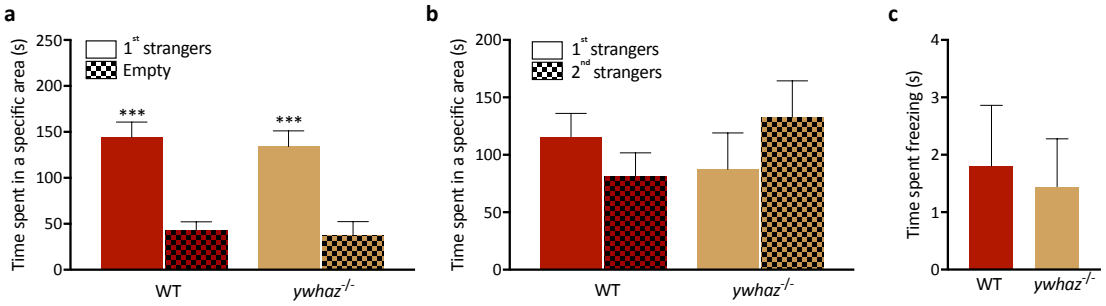

Figure 40. Visually-mediated social preference test with juvenile fish. (a) Social preference. Similar to adults, both WT and *ywhaz*$^{-/-}$ juvenile fish show a significant preference to spend time near a group of unfamiliar fish (1st strangers; $p < 0.001$ for both WT and *ywhaz*$^{-/-}$). **(b)** Preference for social novelty. WT and *ywhaz*$^{-/-}$ juveniles spend equal time close both groups of unfamiliar fish (2nd strangers; $p = 0.077$ and $p = 0.63$ respectively). Two-way ANOVA with Tukey's post hoc comparisons. $n = 10$. *** $p < 0.001$. Mean ± SEM. **(c)** Time spent freezing during the first two minutes after the addition of the second group of unfamiliar fish in the behavioural tank. Neither WT nor *ywhaz*$^{-/-}$ juveniles show any freezing reaction ($p > 0.99$). Mann-Whitney U test. $n = 10$. Mean ± SEM

5.2.2.1.2 Shoaling test

We next examined social behaviour in a group of five fish. We analysed shoaling by measuring the proximity to other conspecifics. Analysis of this behaviour revealed that *ywhaz*$^{-/-}$ does not differ significantly in shoal cohesion compared to WT. This was showed by the nearest neighbour distance (NDD, p = 0.66, Figure 41a), the inter-individual distance (IID, p= 0.91, Figure 41b), the cluster score (p = 0.93, Figure 41c), the polarization (p = 0.53, Figure 41d) and velocity (p = 0.53, Figure 41e) of the shoal, which were similar between *ywhaz*$^{-/-}$ and WT. Shoaling behaviour also appears normal in juveniles (p = 0.33, Figure 41f).

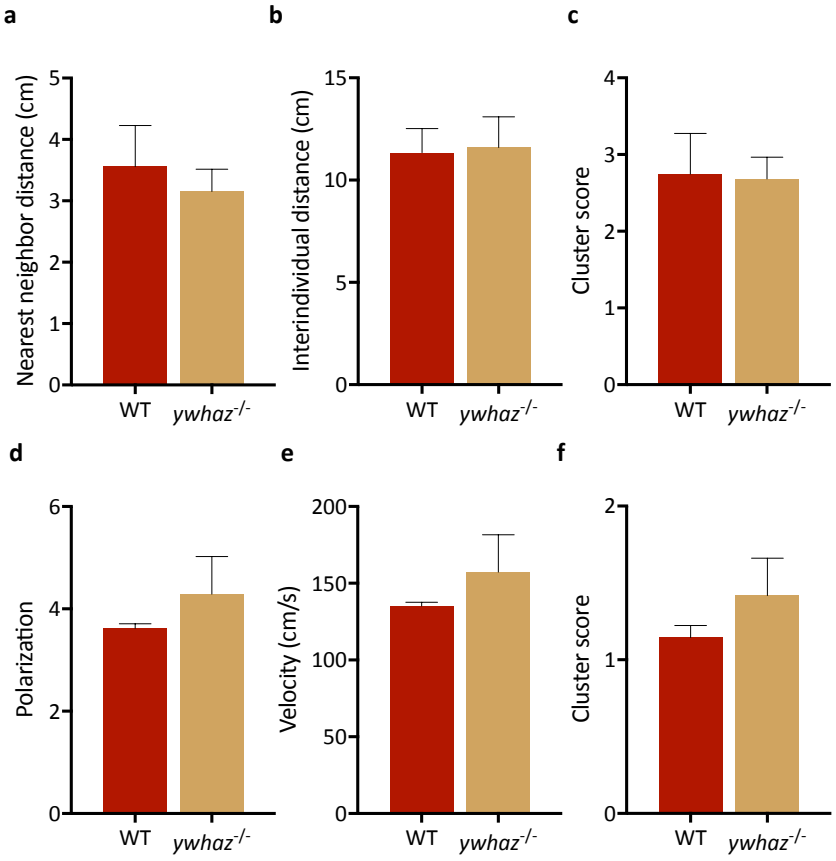

Figure 41. Shoaling behaviour. Adult *ywhaz*$^{-/-}$ display normal shoaling. **(a)** Nearest neighbour distance (p = 0.66), **(b)** inter-individual distance (p = 0.91), **(c)** cluster score (p = 0.93), **(d)** polarization (p = 0.53) and **(e)** velocity (p = 0.53). n = 2 groups of 5 wild-type, n = 2 groups of 5 *ywhaz*$^{-/-}$. Unpaired t-test with Welch's correction. Mean ± SEM. **(f)** Shoaling behaviour is normal in juveniles fish, with equal cluster score between genotypes (p = 0.33). n = 4 groups of 5 wild-type, n = 4 groups of 5 *ywhaz*$^{-/-}$. Unpaired t-test with Welch's correction. Mean ± SEM.

5.2.2.2 Analysis of anxiety-like behaviour and exploratory activity

5.2.2.2.1 Novel tank test (NTT)

We examined anxiety-like behaviour using the NTT. Both genotypes spent most of the time of the experiment at the bottom showing a general baseline of anxiety-like behaviour. No significant difference was found between WT and *ywhaz*$^{-/-}$ in the time spent at the bottom (p = 0.41, Figure 42a) or at the top (p = 0.50, Figure 42b) of a novel tank. Furthermore, no significant differences were observed between genotypes, neither in the time spent freezing (p = 0.13, Figure 42c), locomotion (p = 0.31, Figure 42d), velocity (p = 0.19, Figure 42e) nor angular velocity (p = 0.22, Figure 42f) in the novel tank.

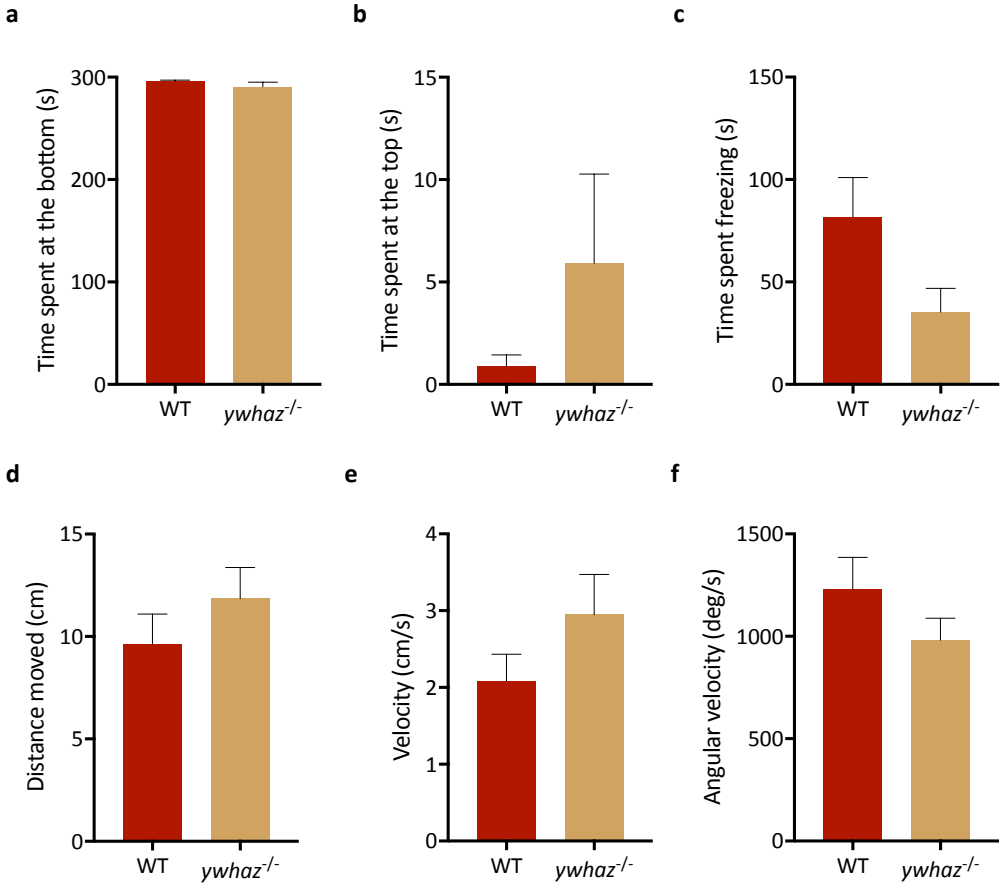

Figure 42. Novel tank test. *ywhaz*$^{-/-}$ exhibit normal anxiety-like behaviour. Time spent **(a)** at the bottom (p = 0.41), **(b)** at the top (p = 0.50), and **(c)** freezing (p = 0.13) in a novel tank. n = 15 wild-type, n = 15 *ywhaz*$^{-/-}$. Mann-Whitney U test. **(d)** Locomotion (p = 0.31), **(e)** velocity (p = 0.19) and **(f)** angular velocity (p = 0.22) in a novel tank. n = 15 wild-type, n = 15 *ywhaz*$^{-/-}$. Unpaired t-test with Welch's correction. Mean ± SEM.

5.2.2.2.2 Open field test

By measuring the time spent in the centre, periphery and side of a large tank we confirmed the lack of anxiety-like phenotype already observed in the NTT test. Both genotypes spent roughly one third of the time in each area of the tank, showing a normal level of exploratory activity. No significant differences were found in the time spent in thigmotaxis (p = 0.42, Figure 43a), in the periphery (p = 0.24, Figure 43b) and in the centre (p = 0.19, Figure 43c) of the open field tank between WT and *ywhaz*$^{-/-}$. The time spent freezing (p = 0.70, Figure 43d), locomotion (p = 0.0574, Figure 43e) and velocity (p = 0.16, Figure 43f) were also not affected in the open field test.

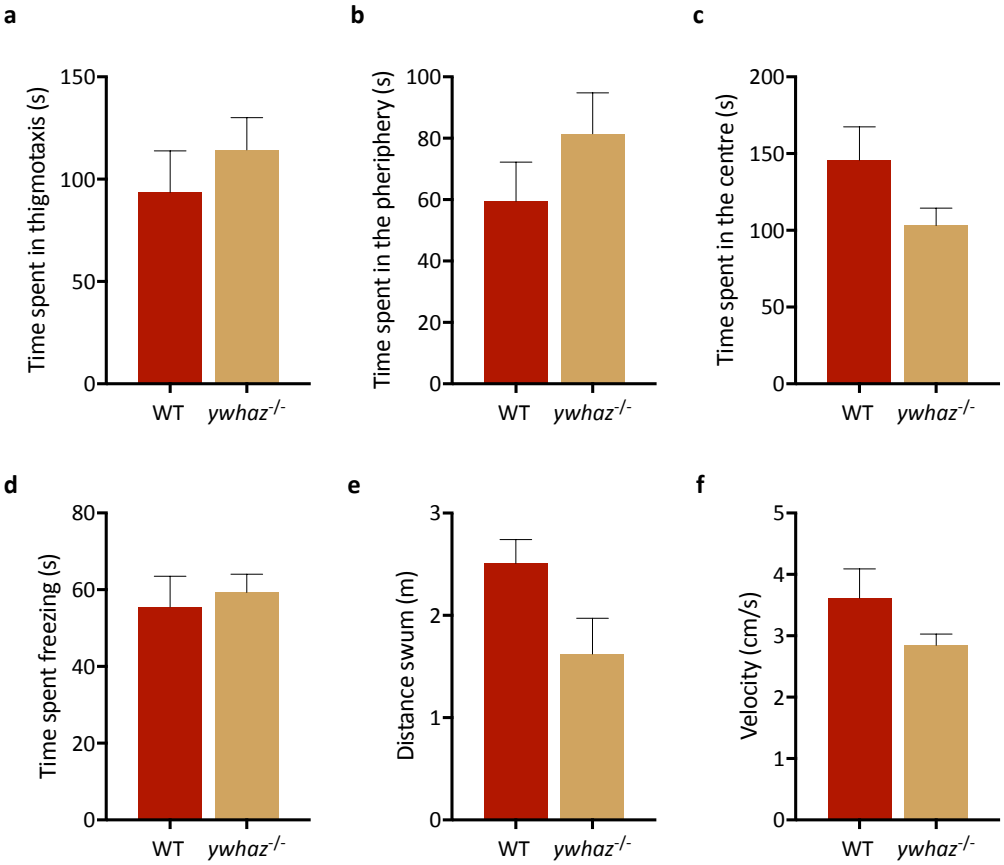

Figure 43. Open field test. *ywhaz*$^{-/-}$ behave similarly to WT in the open field test. **(a)** Time at the side of the tank (p = 0.42), **(b)** in the periphery (p = 0.24), **(c)** in the centre of the tank (p = 0.19) and **(d)** time spent freezing (p = 0.70). n = 15 WT, n = 15 *ywhaz*$^{-/-}$. Unpaired t-test with Welch's correction. **(e)** Locomotion (p = 0.0574). n = 15 wild-type, n = 15 *ywhaz*$^{-/-}$. Mann-Whitney U test. **(f)** Velocity (p = 0.16) is not affected in the open field test. n = 15 WT, n = 15 *ywhaz*$^{-/-}$. Unpaired t-test with Welch's correction. Mean ± SEM.

5.2.2.3 Mirror-induced aggression

We next investigated the behaviour of *ywhaz* mutants in the mirror-induced aggression test. The mutants did not show a different level of aggression compared to WT (Figure 44).

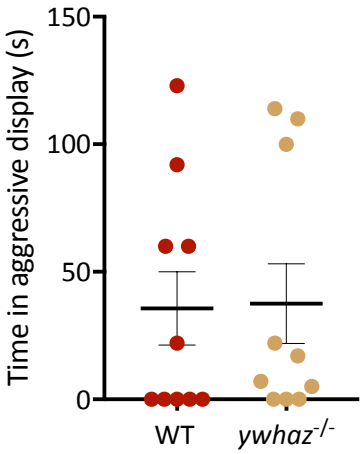

Figure 44. Mirror-induced aggression test. No difference in aggression levels between WT and *ywhaz*$^{-/-}$ (p = 0.72). n = 15 wild-type, n = 15 *ywhaz*$^{-/-}$. Mann-Whitney unpaired t-test. Mean ± SEM.

5.2.3 Analysis of monoamines and their metabolites levels by high-performance liquid chromatography (HPLC)

To investigate whether mutation of *ywhaz* influences levels of monoamines and their metabolites we performed HPLC to measure the basal level of 3,4-dihydroxyphenylacetic acid (DOPAC), dopamine (DA), 5-hydroxyindoleacetic acid (5HIAA) and serotonin (5-HT) in the brain. There was a significant genotype effect on DA and 5-HT levels in the hindbrain, with *ywhaz*$^{-/-}$ decreasing the level of both these neurotransmitters (p = 0.0063 and p = 0.0026 respectively, Figure 45d). No further alterations were found in others area of the brain (Figure 45a-c) nor in the turnover of neurotransmitters (Figure 45e,f).

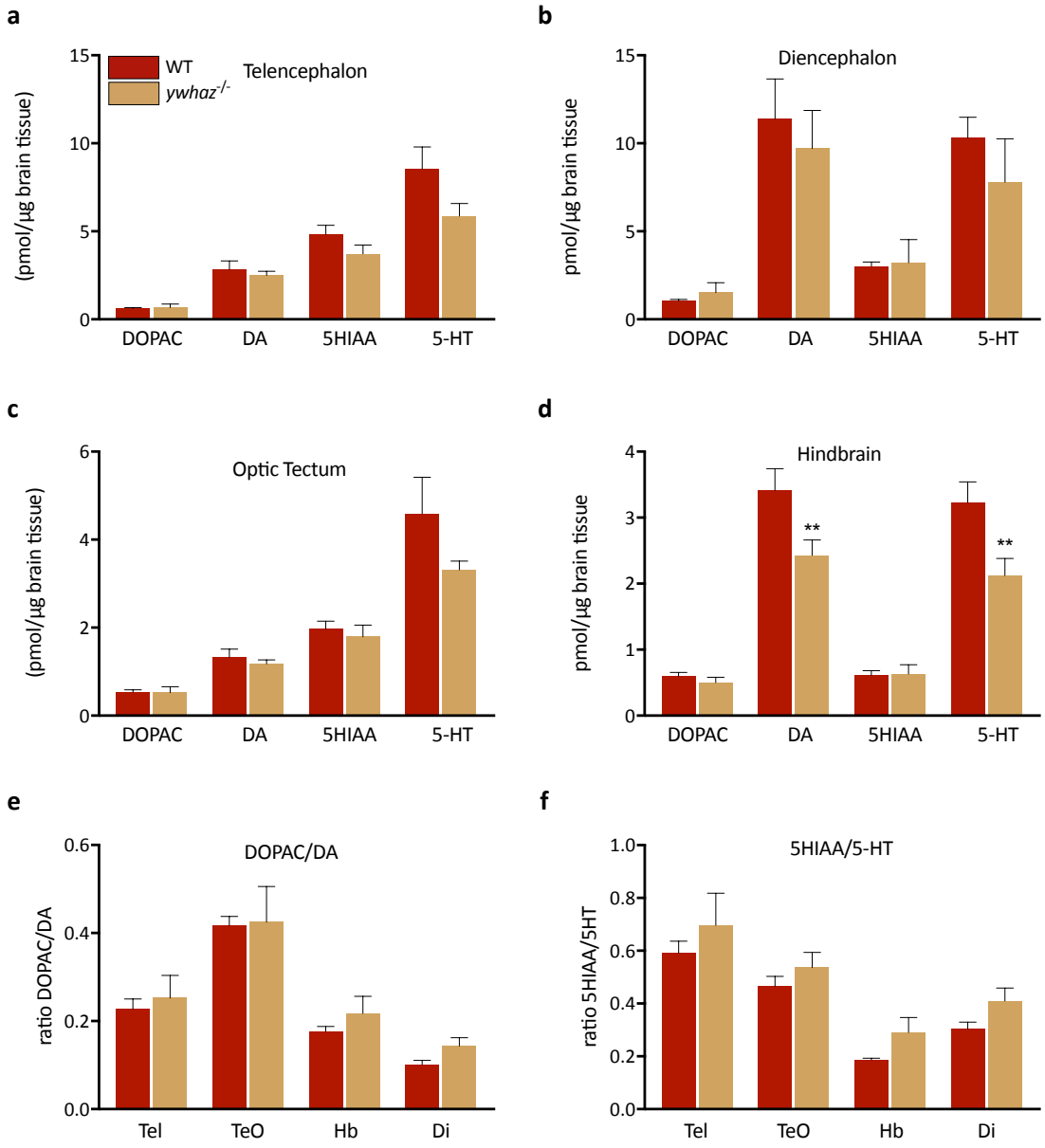

Figure 45. High precision liquid chromatography. DA and 5-HT levels are decreased in the hindbrain of *ywhaz*$^{-/-}$ compared to WT (p = 0.0063 and p = 0.0026 respectively). **(a)** Telencephalon, **(b)** diencephalon, **(c)** optic tectum and **(d)** hindbrain. No differences in the breakdown of **(e)** DOPAC/DA and **(f)** 5HIAA/5-HT. Multiple t-tests with Holm-Sidak correction for multiple comparisons. Abbreviations: DA, dopamine; Di, diencephalon; DOPAC, 3,4-dihydroxyphenylacetic acid; Hb, hindbrain; Tel, telencephalon; TeO, optic tectum; 5-HIAA, 5-hydroxyindoleacetic acid; 5-HT, 5-hydroxytryptamine. n = 7 WT, n = 7 *ywhaz*$^{-/-}$. ** p < 0.01. Mean ± SEM.

5.2.4 Effects of *ywhaz*$^{-/-}$ on gene expression

The reduced levels of DA and 5-HT in *ywhaz*$^{-/-}$ could be explained by a decreased production of these neurotransmitters. Tyrosine hydroxylase (TH), the rate-limiting enzyme in the biosynthesis of DA from its precursor L-tyrosine, is known to be regulated

by 14-3-3 proteins (Aitken, 2006). Among all isoforms YWHAZ plays the most important role in DA synthesis (Wang et al., 2009). YWHAZ binding to TH enhances its phosphorylation and positively regulates its enzymatic activity (Ichimura et al., 1987; Itagaki et al., 1999; Toska et al., 2002). Therefore, we first measured the expression of genes coding for the DA and 5-HT synthesis enzymes TH and Tryptophan hydroxylase (TPH). There was a significant increase in *tryptophan hydroxylase 2* (*tph2*) expression in *ywhaz*$^{-/-}$ compared to WT ($p = 0.0287$), whereas *tph1a*, *tph1b* and both homologues of *tyrosine hydroxylase* (*th1* and *th2*) were equally expressed in both genotypes (Figure 46a). Since defects in *th* or *th2* were not detected we further examined the expression of genes coding for proteins involved in the dopaminergic neurotransmitter pathway: the dopamine transporter *solute carrier family 6 (neurotransmitter transporter), member 3* (*slc6a3*), *dopamine receptor 1* (*drd1*), *dopamine receptor 2a* (*drd2a*), *dopamine receptor 2b* (*drd2b*) and *dopamine receptor 4* (*drd4*). The expression of both isoforms of the *drd2a and drd2b* are increased in *ywhaz*$^{-/-}$ compared to WT ($p = 0.0326$ for *drd2a* and $p = 0.0359$ for *drd2b*, Figure 46b).

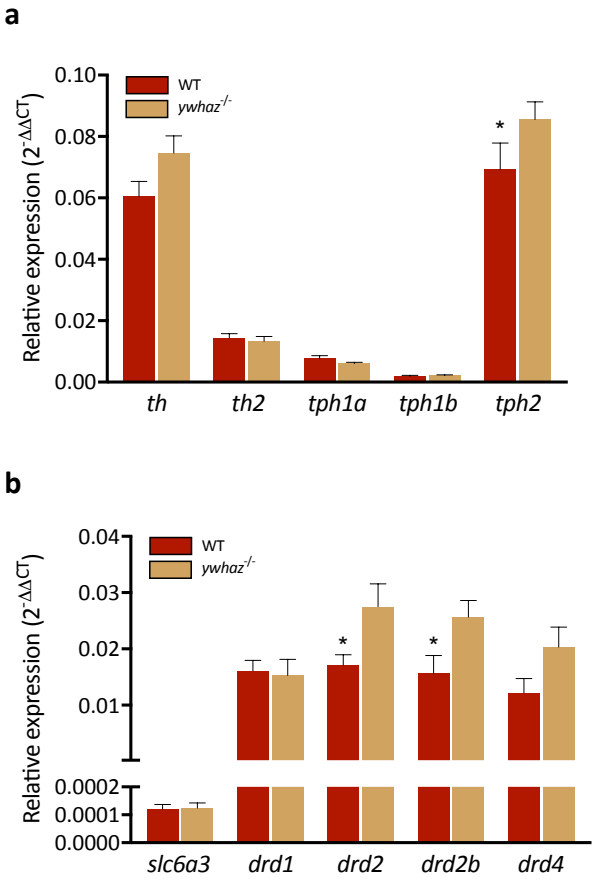

Figure 46. Effects of *ywhaz*$^{-/-}$ on gene expression. (a) Relative expression profile of *tyrosine hydroxylase* (*th*), *tyrosine hydroxylase 2* (*th2*), *tryptophan hydroxylase 1a* (*tph1a*), *tryptophan hydroxylase 1b* (*tph1b*) and *tryptophan hydroxylase 2* (*tph2*), normalised to the reference gene *ribosomal protein L13* (*rpl13*). *ywhaz*$^{-/-}$ have an increased level of *tph2* expression (p = 0.0287). Multiple t-tests with Holm-Sidak correction for multiple comparisons. n = 10 WT, n = 10 *ywhaz*$^{-/-}$. * p < 0.05. Mean ± SEM. **(b)** Relative expression profile of *solute carrier family 6 (neurotransmitter transporter), member 3* (*slc6a3*), *dopamine receptor 1* (*drd1*), *dopamine receptor 2a* (*drd2a*), *dopamine receptor 2b* (*drd2b*) and *dopamine receptor 4* (*drd4*), normalised to the reference gene *elongation factor 1a* (*elf1a*). *ywhaz*$^{-/-}$ have an increased level of *drd2a* and *drd2b* expression (p = 0.0326 and p = 0.0359 respectively). Multiple t-tests with Holm-Sidak correction for multiple comparisons. n = 10 WT, n = 10 *ywhaz*$^{-/-}$. * p < 0.05. Mean ± SEM.

5.2.5 Pharmacological analysis of the of *ywhaz*$^{-/-}$ behavioural phenotype

The major defect in neurotransmitter signalling that we observed in *ywhaz*$^{-/-}$ was a decreased level of 5-HT and DA in the hindbrain. We applied fluoxetine, a selective serotonin reuptake inhibitor (SSRI; Vaswani et al., 2003), to investigate the connection between 5-HT and the behavioural phenotype observed in *ywhaz*$^{-/-}$. Fluoxetine inhibits the reuptake of 5-HT into presynaptic cells, resulting in 5-HT persisting longer when it is released, and thus increasing its extracellular level (Vaswani et al., 2003). Treatment with 5 mg/L fluoxetine significantly decreased the time that *ywhaz*$^{-/-}$ spent freezing after

the addition of the second group of unfamiliar fish (p = 0.0126, Figure 47) without affecting WT behaviour (p = 0.29, Figure 47).

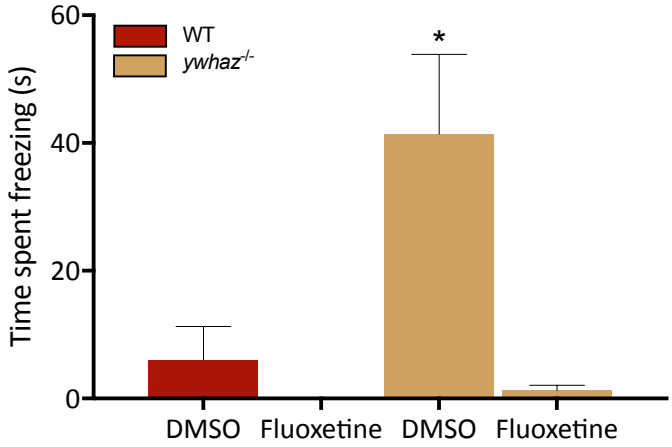

Figure 47. Treatment with 5 mg/L fluoxetine rescues the freezing phenotype in *ywhaz*$^{-/-}$. Treatment with 5 mg/L fluoxetine significantly decreased the time that *ywhaz*$^{-/-}$ spent freezing after the addition of the second group of unfamiliar fish (p = 0.0126) without affecting WT behaviour (p = 0.29). Multiple t-tests with Holm-Sidak correction for multiple comparisons. n = 8 WT, n = 8 *ywhaz*$^{-/-}$. * p < 0.05. Mean ± SEM.

In order to understand the connection between the decreased level of DA, together with increased expression levels of the *drd2a and drd2b* and the *ywhaz*$^{-/-}$ behavioural phenotype we applied quinpirole, a selective D2-like receptor agonist (Millan et al., 2002). We tested different concentrations of quinpirole to examine a wide spectrum of possible effects. Treatment with 0.25 mg/L quinpirole significantly decreased the time that *ywhaz*$^{-/-}$ spent freezing after the addition of the second group of unfamiliar fish (p = 0.0467, Figure 48), whereas higher concentrations, 1 and 4 mg/L, do not reverse the freezing behaviour (p > 0.99 for both concentrations, Figure 48). Quinpirole does not affect the freezing behaviour in WT at any concentration (p > 0.99 for 0.25, 1 and 4 mg/L, Figure 48).

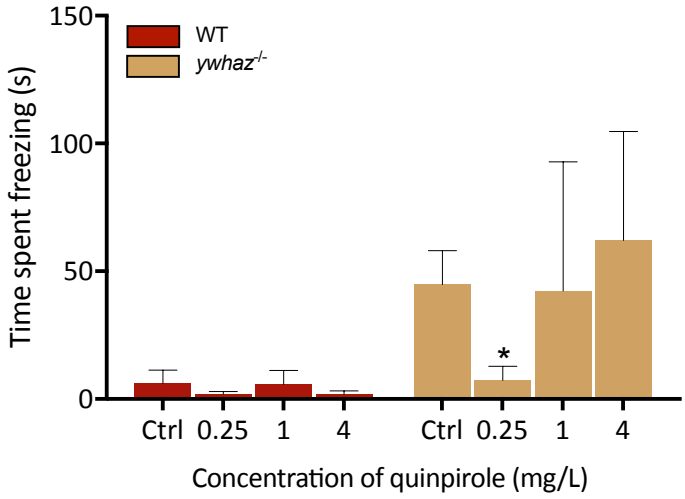

Figure 48. Treatment with 0.25 mg/L quinpirole rescues the freezing phenotype in *ywhaz*$^{-/-}$. Treatment with 0.25 mg/L quinpirole decreased significantly the time that *ywhaz*$^{-/-}$ spent freezing after the addition of the second group of stranger fish ($p = 0.0467$). At higher concentrations, 1 and 4 mg/L, quinpirole does not rescue the freezing behaviour ($p > 0.99$ for both concentrations). Quinpirole does not affect the time spent freezing by WT fish at any concentration ($p > 0.99$ for 0.25, 1 and 4 mg/L). Kruskal-Wallis test with Dunn's multiple comparisons. n = 5 WT and n = 10 *ywhaz*$^{-/-}$. * $p < 0.05$. Mean ± SEM.

5.3 Discussion

5.3.1 *ywhaz* expression is widespread at early stages and become restricted to the Purkinje cell layer in adults

As first step towards understanding the behavioural function of *ywhaz*, we analysed its expression at both developmental and adult stages by *in situ* hybridization. At developmental stages (3, 6 and 9 dpf) *ywhaz* expression is widespread covering almost all brain areas, with a particularly strong signal in the cerebellum. In adults the expression of *ywhaz* becomes restricted to the Purkinje cell layer of the valvula cerebelli (Va) and corpus cerebelli (CCe). It is therefore possible that *ywhaz* may have a wide range of functions during development and more restricted functions at later stages. Zebrafish have widespread and conserved embryonic neurogenesis, which originates from different proliferative neuronal clusters that are distributed along the brain axis (Tropepe and Sive, 2003). Teleost embryogenesis consists of a primary phase which occurs at 16 hpf with the genesis of the first neurons that form an elementary network essential to coordinate larval behaviour (Kimmel et al., 1991). The second phase starts at 2 dpf and produces the sub-regions of the mature brain, contributing significantly to

neuronal development. The positions of axonal tracts in this teleost fish are analogous to the ones of other vertebrates (Tropepe and Sive, 2003). In mouse, *Ywhaz* has been shown to be an essential regulator of neurogenesis and neural differentiation (Cornell and Toyo-Oka, 2017; Toyo-oka et al., 2014). Therefore, given the fact that i) the process of neurogenesis is conserved, and ii) *Ywhaz* is associated with neurogenesis in mice and iii) embryonic neurogenesis in zebrafish is widespread and zebrafish *ywhaz* expression is also widespread, it is tempting to hypothesis that at early stages *ywhaz* might play an important role in neurogenesis. In adults the expression of *ywhaz* becomes restricted to the Purkinje cell layer of the valvula cerebelli (Va) and corpus cerebelli (CCe). This is an interesting result that fits well with published studies about the cerebellum and its link with psychiatric disorders (Stoodley, 2016). Post-mortem studies have shown a reduction in Purkinje cell density in human autistic patients (Skefos et al., 2014), and mutant mice with a decrease in Purkinje functioning show ASD-like behaviours (Tsai et al., 2012). A decreased number of Purkinje cells may lead to ASD-like behaviours by increasing activity in the cerebellum-cortex pathway since the neurons have GABAergic properties. The possible involvement of the cerebellum with ASD will be discussed in more detail in the general discussion (paragraph 6.2). At adult stages *ywhaz* might be essential for the integrity of the cerebellar cytoarchitecture and function. Both impairment in neurogenesis and cerebellar function are linked to ASD (Packer, 2016; Wang et al., 2014a). Thus the expression of *ywhaz* in these regions adds further weight to the idea of *Ywhaz* being involved in the aetiology of ASD.

5.3.2 *ywhaz*$^{-/-}$ freeze in response to novel stimuli

In order to investigate whether *Ywhaz* dysfunction causes behavioural alterations that are reminiscent of ASD symptoms in humans we characterised the behaviour of *ywhaz*$^{-/-}$. Mutants do not show any abnormal aggression or anxiety-like behaviour. We evaluated the social phenotype using the VMSP and shoaling tests which measure different aspects of social behaviour. Zebrafish have strong shoaling tendencies and they tend to approach a group of conspecifics (Miller and Gerlai, 2012). At both adult and juvenile stages, *ywhaz*$^{-/-}$ and WT display similar shoaling behaviour, determined by comparable cluster score values which define the level of group cohesion. Other

shoaling parameters such as NND, IID, polarization and velocity were not impaired in adult *ywhaz*$^{-/-}$ fish. Typically, zebrafish are visually drawn to conspecifics (Krause et al., 2000; Miller and Gerlai, 2011; Saverino and Gerlai, 2008), therefore we utilize this innate inclination to test preference for social interaction and novelty with the VMSP test. Consistent with their normal shoaling behaviour, during the social preference step of the VMSP test both juvenile and adult *ywhaz*$^{-/-}$ fish behaved in the same way as WT, spending most of the time swimming close to the first group of strangers. As soon as the second stimulus group was added the mutants froze before restoring their movement. We hypothesised that this reaction was a form of social anxiety caused by the presence of the second group of strangers. However, when we repeated the experiment using marbles as an inanimate stimulus the neophobic response freezing was still present. This neophobic response is age specific, and only occurs in adults. *ywhaz*$^{-/-}$ juvenile fish subjected to the same test spend an equal amount of time close to both groups of fish after the addition of the second group of strangers. Given the fact that *ywhaz* expression is also age specific, and this impairment only occurs in adults, we suggest that this reaction is linked to *ywhaz* dysfunction in Purkinje cells. Freezing response, which is defined by the absence of any movement excluding respiration, has been studied and analysed in a number of model organisms. In zebrafish, the freezing response has been recently investigated as part of defining personality in fish (Yuan et al., 2018). In animal research, the concept of personality refers to the range of different behavioural and physiological differences that exist among individuals of the same species (Carere and Maestripieri, 2013). These traits are consistent over time and across contexts and some of them, such as stress response, can divide zebrafish into proactive and reactive groups (Ariyomo, 2013; Koolhaas et al., 1999; Wilson, 1994). Proactive fish are dominant in social hierarchies and they tend to take risks, whereas reactive fish are subordinate with the tendency of avoiding risk. This distinction is further observed during acute stress, with reactive fish reacting with a passive “freeze-hide” response while proactive fish adopt an active “fight-flight” response (Buirski et al., 1978; Frost et al., 2013; Magno et al., 2015; Rupia et al., 2016). Therefore, one explanation could be that *ywhaz* fish are more reactive, and the addition of the second stimulus triggers an acute stress response.

One of the diagnostic criteria for ASD reported by the Diagnostic and Statistical Manual of Mental Disorders (DSM-5, Edition 2013) includes information about hypo- or hyper-reactivity to sensory input, stating that autistic patients might have adverse responses to specific sounds or textures and excessive smelling or touching of objects. Given the fact that sensory processing alterations have been identified as being universally present in ASD patients (Genn et al., 2003), Rodriguez-Porcel and colleagues studied the reaction to novel auditory stimuli of a rat autism model (Rodriguez-Porcel et al., 2011). Typically, rats which are presented with a novel auditory stimulus tend to react by stopping their movement and freezing for the full duration of the stimulus before re-establishing their movement slowly after sound termination. When SSRI-exposed rats, a well-defined ASD model, are exposed to a novel auditory stimulus they freeze in a similar way to untreated rats, but it takes them significantly longer to restore their movement. This can be described as over-responsivity to a sensory stimulus (Rodriguez-Porcel et al., 2011). Visual, auditory, tactile and olfactory sensory processing have been reported to be abnormal in individuals with ASD (Leekam et al., 2007). Therefore, the freezing response of *ywhaz*$^{-/-}$ to novel stimuli could indeed represent underlying sensory alterations resulting in auditory and visual hyper-reactivity to novel targets. In conclusion, this neophobic freezing response might be similar to the symptoms observed in ASD patients, highlighting the importance of functional *ywhaz* signalling in the adult brain.

5.3.3 HPLC analysis of monoamines and metabolites reveals decreased level of dopamine and serotonin in the hindbrain of *ywhaz*$^{-/-}$

We carried out HPLC to correlate the *ywhaz*$^{-/-}$ behavioural phenotype to changes in basal levels of monoamine neurotransmitters in the brain. Using this approach we identified decreased levels of DA and 5-HT in the mutant hindbrain. Interestingly, 5-HT not only regulates important aspects of human behaviour, including the hyper- and hyposerotonemia that occurs in ASD patients (Connors et al., 2006; Schain and Freedman, 1961; Yang et al., 2014), but is also known to play a primary trophic role in the development of sensory cortical projections (Chugani, 2002; Rodriguez-Porcel et al., 2011). Growing evidence indicates that ASD might be linked to DAergic dysfunction

through the reward processing circuit (Dichter et al., 2010; Ernst et al., 1997; Schultz, 2013; Scott-Van Zeeland et al., 2010). In fact, DA systems regulate both reward processing and a number of related functions such as motivation, which facilitate approach towards biologically relevant stimuli (Wise, 2008). Since humans and many other species find social interaction rewarding, autism might be caused by a deficit in reward-related social motivation (Gunaydin and Deisseroth, 2014). Animal studies have strengthened this theory by showing that DA neurons increase their activity during normal social interactions (Gunaydin et al., 2014), whereas activity is decreased in the prefrontal cortex of rats exposed to repeated social defeat during adolescence (Watt et al., 2014). The decreased level of DA observed in *ywhaz*$^{-/-}$ could lead to an impairment in social reward motivation, which could contribute to the neophobic freezing response of mutants. The fact that the same response also happens when the stimulus is a group of marbles might be explained by another DA function. Dopamine has a key modulatory role in a number of motor and cognitive functions (Chudasama and Robbins, 2006), and deficits in fine motor skills are observed in autistic patients (Bhat et al., 2011), together with altered cognitive performance (Baron-Cohen, 2004). Studies in animal models have shown that prefrontal cortex needs an optimal level of DA for normal cognitive performance, in fact both excessive or insufficient DA levels are associated with impaired working memory performance (Arnsten and Li, 2005). Therefore, the neophobic phenotype observed in *ywhaz*$^{-/-}$ could also arise from deficits in cognition and motor skills. The effect of *YWHAZ* haploinsufficiency on the dopaminergic system has been already studied in two mouse models which carry the same mutation on two different backgrounds: Sv/129 (Ramshaw et al., 2013) and BALB/c (Xu et al., 2015). The former displays increased total tissue DA levels and reduced levels of DAT, whereas the latter has normal levels of DAT and dopaminergic signalling suggesting that the role of *Ywhaz* in DA neurotransmission is influenced by epistatic interactions (Ramshaw et al., 2013; Xu et al., 2015). In conclusion, given the essential role of 5-HT in sensory processing it is tempting to hypothesise that decreased level of 5-HT might be responsible of the neophobic freezing response to novel stimuli observed in *ywhaz*$^{-/-}$. Moreover, low levels of DA might lead to impairments in social reward motivation, fine

motor skills and cognitive functions that can act synergistically to cause the impaired social behaviour that we observed.

5.3.4 Mutation of *ywhaz* leads to overexpression of *tph2*, *drd2a* and *drd2b*

We first hypothesised that the link between impaired levels of DA and *ywhaz* could be due to altered *tyrosine hydroxylase* (*th*) activity. TH is regulated by 14-3-3 family members and in particularly by YWHAZ (Aitken, 2006). The low level of DA observed in *ywhaz*$^{-/-}$ might arise from impaired dopamine synthesis. However, contrary to what we expected, *ywhaz*$^{-/-}$ possess normal expression levels of *th1* and *th2*. A number of factors can influence dopaminergic neurotransmission: the amount of DA synthesized and released, the number of DA receptors (DRs) at the synapse, and the time that DA spends in the synaptic space, which is regulated by the dopamine transporter (DAT). Given the normal expression level of *th* we also examined the expression of dopaminergic pathway genes, uncovering increased expression of *drd2a and drd2b*. High levels of *drd2* are not likely to be responsible for the decreased levels of DA. Rather, this could a compensation mechanism to overcome DA depletion and ensure normal neurotransmission. In mammals DR2 is coupled to the G-inhibitory proteins (G_i) and results in the inhibition of adenylyl cyclase and suppression of cyclic adenosine monophosphate (cAMP) production (Kebabian and Calne, 1979; Stoof and Kebabian, 1981). D2R is the main presynaptic autoreceptor of the dopaminergic system (Mercuri et al., 1997), and by inhibiting cAMP production it has inhibitory functions. Moreover, schizophrenia is hypothesised to be caused by hyperactivity of DAergic transmission specifically at the D2 receptor because antipsychotic drugs are D2 receptor antagonists (Creese et al., 1976; Seeman et al., 1975). Therefore, in *ywhaz*$^{-/-}$ low levels of DA could give rise to a compensatory increment of *drd2*, which could affect cognitive functions and results in the abnormal phenotype observed.

We also identified increased *tph2* expression levels in *ywhaz*$^{-/-}$. Usually, high levels of this enzyme lead to increased 5-HT levels, but in *ywhaz*$^{-/-}$ the situation is the opposite with mutants displaying increased *tph2* and decreased 5-HT levels. Therefore, it appears

that the reduced levels of 5-HT are not caused by impaired synthesis, but rather it seems that *tph2* is upregulated to compensate for the depletion of 5-HT.

In conclusion, it appears that decreased level of 5-HT and DA in *ywhaz*$^{-/-}$ leads to compensatory effects in both the 5-HTergic and DAergic system. Moreover, the unaltered expression levels of *th* in the mutants suggest that *ywhaz* is not the major isoform which regulates *th* activity in zebrafish. Alternatively, *ywhaz* could act at a post-translational level to regulate Th. Further studies are needed to verify whether Th levels are reduced or not at the protein level in *ywhaz*$^{-/-}$.

5.3.5 Both fluoxetine and quinpirole rescue the abnormal neophobic freezing behaviour in *ywhaz*$^{-/-}$

Two different compounds were tested to try and rescue the abnormal neophobic freezing behaviour of *ywhaz*$^{-/-}$. Since *ywhaz*$^{-/-}$ have decreased level of 5-HT in the hindbrain, we first tested fluoxetine which is a selective serotonin reuptake inhibitor (SSRI) that increases serotonin levels (Vaswani et al., 2003). Numerous studies have shown that fluoxetine can have anxiolytic effects in zebrafish (Dulawa et al., 2004; Egan et al., 2009; Singer et al., 2016; Wong et al., 2010; Wong et al., 2013). Furthermore, fluoxetine can affect social interactions between dominant and subordinate zebrafish. In fact, acute exposure to fluoxetine causes a decreased offensive response in dominant fish whereas the subordinate fish no longer display freezing behaviour after acute fluoxetine treatment (Theodoridi et al., 2017). These changes are accompanied by differences in the expression levels of several genes associated with neural activity, stress and anxiety such as *bdnf*, *c-fos*, serotonin transporters and receptors (Theodoridi et al., 2017). According to our results, acute treatment with fluoxetine restores normal preference for social novelty in *ywhaz*$^{-/-}$. We have already suggested that mutation in *ywhaz* could make the fish be more prone to a subordinate phenotype trait. It is therefore interesting to observe that fluoxetine has the same effect in both *ywhaz*$^{-/-}$ and in the subordinate fish of Theodoridi and colleagues. In addition to this, we speculated about the link between decreased level of 5-HT and impaired sensory processing in the mutant. Indeed, increased level of 5-HT after acute treatment with fluoxetine is able to rescue the exaggerated response to novel stimuli seen in *ywhaz*$^{-/-}$.

ywhaz$^{-/-}$ also show a decreased level of DA accompanied by increased expression of *drd2*. DA influences locomotor activity, mainly by acting on D1 and D2 receptors. Thus, the second drug tested was quinpirole which is a D2-like receptor selective agonist. In humans, quinpirole activates D2-like receptors, which either modulate calcium or potassium channels or inhibit protein kinase A (PKA) and Akt signalling (Beaulieu and Gainetdinov, 2011; Missale et al., 1998). D2 receptors are widespread in various regions of the brain encompassing both pre- and postsynaptic areas. Therefore their activation might have several different effects based upon their location and the level of activation (De Mei et al., 2009). For instance, a low concentration of D2 agonists mainly activates presynaptic receptors, reducing DA release and decreasing locomotion, while high concentrations of D2 agonists activate postsynaptic neurons inducing hyperactivity (Beaulieu and Gainetdinov, 2011; Missale et al., 1998). Quinpirole administration in mammals results in such a U-shaped response with biphasic dose dependent effects (Li et al., 2010). In zebrafish the situation is controversial, with one group showing that high and low concentrations do not affect locomotion whereas an intermediate concentration results in increased activity (Irons et al., 2013). However, another study showed that locomotion decreases exponentially after drug treatment (Lange et al., 2018). In *ywhaz*$^{-/-}$, the neophobic freezing response is rescued by a low concentration of quinpirole whereas higher concentrations had no effect. Given the importance of the dopaminergic system for cognitive function, the serotoninergic system for sensory processing, and the fact that both quinpirole and fluoxetine are able to rescue the neophobic freezing phenotype, it is possible to speculate that the combined impairment in dopamine and serotonin signalling might cause the alterations to behaviour observed in this mutant.

Chapter 6 Final conclusions

The overall aim of this thesis was to investigate the function of two autism spectrum disorder (ASD) candidate genes: *reelin* (*reln*) and *ywhaz* (Lammert and Howell, 2016; Toma et al., 2014). To do so, we have used zebrafish as model organism since animal studies based on candidate genes can be used to gain insights into the neurological basis of this disease.

6.1 Main findings

In the third chapter we have shown that Reln localises to laminated central nervous system (CNS) structures, such as the stratum fibrosum et griseum superficiale (sfgs) of the optic tectum which seems to have neuronal ectopia defects, enhancing the evidence for a conserved role for Reln in neuronal migration. Reln is also highly present in CNS structures that regulate cognition, emotion, learning and synaptic activity, and deficits in these features are the main hallmarks of ASD (Gilbert and Man, 2017).

Behaviourally, *reln*$^{-/-}$ do not show any deficit in aggression or anxiety-like behaviour, but they differ from WT in the visually-mediated social preference (VMSP) test since *reln*$^{-/-}$ do not switch preference when a second group of unfamiliar fish are presented. This impaired behaviour might arise either from lack of interest in the novel social stimulus, or due to an abnormal increase in attention towards the first group of fish which is already present in the tank. Both social deficits and restricted interests with abnormal focus intensity are part of the diagnostic criteria for ASD reported by the Diagnostic and Statistical Manual of Mental Disorders (DSM-5, Edition 2013). Thus, the presence of Reln in regions which are important for neuronal migration and the regulation of processes which are impaired in ASD, together with the behaviour of *reln*$^{-/-}$ which resembles autistic symptoms, strengthen the idea of Reln being involved in the aetiology of ASD.

Reln activity is mediated by different downstream pathways including canonical signalling, which acts via Dab1 and VLDLR (Bock and May, 2016). Since genetic and

epigenetic impairments of Dab1 and VLDLR are linked to ASD risk we analysed *dab1a*$^{-/-}$ and *vldlr*$^{-/-}$ to check whether canonical signalling pathways might be involved in the phenotype observed in *reln*$^{-/-}$ zebrafish. *dab1a*$^{-/-}$ and *vldlr*$^{-/-}$ displayed different behavioural profiles, but none of the two showed impairments related to any of the core features of ASD, or resemble the specific alteration in social interactions seen in *reln*$^{-/-}$. Therefore, the impaired behaviour of *reln*$^{-/-}$ does not seem to involve the canonical signalling pathway mediated by *dab1a* and *vldlr*.

We next correlated the behavioural abnormalities observed in *reln*$^{-/-}$ to neurotransmitter signalling. Thus, we analysed the level of monoamine neurotransmitters in the brain by high precision liquid chromatography (HPLC) analysis, which revealed an increased level of serotonin (5-HT) in the hindbrain of mutants. 5-HT plays a key role in shaping social responses since it influences the sensitivity and reaction to social stimuli, and the 5-HTergic system itself is highly responsive to social influences (Kiser et al., 2012). Intriguingly, hyperserotonemia occurs also in ASD patients (Connors et al., 2006; Schain and Freedman, 1961; Yang et al., 2014). In *reln*$^{-/-}$, the increased level of 5-HT is specifically revealed in the hindbrain, and it has been shown that cerebellar dysfunction is evident in autism (Stoodley, 2016). The role of cerebellum in autism will be further discussed later in this chapter.

Considering the lack of drug therapies to ameliorate the core symptoms of ASD, we tested different compounds to check if any treatment was able to rescue the impaired preference for social novelty seen in *reln*$^{-/-}$. Three compounds with different mechanisms of action were tested. i) Buspirone was selected for its action on the 5-HTergic system in order to decrease 5-HT levels in *reln*$^{-/-}$ and for its well established role as anxiolytic with pro-social effects (Barba-Escobedo and Gould, 2012; Bencan et al., 2009; File and Seth, 2003; Gould, 2011; Gould et al., 2012; Maaswinkel et al., 2013; Maaswinkel et al., 2012). ii) Oxytocin was selected based on the fact that its signalling has been suggested to be impaired in ASD patients, and for its proved role in improving social function and reducing repetitive behaviour in autistic individuals and ASD mouse models (Andari et al., 2010; Guastella et al., 2010; Higashida et al., 2012; Hollander et al., 2007; Hollander et al., 2003; Striepens et al., 2011; Teng et al., 2013). iii) Risperidone is one of the only two medications approved by the Food and Drug Administration (FDA)

to treat symptoms associated with ASD (DeFilippis and Wagner, 2016). None of these drug treatments rescued the impaired preference for social novelty observed in *reln*$^{-/-}$. Among them, buspirone, acting on the 5-HTergic system, seems to be the most promising drug, since it slightly increases the preference for social novelty in *reln*$^{-/-}$. Usually drug treatments for ASD patients are only effective when administrated chronically for months (DeFilippis and Wagner, 2016). In fact, oxytocin administration to mouse models with face validity to core ASD symptoms, ameliorated social deficits and repetitive behaviour only upon chronic administration lasting for weeks (Teng et al., 2013). Given the promising effect of buspirone with single acute administration, our preclinical findings indicate that buspirone might have beneficial effects in treating ASD symptoms but its effect in *reln*$^{-/-}$ has to be further tested under chronic administration regimen.

Overall, the third chapter provide significant information regarding the relationship between Reln activity and neurotransmitter signalling, shedding light on the role of the 5-HTergic system in ASD. Homozygous *reln*$^{-/-}$ zebrafish mutants might be considered a good novel model to analyse some features which resemble specific symptoms of ASD. Further study with chronic administration of buspirone might rescue the sociability phenotype of this mutant. In conclusion these results provide novel insights into Reln function and its association with ASD.

The fourth chapter described the generation of *ywhaz*$^{-/-}$ mutant line using the Clustered Regularly Interspaced Short Palindromic Repeats/CRISPR associated protein-9 nuclease (CRISPR/Cas9) technique. Protocols from Auer and Del Bene, Gagnon and colleagues, and Hwang and colleagues (Auer and Del Bene, 2014; Gagnon et al., 2014; Hwang et al., 2013) were available, but specific adjustments and modifications were necessary to use this technique in this project. For examples, several trials have been performed before reaching the conclusion that the optimal concentration of Cas9-encoding mRNA to be injected was 250 ng/µl together with 25 ng/µl sgRNA. These concentrations are specific for every single sgRNA. Moreover, the genotyping protocol required few steps of optimizations since the strategy which relied on the digestion of the unique restriction enzyme site in the mutants was not satisfactory. Therefore, we had to design a multiplex PCR reaction with specific primers that recognised the presence or the absence of the

Δ7 allele, plus a pair of control primers which amplified a region upstream in the *ywhaz* gene. Overall, merging the contents of three different protocols and making the appropriate adjustments we were able to generate a novel *ywhaz*$^{-/-}$ mutant line that carries a 7 bp deletion, which causes a frameshift leading to degradation of the truncated *ywhaz* mRNA. This mutant line has been used in the fifth chapter to examine Ywhaz function in zebrafish.

In the fifth chapter we have shown that at developmental stages *ywhaz* expression is widespread covering almost all brain areas, whereas in adults it becomes restricted to the Purkinje cell layer of the valvula cerebelli (Va) and corpus cerebelli (CCe). We therefore hypothesized that *ywhaz* may have an important role in neurogenesis during development while at adult stages it might be essential for the integrity of the cerebellar cytoarchitecture and function. Both impaired neurogenesis and deficits in cerebellar function are linked to ASD (Packer, 2016; Stoodley, 2016; Wang et al., 2014a).

Behaviourally, *ywhaz*$^{-/-}$ do not show abnormal aggression or anxiety-like behaviour, however in the second step of the VMSP step they exhibit an age-specific neophobic reaction in response to both social stimuli and marbles. Given the fact that *ywhaz* expression is also age-specific, we hypothesised that the impaired behaviour observed could arise from *ywhaz* dysfunction in Purkinje cells. In particular, *ywhaz* impairments might lead to either sensory alterations, causing over-responsivity to sensory stimuli, which is a typical symptom of ASD (Leekam et al., 2007) or might lead the fish to be more likely to express a “reactive” phenotype. Thus, the addition of the second stimulus might trigger an acute stress response.

We identified decreased levels of dopamine (DA) and 5-HT in the mutant hindbrain. Intriguingly, 5-HT also plays a primary trophic role in the development of sensory cortical projections (Chugani, 2002; Rodriguez-Porcel et al., 2011), and the DA system is known to regulate social reward processing and a number of motor and cognitive functions (Chudasama and Robbins, 2006; Wise, 2008). Therefore, we hypothesised that decreased level of 5-HT and DA could affect the development of sensory cortical projections, reward motivation and cognitive functions which synergistically might be responsible for the neophobic freezing response to novel stimuli observed in *ywhaz*$^{-/-}$. Moreover, it appears that a decreased level of 5-HT and DA in *ywhaz*$^{-/-}$ leads to

compensatory effects in both the 5-HTergic and DAergic system, leading to the overexpression of *tph2*, *drd2a* and *drd2b*. Finally, *th* levels in *ywhaz*$^{-/-}$ are normal, suggesting that *ywhaz* is not the major isoform which regulates *th* activity in zebrafish.

Therapeutically, both fluoxetine, a selective serotonin reuptake inhibitor (SSRI) which increases serotonin levels and has anxiolytic effects (Vaswani et al., 2003), and quinpirole which is a selective D2-like receptor agonist are able to rescue the neophobic freezing phenotype. The positive outcome upon drug treatments suggest that a combined impairment in DA and 5-HT signalling might underlie impaired phenotype observed in this mutant.

Overall, the fifth chapter highlighted the importance of functional *ywhaz* signalling in the adult brain, shedding light on the role of both the 5-HTergic and DAergic system in ASD. The *ywhaz*$^{-/-}$ mutant line that we generated in the laboratory could therefore be considered a suitable novel model to analyse some defects which occur in ASD. Translational studies in mammals will be needed to validate the efficacy and verify the side effects of fluoxetine and quinpirole as a treatment for some ASD traits. In conclusion these results increase the understanding of Ywhaz function and its association with ASD.

6.2 The role of the cerebellum in autism spectrum disorder

The cerebellum is one of the most consistent areas of abnormality reported in ASD, with post-mortem, genetic, animal model, and neuroimaging studies revealing cerebellar impairments (Becker and Stoodley, 2013; Wang et al., 2014a). Cerebellar damage is associated with an increased risk of ASD symptoms, suggesting that cerebellar dysfunction may have a critical role in the aetiology of this disorder (Allen, 2005; Fatemi et al., 2012). Moreover, normal cerebellum function is essential during development, and impairments to the cerebellum at this stage can have long-term effects on cognition, movement, and affective regulation. Nevertheless early cerebellar damage is usually associated with worse outcomes than cerebellar impairments in adulthood (Wang et al., 2014a).

The human cerebellum appears as a separate structure attached to the bottom of the brain, underneath the cerebral hemispheres. Even though it covers only the 10% of total brain volume it contains more neurons than the rest of the brain, having approximately a cell density four times greater than the neocortex (Herculano-Houzel, 2010). Morphologically, the cerebellum is subdivided into a central vermis flanked by two hemispheres, and it is composed of an outer layer of grey matter, the cerebellar cortex, which encloses an internal layer of white matter and three pairs of embedded deep nuclei. Moreover, the cerebellum is subdivided into 3 lobes and 10 lobules (I–X). Some of the brain abnormalities that have been detected in ASD patients correspond to hypoplasia of the posterior vermis, decreased cerebellar cortical volume (Becker and Stoodley, 2013), grey matter reductions in the right lobule VII, left lobule VIII and medial IX (Stoodley, 2014), and in the cerebellar peduncles (Becker and Stoodley, 2013). Moreover, the valproic acid mouse model, one of the most widely used animal models of ASD, exhibit cerebellar atrophy (Ingram et al., 2000). The human cerebellar cortex has three layers and consists of five major cell types: the inhibitory stellate and basket cells, Golgi and Purkinje neurons, and the excitatory granule cells (GCs) (Becker and Stoodley, 2013). It receives input exclusively from the cerebral cortex and its neurons are arranged in repeating circuit modules ensuring precise connections. In fact, the cerebellum receives two types of excitatory inputs, from the mossy fibers which originate in the precerebellar nuclei and from the climbing fibers coming from the inferior olive. The Purkinje cells are the only output of the cerebellar cortex, and their axons project to neurons in the cerebellar nuclei, which then project to specific regions of the brain. One of the most consistent cerebellar impairments associated with ASD is decreased GABAergic Purkinje cell counts in the cerebellar cortex of autistic patients (Bauman and Kemper, 2005; Fatemi et al., 2002; Williams et al., 1980), and interestingly, ASD symptoms can be induced by specifically targeting cerebellar Purkinje cells in mutant mice (Tsai et al., 2012). These cerebellar structural and functional abnormalities may have functional impacts on specific cerebro-cerebellar circuits, since the cerebellum is connected with most of the cerebral cortex areas, thanks to specific closed-loop cerebello-thalamo-cortico-pontine-cerebellar circuits, which define different cerebellar functionality based on their patterns of connectivity with the cerebral cortex (Stoodley and Schmahmann, 2010). For example, the cortico-ponto-

cerebellar and cerebello-thalamo-cortical pathways allow the cerebellum to control cognitive and emotional processes, and the cerebellum also coordinates language (Booth et al., 2007), sensation, reward, motivation (Paulin, 1993), attention (Kellermann et al., 2012), memory (Heath and Harper, 1974), social processing (Jack and Pelphrey, 2014), and the spatial and temporal coordination of movement (Bugalho et al., 2006). Based on these anatomical circuits, cerebellar dysfunctions could result in behavioural outcomes which can affect the large spectrum of ASD symptoms, depending on which cerebro-cerebellar connections affected (Rogers et al., 2013).

Intriguingly both *reln* and *ywhaz* are expressed in specific areas of the cerebellum, and the correspondent mutant lines show impaired behaviour accompanied by neurotransmitter alterations in the hindbrain. Therefore, it is possible to hypothesise that ablation of these two genes might lead to disruptions in specific cerebro-cerebellar loops which might regulate the functions of cortical regions involved in ASD-like behaviour. It is possible to investigate and make predictions about the role of *reln* and *ywhaz* in the zebrafish cerebellum in relation to the human cerebro-cerebellar circuits because of the well-known structure of the zebrafish cerebellum, which is described below.

6.2.1 Zebrafish cerebellum

In zebrafish the cerebellum is located in the dorsal anterior hindbrain and similar to mammals it has an important role in the integration of sensory perception and motor control. Moreover, cerebellar development is conserved between zebrafish and mammals, and is controlled by similar genes. In both species, the cerebellum contains a number of different types of neurons that are categorized into glutamatergic and GABAergic groups according to their major neurotransmitter (Bae et al., 2009; Butler and Hodos, 2005). The excitatory glutamatergic neurons encompass unipolar brush cells, granule cells, and eurydendroid cells; the latter are functionally equivalent to the neurons in the mammalian deep cerebellar nuclei. The inhibitory GABAergic neurons include Purkinje cells, Golgi cells and stellate cells. These neurons and glial cells are arranged in a three-layered structure (from superficial to deep): the molecular layer,

Purkinje cell layer (PCL), and granule cell layer (GCL). From rostral to caudal the cerebellum is organized in three lobular structures: the valvula cerebelli (Va), the corpus cerebelli (CCe), and the vestibulolateral lobe. The latter includes the eminentia granularis (EG) and the lobus caudalis cerebelli (LCa). The Va, the CCe, and the LCa are all composed of three-layers whereas the EG contains only the GCL (Figure 49a) (Bae et al., 2009; Miyamura and Nakayasu, 2001; Wullimann et al., 1996). This structure is only partly homologous to its mammalian counterpart. In fact the CCe, which is considered the most primitive part of the teleost cerebellum, is thought to be homologous to the vermis of mammals, whereas the Va is a unique structure of teleost fish (Delgado and Schmachtenberg, 2008). In zebrafish the granule cells receive inputs from the mossy fibers (MFs), which are neuronal axons emanating from precerebellar nuclei located in several brain regions. Purkinje cells receive inputs from the climbing fibers (CFs), which are axons projecting from the inferior olive nuclei (IO) located in the ventro-posterior hindbrain. The MFs send their signals to the Purkinje cell dendrites through granule cell axons, also known as parallel fibers. Therefore, Purkinje cells integrate the signals carried by both the MFs and the CFs (Takeuchi et al., 2015). Purkinje cell axons and parallel fibers send their signal to the eurydendroid cells which further integrate information and project their axons to targets outside the cerebellum (Ikenaga et al., 2006), and to vestibular nuclei in the hindbrain forming the cerebellovestibular tracts (Han and Bell, 2003; Meek, 1992). Bergmann glia cells are involved in the development and function of the cerebellum (Buffo and Rossi, 2013)(Figure 49b). The granule cells of the CCe and Va send their axons to Purkinje cells in the ML of the cerebellum, whereas the granule cells of the LCa also send their axons to the dendrites of crest cells in the CC of the dorsal hindbrain, forming two distinct types of circuits: rostral non-vestibulocerebellar and caudal vestibulocerebellar circuits (Bae et al., 2009; Volkmann et al., 2008; Wullimann and Grothe, 2013).

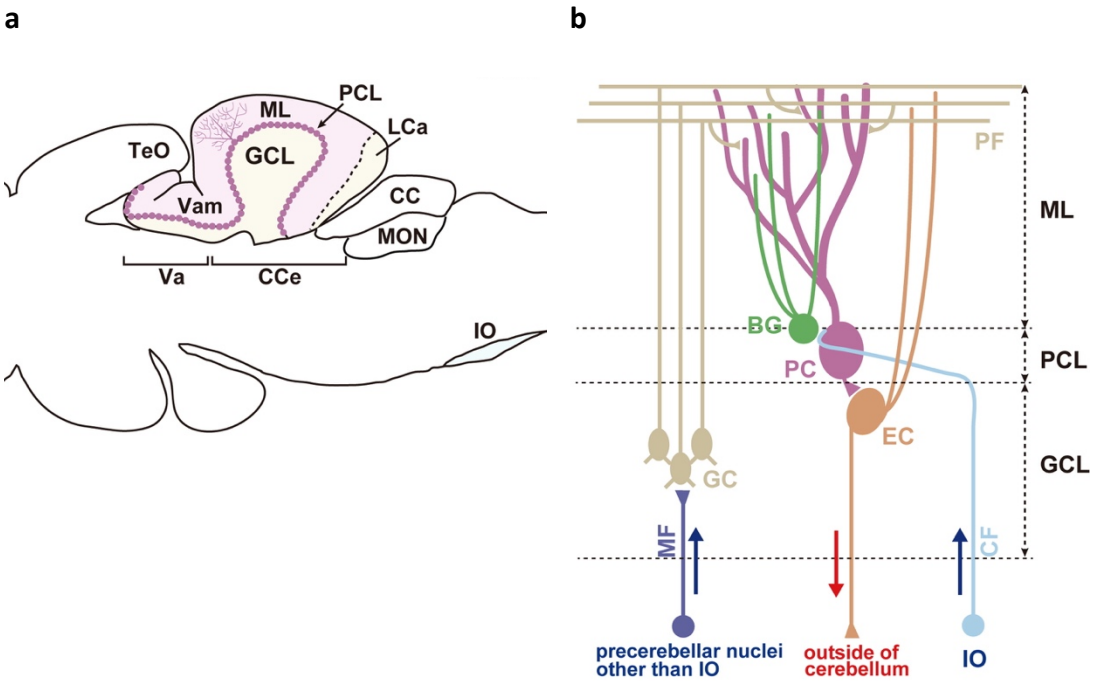

Figure 49. Structure of the zebrafish cerebellum. (a) Schematic representation of a sagittal section of the adult cerebellum. **(b)** Schematic representation of cerebellar neural circuitry. Abbreviations: BG, Bergmann glia; CC, Crista cerebellaris; CCe, Corpus cerebelli; CF, Climbing fiber; EC, Eurydendroid cells; GC, Granule cells; GCL, Granule cell layer; IO, Inferior olive nuclei; LCa, Lobus caudalis cerebelli; ML, Molecular layer; MON, Medial octavolateral nucleus; MF, Mossy fiber; PC, Purkinje cells; PCL, Purkinje cell layer; PF, Parallel fibers; TeO, Optic tectum; Va, Valvula cerebelli; Vam, Medial division of valvula cerebelli; Val, Lateral division of valvula cerebelli. Figure adapted from Takeuchi et al, 2015.

6.2.2 Cerebellar defects in *reln*$^{-/-}$

Reln is an extracellular matrix molecule that is essential for normal brain development. It is involved in granule cell migration, normal development of cerebellar lamination, arrangement of the Purkinje cell monolayer and alignment of Bergmann glia fibres (Folsom and Fatemi, 2013). In agreement with these functions, we found Reln to be present in several zebrafish brain regions. In particular, in the cerebellum Reln was localised in the granule cell layer of the CCe, in the LCa and in the CC. Unexpectedly, we did not uncover obvious cerebellar malformations in *reln*$^{-/-}$. However, given Reln function and its localisation within the granule cell layer of the cerebellum, it is tempting to hypothesise that Reln deficits might still cause subtle neuronal dysfunction without affecting the entire cerebellar structure. We were able to reveal an increase in 5-HT levels in the hindbrain of *reln*$^{-/-}$. It is well-known that the cerebellum receives dense innervation by 5-HTergic fibers. These inputs originate from the medullary and pontine reticular formation and reach both cerebellar nuclei and the cortex (Bishop and Ho,

1985; Chan-Palay, 1975), with the latter expressing multiple subtypes of 5-HT receptors (5-HTRs) (Geurts et al., 2002; Oostland et al., 2014; Pazos and Palacios, 1985). This widespread distribution of 5-HTergic innervation through the cerebellar cortex and the variety of signals evoked by different 5-HTR subtypes, allows 5-HT to modulate both excitatory and inhibitory synaptic signals throughout the cerebellar network. For example, some 5-HTR subtypes have inhibitory functions which reduce the release of glutamate from the parallel fibers to Purkinje cells (Maura et al., 1986), enhancing the inhibitory synaptic transmission onto Purkinje cells (Mitoma et al., 1994; Mitoma and Konishi, 1999), whereas others are involved in plasticity of the parallel fiber-Purkinje cell synapse. Therefore, in *reln*$^{-/-}$, a heightened level of 5-HT in the hindbrain could impair normal neural circuit activity, causing unbalanced excitatory-inhibitory neurotransmission, which in turn could lead to symptoms that resemble core features of autism.

6.2.3 Cerebellar defects in *ywhaz*$^{-/-}$

Even though it is well-recognised that impaired Purkinje cell physiology contributes to ASD behavioural phenotypes, the mechanism by which this occurs is not well understood. Given the expression of *ywhaz* specifically within Purkinje cells, and the fact that *ywhaz*$^{-/-}$ have a behavioural phenotype which resembles some of the core symptoms of ASD, this model could help understand cerebellar dysfunction which can lead to ASD symptoms. Intriguingly, there are studies that describe the interaction between $GABA_B$ receptors and two members of the 14-3-3 protein family, 14-3-3ζ and 14-3-3η (Couve et al., 2001). $GABA_B$ receptors localise to the cell bodies of Purkinje cells in zebrafish, having a distribution pattern similar to the mammalian cerebellar cortex. $GABA_B$ receptors require the formation of a heterodimer between their subunits, $GABA_B$ R1 and $GABA_B$ R2, to mediate prolonged inhibitory responses that regulate neurotransmission (Delgado and Schmachtenberg, 2008). Couve and colleagues propose that 14-3-3ζ is involved in coupling $GABA_B$ receptors and since 14-3-3ζ is present both pre- and postsynaptically, it may regulate aspects of neurotransmitter release or membrane hyperpolarization in pre- and postsynaptic neurons respectively (Couve et al., 2001). In zebrafish, *ywhaz* ablation could impair the normal

heterodimerization of the $GABA_B$ receptors affecting the balance between excitatory and inhibitory neurotransmission that is necessary for normal brain function and homeostasis. In fact, defects in $GABA_B$ receptors might heighten postsynaptic neuronal excitability resulting in hyperstimulation of neurons and leading to impairments in reacting to external stimuli (Casanova et al., 2003; Casanova et al., 2006). In addition to this, *ywhaz*$^{-/-}$ also have a decreased level of 5-HT and DA in the hindbrain that could potentially further impair the crucial balance between excitatory and inhibitory neurotransmission. In conclusion, these data support the idea that abnormalities in the cerebellum can lead to ASD-like behavioural symptoms in zebrafish.

6.3 Final conclusions and future perspectives

The idea that disruption of certain cerebellar areas, especially at developmental stages, can result in the core symptoms of ASD has been thoroughly investigated in recent years (D'Mello and Stoodley, 2015). In this project we have studied two candidate genes for ASD, and both *reln* and *ywhaz* are expressed in specific cerebellar areas. Intriguingly these proteins have a specific function within the cerebellum, with RELN being involved in neural migration, and YWHAZ interacting with $GABA_B$ receptors, suggesting that their ablation could alter the inhibitory:excitatory balance in this brain area. Moreover, the respective zebrafish models analysed in this project, *reln*$^{-/-}$ and *ywhaz*$^{-/-}$, show behavioural alterations which resemble some autistic features accompanied by impaired levels of neurotransmitters in the hindbrain. Further research is still needed to better understand the mechanisms that link *reln*$^{-/-}$ and *ywhaz*$^{-/-}$ abnormalities in different cerebellar areas with behavioural symptoms related to the functional disruption of specific cerebro-cerebellar circuits. Given the fact that: i) Purkinje cells are the only output cells of the cerebellar cortex, ii) the firing rate of the Purkinje cells is thought to be critical for encoding correct cerebellar output in deep cerebellar nuclei, iii) *ywhaz* is expressed within Purkinje cells and iv) Reln is localised in the granular cell layer which project to Purkinje cells, it will be essential to examine, via electrophysiological experiments, if the excitability of Purkinje cells is normal or altered in *reln*$^{-/-}$ and *ywhaz*$^{-/-}$. In fact, measuring Purkinje cell firing parameters such as

frequency, intensity and regularity in these mutants might confirm or reject the hypothesis that these cells have a key role in the behavioural symptoms that we observed.

In conclusion, both the mutant lines analysed in this project, *reln*$^{-/-}$ and *ywhaz*$^{-/-}$, can be considered suitable models to analyse some defects which occur in ASD, and in particularly cerebellar defects. Overall this study increases the understanding of Reln and Ywhaz function in the brain and their association with ASD.

References

Ahmad, F., et al., 2012. Zebrafish embryos and larvae in behavioural assays. Behaviour. 149**,** 1241-1281.

Ahn, A. H., et al., 1994. The cloning of zebrin II reveals its identity with aldolase C. Development. 120**,** 2081-2090.

Aitken, A., 2006. 14-3-3 proteins: a historic overview. Semin Cancer Biol. 16**,** 162-72.

Aitken, A., 2011. Post-translational modification of 14-3-3 isoforms and regulation of cellular function. Seminars in Cell & Developmental Biology. 22**,** 673-680.

Alcántara, S., et al., 1998. Regional and cellular patterns of reelin mRNA expression in the forebrain of the developing and adult mouse. Journal of Neuroscience. 18**,** 7779-7799.

Allen, G., 2005. The cerebellum in autism. Clin Neuropsychiatry. 2**,** 321-337.

Alvarado, O., et al. The Florida State University, Tallahassee, National High Magnetic Field Laboratory.

Amaral, D. G., et al., 2008. Neuroanatomy of autism. Trends in Neurosciences. 31**,** 137-145.

Amo, R., et al., 2010. Identification of the zebrafish ventral habenula as a homolog of the mammalian lateral habenula. Journal of Neuroscience. 30**,** 1566-1574.

Andari, E., et al., 2010. Promoting social behavior with oxytocin in high-functioning autism spectrum disorders. Proceedings of the National Academy of Sciences. 107**,** 4389-4394.

Anderson, G. M., et al., 1987. WHOLE BLOOD SEROTONIN IN AUTISTIC AND NORMAL SUBJECTS. Journal of Child Psychology and Psychiatry. 28**,** 885-900.

Arcangelo, G. D., et al., 1995. A protein related to extracellular matrix proteins deleted in the mouse mutant reeler. Nature. 374**,** 719.

Ariyomo, T. O., Personality traits of the zebrafish, Danio rerio and the guppy, Poecilia reticulata. University of Sheffield, 2013.

Arnaud, L., et al., 2003. Regulation of Protein Tyrosine Kinase Signaling by Substrate Degradation during Brain Development. Molecular and Cellular Biology. 23**,** 9293-9302.

Arnsten, A. F., Li, B.-M., 2005. Neurobiology of executive functions: catecholamine influences on prefrontal cortical functions. Biological psychiatry. 57**,** 1377-1384.

Ashley-Koch, A., et al., 1999. Genetic Studies of Autistic Disorder and Chromosome 7. Genomics. 61**,** 227-236.

Auer, T. O., Del Bene, F., 2014. CRISPR/Cas9 and TALEN-mediated knock-in approaches in zebrafish. Methods. 69**,** 142-150.

Bae, Y. K., et al., 2009. Anatomy of zebrafish cerebellum and screen for mutations affecting its development. Dev Biol. 330**,** 406-26.

Bailey, A., 1998. A clinicopathological study of autism. Brain. 121**,** 889-905.

Baldessarini, R., 1996. Drugs and Treatment of Psychiatric Disorders: Psychosis and Anxiety. Goodman and Gilman s The Pharmacological Basis of therapeutics. International Edition. 419-427.

Banerjee, A., et al., 2012. Impairment of cortical GABAergic synaptic transmission in an environmental rat model of autism. The International Journal of Neuropsychopharmacology. 16**,** 1309-1318.

Bar, I., et al., 1995. A YAC contig containing the reeler locus with preliminary characterization of candidate gene fragments. Genomics. 26**,** 543-549.

Barba-Escobedo, P. A., Gould, G. G., 2012. Visual social preferences of lone zebrafish in a novel environment: strain and anxiolytic effects. Genes, Brain and Behavior. 11**,** 366-373.

Baron-Cohen, S., The cognitive neuroscience of autism. BMJ Publishing Group Ltd, 2004.

Barr, A. M., et al., 2008. Heterozygous reeler mice exhibit alterations in sensorimotor gating but not presynaptic proteins. European Journal of Neuroscience. 27**,** 2568-2574.

Barreto-Valer, K., et al., 2012. Modulation by cocaine of dopamine receptors through miRNA-133b in zebrafish embryos. PLoS One. 7**,** e52701.

Barrett, S., et al., 1999. An autosomal genomic screen for autism. Collaborative linkage study of autism. American journal of medical genetics. 88**,** 609-615.

Bauman, M. L., Kemper, T. L., 2005. Neuroanatomic observations of the brain in autism: a review and future directions. International journal of developmental neuroscience. 23**,** 183-187.

Bearden, C., Freimer, N., 2006. Endophenotypes for psychiatric disorders: ready for primetime? Trends in Genetics. 22**,** 306-313.

Beaulieu, J.-M., Gainetdinov, R. R., 2011. The physiology, signaling, and pharmacology of dopamine receptors. Pharmacological reviews. 63**,** 182-217.

Becker, E. B. E., Stoodley, C. J., Autism Spectrum Disorder and the Cerebellum. International Review of Neurobiology. Elsevier, 2013, pp. 1-34.

Beffert, U., et al., 2005. Modulation of Synaptic Plasticity and Memory by Reelin Involves Differential Splicing of the Lipoprotein Receptor Apoer2. Neuron. 47**,** 567-579.

Bell, R., et al., 2000. Systematic screening of the 14-3-3 eta (?) chain gene for polymorphic variants and case-control analysis in schizophrenia. American Journal of Medical Genetics. 96**,** 736-743.

Bellipanni, G., et al., 2002. Cloning of two tryptophan hydroxylase genes expressed in the diencephalon of the developing zebrafish brain. Mechanisms of Development. 119**,** S215-S220.

Bencan, Z., Levin, E. D., 2008. The role of α7 and α4β2 nicotinic receptors in the nicotine-induced anxiolytic effect in zebrafish. Physiology & behavior. 95**,** 408-412.

Bencan, Z., et al., 2009. Buspirone, chlordiazepoxide and diazepam effects in a zebrafish model of anxiety. Pharmacology Biochemistry and Behavior. 94**,** 75-80.

Benzinger, A., et al., 2005. The crystal structure of the non-liganded 14-3-3σ protein: insights into determinants of isoform specific ligand binding and dimerization. Cell Research. 15**,** 219-227.

Berg, D., et al., 2003. 14-3-3 proteins in the nervous system. Nature Reviews Neuroscience. 4**,** 752.

Berry-Kravis, E., 2014. Mechanism-based treatments in neurodevelopmental disorders: fragile X syndrome. Pediatric neurology. 50**,** 297-302.

Bertotto, L. B., et al., 2018. Effects of bifenthrin exposure on the estrogenic and dopaminergic pathways in zebrafish embryos and juveniles. Environmental toxicology and chemistry. 37**,** 236-246.

Bhat, A. N., et al., 2011. Current perspectives on motor functioning in infants, children, and adults with autism spectrum disorders. Physical therapy. 91**,** 1116-1129.

Biamonte, F., et al., 2009. Interactions between neuroactive steroids and reelin haploinsufficiency in Purkinje cell survival. Neurobiology of Disease. 36**,** 103-115.

Biechl, D., et al., 2016. Eppur Si Muove: Evidence for an External Granular Layer and Possibly Transit Amplification in the Teleostean Cerebellum. Front Neuroanat. 10**,** 49.

Bishop, G. A., Ho, R. H., 1985. The distribution and origin of serotonin immunoreactivity in the rat cerebellum. Brain Research. 331**,** 195-207.

Blaser, R. E., Vira, D. G., 2014. Experiments on learning in zebrafish (Danio rerio): A promising model of neurocognitive function. Neuroscience & Biobehavioral Reviews. 42**,** 224-231.

Blatt, G. J., et al., 2001. Journal of Autism and Developmental Disorders. 31**,** 537-543.

Bleuler, E. P., 1930. The physiogenic and psychogenic in schizophrenia. American Journal of Psychiatry. 87**,** 203-211.

Bock, H. H., Herz, J., 2003. Reelin Activates Src Family Tyrosine Kinases in Neurons. Current Biology. 13**,** 18-26.

Bock, H. H., May, P., 2016. Canonical and non-canonical reelin signaling. Frontiers in cellular neuroscience. 10.

Bonora, E., et al., 2003. Analysis of reelin as a candidate gene for autism. Molecular Psychiatry. 8**,** 885-892.

Booth, J. R., et al., 2007. The role of the basal ganglia and cerebellum in language processing. Brain Research. 1133**,** 136-144.

Born, G., et al., 2015. Genetic targeting of NRXN2 in mice unveils role in excitatory cortical synapse function and social behaviors. Frontiers in synaptic neuroscience. 7**,** 3.

Boyle, M. P., et al., 2011. Cell-type-specific consequences of reelin deficiency in the mouse neocortex, hippocampus, and amygdala. Journal of Comparative Neurology. 519**,** 2061-2089.

Bridges, D., Moorhead, G. B. G., 2005. 14-3-3 Proteins: A Number of Functions for a Numbered Protein. Science Signaling. 2005**,** re10-re10.

Brix, M. K., et al., 2015. Brain MR spectroscopy in autism spectrum disorder—the GABA excitatory/inhibitory imbalance theory revisited. Frontiers in human neuroscience. 9**,** 365.

Brocal, I., et al., 2016. Efficient identification of CRISPR/Cas9-induced insertions/deletions by direct germline screening in zebrafish. BMC Genomics. 17**,** 259.

Bromley, R., et al., 2008. Autism spectrum disorders following in utero exposure to antiepileptic drugs. Neurology. 71**,** 1923-1924.

Brunet, A., et al., 2002. 14-3-3 transits to the nucleus and participates in dynamic nucleocytoplasmic transport. The Journal of Cell Biology. 156**,** 817-828.

Brunne, B., et al., 2013. Role of the postnatal radial glial scaffold for the development of the dentate gyrus as revealed by reelin signaling mutant mice. Glia. 61**,** 1347-1363.

Buffo, A., Rossi, F., 2013. Origin, lineage and function of cerebellar glia. Progress in Neurobiology. 109**,** 42-63.

Bufill, E., et al., 2013. Reelin Signaling Pathway Genotypes and Alzheimer Disease in a Spanish Population. Alzheimer Disease & Associated Disorders. 1.

Bugalho, P., et al., 2006. Role of the cerebellum in cognitive and behavioural control: scientific basis and investigation models. Acta medica portuguesa. 19**,** 257-67.

Buirski, P., et al., 1978. Sex differences, dominance, and personality in the chimpanzee. Animal Behaviour. 26**,** 123-129.

Butler, A. B., Hodos, W., Comparative Vertebrate Neuroanatomy. John Wiley & Sons, Inc., 2005.

Butts, T., et al., 2014. Development of the cerebellum: simple steps to make a 'little brain'. Development. 141**,** 4031-4041.

Buxbaum, J., et al., 2002. Association between a GABRB3 polymorphism and autism. Molecular psychiatry. 7**,** 311.

Campbell, J. K., et al., 1997. Activation of the 43 kDa Inositol Polyphosphate 5-Phosphatase by 14-3-3ζ†. Biochemistry. 36**,** 15363-15370.

Candy, J., Collet, C., 2005. Two tyrosine hydroxylase genes in teleosts. Biochimica et Biophysica Acta (BBA) - Gene Structure and Expression. 1727**,** 35-44.

Carere, C., Maestripieri, D., 2013. Animal personalities: behavior, physiology, and evolution. University of Chicago Press.

Carter, C. J., Blizard, R., 2016. Autism genes are selectively targeted by environmental pollutants including pesticides, heavy metals, bisphenol A, phthalates and many others in food, cosmetics or household products. Neurochemistry international. 101**,** 83-109.

Casanova, M. F., et al., 2003. Disruption in the Inhibitory Architecture of the Cell Minicolumn: Implications for Autisim. The Neuroscientist. 9**,** 496-507.

Casanova, M. F., et al., 2006. Minicolumnar abnormalities in autism. Acta neuropathologica. 112**,** 287.

Cellot, G., Cherubini, E., 2014. GABAergic signaling as therapeutic target for autism spectrum disorders. Frontiers in pediatrics. 2**,** 70.

Chan-Palay, V., 1975. Fine structure of labelled axons in the cerebellar cortex and nuclei of rodents and primates after intraventricular infusions with tritiated serotonin. Anatomy and Embryology. 148**,** 235-265.

Chaudhri, M., et al., 2003. Mammalian and yeast 14-3-3 isoforms form distinct patterns of dimers in vivo. Biochemical and Biophysical Research Communications. 300**,** 679-685.

Cheah, P. S., et al., 2012. Neurodevelopmental and neuropsychiatric behaviour defects arise from 14-3-3zeta deficiency. Mol Psychiatry. 17**,** 451-66.

Cheh, M. A., et al., 2006. En2 knockout mice display neurobehavioral and neurochemical alterations relevant to autism spectrum disorder. Brain Research. 1116**,** 166-176.

Chen, N., Reith, M. E., 2000. Structure and function of the dopamine transporter. European journal of pharmacology. 405**,** 329-339.

Chen, Y., 2005. Reelin Modulates NMDA Receptor Activity in Cortical Neurons. Journal of Neuroscience. 25**,** 8209-8216.

Chen, Y., et al., 2010. ApoE4 reduces glutamate receptor function and synaptic plasticity by selectively impairing ApoE receptor recycling. Proceedings of the National Academy of Sciences. 107**,** 12011-12016.

Chevallier, C., et al., 2012. The social motivation theory of autism. Trends in Cognitive Sciences. 16**,** 231-239.

Christensen, D. L., et al., 2016. Prevalence and characteristics of autism spectrum disorder among 4-year-old children in the autism and developmental disabilities monitoring network. Journal of Developmental & Behavioral Pediatrics. 37**,** 1-8.

Chudasama, Y., Robbins, T., 2006. Functions of frontostriatal systems in cognition: comparative neuropsychopharmacological studies in rats, monkeys and humans. Biological psychology. 73**,** 19-38.

Chugani, D., 2002. Role of altered brain serotonin mechanisms in autism. Molecular Psychiatry. 7**,** S16.

Chugani, D. C., et al., 1999. Developmental changes in brain serotonin synthesis capacity in autistic and nonautistic children. Annals of Neurology: Official Journal of the American Neurological Association and the Child Neurology Society. 45**,** 287-295.

Cocco, A., et al., 2017. Characterization of the γ-aminobutyric acid signaling system in the zebrafish (Danio rerio Hamilton) central nervous system by reverse transcription-quantitative polymerase chain reaction. Neuroscience. 343**,** 300-321.

Coghlan, S., et al., 2012. GABA system dysfunction in autism and related disorders: from synapse to symptoms. Neuroscience & Biobehavioral Reviews. 36**,** 2044-2055.

Comparot, S., et al., 2003a. Function and specificity of 14-3-3 proteins in the regulation of carbohydrate and nitrogen metabolism. Journal of Experimental Botany. 54**,** 595-604.

Comparot, S., et al., 2003b. Function and specificity of 14-3-3 proteins in the regulation of carbohydrate and nitrogen metabolism. Journal of Experimental Botany. 54**,** 595-604.

Connaughton, V. P., et al., 2008. Electrophysiological evidence of GABAA and GABAC receptors on zebrafish retinal bipolar cells. Visual Neuroscience. 25**,** 139-153.

Connors, S. L., et al., 2006. Plasma serotonin in autism. Pediatric neurology. 35, 182-186.

Consortium, I. M. G. S. o. A., 2001. Further characterization of the autism susceptibility locus AUTS1 on chromosome 7q. Human Molecular Genetics. 10, 973-982.

Cook, E. H., et al., 1998. Linkage-Disequilibrium Mapping of Autistic Disorder, with 15q11-13 Markers. The American Journal of Human Genetics. 62, 1077-1083.

Cook, E. H., Leventhal, B. L., 1996. The serotonin system in autism. Current opinion in pediatrics. 8, 348-354.

Cookson, M. R., Bandmann, O., 2010. Parkinson's disease: insights from pathways. Human Molecular Genetics. 19, R21-R27.

Corbo, C. P., et al., 2012. Use of different morphological techniques to analyze the cellular composition of the adult zebrafish optic tectum. Microscopy research and technique. 75, 325-333.

Cornell, B., Toyo-oka, K., 2016. Deficiency of 14-3-3ε and 14-3-3ζ by the Wnt1 promoter-driven Cre recombinase results in pigmentation defects. BMC Research Notes. 9.

Cornell, B., Toyo-Oka, K., 2017. 14-3-3 proteins in brain development: neurogenesis, neuronal migration and neuromorphogenesis. Frontiers in molecular neuroscience. 10, 318.

Cornell, B., et al., 2016. Regulation of neuronal morphogenesis by 14-3-3epsilon (Ywhae) via the microtubule binding protein, doublecortin. Human Molecular Genetics. ddw270.

Costa, E., 2002. The heterozygote reeler mouse as a model for the development of a new generation of antipsychotics. Current Opinion in Pharmacology. 2, 56-62.

Costagli, A., et al., 2002. Conserved and divergent patterns of Reelin expression in the zebrafish central nervous system. Journal of Comparative Neurology. 450, 73-93.

Cotzias, G. C., Dole, V. P., 1951. Metabolism of Amines. II: Mitochondrial Localization of Monoamine Oxidase. Experimental Biology and Medicine. 78, 157-160.

Courchesne, E., 2003. Evidence of Brain Overgrowth in the First Year of Life in Autism.

Courchesne, E., 2004. Brain development in autism: Early overgrowth followed by premature arrest of growth. Mental Retardation and Developmental Disabilities Research Reviews. 10, 106-111.

Courchesne, E., et al., 2000. Normal brain development and aging: quantitative analysis at in vivo MR imaging in healthy volunteers. Radiology. 216, 672-682.

Courchesne, E., Pierce, K., 2005. Brain overgrowth in autism during a critical time in development: implications for frontal pyramidal neuron and interneuron development and connectivity. International Journal of Developmental Neuroscience. 23, 153-170.

Courchesne, E., et al., 2004. The autistic brain: birth through adulthood. Current Opinion in Neurology. 17, 489-496.

Couve, A., et al., 2001. Association of GABAB receptors and members of the 14-3-3 family of signaling proteins. Molecular and Cellular Neuroscience. 17, 317-328.

Creese, I., et al., 1976. Dopamine receptor binding predicts clinical and pharmacological potencies of antischizophrenic drugs. Science. 192**,** 481-483.

Cristino, A. S., et al., 2014. Neurodevelopmental and neuropsychiatric disorders represent an interconnected molecular system. Mol Psychiatry. 19**,** 294-301.

Curran, T., D'Arcangelo, G., 1998. Role of reelin in the control of brain development1Published on the World Wide Web on 21 October 1997.1. Brain Research Reviews. 26**,** 285-294.

D'Arcangelo, G., The Reeler Mouse: Anatomy of a Mutant. International Review of Neurobiology. Elsevier, 2005, pp. 383-417.

D'Arcangelo, G., 2014. Reelin in the Years: Controlling Neuronal Migration and Maturation in the Mammalian Brain. Advances in Neuroscience. 2014**,** 1-19.

D'Arcangelo, G., Curran, T., 1998. Reeler: new tales on an old mutant mouse. Bioessays. 20**,** 235-244.

D'Arcangelo, G., et al., 1995. A protein related to extracellular matrix proteins deleted in the mouse mutant reeler. Nature. 374**,** 719-723.

D'Arcangelo, G., et al., 2017. Reelin-related neurological disorders and animal models. Frontiers in cellular neuroscience. 10**,** 299.

D'Mello, A. M., Stoodley, C. J., 2015. Cerebro-cerebellar circuits in autism spectrum disorder. Frontiers in neuroscience. 9**,** 408.

Dai, J.-G., Murakami, K., 2002. Constitutively and autonomously active protein kinase C associated with 14-3-3 ζ in the rodent brain. Journal of Neurochemistry. 84**,** 23-34.

Dalla Vecchia, E., et al., 2018. Cross-species models of attention-deficit/hyperactivity disorder and autism spectrum disorder: lessons from CNTNAP2, ADGRL3, and PARK2. Psychiatric genetics.

Dar, A., et al., 2014. 14-3-3 Proteins Play a Role in the Cell Cycle by Shielding Cdt2 from Ubiquitin-Mediated Degradation. Molecular and Cellular Biology. 34**,** 4049-4061.

Davezac, N., et al., 2000. Regulation of CDC25B phosphatases subcellular localization. Oncogene. 19**,** 2179-2185.

Davis, P. E., et al., 2015. Tuberous Sclerosis: A New Frontier in Targeted Treatment of Autism. Neurotherapeutics. 12**,** 572-583.

Dawson, G., 2008. Early behavioral intervention, brain plasticity, and the prevention of autism spectrum disorder. Development and Psychopathology. 20.

De Mei, C., et al., 2009. Getting specialized: presynaptic and postsynaptic dopamine D2 receptors. Current opinion in pharmacology. 9**,** 53-58.

De Rubeis, S., et al., 2014. Synaptic, transcriptional and chromatin genes disrupted in autism. Nature. 515**,** 209-215.

De Sarno, P., et al., 2002. Regulation of Akt and glycogen synthase kinase-3β phosphorylation by sodium valproate and lithium. Neuropharmacology. 43**,** 1158-1164.

DeFilippis, M., Wagner, K. D., 2016. Treatment of autism spectrum disorder in children and adolescents. Psychopharmacology bulletin. 46**,** 18.

Delavest, M., et al., 2012. Association of the intronic rs2072621 polymorphism of the X-linked GPR50 gene with affective disorder with seasonal pattern. European Psychiatry. 27**,** 369-371.

Delgado, L., Schmachtenberg, O., 2008. Immunohistochemical localization of GABA, GAD65, and the receptor subunits GABA Aα1 and GABA B1 in the zebrafish cerebellum. The Cerebellum. 7**,** 444-450.

Delorey, T., et al., 2008. Gabrb3 gene deficient mice exhibit impaired social and exploratory behaviors, deficits in non-selective attention and hypoplasia of cerebellar vermal lobules: A potential model of autism spectrum disorder. Behavioural Brain Research. 187**,** 207-220.

Delorme, R., et al., 2013. Progress toward treatments for synaptic defects in autism. Nature medicine. 19**,** 685.

DeSilva, U., et al., 1997. The human reelin gene: isolation, sequencing, and mapping on chromosome 7. Genome Research. 7**,** 157-164.

Dhossche, D. M., et al., Is There A Connection Between Autism, Prader-Willi Syndrome, Catatonia, And GABA? , International Review of Neurobiology. Elsevier, 2005, pp. 189-216.

Di Donato, V., et al., 2018. An Attractive Reelin Gradient Establishes Synaptic Lamination in the Vertebrate Visual System. Neuron. 97**,** 1049-1062. e6.

Dichter, G. S., et al., 2010. Reward circuitry function in autism spectrum disorders. Social Cognitive and Affective Neuroscience. 7**,** 160-172.

Dichter, G. S., et al., 2011. Reward Circuitry Function in Autism During Face Anticipation and Outcomes. Journal of Autism and Developmental Disorders. 42**,** 147-160.

DiLalla, L. F., et al., A review of endophenotypes in schizophrenia and autism: The next phase for understanding genetic etiologies. American Journal of Medical Genetics Part C: Seminars in Medical Genetics, Vol. 175. Wiley Online Library, 2017, pp. 354-361.

Dobbing, J., 1982. The later development of the brain and its vulnerability. Journal of Inherited Metabolic Disease. 5**,** 88-88.

DSM-5, Edition 2013. Diagnostic and statistical manual of mental disorders. Am Psychiatric Assoc.

Duan, H., Wang, J., 2010. Selective Transport of Monoamine Neurotransmitters by Human Plasma Membrane Monoamine Transporter and Organic Cation Transporter 3. Journal of Pharmacology and Experimental Therapeutics. 335**,** 743-753.

Dulawa, S. C., et al., 2004. Effects of Chronic Fluoxetine in Animal Models of Anxiety and Depression. Neuropsychopharmacology. 29**,** 1321-1330.

Durand, C. M., et al., 2007. Mutations in the gene encoding the synaptic scaffolding protein SHANK3 are associated with autism spectrum disorders. Nature genetics. 39**,** 25.

Dutta, S., et al., 2006. Reelin gene polymorphisms in the Indian population: A possible paternal 5'UTR-CGG-repeat-allele effect on autism. American Journal of Medical Genetics Part B: Neuropsychiatric Genetics. 144B**,** 106-112.

Dutta, S., et al., 2008. Genetic analysis of reelin gene (RELN) SNPs: No association with autism spectrum disorder in the Indian population. Neuroscience Letters. 441**,** 56-60.

Eastwood, S. L., Harrison, P. J., 2006. Cellular Basis of Reduced Cortical Reelin Expression in Schizophrenia. American Journal of Psychiatry. 163**,** 540-542.

Eberle, A. B., et al., 2008. Posttranscriptional Gene Regulation by Spatial Rearrangement of the 3' Untranslated Region. PLoS Biology. 6**,** e92.

Egan, R. J., et al., 2009. Understanding behavioral and physiological phenotypes of stress and anxiety in zebrafish. Behavioural Brain Research. 205**,** 38-44.

El-Ansary, A., Al-Ayadhi, L., 2014. GABAergic/glutamatergic imbalance relative to excessive neuroinflammation in autism spectrum disorders. Journal of Neuroinflammation. 11.

El-Kordi, A., et al., 2013. Development of an autism severity score for mice using Nlgn4 null mutants as a construct-valid model of heritable monogenic autism. Behavioural brain research. 251**,** 41-49.

Emamian, E. S., et al., 2004. Convergent evidence for impaired AKT1-GSK3β signaling in schizophrenia. Nature Genetics. 36**,** 131-137.

English, J. A., et al., 2011. The neuroproteomics of schizophrenia. Biol Psychiatry. 69**,** 163-72.

Eriksen, J., et al., 2010. Regulation of dopamine transporter function by protein-protein interactions: new discoveries and methodological challenges. Journal of neurochemistry. 113**,** 27-41.

Ernst, M., et al., 1997. Low medial prefrontal dopaminergic activity in autistic children. The Lancet. 350**,** 638.

Evans, D. H., Claiborne, J. B., 2005. The physiology of fishes.

Fagiolini, M., et al., 2009. Epigenetic influences on brain development and plasticity. Current opinion in neurobiology. 19**,** 207-212.

Falconer, D., 1951. Two new mutants,'trembler'and 'reeler', with neurological actions in the house mouse (Mus musculus L.). Journal of genetics. 50**,** 192-205.

Farrant, M., Nusser, Z., 2005. Variations on an inhibitory theme: phasic and tonic activation of GABAA receptors. Nature Reviews Neuroscience. 6**,** 215-229.

Fatemi, S. H., 2001. Reelin mutations in mouse and man: from reeler mouse to schizophrenia, mood disorders, autism and lissencephaly. Molecular Psychiatry. 6**,** 129-133.

Fatemi, S. H., 2002. The role of Reelin in pathology of autism. Molecular Psychiatry. 7**,** 919-920.

Fatemi, S. H., et al., 2012. Consensus Paper: Pathological Role of the Cerebellum in Autism. The Cerebellum. 11**,** 777-807.

Fatemi, S. H., et al., 2002. Purkinje cell size is reduced in cerebellum of patients with autism. Cellular and molecular neurobiology. 22**,** 171-175.

Fatemi, S. H., et al., 2010. mRNA and Protein Levels for GABAAα4, α5, β1 and GABABR1 Receptors are Altered in Brains from Subjects with Autism. Journal of Autism and Developmental Disorders. 40**,** 743-750.

Fatemi, S. H., et al., 2014. Downregulation of GABAA Receptor Protein Subunits α6, β2, δ, ε, γ2, θ, and ρ2 in Superior Frontal Cortex of Subjects with Autism. Journal of Autism and Developmental Disorders. 44**,** 1833-1845.

Fatemi, S. H., et al., 2008. GABAA Receptor Downregulation in Brains of Subjects with Autism. Journal of Autism and Developmental Disorders. 39**,** 223-230.

Fatemi, S. H., et al., 2005. Reelin signaling is impaired in autism. Biological psychiatry. 57**,** 777-787.

Feng, L., et al., 2007. Cullin 5 regulates Dab1 protein levels and neuron positioning during cortical development. Genes & Development. 21**,** 2717-2730.

Ferl, R. J., et al., 2002. Genome Biology. 3**,** reviews3010.1.

Filby, A. L., et al., 2010. Unravelling the neurophysiological basis of aggression in a fish model. BMC Genomics. 11**,** 498.

File, S. E., Seth, P., 2003. A review of 25 years of the social interaction test. European journal of pharmacology. 463**,** 35-53.

Fischer, A., et al., 2008. Regulation of RAF Activity by 14-3-3 Proteins. Journal of Biological Chemistry. 284**,** 3183-3194.

Flashner, B. M., et al., 2013. Epigenetic factors and autism spectrum disorders. Neuromolecular medicine. 15**,** 339-350.

Folgueira, M., et al., 2012. Morphogenesis underlying the development of the everted teleost telencephalon. Neural development. 7**,** 212.

Folsom, T. D., Fatemi, S. H., 2013. The involvement of Reelin in neurodevelopmental disorders. Neuropharmacology. 68**,** 122-135.

Folstein, S., Rutter, M., 1977. Infantile autism: a genetic study of 21 twin pairs. Journal of Child psychology and Psychiatry. 18**,** 297-321.

Fombonne, E., 2003. The prevalence of autism. Jama. 289**,** 87-89.

Foote, M., Zhou, Y., 2012. 14-3-3 proteins in neurological disorders. International journal of biochemistry and molecular biology. 3**,** 152.

Fountoulakis, M., et al., Increased levels of 14-3-3 gamma and epsilon proteins in brain of patients with Alzheimer's disease and Down Syndrome. The Molecular Biology of Down Syndrome. Springer Vienna, 1999, pp. 323-335.

Fraley, E., et al., 2016. Mice with Dab1 or Vldlr insufficiency exhibit abnormal neonatal vocalization patterns. Scientific Reports. 6**,** 25807.

Franco, S. J., et al., 2011. Reelin Regulates Cadherin Function via Dab1/Rap1 to Control Neuronal Migration and Lamination in the Neocortex. Neuron. 69**,** 482-497.

Freeman, A. K., Morrison, D. K., 2011. 14-3-3 Proteins: Diverse functions in cell proliferation and cancer progression. Seminars in Cell & Developmental Biology. 22**,** 681-687.

Frith, U., et al., 1991. The cognitive basis of a biological disorder: Autism. Trends in neurosciences. 14**,** 433-438.

Frost, A. J., et al., 2013. Environmental change alters personality in the rainbow trout, Oncorhynchus mykiss. Animal behaviour. 85**,** 1199-1207.

Frykman, P. K., et al., 1995. Normal plasma lipoproteins and fertility in gene-targeted mice homozygous for a disruption in the gene encoding very low density lipoprotein receptor. Proceedings of the National Academy of Sciences. 92**,** 8453-8457.

Fu, H., et al., 1993. The eukaryotic host factor that activates exoenzyme S of Pseudomonas aeruginosa is a member of the 14-3-3 protein family. Proceedings of the National Academy of Sciences. 90**,** 2320-2324.

Fu, H., et al., 2000. 14-3-3 proteins: structure, function, and regulation. Annual review of pharmacology and toxicology. 40**,** 617-647.

Fu, Y., et al., 2013. High-frequency off-target mutagenesis induced by CRISPR-Cas nucleases in human cells. Nature biotechnology. 31**,** 822.

Földy, C., et al., 2013. Autism-Associated Neuroligin-3 Mutations Commonly Disrupt Tonic Endocannabinoid Signaling. Neuron. 78**,** 498-509.

Förster, E., et al., 2010. Emerging topics in Reelin function. European Journal of Neuroscience. no-no.

Gadow, K. D., et al., 2010. Association of DRD4 polymorphism with severity of oppositional defiant disorder, separation anxiety disorder and repetitive behaviors in children with autism spectrum disorder. European Journal of Neuroscience. 32**,** 1058-1065.

Gaetz, W., et al., 2014. GABA estimation in the brains of children on the autism spectrum: measurement precision and regional cortical variation. Neuroimage. 86**,** 1-9.

Gagnon, J. A., et al., 2014. Efficient Mutagenesis by Cas9 Protein-Mediated Oligonucleotide Insertion and Large-Scale Assessment of Single-Guide RNAs. PLoS ONE. 9**,** e98186.

Gallagher, E., et al., 1998. Cerebellar abnormalities in the disabled (mdab1-1) mouse. The Journal of Comparative Neurology. 402**,** 238-251.

Ganguly, S., et al., 2001. Role of a pineal cAMP-operated arylalkylamine N-acetyltransferase/14-3-3-binding switch in melatonin synthesis. Proceedings of the National Academy of Sciences. 98**,** 8083-8088.

Ganz, J., et al., 2014. Subdivisions of the adult zebrafish pallium based on molecular marker analysis. F1000Research. 3.

Gardener, H., et al., 2009. Prenatal risk factors for autism: comprehensive meta-analysis. The British journal of psychiatry. 195**,** 7-14.

Gardino, A. K., et al., 2006. Structural determinants of 14-3-3 binding specificities and regulation of subcellular localization of 14-3-3-ligand complexes: A comparison of the X-ray crystal structures of all human 14-3-3 isoforms. Seminars in Cancer Biology. 16**,** 173-182.

Gardino, A. K., Yaffe, M. B., 2011. 14-3-3 proteins as signaling integration points for cell cycle control and apoptosis. Seminars in Cell & Developmental Biology. 22**,** 688-695.

Gasiunas, G., et al., 2012. Cas9-crRNA ribonucleoprotein complex mediates specific DNA cleavage for adaptive immunity in bacteria. Proceedings of the National Academy of Sciences. 109**,** E2579-E2586.

Gaspar, P., et al., 2003. The developmental role of serotonin: news from mouse molecular genetics. Nature Reviews Neuroscience. 4**,** 1002.

Gaspar, P., Lillesaar, C., 2012. Probing the diversity of serotonin neurons. Philosophical Transactions of the Royal Society B: Biological Sciences. 367**,** 2382-2394.

Gauducheau, M., et al., 2017. Age-specific autistic-like behaviors in heterozygous Fmr1-KO female mice. Autism Research. 10**,** 1067-1078.

Gebhardt, C., et al., 2013. Direction selectivity in the visual system of the zebrafish larva. Frontiers in neural circuits. 7**,** 111.

Genn, R. F., et al., 2003. Dietary restriction and nicotine can reduce anxiety in female rats. Neuropsychopharmacology. 28**,** 1257.

Gerlai, R., et al., 2000. Drinks like a fish: zebra fish (Danio rerio) as a behavior genetic model to study alcohol effects. Pharmacology biochemistry and behavior. 67**,** 773-782.

Geschwind, D. H., Levitt, P., 2007. Autism spectrum disorders: developmental disconnection syndromes. Current Opinion in Neurobiology. 17**,** 103-111.

Geurts, F. J., et al., 2002. Localization of 5-HT2A, 5-HT3, 5-HT5A and 5-HT7 receptor-like immunoreactivity in the rat cerebellum. Journal of Chemical Neuroanatomy. 24**,** 65-74.

Gil-Sanz, C., et al., 2013. Cajal-Retzius Cells Instruct Neuronal Migration by Coincidence Signaling between Secreted and Contact-Dependent Guidance Cues. Neuron. 79**,** 461-477.

Gilbert, J., Man, H.-Y., 2017. Fundamental elements in autism: from neurogenesis and neurite growth to synaptic plasticity. Frontiers in cellular neuroscience. 11**,** 359.

Gillis, J., et al., 2011. Long QT, syndactyly, joint contractures, stroke and novel CACNA1C mutation: Expanding the spectrum of Timothy syndrome. American Journal of Medical Genetics Part A. 158A**,** 182-187.

Go, G.-w., Mani, A., 2012. Low-density lipoprotein receptor (LDLR) family orchestrates cholesterol homeostasis. The Yale journal of biology and medicine. 85**,** 19.

Goffinet, A. M., 1983. The embryonic development of the cerebellum in normal and reeler mutant mice. Anatomy and Embryology. 168**,** 73-86.

González, J. L., et al., 1997. Birthdate and Cell Marker Analysis of Scrambler: A Novel Mutation Affecting Cortical Development with a Reeler-Like Phenotype. The Journal of Neuroscience. 17**,** 9204-9211.

Gotham, K., et al., 2015. Depressive and anxiety symptom trajectories from school age through young adulthood in samples with autism spectrum disorder and developmental delay. Journal of the American Academy of Child & Adolescent Psychiatry. 54**,** 369-376. e3.

Gottesman, I. I., Gould, T. D., 2003. The Endophenotype Concept in Psychiatry: Etymology and Strategic Intentions. American Journal of Psychiatry. 160**,** 636-645.

Gould, G. G., Aquatic light/dark plus maze novel environment for assessing anxious versus exploratory behavior in zebrafish (Danio rerio) and other small teleost fish. Zebrafish Neurobehavioral Protocols. Springer, 2011, pp. 99-108.

Gould, G. G., et al., 2012. Acetaminophen differentially enhances social behavior and cortical cannabinoid levels in inbred mice. Progress in Neuro-Psychopharmacology and Biological Psychiatry. 38**,** 260-269.

Gould, T. D., Gottesman, I. I., 2006. Psychiatric endophenotypes and the development of valid animal models. Genes, Brain and Behavior. 5**,** 113-119.

Gray, P. A., 2013. Transcription factors define the neuroanatomical organization of the medullary reticular formation. Frontiers in Neuroanatomy. 7**,** 7.

Green, A. J., et al., 1994. The tuberous sclerosis gene on chromosome 9q34 acts as a growth suppressor. Human Molecular Genetics. 3**,** 1833-1834.

Guastella, A. J., et al., 2010. Intranasal Oxytocin Improves Emotion Recognition for Youth with Autism Spectrum Disorders. Biological Psychiatry. 67**,** 692-694.

Guidotti, A., et al., 2000. Decrease in Reelin and Glutamic Acid Decarboxylase67 (GAD67) Expression in Schizophrenia and Bipolar Disorder. Archives of General Psychiatry. 57**,** 1061.

Gunaydin, L. A., Deisseroth, K., Dopaminergic dynamics contributing to social behavior. Cold Spring Harbor symposia on quantitative biology, Vol. 79. Cold Spring Harbor Laboratory Press, 2014, pp. 221-227.

Gunaydin, L. A., et al., 2014. Natural neural projection dynamics underlying social behavior. Cell. 157**,** 1535-1551.

Guptill, J. T., et al., 2006. [3H]-Flunitrazepam-labeled Benzodiazepine Binding Sites in the Hippocampal Formation in Autism: A Multiple Concentration Autoradiographic Study. Journal of Autism and Developmental Disorders. 37**,** 911-920.

Gururajan, A., van den Buuse, M., 2013. Is the mTOR-signalling cascade disrupted in Schizophrenia? Journal of Neurochemistry. 129**,** 377-387.

Haber, S. N., 2014. The place of dopamine in the cortico-basal ganglia circuit. Neuroscience. 282**,** 248-257.

Hadj-Sahraoui, N., et al., 1996. Gender Effect on Purkinje Cell Loss in the Cerebellum of the Heterozygous Reeler Mouse. Journal of Neurogenetics. 11**,** 45-58.

Hallmayer, J., et al., 2011. Genetic heritability and shared environmental factors among twin pairs with autism. Archives of general psychiatry. 68**,** 1095-1102.

Hamaguchi, A., et al., 2003. Sphingosine-dependent Protein Kinase-1, Directed to 14-3-3, Is Identified as the Kinase Domain of Protein Kinase Cδ. Journal of Biological Chemistry. 278**,** 41557-41565.

Hamilton, S. M., et al., 2014. Fmr1 and Nlgn3 knockout rats: Novel tools for investigating autism spectrum disorders. Behavioral neuroscience. 128**,** 103.

Hampson, D. R., Blatt, G. J., 2015. Autism spectrum disorders and neuropathology of the cerebellum. Front Neurosci. 9**,** 420.

Han, V. Z., Bell, C. C., 2003. Physiology of cells in the central lobes of the mormyrid cerebellum. Journal of Neuroscience. 23**,** 11147-11157.

Hanley, H. G., 1977. Hyperserotonemia and Amine Metabolites in Autistic and Retarded Children. Archives of General Psychiatry. 34**,** 521.

Harada, M., et al., 2011. Non-invasive evaluation of the GABAergic/glutamatergic system in autistic patients observed by MEGA-editing proton MR spectroscopy using a clinical 3 tesla instrument. Journal of autism and developmental disorders. 41**,** 447-454.

Hatten, M. E., 2002. New directions in neuronal migration. Science. 297**,** 1660-1663.

He, Y., et al., 2011. No significant association between RELN polymorphism and autism in case-control and family-based association study in Chinese Han population. Psychiatry Research. 187**,** 462-464.

Heath, R. G., Harper, J. W., 1974. Ascending projections of the cerebellar fastigial nucleus to the hippocampus, amygdala, and other temporal lobe sites: Evoked potential and histological studies in monkeys and cats. Experimental Neurology. 45**,** 268-287.

Herculano, A. M., Maximino, C., 2014. Serotonergic modulation of zebrafish behavior: towards a paradox. Progress in Neuro-Psychopharmacology and Biological Psychiatry. 55**,** 50-66.

Herculano-Houzel, S., 2010. Coordinated scaling of cortical and cerebellar numbers of neurons. Frontiers in neuroanatomy. 4**,** 12.

Hermeking, H., Benzinger, A., 2006. 14-3-3 proteins in cell cycle regulation. Seminars in Cancer Biology. 16**,** 183-192.

Herz, J., Chen, Y., 2006. Reelin, lipoprotein receptors and synaptic plasticity. Nature Reviews Neuroscience. 7**,** 850-859.

Hethorn, W. R., et al., 2015. Reelin supplementation recovers synaptic plasticity and cognitive deficits in a mouse model for Angelman syndrome. European Journal of Neuroscience. 41**,** 1372-1380.

Higashida, H., et al., 2012. Social memory, amnesia, and autism: Brain oxytocin secretion is regulated by NAD+ metabolites and single nucleotide polymorphisms of CD38. Neurochemistry International. 61**,** 828-838.

Hirotsune, S., et al., 1995. The reeler gene encodes a protein with an EGF–like motif expressed by pioneer neurons. Nature Genetics. 10**,** 77-83.

Hollander, E., et al., 2007. Oxytocin Increases Retention of Social Cognition in Autism. Biological Psychiatry. 61**,** 498-503.

Hollander, E., et al., 2003. Oxytocin Infusion Reduces Repetitive Behaviors in Adults with Autistic and Asperger's Disorders. Neuropsychopharmacology. 28**,** 193-198.

Homayouni, R., et al., 1999. Disabled-1 binds to the cytoplasmic domain of amyloid precursor-like protein 1. The Journal of neuroscience : the official journal of the Society for Neuroscience. 19**,** 7507-15.

Hong, S. E., et al., 2000. Autosomal recessive lissencephaly with cerebellar hypoplasia is associated with human RELN mutations. Nature Genetics. 26**,** 93-96.

Horev, G., et al., 2011. Dosage-dependent phenotypes in models of 16p11.2 lesions found in autism. Proceedings of the National Academy of Sciences. 108**,** 17076-17081.

Howe, K., et al., 2013. The zebrafish reference genome sequence and its relationship to the human genome. Nature. 496**,** 498.

Howell, B. W., 1997. Mouse disabled (mDab1): a Src binding protein implicated in neuronal development. The EMBO Journal. 16**,** 121-132.

Howell, B. W., et al., 1997. Neuronal position in the developing brain is regulated by mouse disabled-1. Nature. 389**,** 733-737.

Howell, B. W., et al., 1999. Reelin-induced tryosine phosphorylation of Disabled 1 during neuronal positioning. Genes & Development. 13**,** 643-648.

Howell, B. W., Herz, J., 2001. The LDL receptor gene family: signaling functions during development. Current Opinion in Neurobiology. 11**,** 74-81.

Huguet, G., et al., 2013. The genetic landscapes of autism spectrum disorders. Annual review of genomics and human genetics. 14**,** 191-213.

Hussman, J. P., 2001. Letters to the editor: suppressed GABAergic inhibition as a common factor in suspected etiologies of autism. Journal of autism and developmental disorders. 31**,** 247-248.

Hwang, W. Y., et al., 2013. Efficient genome editing in zebrafish using a CRISPR-Cas system. Nat Biotechnol. 31**,** 227-9.

Iafrati, J., et al., 2013. Reelin, an extracellular matrix protein linked to early onset psychiatric diseases, drives postnatal development of the prefrontal cortex via GluN2B-NMDARs and the mTOR pathway. Molecular Psychiatry. 19**,** 417-426.

Ichihara, H., et al., 2001. Three novel repetitive units of reelin. Molecular Brain Research. 97**,** 190-193.

Ichimura, T., et al., 1988. Molecular cloning of cDNA coding for brain-specific 14-3-3 protein, a protein kinase-dependent activator of tyrosine and tryptophan hydroxylases. Proceedings of the National Academy of Sciences. 85**,** 7084-7088.

Ichimura, T., et al., 1987. Brain 14-3-3 protein is an activator protein that activates tryptophan 5-monooxygenase and tyrosine 3-monooxygenase in the presence of Ca2+ ,calmodulin-dependent protein kinase II. FEBS Letters. 219**,** 79-82.

Ikeda, M., et al., 2008. Identification of YWHAE, a gene encoding 14-3-3epsilon, as a possible susceptibility gene for schizophrenia. Human Molecular Genetics. 17**,** 3212-3222.

Ikeda, Y., Terashima, T., 1997. Expression of reelin, the gene responsible for the reeler mutation, in embryonic development and adulthood in the mouse. Developmental dynamics: an official publication of the American Association of Anatomists. 210**,** 157-172.

Ikenaga, T., et al., 2006. Cerebellar efferent neurons in teleost fish. The Cerebellum. 5**,** 268-274.

Imai, H., et al., 2016. Dorsal Forebrain-Specific Deficiency of Reelin-Dab1 Signal Causes Behavioral Abnormalities Related to Psychiatric Disorders. Cerebral Cortex. 27**,** 3485-3501.

Ingram, J. L., et al., 2000. Prenatal exposure of rats to valproic acid reproduces the cerebellar anomalies associated with autism. Neurotoxicology and Teratology. 22**,** 319-324.

Irons, T., et al., 2013. Acute administration of dopaminergic drugs has differential effects on locomotion in larval zebrafish. Pharmacology Biochemistry and Behavior. 103**,** 792-813.

Itagaki, C., et al., 1999. Stimulus-Coupled Interaction of Tyrosine Hydroxylase with 14-3-3 Proteins†. Biochemistry. 38**,** 15673-15680.

Iwata, K., et al., 2012. Vldlr overexpression causes hyperactivity in rats. Molecular autism. 3**,** 11.

Jack, A., Pelphrey, K. A., 2014. Neural Correlates of Animacy Attribution Include Neocerebellum in Healthy Adults. Cerebral Cortex. 25**,** 4240-4247.

Jacquelin, C., et al., 2013. Neurobehavioral performances and brain regional metabolism in Dab1 scm (scrambler) mutant mice. Behavioural brain research. 252**,** 92-100.

Jacquelin, C., et al., 2012. Neurologic function during developmental and adult stages in Dab1 scm (scrambler) mutant mice. Behavioural brain research. 226**,** 265-273.

Jamain, S., et al., 2003. Mutations of the X-linked genes encoding neuroligins NLGN3 and NLGN4 are associated with autism. Nature Genetics. 34**,** 27-29.

Jia, Y., et al., 2004. An association study between polymorphisms in three genes of 14-3-3 (tyrosine 3-monooxygenase/tryptophan 5-monooxygenase activation protein) family and paranoid schizophrenia in northern Chinese population. European Psychiatry. 19**,** 377-379.

Jiang, Y.-h., Ehlers, M. D., 2013. Modeling autism by SHANK gene mutations in mice. Neuron. 78**,** 8-27.

Jinek, M., et al., 2012. A programmable dual-RNA–guided DNA endonuclease in adaptive bacterial immunity. Science. 337**,** 816-821.

Jones, L. J., et al., 2015. Neurochemical measurements in the zebrafish brain. Front Behav Neurosci. 9**,** 246.

Jossin, Y., 2004. The Central Fragment of Reelin, Generated by Proteolytic Processing In Vivo, Is Critical to Its Function during Cortical Plate Development. Journal of Neuroscience. 24**,** 514-521.

Jossin, Y., Cooper, J. A., 2011. Reelin, Rap1 and N-cadherin orient the migration of multipolar neurons in the developing neocortex. Nature Neuroscience. 14**,** 697-703.

Jossin, Y., Goffinet, A. M., 2007. Reelin Signals through Phosphatidylinositol 3-Kinase and Akt To Control Cortical Development and through mTor To Regulate Dendritic Growth. Molecular and Cellular Biology. 27**,** 7113-7124.

Kabir, Z., et al., 2017. Rescue of impaired sociability and anxiety-like behavior in adult cacna1c-deficient mice by pharmacologically targeting eIF2α. Molecular psychiatry. 22**,** 1096.

Kaiser-McCaw, B., et al., 1980. Fragile X-linked mental retardation. American Journal of Medical Genetics. 7**,** 503-505.

Kalueff, A. V., et al., 2013. Towards a Comprehensive Catalog of Zebrafish Behavior 1.0 and Beyond. Zebrafish. 10**,** 70-86.

Kalueff, A. V., et al., 2014. Zebrafish as an emerging model for studying complex brain disorders. Trends in Pharmacological Sciences. 35**,** 63-75.

Kanner, L., et al., 1943. Library of the History of Autism Research, Behaviorism & Psychiatry. Nervous Child. 2**,** 217-50.

Karousis, E. D., et al., 2016. Nonsense-mediated mRNA decay: novel mechanistic insights and biological impact. Wiley Interdisciplinary Reviews: RNA. 7**,** 661-682.

Katsuyama, Y., Terashima, T., 2009. Developmental anatomy of reeler mutant mouse. Development, growth & differentiation. 51**,** 271-286.

Kaufman, D. L., et al., 1991. Two Forms of the ?-Aminobutyric Acid Synthetic Enzyme Glutamate Decarboxylase Have Distinct Intraneuronal Distributions and Cofactor Interactions. Journal of Neurochemistry. 56**,** 720-723.

Kaufman, S., 1995. Tyrosine hydroxylase. Advances in enzymology and related areas of molecular biology. 70**,** 103-220.

Kawamoto, Y., et al., 2002. 14-3-3 Proteins in Lewy Bodies in Parkinson Disease and Diffuse Lewy Body Disease Brains. Journal of Neuropathology & Experimental Neurology. 61**,** 245-253.

Kebabian, J. W., Calne, D. B., 1979. Multiple receptors for dopamine. Nature. 277**,** 93-96.

Kellermann, T., et al., 2012. Effective Connectivity of the Human Cerebellum during Visual Attention. Journal of Neuroscience. 32**,** 11453-11460.

Kemper, T. L., Bauman, M., 1998. Neuropathology of Infantile Autism. Journal of Neuropathology and Experimental Neurology. 57**,** 645-652.

Kim, H.-G., et al., 2008. Disruption of neurexin 1 associated with autism spectrum disorder. The American Journal of Human Genetics. 82**,** 199-207.

Kim, Y.-J., et al., 2004. Identification and functional evidence of GABAergic neurons in parts of the brain of adult zebrafish (Danio rerio). Neuroscience letters. 355**,** 29-32.

Kimmel, C. B., et al., 1991. Genetic control of primary neuronal development in zebrafish. Development. 113**,** 47-57.

Kiser, D., et al., 2012. The reciprocal interaction between serotonin and social behaviour. Neuroscience & Biobehavioral Reviews. 36**,** 786-798.

Kitada, T., et al., 1998. Mutations in the parkin gene cause autosomal recessive juvenile parkinsonism. Nature. 392**,** 605-608.

Kligys, K., et al., 2009. 14-3-3ζ/τ heterodimers regulate Slingshot activity in migrating keratinocytes. Biochemical and Biophysical Research Communications. 383**,** 450-454.

Kohno, T., et al., 2015. Importance of Reelin C-terminal region in the development and maintenance of the postnatal cerebral cortex and its regulation by specific proteolysis. Journal of Neuroscience. 35**,** 4776-4787.

Kojima, T., et al., 2000. The disabled 1 gene is disrupted by a replacement with L1 fragment in yotari mice. Molecular brain research. 75**,** 121-127.

Koolhaas, J., et al., 1999. Coping styles in animals: current status in behavior and stress-physiology. Neuroscience & Biobehavioral Reviews. 23**,** 925-935.

Kosaka, Y., et al., 2012. 14-3-3 Plays a Role in Cardiac Ventricular Compaction by Regulating the Cardiomyocyte Cell Cycle. Molecular and Cellular Biology. 32**,** 5089-5102.

Koshimizu, E., et al., 2013. Performance Comparison of Bench-Top Next Generation Sequencers Using Microdroplet PCR-Based Enrichment for Targeted Sequencing in Patients with Autism Spectrum Disorder. PLoS ONE. 8**,** e74167.

Krause, J., et al., 2000. The social organization of fish shoals: a test of the predictive power of laboratory experiments for the field. Biological Reviews. 75**,** 477-501.

Krebs, M. O., et al., 2002. Absence of association between a polymorphic GGC repeat in the 5′ untranslated region of the reelin gene and autism. Molecular Psychiatry. 7**,** 801-804.

Kriegebaum, C., et al., 2010. Brain-specific conditional and time-specific inducible Tph2 knockout mice possess normal serotonergic gene expression in the absence of serotonin during adult life. Neurochemistry international. 57**,** 512-517.

Krueger, D. D., et al., 2006. Assessment of cognitive function in the heterozygous reeler mouse. Psychopharmacology. 189**,** 95-104.

Kumar, M., et al., 2008. Intranasal nanoemulsion based brain targeting drug delivery system of risperidone. International Journal of Pharmaceutics. 358**,** 285-291.

Kumar, M., et al., 2009. Formulation and Characterization of Nanoemulsion-Based Drug Delivery System of Risperidone. Drug Development and Industrial Pharmacy. 35**,** 387-395.

Kutiyanawalla, A., et al., 2011. Cysteamine treatment ameliorates alterations in GAD67 expression and spatial memory in heterozygous reeler mice. The International Journal of Neuropsychopharmacology. 15**,** 1073-1086.

Labun, K., et al., 2016. CHOPCHOP v2: a web tool for the next generation of CRISPR genome engineering. Nucleic acids research. 44**,** W272-W276.

Laggerbauer, B., 2001. Evidence that fragile X mental retardation protein is a negative regulator of translation. Human Molecular Genetics. 10**,** 329-338.

Lai, M.-C., et al., 2013. Subgrouping the autism “Spectrum": reflections on DSM-5. PLoS biology. 11**,** e1001544.

Lalle, M., et al., 2010. Involvement of 14-3-3 protein post-translational modifications in Giardia duodenalis encystation. International Journal for Parasitology. 40**,** 201-213.

Lam, K. S., et al., 2006. Neurochemical correlates of autistic disorder: a review of the literature.

Lammert, D. B., Howell, B. W., 2016. RELN Mutations in Autism Spectrum Disorder. Front Cell Neurosci. 10**,** 84.

Lange, M., et al., 2018. Pharmacological analysis of zebrafish lphn3. 1 morphant larvae suggests that saturated dopaminergic signaling could underlie the ADHD-like locomotor hyperactivity. Progress in Neuro-Psychopharmacology and Biological Psychiatry. 84**,** 181-189.

Lau, J. M., et al., 2006. Differential role of 14-3-3 family members in Xenopus development. Developmental dynamics: an official publication of the American Association of Anatomists. 235**,** 1761-1776.

Laviola, G., et al., 2009. Gene–environment interaction during early development in the heterozygous reeler mouse: clues for modelling of major neurobehavioral syndromes. Neuroscience & Biobehavioral Reviews. 33**,** 560-572.

Lawrence, Y. A., et al., 2010. Parvalbumin-, calbindin-, and calretinin-immunoreactive hippocampal interneuron density in autism. Acta Neurologica Scandinavica. 121**,** 99-108.

Layfield, R., et al., 1996. Neurofibrillary tangles of Alzheimer's disease brains contain 14-3-3 proteins. Neuroscience Letters. 209**,** 57-60.

Leblond, C. S., et al., 2012. Genetic and functional analyses of SHANK2 mutations suggest a multiple hit model of autism spectrum disorders. PLoS genetics. 8**,** e1002521.

Leboyer, M., et al., 1999. Whole blood serotonin and plasma beta-endorphin in autistic probands and their first-degree relatives. Biological Psychiatry. 45**,** 158-163.

Lee, E.-J., et al., 2015. NMDA receptor dysfunction in autism spectrum disorders. Current opinion in pharmacology. 20**,** 8-13.

Lee, G. H., et al., 2014. Reelin Induces Erk1/2 Signaling in Cortical Neurons Through a Non-canonical Pathway. Journal of Biological Chemistry. 289**,** 20307-20317.

Lee, G. H., D'Arcangelo, G., 2016. New insights into reelin-mediated signaling pathways. Frontiers in cellular neuroscience. 10**,** 122.

Leekam, S. R., et al., 2007. Describing the sensory abnormalities of children and adults with autism. Journal of autism and developmental disorders. 37**,** 894-910.

Leonelli, S., Ankeny, R. A., 2013. What makes a model organism? Endeavour. 37**,** 209-212.

Levenson, J. M., et al., 2008. The role of reelin in adult synaptic function and the genetic and epigenetic regulation of the reelin gene. Biochimica et Biophysica Acta (BBA) - Gene Regulatory Mechanisms. 1779**,** 422-431.

Leventhal, B. L., et al., 1990. Relationships of whole blood serotonin and plasma norepinephrine within families. Journal of Autism and Developmental Disorders. 20**,** 499-511.

Levitt, P., 2005. Disruption of Interneuron Development. Epilepsia. 46**,** 22-28.

Levy, A. D., et al., 2014. Extracellular matrix control of dendritic spine and synapse structure and plasticity in adulthood. Frontiers in Neuroanatomy. 8.

Lewis, M., Kim, S.-J., 2009. The pathophysiology of restricted repetitive behavior. Journal of Neurodevelopmental Disorders. 1**,** 114-132.

Lewis, M., et al., 2007. Animal models of restricted repetitive behavior in autism. Behavioural Brain Research. 176**,** 66-74.

Leyfer, O. T., et al., 2006. Comorbid psychiatric disorders in children with autism: interview development and rates of disorders. Journal of autism and developmental disorders. 36**,** 849-861.

Li, H., et al., 2008. The association analysis of RELN and GRM8 genes with autistic spectrum disorder in chinese han population. American Journal of Medical Genetics Part B: Neuropsychiatric Genetics. 147B**,** 194-200.

Li, J., et al., 2013. Association study between genes in Reelin signaling pathway and autism identifies DAB1 as a susceptibility gene in a Chinese Han population. Progress in Neuro-Psychopharmacology and Biological Psychiatry. 44**,** 226-232.

Li, J., et al., 2004. Lack of evidence for an association between WNT2 and RELN polymorphisms and autism. American Journal of Medical Genetics. 126B**,** 51-57.

Li, S.-M., et al., 2010. Yawning and locomotor behavior induced by dopamine receptor agonists in mice and rats. Behavioural pharmacology. 21**,** 171.

Li, W., et al., 2015. Evaluating the relationship between reelin gene variants (rs7341475 and rs262355) and schizophrenia: A meta-analysis. Neuroscience Letters. 609**,** 42-47.

Liang, X., et al., 2008. An Obligatory Heterodimer of 14-3-3β and 14-3-3ϵ Is Required for Aldosterone Regulation of the Epithelial Sodium Channel. Journal of Biological Chemistry. 283**,** 27418-27425.

Liu, D., et al., 1995. Crystal structure of the zeta isoform of the 14-3-3 protein. Nature. 376**,** 191.

Liu, Z., et al., 2016. Autism-like behaviours and germline transmission in transgenic monkeys overexpressing MeCP2. Nature. 530**,** 98.

Livak, K. J., Schmittgen, T. D., 2001. Analysis of relative gene expression data using real-time quantitative PCR and the 2− ΔΔCT method. methods. 25**,** 402-408.

Loane, C., Politis, M., 2012. Buspirone: what is it all about? Brain research. 1461**,** 111-118.

Loughran, G., et al., 2014. Evidence of efficient stop codon readthrough in four mammalian genes. Nucleic Acids Research. 42**,** 8928-8938.

Maaswinkel, H., et al., 2013. Dissociating the effects of habituation, black walls, buspirone and ethanol on anxiety-like behavioral responses in shoaling zebrafish. A 3D approach to social behavior. Pharmacology Biochemistry and Behavior. 108**,** 16-27.

Maaswinkel, H., et al., 2012. The immediate and the delayed effects of buspirone on zebrafish (Danio rerio) in an open field test: a 3-D approach. Behavioural brain research. 234**,** 365-374.

Mabunga, D. F. N., et al., 2015. Exploring the validity of valproic acid animal model of autism. Experimental neurobiology. 24**,** 285-300.

MacDonald, R. B., et al., 2013. The ascl1a and dlx genes have a regulatory role in the development of GABAergic interneurons in the zebrafish diencephalon. Developmental Biology. 381**,** 276-285.

Magno, L. D. P., et al., 2015. Pharmacological study of the light/dark preference test in zebrafish (Danio rerio): Waterborne administration. Pharmacology Biochemistry and Behavior. 135**,** 169-176.

Maloku, E., et al., 2010. Lower number of cerebellar Purkinje neurons in psychosis is associated with reduced reelin expression. Proceedings of the National Academy of Sciences. 107**,** 4407-4411.

Manent, J.-B., Represa, A., 2007. Neurotransmitters and Brain Maturation: Early Paracrine Actions of GABA and Glutamate Modulate Neuronal Migration. The Neuroscientist. 13, 268-279.

Markram, H., 2007. The intense world syndrome – an alternative hypothesis for autism. Frontiers in Neuroscience. 1, 77-96.

Markram, K., Markram, H., 2010. The Intense World Theory – A Unifying Theory of the Neurobiology of Autism. Frontiers in Human Neuroscience. 4.

Marraffini, L. A., Sontheimer, E. J., 2010. Self versus non-self discrimination during CRISPR RNA-directed immunity. Nature. 463, 568.

Martin, H., et al., 1993. Antibodies against the major brain isoforms of 14-3-3 protein. FEBS letters. 331, 296-303.

Masters, S. C., et al., 1999. Interaction of 14-3-3 with a Nonphosphorylated Protein Ligand, Exoenzyme S ofPseudomonas aeruginosa†. Biochemistry. 38, 5216-5221.

Mathur, P., Guo, S., 2010. Use of zebrafish as a model to understand mechanisms of addiction and complex neurobehavioral phenotypes. Neurobiology of Disease. 40, 66-72.

Maura, G., et al., 1986. Serotonin inhibits the depolarization-evoked release of endogenous glutamate from rat cerebellar nerve endings. Neuroscience Letters. 67, 218-222.

Maximino, C., Herculano, A. M., 2010. A Review of Monoaminergic Neuropsychopharmacology in Zebrafish. Zebrafish. 7, 359-378.

Maximino, C., et al., 2013. The serotonergic system of zebrafish: genomics, neuroanatomy and neuropharmacology. Serotonin Biosynthesis, Regul Heal Implic. New York, NY: Nova Science. 53-67.

McDougle, C., et al., 1996. Effects of tryptophan depletion in drug-free adults with autistic disorder. Archives of general psychiatry. 53, 993-1000.

McDougle, C. J., et al., 2005. Risperidone for the core symptom domains of autism: results from the study by the autism network of the research units on pediatric psychopharmacology. American Journal of Psychiatry. 162, 1142-1148.

McFarland, K. A., et al., 2008. Hh and Wnt signaling regulate formation of olig2+ neurons in the zebrafish cerebellum. Dev Biol. 318, 162-71.

McLean, D. L., Fetcho, J. R., 2004. Ontogeny and innervation patterns of dopaminergic, noradrenergic, and serotonergic neurons in larval zebrafish. The Journal of Comparative Neurology. 480, 38-56.

McPheeters, M. L., et al., 2011. A systematic review of medical treatments for children with autism spectrum disorders. Pediatrics. peds. 2011-0427.

Meek, J., 1992. Comparative aspects of cerebellar organization. From mormyrids to mammals. European journal of morphology. 30, 37-51.

Meffre, J., et al., 2012. 5-HT6receptor recruitment of mTOR as a mechanism for perturbed cognition in schizophrenia. EMBO Molecular Medicine. 4, 1043-1056.

Meloni, I., et al., 2000. A Mutation in the Rett Syndrome Gene, MECP2, Causes X-Linked Mental Retardation and Progressive Spasticity in Males. The American Journal of Human Genetics. 67**,** 982-985.

Mercuri, N., et al., 1997. Loss of autoreceptor function in dopaminergic neurons from dopamine D2 receptor deficient mice. Neuroscience. 79**,** 323-327.

Meyer, G., 2007. Genetic control of neuronal migrations in human cortical development. Springer Science & Business Media.

Meyer, G., et al., 2003. Disabled-1 mRNA and protein expression in developing human cortex. European Journal of Neuroscience. 17**,** 517-525.

Michetti, C., et al., 2014. Mapping pathological phenotypes in reelin mutant mice. Frontiers in pediatrics. 2**,** 95.

Middleton, F. A., et al., 2005. Altered Expression of 14-3-3 Genes in the Prefrontal Cortex of Subjects with Schizophrenia. Neuropsychopharmacology. 30**,** 974-983.

Millan, M. J., et al., 2002. Differential actions of antiparkinson agents at multiple classes of monoaminergic receptor. I. A multivariate analysis of the binding profiles of 14 drugs at 21 native and cloned human receptor subtypes. Journal of Pharmacology and Experimental Therapeutics. 303**,** 791-804.

Miller, N., Gerlai, R., 2012. From schooling to shoaling: patterns of collective motion in zebrafish (Danio rerio). PLoS One. 7**,** e48865.

Miller, N. Y., Gerlai, R., 2011. Shoaling in zebrafish: what we don't know. Reviews in the Neurosciences. 22**,** 17-25.

Minshew, N. J., Williams, D. L., 2007. The New Neurobiology of Autism. Archives of Neurology. 64**,** 945.

Missale, C., et al., 1998. Dopamine receptors: from structure to function. Physiological reviews. 78**,** 189-225.

Mitchell, K. J., 2011. The genetics of neurodevelopmental disease. Curr Opin Neurobiol. 21**,** 197-203.

Mitoma, H., et al., 1994. Enhancement by serotonin of GABA-mediated inhibitory synaptic currents in rat cerebellar Purkinje cells. Neuroscience Letters. 173**,** 127-130.

Mitoma, H., Konishi, S., 1999. Monoaminergic long-term facilitation of GABA-mediated inhibitory transmission at cerebellar synapses. Neuroscience. 88**,** 871-883.

Miyamura, Y., Nakayasu, H., 2001. Zonal distribution of Purkinje cells in the zebrafish cerebellum: analysis by means of a specific monoclonal antibody. Cell and tissue research. 305**,** 299-305.

Miyata, T., et al., 1997. Regulation of Purkinje cell alignment by reelin as revealed with CR-50 antibody. The Journal of neuroscience : the official journal of the Society for Neuroscience. 17**,** 3599-609.

Mizuno, E., et al., 2007. 14-3-3-dependent inhibition of the deubiquitinating activity of UBPY and its cancellation in the M phase. Experimental Cell Research. 313**,** 3624-3634.

Montague, T. G., et al., 2014. CHOPCHOP: a CRISPR/Cas9 and TALEN web tool for genome editing. Nucleic acids research. 42**,** W401-W407.

Morris, J. A., Zebrafish: a model system to examine the neurodevelopmental basis of schizophrenia. Progress in Brain Research. Elsevier, 2009, pp. 97-106.

Morrison, D. K., 2009. The 14-3-3 proteins: integrators of diverse signaling cues that impact cell fate and cancer development. Trends in Cell Biology. 19**,** 16-23.

Mueller, T., 2012. What is the Thalamus in Zebrafish? Frontiers in Neuroscience. 6.

Mueller, T., et al., 2011. The dorsal pallium in zebrafish, Danio rerio (Cyprinidae, Teleostei). Brain research. 1381**,** 95-105.

Muller, C. L., et al., 2016. The serotonin system in autism spectrum disorder: from biomarker to animal models. Neuroscience. 321**,** 24-41.

Muratake, T., et al., 1996. Structural Organization and Chromosomal Assignment of the Human 14-3-3 η Chain Gene (YWHAH). Genomics. 36**,** 63-69.

Musiani, F., et al., 2011. Interaction of Selenoprotein W with 14-3-3 Proteins: A Computational Approach. Journal of Proteome Research. 10**,** 968-976.

Muslin, A. J., Lau, J. M., 2005. 8 Differential Functions of 14-3-3 Isoforms in Vertebrate Development. Current topics in developmental biology. 65**,** 211-228.

Muslin, A. J., et al., 1996. Interaction of 14-3-3 with Signaling Proteins Is Mediated by the Recognition of Phosphoserine. Cell. 84**,** 889-897.

Männistö, P. T., Kaakkola, S., 1999. Catechol-O-methyltransferase (COMT): biochemistry, molecular biology, pharmacology, and clinical efficacy of the new selective COMT inhibitors. Pharmacological reviews. 51**,** 593-628.

Nagamani, S. C., et al., 2009. Microdeletions including YWHAE in the Miller-Dieker syndrome region on chromosome 17p13.3 result in facial dysmorphisms, growth restriction, and cognitive impairment. Journal of Medical Genetics. 46**,** 825-833.

Nagaraj, R., et al., 2006. Risperidone in Children With Autism: Randomized, Placebo-Controlled, Double-Blind Study. Journal of Child Neurology. 21**,** 450-455.

Neale, B. M., et al., 2012. Patterns and rates of exonic de novo mutations in autism spectrum disorders. Nature. 485**,** 242-245.

Neelkantan, N., et al., 2013. Perspectives on Zebrafish Models of Hallucinogenic Drugs and Related Psychotropic Compounds. ACS Chemical Neuroscience. 4**,** 1137-1150.

Neu-Yilik, G., et al., 2011. Mechanism of escape from nonsense-mediated mRNA decay of human -globin transcripts with nonsense mutations in the first exon. RNA. 17**,** 843-854.

Nicolini, C., Fahnestock, M., 2017. The valproic acid-induced rodent model of autism. Experimental neurology.

Nieuwenhuys, R., 1994. The neocortex. Anatomy and embryology. 190**,** 307-337.

NIH, Model organisms for biomedical research. In: N. I. o. Health, M. Bethesda, (Eds.), 2010.

Northmore, D. P., 2017. Holding visual attention for 400 million years: A model of tectum and torus longitudinalis in teleost fishes. Vision research. 131**,** 44-56.

Norton, W. H., et al., 2008. Comparative analysis of serotonin receptor (HTR1A/HTR1B families) and transporter (slc6a4a/b) gene expression in the zebrafish brain. J Comp Neurol. 511**,** 521-42.

Norton, W. H., et al., 2011. Modulation of Fgfr1a signaling in zebrafish reveals a genetic basis for the aggression-boldness syndrome. J Neurosci. 31**,** 13796-807.

Oberman, L. M., 2012. mGluR antagonists and GABA agonists as novel pharmacological agents for the treatment of autism spectrum disorders. Expert opinion on investigational drugs. 21**,** 1819-1825.

Obsil, T., et al., 2003. Two 14-3-3 Binding Motifs Are Required for Stable Association of Forkhead Transcription Factor FOXO4 with 14-3-3 Proteins and Inhibition of DNA Binding. Biochemistry. 42**,** 15264-15272.

Obsil, T., et al., 2001. Crystal Structure of the 14-3-3ζ:Serotonin N-Acetyltransferase Complex. Cell. 105**,** 257-267.

Obsil, T., Obsilova, V., Structural basis of 14-3-3 protein functions. Seminars in cell & developmental biology, Vol. 22. Elsevier, 2011, pp. 663-672.

Obsilova, V., et al., 2008. The 14-3-3 Protein Affects the Conformation of the Regulatory Domain of Human Tyrosine Hydroxylase†. Biochemistry. 47**,** 1768-1777.

Ogawa, M., et al., 1995. The reeler gene-associated antigen on cajal-retzius neurons is a crucial molecule for laminar organization of cortical neurons. Neuron. 14**,** 899-912.

Ohlsen, R., Pilowsky, L., 2005. The place of partial agonism in psychiatry: recent developments. Journal of Psychopharmacology. 19**,** 408-413.

Oostland, M., et al., 2014. Distinct Temporal Expression of 5-HT1A and 5-HT2A Receptors on Cerebellar Granule Cells in Mice. The Cerebellum. 13**,** 491-500.

Ostrerova, N., et al., 1999. α-Synuclein Shares Physical and Functional Homology with 14-3-3 Proteins. The Journal of Neuroscience. 19**,** 5782-5791.

Ottmann, C., et al., 2007. Structure of a 14-3-3 Coordinated Hexamer of the Plant Plasma Membrane H+-ATPase by Combining X-Ray Crystallography and Electron Cryomicroscopy. Molecular Cell. 25**,** 427-440.

Ovadia, G., Shifman, S., 2011. The Genetic Variation of RELN Expression in Schizophrenia and Bipolar Disorder. PLoS ONE. 6**,** e19955.

O'Dell, R. S., et al., 2012. Layer 6 cortical neurons require Reelin-Dab1 signaling for cellular orientation, Golgi deployment, and directed neurite growth into the marginal zone. Neural development. 7**,** 25.

Packer, A., 2016. Neocortical neurogenesis and the etiology of autism spectrum disorder. Neuroscience & Biobehavioral Reviews. 64**,** 185-195.

Pandina, G. J., et al., 2006. Risperidone Improves Behavioral Symptoms in Children with Autism in a Randomized, Double-Blind, Placebo-Controlled Trial. Journal of Autism and Developmental Disorders. 37**,** 367-373.

Panula, P., et al., 2010. The comparative neuroanatomy and neurochemistry of zebrafish CNS systems of relevance to human neuropsychiatric diseases. Neurobiology of Disease. 40**,** 46-57.

Panula, P., et al., 2006. Modulatory Neurotransmitter Systems and Behavior: Towards Zebrafish Models of Neurodegenerative Diseases. Zebrafish. 3**,** 235-247.

Pappas, G. D., et al., 2002. Reelin in the extracellular matrix and dendritic spines of the cortex and hippocampus: a comparison between wild type and heterozygous reeler mice by immunoelectron microscopy. Journal of neurocytology. 30**,** 413-425.

Parker, M. O., et al., 2013. Behavioral phenotyping of casper mutant and 1-pheny-2-thiourea treated adult zebrafish. Zebrafish. 10**,** 466-471.

Paulin, M. G., 1993. The role of the cerebellum in motor control and perception. Brain, Behavior and Evolution. 41**,** 39-50.

Pazos, A., Palacios, J. M., 1985. Quantitative autoradiographic mapping of serotonin receptors in the rat brain. I. Serotonin-1 receptors. Brain Research. 346**,** 205-230.

Penagarikano, O., 2015. New Therapeutic Options for Autism Spectrum Disorder: Experimental Evidences. Exp Neurobiol. 24**,** 301-11.

Perez, M. a., 1967. Physiological and

Biochemical Aspects of Nervous Integration. pp. 343-359.

Persico, A. M., et al., 2001. Reelin gene alleles and haplotypes as a factor predisposing to autistic disorder. Molecular Psychiatry. 6**,** 150-159.

Persico, A. M., Napolioni, V., 2013. Autism genetics. Behav Brain Res. 251**,** 95-112.

Pesold, C., et al., 1998. Reelin is preferentially expressed in neurons synthesizing γ-aminobutyric acid in cortex and hippocampus of adult rats. Proceedings of the National Academy of Sciences. 95**,** 3221-3226.

Petosa, C., et al., 1998. 14-3-3ζ Binds a Phosphorylated Raf Peptide and an Unphosphorylated Peptide via Its Conserved Amphipathic Groove. Journal of Biological Chemistry. 273**,** 16305-16310.

Peyrl, A., et al., 2002. Aberrant expression of signaling-related proteins 14-3-3 gamma and RACK1 in fetal Down Syndrome brain (trisomy 21). ELECTROPHORESIS. 23**,** 152.

Philippe, A., et al., 1999. Genome-Wide Scan for Autism Susceptibility Genes. Human Molecular Genetics. 8**,** 805-812.

Picci, G., Scherf, K. S., 2015. A two-hit model of autism: Adolescence as the second hit. Clinical Psychological Science. 3**,** 349-371.

Piochon, C., et al., 2014. Cerebellar plasticity and motor learning deficits in a copy-number variation mouse model of autism. Nature communications. 5**,** 5586.

Pizzarelli, R., Cherubini, E., 2013. Developmental regulation of GABAergic signalling in the hippocampus of neuroligin 3 R451C knock-in mice: an animal model of Autism. Frontiers in Cellular Neuroscience. 7.

Podhorna, J., Didriksen, M., 2004. The heterozygous reeler mouse: behavioural phenotype. Behavioural brain research. 153**,** 43-54.

Politte, L. C., et al., 2014. Psychopharmacological interventions in autism spectrum disorder. Harv Rev Psychiatry. 22**,** 76-92.

Presti, M. F., et al., 2003. Selective blockade of spontaneous motor stereotypy via intrastriatal pharmacological manipulation. Pharmacology Biochemistry and Behavior. 74**,** 833-839.

Prieto, M., 2014. G4.5 Pamam Dendrimer-Risperidone: Biodistribution and Behavioral Changes in In Vivo Model. Journal of Nanomedicine & Biotherapeutic Discovery. 04.

Prieto, M. J., et al., 2014. Optimization and In Vivo Toxicity Evaluation of G4.5 Pamam Dendrimer-Risperidone Complexes. PLoS ONE. 9**,** e90393.

Prieto, M. J., et al., 2011. Optimization and in vitro toxicity evaluation of G4 PAMAM dendrimer–risperidone complexes. European Journal of Medicinal Chemistry. 46**,** 845-850.

Puts, N. A., et al., 2017. Reduced GABA and altered somatosensory function in children with autism spectrum disorder. Autism Research. 10**,** 608-619.

Puttonen, H., et al., 2018. Knockout of histamine receptor H3 alters adaptation to sudden darkness and monoamine levels in the zebrafish. Acta Physiologica. 222**,** e12981.

Qiu, S., et al., 2006. Cognitive disruption and altered hippocampus synaptic function in Reelin haploinsufficient mice. Neurobiology of Learning and Memory. 85**,** 228-242.

Ramshaw, H., et al., 2013. Locomotor hyperactivity in 14-3-3zeta KO mice is associated with dopamine transporter dysfunction. Transl Psychiatry. 3**,** e327.

Redcay, E., Courchesne, E., 2005. When is the brain enlarged in autism? A meta-analysis of all brain size reports. Biological psychiatry. 58**,** 1-9.

Reeber, S. L., et al., 2013. New roles for the cerebellum in health and disease. Frontiers in systems neuroscience. 7**,** 83.

Ren, G., et al., 2013. Zebrafish Tyrosine Hydroxylase 2 Gene Encodes Tryptophan Hydroxylase. Journal of Biological Chemistry. 288**,** 22451-22459.

Rice, D. S., et al., 1998. Disabled-1 acts downstream of Reelin in a signaling pathway that controls laminar organization in the mammalian brain. Development. 125**,** 3719-3729.

Rink, E., Guo, S., 2004. The too few mutant selectively affects subgroups of monoaminergic neurons in the zebrafish forebrain. Neuroscience. 127**,** 147-154.

Rink, E., Wullimann, M. F., 2001. The teleostean (zebrafish) dopaminergic system ascending to the subpallium (striatum) is located in the basal diencephalon (posterior tuberculum). Brain Research. 889**,** 316-330.

Rink, E., Wullimann, M. F., 2002a. Connections of the ventral telencephalon and tyrosine hydroxylase distribution in the zebrafish brain (Danio rerio) lead to identification of an ascending dopaminergic system in a teleost. Brain Research Bulletin. 57**,** 385-387.

Rink, E., Wullimann, M. F., 2002b. Development of the catecholaminergic system in the early zebrafish brain: an immunohistochemical study. Developmental Brain Research. 137**,** 89-100.

Rittinger, K., et al., 1999. Structural Analysis of 14-3-3 Phosphopeptide Complexes Identifies a Dual Role for the Nuclear Export Signal of 14-3-3 in Ligand Binding. Molecular Cell. 4**,** 153-166.

Ritvo, E. R., 1970. Increased Blood Serotonin and Platelets in Early Infantile Autism. Archives of General Psychiatry. 23**,** 566.

Ritvo, E. R., et al., 1986. Lower Purkinje cell counts in the cerebella of four autistic subjects: Initial findings of the UCLA-NSAC research report. The American journal of psychiatry.

Roberts, E., Kuriyama, K., 1968. Biochemical-physiology correlations in studies of the γ-aminobutyric acid system. Brain Research. 8**,** 1-35.

Rodriguez-Porcel, F., et al., 2011. Neonatal exposure of rats to antidepressants affects behavioral reactions to novelty and social interactions in a manner analogous to autistic spectrum disorders. The Anatomical Record. 294**,** 1726-1735.

Rogers, T. D., et al., 2013. Is autism a disease of the cerebellum? An integration of clinical and pre-clinical research. Frontiers in Systems Neuroscience. 7.

Rommelse, N. N., 2008. Endophenotypes in the genetic research of ADHD over the last decade: have they lived up to their expectations? Expert Review of Neurotherapeutics. 8**,** 1425-1429.

Rosenberg, R. E., et al., 2009. Characteristics and concordance of autism spectrum disorders among 277 twin pairs. Archives of pediatrics & adolescent medicine. 163**,** 907-914.

Rubenstein, E., et al., 2015. A review of the differences in developmental, psychiatric, and medical endophenotypes between males and females with autism spectrum disorder. Journal of Developmental and Physical Disabilities. 27**,** 119-139.

Rupia, E. J., et al., 2016. Fight-flight or freeze-hide? Personality and metabolic phenotype mediate physiological defence responses in flatfish. Journal of Animal Ecology. 85**,** 927-937.

Russo, A. J., 2013. Correlation between Hepatocyte Growth Factor (HGF) and Gamma-Aminobutyric Acid (GABA) Plasma Levels in Autistic Children. Biomarker Insights. 8**,** BMI.S11448.

Rutter, M., et al., 1999. Quasi-autistic patterns following severe early global privation. The Journal of Child Psychology and Psychiatry and Allied Disciplines. 40**,** 537-549.

Sakai, K., et al., 2016. Mice that lack the C-terminal region of Reelin exhibit behavioral abnormalities related to neuropsychiatric disorders. Scientific reports. 6**,** 28636.

Salas, C., et al., 1996. Spatial learning and memory deficits after telencephalic ablation in goldfish trained in place and turn maze procedures. Behavioral Neuroscience. 110**,** 965-980.

Salvage, J., 2011. Global Institutions – The World Health Organization (WHO)Global Institutions – The World Health Organization (WHO). Nursing Standard. 25**,** 30-30.

Sato, S., et al., 2005. 14-3-3η is a novel regulator of parkin ubiquitin ligase. The EMBO Journal. 25**,** 211-221.

Saverino, C., Gerlai, R., 2008. The social zebrafish: behavioral responses to conspecific, heterospecific, and computer animated fish. Behavioural brain research. 191**,** 77-87.

Schain, R. J., Freedman, D. X., 1961. Studies on 5-hydroxyindole metabolism in autistic and other mentally retarded children. The Journal of pediatrics. 58**,** 315-320.

Schmittgen, T. D., Livak, K. J., 2008. Analyzing real-time PCR data by the comparative C T method. Nature protocols. 3**,** 1101.

Schultz, W., 2013. Updating dopamine reward signals. Current opinion in neurobiology. 23**,** 229-238.

Schumann, C. M., 2004. The Amygdala Is Enlarged in Children But Not Adolescents with Autism; the Hippocampus Is Enlarged at All Ages. Journal of Neuroscience. 24**,** 6392-6401.

Schumann, C. M., Amaral, D. G., 2005. Stereological estimation of the number of neurons in the human amygdaloid complex. The Journal of Comparative Neurology. 491**,** 320-329.

Schumann, C. M., Amaral, D. G., 2006. Stereological Analysis of Amygdala Neuron Number in Autism. Journal of Neuroscience. 26**,** 7674-7679.

Scott-Van Zeeland, A. A., et al., 2010. Reward processing in autism. Autism Research. n/a-n/a.

Seeman, P., et al., 1975. Brain receptors for antipsychotic drugs and dopamine: direct binding assays. Proceedings of the National Academy of Sciences. 72**,** 4376-4380.

Sekine, K., et al., 2012. Reelin controls neuronal positioning by promoting cell-matrix adhesion via inside-out activation of integrin α5β1. Neuron . doi: 10.1016/j.neuron..07.020. 76 DOI - Sekine, K., Kawauchi, T., Kubo, K., Honda, T., Herz, J., Hattori, M., et al. (2012). Reelin controls neuronal positioning by promoting cell-matrix adhesion via inside-out activation of integrin α5β1. Neuron 76, 353-369. doi: 10.1016/j.neuron.2012.07.020 SRC - BaiduScholar**,** 353-369.

Serajee, F. J., et al., 2006. Association of Reelin gene polymorphisms with autism. Genomics. 87**,** 75-83.

Setini, A., et al., 2005. Molecular characterization of monoamine oxidase in zebrafish (Danio rerio). Comparative Biochemistry and Physiology Part B: Biochemistry and Molecular Biology. 140**,** 153-161.

Shea, S., 2004. Risperidone in the Treatment of Disruptive Behavioral Symptoms in Children With Autistic and Other Pervasive Developmental Disorders. PEDIATRICS. 114**,** e634-e641.

Sheldon, M., et al., 1997. Scrambler and yotari disrupt the disabled gene and produce a reeler -like phenotype in mice. Nature. 389**,** 730-733.

Shin, J., et al., 2003. Neural cell fate analysis in zebrafish using olig2 BAC transgenics. Methods in Cell Science. 25**,** 7-14.

Silva, A. C., et al., 2012. Long-term stability, biocompatibility and oral delivery potential of risperidone-loaded solid lipid nanoparticles. International Journal of Pharmaceutics. 436**,** 798-805.

Singer, M. L., et al., 2016. Anxiolytic effects of fluoxetine and nicotine exposure on exploratory behavior in zebrafish. PeerJ. 4**,** e2352.

Skefos, J., et al., 2014. Regional alterations in purkinje cell density in patients with autism. PLoS One. 9**,** e81255.

Skoulakis, E. M., Davis, R. L., 1998. 14-3-3 proteins in neuronal development and function. Molecular neurobiology. 16**,** 269-284.

Staal, W. G., et al., 2015. DRD3 gene and striatum in autism spectrum disorder. British Journal of Psychiatry. 206**,** 431-432.

Steinacker, P., et al., 2005. Unchanged survival rates of 14-3-3γ knockout mice after inoculation with pathological prion protein. Molecular and cellular biology. 25**,** 1339-1346.

Stewart, A. M., et al., 2014. Developing zebrafish models of autism spectrum disorder (ASD). Prog Neuropsychopharmacol Biol Psychiatry. 50**,** 27-36.

Stolt, P. C., et al., 2003. Origins of Peptide Selectivity and Phosphoinositide Binding Revealed by Structures of Disabled-1 PTB Domain Complexes. Structure. 11**,** 569-579.

Stoner, R., et al., 2014. Patches of Disorganization in the Neocortex of Children with Autism. New England Journal of Medicine. 370**,** 1209-1219.

Stoodley, C. J., 2014. Distinct regions of the cerebellum show gray matter decreases in autism, ADHD, and developmental dyslexia. Frontiers in Systems Neuroscience. 8.

Stoodley, C. J., 2016. The Cerebellum and Neurodevelopmental Disorders. Cerebellum. 15**,** 34-7.

Stoodley, C. J., Schmahmann, J. D., 2010. Evidence for topographic organization in the cerebellum of motor control versus cognitive and affective processing. Cortex. 46**,** 831-844.

Stoof, J., Kebabian, J., 1981. Opposing roles for D-1 and D-2 dopamine receptors in efflux of cyclic AMP from rat neostriatum. Nature. 294**,** 366.

Strazielle, C., et al., 2012. Abnormal grooming activity in Dab1 scm (scrambler) mutant mice. Behavioural brain research. 233**,** 24-28.

Striepens, N., et al., 2011. Prosocial effects of oxytocin and clinical evidence for its therapeutic potential. Frontiers in Neuroendocrinology. 32**,** 426-450.

Sweet, H. O., et al., 1996. Scrambler, a new neurological mutation of the mouse with abnormalities of neuronal migration. Mammalian Genome. 7**,** 798-802.

Szatmari, P., et al., 2007. Mapping autism risk loci using genetic linkage and chromosomal rearrangements. Nature genetics. 39**,** 319.

Tabuchi, K., et al., 2007. A Neuroligin-3 Mutation Implicated in Autism Increases Inhibitory Synaptic Transmission in Mice. Science. 318**,** 71-76.

Takahashi, S., et al., 1976. Reassessment of elevated serotonin levels in blood platelets in early infantile autism. Journal of Autism and Childhood Schizophrenia. 6**,** 317-326.

Takeuchi, M., et al., 2015. Establishment of Gal4 transgenic zebrafish lines for analysis of development of cerebellar neural circuitry. Developmental biology. 397**,** 1-17.

Tanabe, K., et al., 2010. Atypical protein kinase C regulates primary dendrite specification of cerebellar Purkinje cells by localizing Golgi apparatus. Journal of Neuroscience. 30**,** 16983-16992.

Teixeira, C. M., et al., 2011. Overexpression of Reelin Prevents the Manifestation of Behavioral Phenotypes Related to Schizophrenia and Bipolar Disorder. Neuropsychopharmacology. 36**,** 2395-2405.

Teixeira, C. M., et al., 2014. Transient downregulation of Dab1 protein levels during development leads to behavioral and structural deficits: relevance for psychiatric disorders. Neuropsychopharmacology. 39**,** 556.

Teng, B. L., et al., 2013. Prosocial effects of oxytocin in two mouse models of autism spectrum disorders. Neuropharmacology. 72**,** 187-196.

Teraoka, H., et al., 2004. Hedgehog and Fgf signaling pathways regulate the development of tphR-expressing serotonergic raphe neurons in zebrafish embryos. Journal of neurobiology. 60**,** 275-288.

Theodoridi, A., et al., 2017. Acute exposure to fluoxetine alters aggressive behavior of zebrafish and expression of genes involved in serotonergic system regulation. Frontiers in neuroscience. 11**,** 223.

Thomas, A. M., et al., 2017. Sleep/Wake Physiology and Quantitative Electroencephalogram Analysis of the Neuroligin-3 Knockout Rat Model of Autism Spectrum Disorder. Sleep. 40.

Thomson, P. A., et al., 2004. Sex-specific association between bipolar affective disorder in women and GPR50, an X-linked orphan G protein-coupled receptor. Molecular Psychiatry. 10**,** 470-478.

Toma, C., et al., 2014. Exome sequencing in multiplex autism families suggests a major role for heterozygous truncating mutations. Mol Psychiatry. 19**,** 784-90.

Tordjman, S., et al., 2014. Gene× Environment interactions in autism spectrum disorders: role of epigenetic mechanisms. Frontiers in psychiatry. 5**,** 53.

Toska, K., et al., 2002. Regulation of tyrosine hydroxylase by stress-activated protein kinases. Journal of Neurochemistry. 83**,** 775-783.

Toyo-oka, K., et al., 2003. 14-3-3ε is important for neuronal migration by binding to NUDEL: a molecular explanation for Miller–Dieker syndrome. Nature Genetics. 34**,** 274-285.

Toyo-oka, K., et al., 2014. 14-3-3 and Regulate Neurogenesis and Differentiation of Neuronal Progenitor Cells in the Developing Brain. Journal of Neuroscience. 34**,** 12168-12181.

Toyooka, K., et al., 1999. 14-3-3 protein ? chain gene (YWHAH) polymorphism and its genetic association with schizophrenia. American Journal of Medical Genetics. 88**,** 164-167.

Tremolizzo, L., et al., 2002. An epigenetic mouse model for molecular and behavioral neuropathologies related to schizophrenia vulnerability. Proceedings of the National Academy of Sciences. 99**,** 17095-17100.

Trommsdorff, M., et al., 1999. Reeler/Disabled-like disruption of neuronal migration in knockout mice lacking the VLDL receptor and ApoE receptor 2. Cell 97 doi 101016s0092807825. 8674**,** 689-701.

Tropepe, V., Sive, H. L., 2003. Can zebrafish be used as a model to study the neurodevelopmental causes of autism? Genes, Brain and Behavior. 2**,** 268-281.

Trotter, J., et al., 2013. Dab1 is required for synaptic plasticity and associative learning. J Neurosci doi 101523JNEUROSCI13. 33 DOI - Trotter, J., Lee, G. H., Kazdoba, T. M., Crowell, B., Domogauer, J., Mahoney, H. M., et al. (2013). Dab1 is required for synaptic plasticity and associative learning. J. Neurosci. 33, 15652-15668. doi: 10.1523/JNEUROSCI.2010-13.2013 SRC - BaiduScholar**,** 15652-15668.

Truong, A. B., et al., 2002. Role of the 14-3-3 C-terminal loop in ligand interaction. Proteins: Structure, Function, and Bioinformatics. 49**,** 321-325.

Tsai, P. T., et al., 2012. Autistic-like behaviour and cerebellar dysfunction in Purkinje cell Tsc1 mutant mice. Nature. 488**,** 647-51.

Tuchman, R., Rapin, I., 2002. Epilepsy in autism. The Lancet Neurology. 1**,** 352-358.

Tueting, P., et al., 1999. The phenotypic characteristics of heterozygous reeler mouse. NeuroReport. 10**,** 1329-1334.

Tzivion, G., Avruch, J., 2001. 14-3-3 Proteins: Active Cofactors in Cellular Regulation by Serine/Threonine Phosphorylation. Journal of Biological Chemistry. 277**,** 3061-3064.

Ubl, A., et al., 2002. 14-3-3 protein is a component of Lewy bodies in Parkinson's disease—Mutation analysis and association studies of 14-3-3 eta. Molecular Brain Research. 108**,** 33-39.

van Hemert, M. J., et al., 2001. 14-3-3 proteins: key regulators of cell division, signalling and apoptosis. BioEssays. 23**,** 936-946.

van Kooten, I. A. J., et al., 2008. Neurons in the fusiform gyrus are fewer and smaller in autism. Brain. 131**,** 987-999.

Varela, M., et al., 2015. Reelin influences the expression and function of dopamine D2 and serotonin 5-HT2A receptors: a comparative study. Neuroscience. 290**,** 165-174.

Vaswani, M., et al., 2003. Role of selective serotonin reuptake inhibitors in psychiatric disorders: a comprehensive review. Progress in neuro-psychopharmacology and biological psychiatry. 27**,** 85-102.

Vawter, M. P., et al., 2001. Application of cDNA microarrays to examine gene expression differences in schizophrenia. Brain Research Bulletin. 55**,** 641-650.

Viding, E., Blakemore, S.-J., 2007. Endophenotype approach to developmental psychopathology: implications for autism research. Behavior Genetics. 37**,** 51-60.

Vijayakumar, N. T., Judy, M., 2016. Autism spectrum disorders: integration of the genome, transcriptome and the environment. Journal of the neurological sciences. 364**,** 167-176.

Vincenz, C., Dixit, V. M., 1996. 14-3-3 Proteins Associate with A20 in an Isoform-specific Manner and Function Both as Chaperone and Adapter Molecules. Journal of Biological Chemistry. 271**,** 20029-20034.

Viswanath, H., et al., 2014. The medial habenula: still neglected. Frontiers in human neuroscience. 7**,** 931.

Volkmann, K., et al., 2008. The zebrafish cerebellar rhombic lip is spatially patterned in producing granule cell populations of different functional compartments. Developmental biology. 313**,** 167-180.

Volkmar, F. R., McPartland, J. C., 2014. From Kanner to DSM-5: autism as an evolving diagnostic concept. Annual review of clinical psychology. 10**,** 193-212.

Wang, H., et al., 1998. Mutations in the Hydrophobic Surface of an Amphipathic Groove of 14-3-3ζ Disrupt Its Interaction with Raf-1 Kinase. Journal of Biological Chemistry. 273**,** 16297-16304.

Wang, J., et al., 2009. 14-3-3ζ Contributes to Tyrosine Hydroxylase Activity in MN9D Cells. Journal of Biological Chemistry. 284**,** 14011-14019.

Wang, S. S.-H., et al., 2014a. The cerebellum, sensitive periods, and autism. Neuron. 83**,** 518-532.

Wang, Samuel S. H., et al., 2014b. The Cerebellum, Sensitive Periods, and Autism. Neuron. 83**,** 518-532.

Wang, Y., et al., 2016. Vesicular monoamine transporter 2 (Vmat2) knockdown elicits anxiety-like behavior in zebrafish. Biochemical and biophysical research communications. 470**,** 792-797.

Wang, Z., et al., 2014c. Reelin gene variants and risk of autism spectrum disorders: an integrated meta-analysis. Am J Med Genet B Neuropsychiatr Genet. 165B**,** 192-200.

Ware, M. L., et al., 1997. Aberrant Splicing of a Mouse disabled Homolog, mdab1, in the scrambler Mouse. Neuron. 19**,** 239-249.

Watanabe, M., et al., GABA and GABA receptors in the central nervous system and other organs. International review of cytology. Elsevier, 2002, pp. 1-47.

Watt, M. J., et al., 2014. Decreased prefrontal cortex dopamine activity following adolescent social defeat in male rats: role of dopamine D 2 receptors. Psychopharmacology. 231**,** 1627-1636.

Weeber, E. J., et al., 2002. Reelin and ApoE Receptors Cooperate to Enhance Hippocampal Synaptic Plasticity and Learning. Journal of Biological Chemistry. 277**,** 39944-39952.

Wen, L., et al., 2008. Visualization of monoaminergic neurons and neurotoxicity of MPTP in live transgenic zebrafish. Developmental biology. 314**,** 84-92.

Werling, D. M., Geschwind, D. H., 2013. Understanding sex bias in autism spectrum disorder. Proc Natl Acad Sci U S A. 110**,** 4868-9.

Wiedenheft, B., et al., 2012. RNA-guided genetic silencing systems in bacteria and archaea. Nature. 482**,** 331-8.

Wilker, E. W., et al., 2005. A Structural Basis for 14-3-3σ Functional Specificity. Journal of Biological Chemistry. 280**,** 18891-18898.

Williams, K., et al., 2011. Cochrane review: selective serotonin reuptake inhibitors (SSRIs) for autism spectrum disorders (ASD). Evidence-Based Child Health: A Cochrane Review Journal. 6**,** 1044-1078.

Williams, R. S., et al., 1980. Autism and mental retardation: neuropathologic studies performed in four retarded persons with autistic behavior. Archives of neurology. 37**,** 749-753.

Willner, P., Methods for assessing the validity of animal models of human psychopathology. Animal models in psychiatry, I. Springer, 1991, pp. 1-23.

Wilson, D. S., 1994. Adaptive genetic variation and human evolutionary psychology. Evolution and Human Behavior. 15**,** 219-235.

Wiltfang, J., et al., 2002. Isoform Pattern of 14-3-3 Proteins in the Cerebrospinal Fluid of Patients with Creutzfeldt-Jakob Disease. Journal of Neurochemistry. 73**,** 2485-2490.

Wise, R. A., 2008. Dopamine and reward: the anhedonia hypothesis 30 years on. Neurotoxicity research. 14**,** 169-183.

Wolpert, C. M., et al., 2000. Three probands with autistic disorder and isodicentric chromosome 15. American Journal of Medical Genetics. 96**,** 365-372.

Wong, A. H. C., et al., 2005. Genetic and post-mortem mRNA analysis of the 14-3-3 genes that encode phosphoserine/threonine-binding regulatory proteins in schizophrenia and bipolar disorder. Schizophrenia Research. 78**,** 137-146.

Wong, A. H. C., et al., 2003. Identification of candidate genes for psychosis in rat models and possible association between schizophrenia and the 14-3-3η gene. Molecular Psychiatry. 8**,** 156-166.

Wong, K., et al., 2010. Analyzing habituation responses to novelty in zebrafish (Danio rerio). Behavioural Brain Research. 208**,** 450-457.

Wong, R. Y., et al., 2013. Behavioral and neurogenomic transcriptome changes in wild-derived zebrafish with fluoxetine treatment. BMC genomics. 14**,** 348.

Wullimann, M. F., Grothe, B., The central nervous organization of the lateral line system. The Lateral Line System. Springer, 2013, pp. 195-251.

Wullimann, M. F., et al., The brain of the zebrafish Danio rerio: a neuroanatomical atlas. Neuroanatomy of the Zebrafish Brain. Birkhäuser Basel, 1996, pp. 19-87.

Xiao, B., et al., 1995. Structure of a 14-3-3 protein and implications for coordination of multiple signalling pathways. Nature. 376**,** 188-191.

Xu, X., et al., 2015. 14-3-3ζ deficient mice in the BALB/c background display behavioural and anatomical defects associated with neurodevelopmental disorders. Scientific Reports. 5.

Yaffe, M. B., et al., 1997. The structural basis for 14-3-3: phosphopeptide binding specificity. Cell. 91**,** 961-971.

Yang, C.-J., et al., 2014. The developmental disruptions of serotonin signaling may involved in autism during early brain development. Neuroscience. 267**,** 1-10.

Yang, X., et al., 2006. Structural basis for protein-protein interactions in the 14-3-3 protein family. Proceedings of the National Academy of Sciences. 103**,** 17237-17242.

Yasui, N., et al., 2007. Structure of a receptor-binding fragment of reelin and mutational analysis reveal a recognition mechanism similar to endocytic receptors. Proceedings of the National Academy of Sciences. 104**,** 9988-9993.

Yasui, N., et al., 2010. Structural basis for specific recognition of reelin by its receptors. Structure. 18**,** 320-331.

Yoneshima, H., et al., 1997. A novel neurological mutant mouse, yotari, which exhibits reeler-like phenotype but expresses CR-50 antigen/reelin. Neuroscience research. 29**,** 217-223.

Young, A. M., 2004. Increased extracellular dopamine in nucleus accumbens in response to unconditioned and conditioned aversive stimuli: studies using 1 min microdialysis in rats. Journal of neuroscience methods. 138**,** 57-63.

Yuan, M., et al., 2018. Behavioral and metabolic phenotype indicate personality in zebrafish (Danio rerio). Frontiers in physiology. 9**,** 653.

Yuen, R. K. C., et al., 2015. Whole-genome sequencing of quartet families with autism spectrum disorder. Nature Medicine. 21**,** 185-191.

Zhang, F., et al., 2014. CRISPR/Cas9 for genome editing: progress, implications and challenges. Human molecular genetics. 23**,** R40-R46.

Zhang, H., et al., 2002. Reelin gene alleles and susceptibility to autism spectrum disorders. Molecular Psychiatry. 7**,** 1012-1017.

Zhang, X.-H., et al., 2015a. Off-target effects in CRISPR/Cas9-mediated genome engineering. Molecular Therapy-Nucleic Acids. 4**,** e264.

Zhang, Y., et al., 2015b. Gene Mutation Analysis in 253 Chinese Children with Unexplained Epilepsy and Intellectual/Developmental Disabilities. PLOS ONE. 10**,** e0141782.

Zhou, Q., Sheng, M., 2013. NMDA receptors in nervous system diseases. Neuropharmacology. 74**,** 69-75.